THE CAFETERIA DIET MODEL OF METABOLIC SYNDROME AND ITS EFFECTS ON CEREBROVASCULAR FORM AND FUNCTION

A thesis submitted to the

Faculty of Graduate and Postdoctoral Studies

in partial fulfillment of the requirements for the

Doctorate in Philosophy degree in Neuroscience

by

Mariana Gomez-Smith

Department of Cellular and Molecular Medicine, Neuroscience Program

Faculty of Medicine

University of Ottawa

April 2017

Abstract

The global occurrence of metabolic syndrome has reached epidemic proportions and is a contributing factor in the rising incidence of cognitive decline in the aging population. While pre-clinical research has advanced our understanding of many of the mechanisms underlying metabolic syndrome, animal models often do not reflect the complexity of human disease. For example, animal models that investigate the role played by diet in metabolic syndrome have generally focused on a single macronutrient, in particular fat or carbohydrate. As a result, although a balanced diet and increased physical activity are commonly recommended to treat metabolic syndrome symptomatology, their long-term cerebrovascular benefits are uncertain. To address these gaps in knowledge, a "Cafeteria" diet consisting of 16 common ultra-processed grocery store food items was used to model human metabolic syndrome in the rat. I compared rats fed a Cafeteria diet (CAF) to those fed "standard" chow (SD) as well as to a third group that underwent a switch to chow after chronic exposure to the Cafeteria diet (SWT). In a first study, I showed that three months of exposure to the Cafeteria diet produced metabolic syndrome as well as hippocampal neuroinflammation with increased microglial proliferation. These were fully reversed in SWT rats. Nonetheless, the Cafeteria diet did not worsen spatial learning and memory performance as assessed using the Barnes maze. In a second study, brain perfusion was examined using continuous arterial spin labeling magnetic resonance imaging (CASL MRI). Cortical and hippocampal resting perfusion was increased in CAF rats while cerebrovascular reactivity in response to a 10% CO_2 vasodilatory challenge was reduced. Furthermore, while resting perfusion improved in SWT rats, cerebrovascular reactivity remained impaired. These cerebral blood flow outcomes were

not accompanied by alterations in microvascular architecture or integrity as determined by rat endothelial cell antigen-1 (RECA-1) and immunoglobulin G (IgG) histology. Taken together, these results demonstrate that the Cafeteria diet is an effective model of metabolic syndrome that negatively impacts brain hemodynamic function. Moreover, while a dietary lifestyle intervention can recover peripheral features of metabolic syndrome, neuroinflammation, and resting perfusion, it is insufficient to completely reverse deficits in cerebrovascular reactivity. These findings are compelling as they speak to the detrimental effects of ultra-processed food consumption on cerebrovascular reserve capacity, believed to be an important factor in cognitive decline.

Table of Contents

Tables

Figures

Abbreviations

7T: 7 Tesla

ABC: avidin-biotin complex

AHA: American Heart Association

ANOVA: analysis of variance

AP: anterior-posterior

ARRIVE guidelines: Animal Research Reporting of In Vivo Experiments guidelines

ASL: arterial spin labeling

BBB: blood-brain barrier

BDNF: brain-derived neurotrophic factor

BMI: body-mass index

CA1: cornu ammonis 1

CA3: cornu ammonis 3

CAF: Cafeteria diet-fed rats

CASL: continuous arterial spin labeling

CBF: cerebral blood flow

CCHS: Canadian Community Health Survey

CO_2: carbon dioxide

CVD: cerebrovascular disease

Cx: cortical ROI

DAB: 3,3´-diaminobenzidine tetrahydrochloride

db/db: leptin receptor mutant mouse

DG: dentate gyrus

EPI: echo planar images

$FiCO_2$: fractional concentration of inspired CO_2

FOV: field of view

GLUT2: glucose transporter-2

GTT: glucose tolerance test

gWAT: gonadal white adipose tissue

H&E: haematoxylin and eosin

Hc: hippocampal ROI

HDL: high-density lipoprotein

HRP: horseradish peroxidase

i.m.: intramuscular injection

i.p.: intraperitoneal injection

i.v.: intravenous injection

Iba1: ionized calcium-binding adapter molecule 1

IDF: International Diabetes Federation

IgG: immunoglobulin G

IL1β: interleukin-1 beta

ITT: insulin tolerance test

LDL/VLDL: low density lipoprotein/very-low density lipoprotein

Look AHEAD: Action for Health in Diabetes study

MELAS: mitochondrial encephalomyopathy, lactic acidosis, and stroke-like episodes

ML: medial-lateral

MRI: magnetic resonance imaging

NHLBI: National Heart, Lung and Blood Institute

NO: nitric oxide

ob/ob: leptin mutant mouse

OLETF: Otsuka Long-Evans Tokushima Fatty rat

PBS: phosphate-buffered saline

PFA: paraformaldehyde

PREDIMED: Prevención con Dieta Mediterránea study

RARE: rapid acquisition with relaxation enhancement sequence

RECA-1: rat endothelial cell antigen-1

REML: restricted maximum likelihood method

RF: radio-frequency pulse

ROI: region of interest

s.q.: subcutaneous injection

SAT: subcutaneous adipose tissue

SCFA: short-chain fatty acids

SD: standard chow diet rats

SEM: standard error of the mean

STZ: streptozotocin

SUR1: sulfonylurea receptor-1

SWT: switch diet rats

T1W-RARE: T1-weighted rapid acquisition with relaxation enhancement sequence

T2: T2-weighted imaging

$tcPCO_2$: transcutaneous partial pressure of CO_2

TNFα: tumor necrosis factor alpha

TR/TE: repetition time/echo time

VAT: visceral adipose tissue

ZDF: Zucker diabetic fatty rat

Acknowledgements

I am immensely grateful to have had the opportunity to pursue a PhD. These many years contributing to the body of scientific knowledge would not have been possible without vast intellectual, emotional, and financial support and commitment. I will forever be thankful to my colleagues, friends, and family for selflessly sharing their advice and skills with me; they've been an endless source of encouragement. Each relationship has helped me to mature as a scientist and as a person, driving me to push through adversity.

Dale, you have been an inspiring role model who has taught me the value of appreciating and emphasizing the positive in every situation. Matthew, I have striven to emulate your resolve and professionalism; I hope that one day these qualities will be as developed in me as they are in you. To all my Corbett lab mates, past and present, your diverse experiences, points of view, and personality were continuously stimulating, making you all an extreme joy to work with. To Hsiao-Huei, Xun, Tina, Phil, and Erik, you were my first lab mates on my return to Canada, and what a time it was! That rollercoaster ride was a great insight into what fuels scientific curiosity and passion.

Thank you to my thesis advisory committee members, Drs. Slack, Lagace, and Albert, for your invaluable input and for helping to keep me focused on the end game. To my thesis examiners, Drs. Paterson, Schlossmacher, Lacoste, and Ismail, thank you for taking the time to evaluate my thesis and for helping me to put the finishing touches on this labour of love.

My dear friends, particularly Keren, Quenby, Anne, and Ben, thank you for dropping everything whenever I needed to talk. Thank you, dad, for inspiring me to never stop asking questions and for instilling in me the need to run after the ball. Thank you, Jav, for

sharing your love of the majestic universe with me. Thank you, mom, for your gift of empathy that enabled me to continually grow and learn. I can't thank my husband, John, enough for his limitless patience and for never letting me give up.

Finally, I wish to express my gratitude to the University of Ottawa, the governments of Ontario and Quebec, the Heart and Stroke Foundation, and the Canadian Partnership for Stroke Recovery for providing the financial support needed to pursue this research.

List of Manuscripts

1) **Gomez-Smith M**, Karthikeyan S, Jeffers MS, Janik R, Thomason LA, Stefanovic B & Corbett D (2016). A physiological characterization of the Cafeteria diet model of metabolic syndrome in the rat. *Physiol. Behav* **167,** 382–391.
2) **Gomez-Smith M**, Janik R, Lake EM, Thomason LA, Adams C, Jeffers MS, Stefanovic B & Corbett D. Reduced cerebrovascular reactivity and increased resting cerebral perfusion in rats exposed to a Cafeteria Diet. Submitted to *Neuroscience*, April 20th, 2017.

List of Appended Publications

1) Schuch CP, Jeffers MS, Antonescu S, Nguemeni C, **Gomez-Smith M**, Pereira LO, Morshead CM & Corbett D (2016). Enriched rehabilitation promotes motor recovery in rats exposed to neonatal hypoxia-ischemia. *Behav Brain Res*. **1**, 42-50.
2) Nguemeni C, **Gomez-Smith M**, Jeffers MS, Schuch CP & Corbett D (2015). Time course of neuronal death following endothelin-1 induced focal ischemia in rats. *J. Neurosci. Method* **15**, 72-6.
3) Corbett D, Jeffers M, Nguemeni C, **Gomez-Smith M** & Livingston-Thomas (2015). Lost in translation: rethinking approaches to stroke recovery. *J Prog Brain Res*. **218**, 413-434.
4) Corbett D, Nguemeni C & **Gomez-Smith M** (2014). How can you mend a broken brain? - Neurorestorative approaches to stroke recovery. *Cerebrovasc Dis*. **38**, 233-239.

"Dying Off the Fat of the Land"

An artist's response to the press release covering my research, presented at the 2012 Canadian Stroke Congress in Calgary.

− Hung, Drawn and Cultured, Ian Hampton's Daily Drawings

(reproduced with permission from the artist)

Chapter 1 - General Introduction

1. Metabolic Syndrome and Cardiovascular Disease

a. History of the metabolic syndrome concept

The observation that several disorders of metabolic origin frequently present together was first reported in 1923 by Eskil Kylin in describing the association between diabetes, hypertension, and kidney disease (Kylin, 1923). Jean Vague added obesity to this clustering with a quantifiable description of gender-specific adipose tissue distribution and its differential role in peripheral metabolism (Vague, 1947). Over the course of the following three decades, epidemiological evidence began to link cardiovascular disease (i.e. coronary heart disease, cerebrovascular disease, peripheral arterial disease) (World Health Organization, 2016) to metabolic disorders (Haller, 1977).

During this same period, the rapidly increasing rate of obesity in the United States (Flegal *et al.*, 1998) was viewed as the leading cause of many health complications (Bray, 1985). However, the nature of the relationship between obesity and cardiovascular disease, whether causal or correlational, is still unclear (Antonopoulos *et al.*, 2016) with some considering insulin resistance to be the primary mechanism underlying cardiovascular disease (Reaven, 2006). In fact, in his 1988 Banting lecture, Gerald Reaven highlighted the role of insulin resistance and hyperinsulinemia in the development of hypertriglyceridemia and hypertension, coining the term 'Syndrome X' to identify this cluster of metabolic disturbances (Reaven, 1988). Syndrome X would become the forerunner to metabolic syndrome.

b. Institutional definitions of metabolic syndrome

In an effort to develop a working guideline for clinicians and researchers, national and international organizations including the World Health Organization (Alberti & Zimmet, 1998), the European Group for the Study of Insulin Resistance (Hills *et al.*, 1999), the National Heart, Lung and Blood Institute (NHLBI) (Expert Panel on Detection Evaluation and Treatment of High Blood Cholesterol in Adults., 2001), and the International Diabetes Federation (IDF) (Alberti *et al.*, 2005) each proposed a definition of metabolic syndrome, grouping together the most salient metabolic features shown to increase the risk of cardiovascular disease.

Though these definitions had much in common, they differed in their applicability to different ethnic groups. In particular, this was based on the use of waist circumference as the measure of abdominal obesity, as single cut-off values cannot be standardized across populations (Alberti *et al.*, 2005). To reconcile these differences, the IDF, the NHLBI, and the American Heart Association (AHA) agreed on a harmonized definition of metabolic syndrome (Alberti *et al.*, 2009*a*), requiring that any three out of the following five features be present: abdominal obesity with elevated waist circumference (country-specific); elevated triglyceride ($\geq$ 150 mg/dl); reduced high-density lipoprotein (HDL) ($<$ 40 mg/dl in men, $<$ 50 mg/dl in women); elevated blood pressure (systolic $\geq$ 130 and/or diastolic $\geq$ 85 mmHg); elevated fasted blood glucose ($\geq$ 100 mg/dl).

c. Metabolic syndrome and cardiovascular disease statistics

The global prevalence of metabolic syndrome has grown substantially in recent decades (Batsis *et al.*, 2007). Nonetheless, Canada and the United States lead the world in rates of metabolic syndrome (Monteiro *et al.*, 2013). In Canada, 21% of the adult

population over the age of 18 is affected (Statistics Canada, 2014) while 35% of adults ≥20 years old in the United States have metabolic syndrome (Aguilar *et al.*, 2015).

These numbers are troubling given that metabolic syndrome increases the risk of ischemic stroke and myocardial infarction by 60% (Boden-Albala *et al.*, 2008). This increased ischemic stroke risk disproportionally affects women (hazard ratio of 2.0 in women, 1.1 in men), driven by a higher rate of elevated waist circumference and considerably lower HDL in women.

2. Factors Contributing to Metabolic Syndrome

a. Lifestyle factors

An unhealthy diet and physical inactivity greatly contribute to the rising rates of chronic illness, supported by the results of the 2010 Global Burden of Disease study (Lim *et al.*, 2012). Collectively, these two risk factors explained 10% of disability-adjusted life years lost, leading all of the 67 risk factors studied. Further, the number of years of life lost due to high body-mass index (BMI) and high fasted blood glucose nearly doubled between 1990 and 2010.

i. Dietary factors

These findings from the Global Burden of Disease study are troubling given that ~55% of Canadians do not consume enough fruits and vegetables (at least 5 daily servings) (Public Health Agency of Canada, 2011). Instead, energy-dense ultra-processed foods are preferred, a dietary trend that is becoming adopted globally (Monteiro *et al.*, 2013). These are foods that result from the additional processing of substances that have already been refined from whole foods and that are particularly energy dense and high in

sodium. Combined with physical inactivity, this dietary preference contributes to a positive energy balance. Indeed, the North American diet, characterized especially by the elevated consumption of soda, potato chips, deli meats, and sweets, as well as the low intake of vegetables, whole grains, fruits, and yogurt is associated with an average yearly weight gain of 1 lbs (Mozaffarian *et al.*, 2011).

In particular, refined sugars in sweetened beverages (e.g. soda and fruit juice) play an important role in the development of metabolic syndrome. Because of their liquid form, sweetened beverages are quickly ingested before satiety signals take effect (Gibbs *et al.*, 1973) and the additional kilocalories that they provide are not compensated for by reduced appetite at subsequent meals (Almiron-Roig & Drewnowski, 2003). In fact, the consumption of a single sweetened beverage per day results in a positive energy balance and weight gain (Malik *et al.*, 2008). These detrimental effects are compounded by sugar's high palatability through its activation of reward pathways in the brain in much the same way as drugs of addiction (Avena *et al.*, 2008). Furthermore, combining sugar with fat in ultra-processed foods further enhances food palatability by decreasing sensory-specific satiety, thereby greatly enhancing overall food intake and promoting a positive energy balance (Sørensen et al., 2003).

A positive energy balance is central to the development of the various metabolic syndrome features. Initially, surplus metabolic fuels are preferentially stored in subcutaneous adipose tissue (SAT) which acts as a 'metabolic sink' (Lemieux, 2004). Because of SAT's high expression of lipoprotein lipase that facilitates the removal of triglycerides from circulating cholesterol particles, lipid storage in SAT is cardioprotective (Pouliot et al., 1991). However, once maximal hyperplastic expansion of SAT adipocytes is reached, as determined by environmental and genetic factors,

adipocytes transition to hypertrophic growth, triggering several negative events within SAT tissue (Danforth, 2000). These include the infiltration of immune cells causing the local and systemic release of inflammatory adipokines as well as the development of insulin resistance. SAT insulin resistance does not significantly contribute to whole-body glucose regulation due to the fact that it accounts for just 10% of the glucose load (Gustafson et al., 2015). However, it does alter adipocyte metabolism causing lipids to be funneled towards visceral adipose tissue (VAT) and to ectopic organs such as skeletal muscle, heart, and liver, subsequently elevating circulating triglyceride leading to a concomitant reduction in HDL cholesterol (Després & Lemieux, 2006). Additionally, these ectopic tissues also become insulin resistant, thus precipitating the onset of type 2 diabetes (Boren et al., 2013). Finally, insulin resistance, and more specifically hyperinsulinemia, instigates the development of hypertension as it stimulates renin secretion and greater retention of sodium by the kidneys (Johnson et al., 2015). An overview of these processes and how they contribute to the development of cardiometabolic risk factors is shown in **Figure 1**.

In addition to a positive energy balance, nutritional quality plays an important role in the development of metabolic syndrome, particularly in regulating metabolite oxidation rate, oxidative stress, and appetite (Mozaffarian, 2017). Nonetheless, the question of what constitutes a nutritious diet is fraught with controversy. Historically, healthy diets have been considered from the perspective of single nutrient deficiencies or excesses. An important example of this was the description, in the Seven-Country Study, of a link between elevated dietary saturated fat consumption and increased cardiovascular disease (Keys *et al.*, 1981, 1986). By extension, total dietary fat became considered by researchers and health agencies as *the* most important risk factor for obesity and

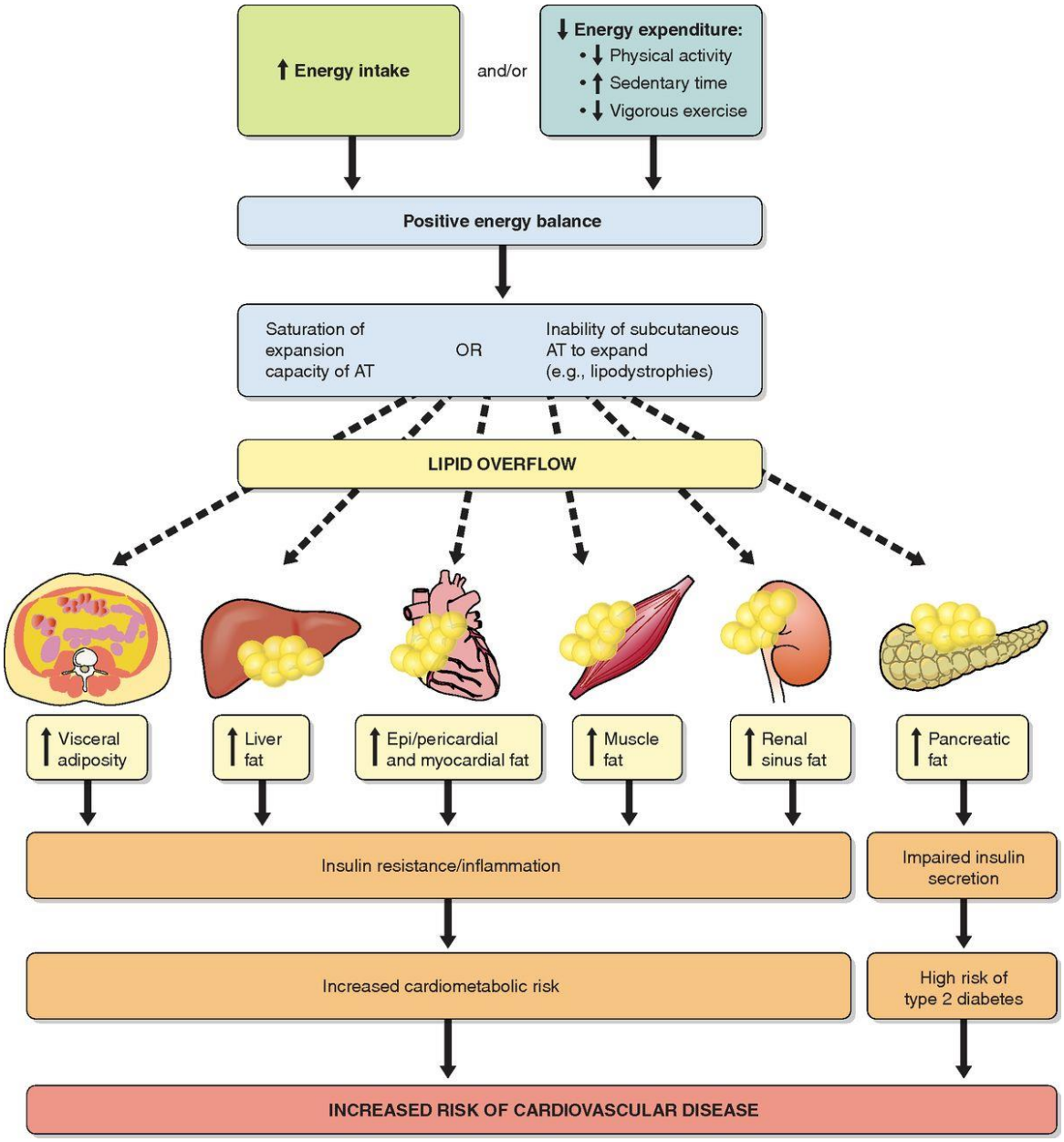

Figure 1: Working model of how a positive energy balance leads to metabolic syndrome with increased cardiovascular disease risk.

Lipid overflow from subcutaneous adipose tissue spills over into visceral adipose tissue as well as into ectopic organs including liver, heart, muscle, kidney and pancreas. This in turn impairs insulin signaling with harmful cardiometabolic consequences.

Adapted from (Tchernof & Després, 2013).

cardiovascular disease (Mozaffarian, 2016). However, recent analysis of internal documents from the Sugar Research Foundation has revealed that this was an intentional misdirection in order to mask the negative impact of refined sugars (Kearns *et al.*, 2016). Large prospective studies and meta-analyses of retrospective studies have since concluded that the nutrient that is replaced, rather than the quantity of saturated fat per se, matters most in predicting cardiovascular disease risk (Micha & Mozaffarian, 2010; Li *et al.*, 2015). Indeed, replacing saturated fat with polyunsaturated fat or high-quality carbohydrates reduces cardiovascular disease outcomes while replacement with refined sugars increases risk (Yang et al., 2014). As such, current recommendations urge the consideration of overall dietary patterns and a food-based research approach rather than focusing on isolated nutrients (Mozaffarian, 2016).

ii. Physical inactivity

Physical inactivity represents the other side of the coin in the development of metabolic syndrome; energy surplus from diet that is not countered by physical activity of sufficient intensity results in a net positive energy balance. Paralleling dietary patterns, intensity of physical activity by the average Canadian is lower than that recommended by healthcare providers, helping to explain the high national rate of metabolic syndrome. Indeed, only one in five adult Canadians meet the recommended 150 minutes of moderate to vigorous physical activity set out by the Canadian Physical Activity Guidelines (Canada, 2015) and ~48% are physically inactive (walking less than 30 min/day) (Public Health Agency of Canada, 2011).

In addition to counterbalancing dietary energy surplus, physical activity exerts several other cardioprotective effects. These include the regulation of the metabolic oxidation

rate via engagement of sympathetic and neuroendocrine systems, the mobilization of progenitor cells to enable tissue repair, and changes to muscle tissue that enhance secretion of beneficial metabolites and the effective disposal of deleterious others (Neufer *et al.*, 2015). Combined, these benefits of physical activity have a cardioprotective value that is estimated to be ~40% greater than that predicted by the improvement of metabolic syndrome features alone (Joyner & Green, 2009). This strong effect is exemplified in a population of individuals that, despite being obese, do not exhibit the other features of metabolic syndrome (Lavie *et al.*, 2014). These 'metabolically healthy obese' individuals are at a lower risk of cardiovascular disease than their metabolically unhealthy obese counterparts, an effect that is in part due to their greater level of cardiorespiratory fitness (Ortega *et al.*, 2013).

b. Genetic factors

Though lifestyle is an incontrovertible cause of metabolic syndrome, common genetic polymorphisms potentiate its features. Indeed, individual metabolic syndrome features are estimated to exhibit 25-60% heritability (Stančáková & Laakso, 2014). Resulting from the selective pressures of historical food shortages, purported 'thrifty genes' promote the onset of obesity and insulin resistance as food has become over abundant in modern times (Neel, 1962). Alternatively, these polymorphisms may have arisen instead from genetic drift and confer no evolutionary advantage (Speakman, 2008).

Regardless of the evolutionary mechanisms driving their appearance, most polymorphisms produce mild phenotypes and only in combination with an energy-dense diet (Groop, 2000). Nevertheless, certain mutations, for example those affecting leptin (Clément *et al.*, 1998) and melanocortin signaling (Vaisse *et al.*, 1998), result in extreme

phenotypes regardless of diet. However, the prevalence of these mutations is low. For example, the frequency of the LEP A19G leptin allele is 0.46% in the Caucasian population while leptin receptor variants are present at rates of 0.25-0.85% (Paracchini *et al.*, 2005). These severe genetic polymorphisms do not, therefore, significantly contribute to the rapid increase in prevalence of metabolic syndrome that has been observed in the past few decades.

c. Gut microbiome

Recent advances in our understanding of the gut microbiome have revealed other mechanisms by which diet leads to the development of metabolic syndrome. In addition to the energy absorbed from food macronutrients, intestinal bacteria, primarily from the *Bacteroidetes* and *Firmicutes* phyla, supply the body with energy from short-chain fatty acids (SCFA) such as butyrate, propionate, and acetate via the fermentation of non-digestible carbohydrates (Komaroff et al., 2017). In particular, *Firmicutes* exhibit a greater ability to generate SCFA, with an increase in the relative abundance of certain classes of *Firmicutes* associated with an 'obese' phenotype in both rodents (Turnbaugh *et al.*, 2006) and humans (Turnbaugh *et al.*, 2009*a*). While the composition of the gut microbiome is largely established at birth (Palmer *et al.*, 2007), diet can dramatically alter its composition after a single day. In particular, mice switched to a high-fat and high-sugar 'Western' diet exhibit a reduction in bacterial diversity and a shift in the relative abundance of bacterial species leading to increased adiposity, features that are transmissible to chow-fed mice within two weeks of a fecal transplant (Turnbaugh *et al.*, 2009*b*).

SCFA, while serving as an additional energy source, also act as signaling molecules that modulate systemic inflammation and brain function (Noble et al., 2017). Butyrate, in particular, is protective of intestinal barrier integrity. Conversely, low butyrate levels decrease epithelial tight junction function, leading to increased gut permeability, low-grade systemic inflammation, and subsequent insulin resistance (Canfora et al., 2015). The actions of SCFA on barrier permeability extend to that of the blood-brain barrier (BBB). Indeed, germ-free mice exhibit low BBB tight junction protein expression which is restored following exposure to gut bacteria from healthy mice (Braniste et al., 2014). Moreover, treatment of germ-free mice with SCFA in drinking water can also restore BBB integrity in addition to normalizing impaired microglial function (Erny et al., 2015). Similar detrimental effects on BBB permeability and neuroinflammation are seen in high-fat diet-fed mice, accompanied by increased anxiety behaviour and decreased memory performance (Bruce-Keller et al., 2015). These features are transmissible to antibiotic-treated chow-fed recipient mice, highlighting the relationship between the composition of the gut microbiome and behavioural outcomes.

3. Lifestyle Interventions in the Treatment of Metabolic Syndrome

The long-time focus on obesity and dietary fat as the main causes of metabolic syndrome have greatly influenced the development of lifestyle interventions aimed at reducing rates of cardiovascular disease. These have primarily targeted weight reduction by employing energy-restricted low-fat diets (Mozaffarian, 2016). An important example of this was the Women's Health Initiative randomized controlled trial in which fat intake was limited to 20% of total energy (Howard et al., 2006). While modest weight loss was achieved over the course of 8 years, other metabolic syndrome features were not different

from those of control subjects nor were cardiovascular disease morbidity and mortality improved. In a similar study, the Look AHEAD trial, an energy-restricted diet was combined with moderate intensity exercise. Though it achieved greater improvements in reducing the severity of metabolic syndrome features, it continued to fail in reducing cardiovascular disease risk (The Look AHEAD Research Group, 2013).

In contrast, significant cardiovascular benefits are obtained when following a Mediterranean diet. In the PREDIMED study, participants consuming an energy-unrestricted Mediterranean diet were compared to control subjects on a low-fat diet (Salas-Salvadó *et al.*, 2011; Estruch *et al.*, 2013). Emphasis was put on consuming large amounts of olive oil, nuts, fish, fruits, and vegetables and limiting intake of certain food categories (red and processed meats, sweets, etc.). The overall number of cardiovascular events, incidence of stroke, and the rate of diabetes were all reduced after four years on the Mediterranean diet.

The stark contrast between these dietary approaches exemplifies the great importance of overall dietary patterns over single-nutrient interventions in improving cardiovascular outcomes (Mozaffarian, 2016). Moreover, these studies highlight the difficulty in reversing the effects of diet on the cardiovascular system and the need to better understand underlying biological mechanisms.

4. Structural and Functional Neurovascular Consequences of Metabolic Syndrome

a. Metabolic syndrome and cognition

A strong negative correlation exists between metabolic syndrome, its causal lifestyle factors, and cognitive performance in humans (Crichton *et al.*, 2014). In particular, high-

saturated fat and low-polyunsaturated fat diets (Eskelinen *et al.*, 2008) as well as diets high in refined sugars (Ye *et al.*, 2011) decrease cognitive function whereas the Mediterranean diet slows cognitive decline in aging populations (Opie *et al.*, 2013).

Studies using animal models have confirmed this link, particularly in respect to hippocampal-dependent spatial memory. Testing rats fed a high-fat/high-carbohydrate diet on the radial arm maze, Kanoski *et al.* demonstrated that spatial memory was impaired after only three days, while deficits in non-spatial memory retention occurred much later, after 30 days (Kanoski & Davidson, 2010). Similarly, using a novel object and place task, both mice (Heyward *et al.*, 2012) and rats (Beilharz et al., 2014) fed obesogenic diets exhibit poor performance on the spatial component of the task but not in the detection of the novel object. These high-energy diets are hypothesized to impair spatial memory by reducing the effectiveness of neuronal satiety signals. These signals normally act to inhibit memories associated with post-ingestive reward and the reduction in their intensity promotes increased memory competition (Davidson et al., 2005). This reduction in memory inhibition has been shown to play a key role in increasing food intake in humans (Attuquayefio *et al.*, 2016). Moreover, it specifically relates to fat and refined sugar intake and not to decreased consumption of fruits and vegetables.

The negative effects of diet on cognition are not limited to hippocampal-dependent spatial memory. Indeed, frontal lobe function is impaired by a high saturated fat diet, as assessed using the Hebb-Williams maze (Greenwood & Winocur, 1990). The variable-interval delayed alternation task, reliant on various brain regions, has also elucidated impairments in rats fed several different high-fat diets (Winocur & Greenwood, 1999). These effects of diet on cognition are related to a number of mechanisms that include

increased neuroinflammation and changes in cereobrovascular hemodynamics (Yates *et al.*, 2012).

b. Metabolic syndrome and neuroinflammation

A positive energy balance is a causal factor in the development of low-grade chronic inflammation (Bettcher & Kramer, 2014). Indeed, surplus metabolic fuels cause mitochondrial and endoplasmic reticulum stress in metabolically active tissues leading to the generation of noxious metabolic by-products and reactive oxygen species (Samuel & Shulman, 2012). In turn, these signals of cellular stress recruit innate immune cells to sites of injury where they act to engage cellular repair mechanisms (Hotamisligil, 2006). Cerebrovascular endothelial cells, in particular, are a primary site of cellular stress due to their high number of mitochondria (Oldendorf *et al.*, 1977).

In the immune-privileged brain, resident microglia surveil the parenchymal microenvironment for signs of inflammation and neuronal damage. Peripheral inflammatory signals also communicate with central microglia via a number of routes, notably by transport of cytokines across the BBB or from circumventricular organs and by signaling vascular endothelial cells (Hoogland *et al.*, 2015). Once stimulated, microglia undergo graded levels of activation that include increased proliferation, progression through various morphological states and release of cytokines and growth factors with both pro- and anti-inflammatory properties (Gomez-Nicola & Perry, 2015). Whether microglial activation is beneficial or detrimental depends on a number of factors including the type of insult and the extent of damage (Marshall *et al.*, 2013).

Dietary insults have been shown to activate microglia, yielding negative effects on neuronal function. Gavage with saturated fat causes microglial proliferation and pro-

inflammatory cytokine production in the hypothalamus, both of which are abolished when microglia are ablated in transgenic mice (Valdearcos *et al.*, 2014). Moreover, microglial ablation improves hypothalamic leptin signaling and reduces food intake despite the continued delivery of saturated fat, thus demonstrating a direct role for microglia in modulating neuronal activity. In addition to increasing cytokine and growth factor release, microglia also regulate neuronal function via synaptic remodeling. In the healthy developing brain, microglia extensively prune synapses, a mechanism that may be reactivated in the pathological adult brain (Salter & Beggs, 2014). Indeed, this appears to occur in rats fed a high-fat diet. After eight weeks, obese adult rats simultaneously exhibit decreased dendritic spine density and highly ramified microglia in the cortex which correlates with impaired capacity for novel object recognition and worsened performance on an attentional set-shifting task (Bocarsly *et al.*, 2015).

c. Metabolic syndrome and the cerebrovasculature

While inflammation exerts direct effects on neuronal function, it also causes diffuse arteriopathy in cerebral arteries and arterioles, disturbing brain perfusion and cerebrovascular reactivity and worsening cognitive impairments (Hainsworth & Markus, 2008). This damage is characterized by vessel wall thickening due to collagen deposition in the basement membrane, vascular smooth muscle cell degeneration, and endothelial cell dysfunction. As a result, vessel stiffness and, consequently, global vascular tone are both increased (Thompson & Hakim, 2009).

Furthermore, inflammation can negatively impact the functional performance of the cerebrovasculature, that is the ability of vessels to contract and dilate in response to changes in local energy and oxygen requirements. Vascular inflammation increases

vasoconstriction by acting upon endothelial cells, simultaneously downregulating nitric oxide synthase activity, thus reducing nitric oxide (NO) production (Katakam *et al.*, 2012) and upregulating the expression of the vasoconstrictor endothelin-1 (Mather *et al.*, 2013). In addition, inflammatory processes cause BBB disruption by interfering with barrier proteins, thereby increasing barrier permeability and further enhancing the transit of inflammatory proteins and increasing neuroinflammation (Obermeier *et al.*, 2013).

An increase in vessel tone and loss of vasodilatory ability results in an eventual reduction in cerebral blood flow (CBF). This subsequently generates a hypoxic microenvironment causing upregulation of hypoxia-inducible factor 1, an initiating factor for angiogenesis (Ergul *et al.*, 2014). However, in combination with diabetic conditions, hypoxic angiogenic processes are dysfunctional, resulting in the aberrant growth of new vessels that are poorly perfused and non-viable (Li *et al.*, 2010). These newly generated blood vessels are vulnerable to additional vascular insults such as an ischemic stroke. In diabetic Goto-Kakizaki rats, for example, cortical vessel density, initially elevated in comparison to control rats, decreases in diabetic animals following middle cerebral artery occlusion (Prakash et al., 2013b).

Figure 2 illustrates some of the pathways by which inflammation, oxidative stress, and hypoxia act on the cerebrovasculature to impair structural integrity and hemodynamic function.

5. Rodent Models of Metabolic Syndrome

a. Genetic models

Metabolic syndrome is often modeled in rodent strains in which a spontaneous mutation causing pronounced obesity, diabetes, or hypertension has arisen. Leptin ligand

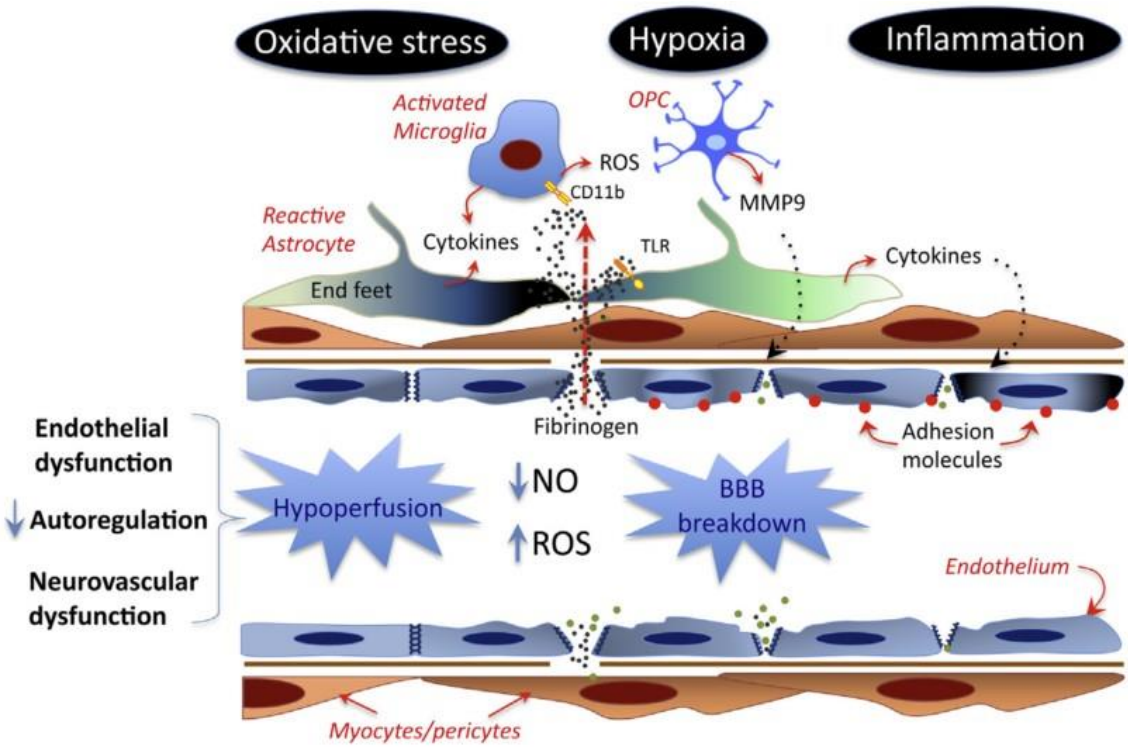

Figure 2: Pathways by which inflammation, oxidative stress, and hypoxia initiate blood vessel damage.

Inflammation, oxidative stress, and hypoxia lead to increased vasoconstriction by reducing NO release. As a result, vessel tone increases, reducing CBF. Moreover, functional and structural damage to the cell layers of vessel walls, in particular the endothelial cell layer, leads to breakdown of the BBB which further perpetuates neuroinflammation and impairs vascular reactivity.

Adapted from (Iadecola, 2013).

and receptor mutants, the ob/ob and db/db mice, as well as the Zucker diabetic fatty (ZDF) rat, were some of the first to be recognized (Panchal & Brown, 2011). A number of other strains have subsequently been isolated, often through selective breeding. A few of these include the cholecystokinin-1 receptor mutant Otsuka Long-Evans Tokushima Fatty (OLETF) rat as well as the polygenic mutant Goto-Kakizaki and spontaneously hypertensive rats, of which the latter is often crossed with other strains to generate a complex metabolic phenotype (Aleixandre de Artiñano & Miguel Castro, 2009). Finally, genetically engineered lines targeting specific gene products, such as neuropeptide Y, agouti-related peptide, or the insulin receptor, have greatly helped to dissect the cellular and molecular pathways responsible for regulating feeding behaviour and energy use (Barrett *et al.*, 2016).

While the genetic approach to studying metabolic syndrome has certain advantages, it is disadvantaged relative to dietary models in several respects. Firstly, genetic models often do not recapitulate the full gamut of metabolic syndrome features (Panchal & Brown, 2011). A summary of metabolic syndrome features observed in several of the above mentioned rodent models is presented in **Table 1**. On the other hand, rodent genetic models sometimes produce exaggerated phenotypes not observed in their human counterparts, such as the case of the pancreatic β-cell glucose transporter 2 (GLUT2) transgenic mouse. Similar human mutations result in gross glucose homeostatic dysregulation without abnormal insulin secretion, whereas mice expressing the GLUT2 antisense mRNA in β-cells are hypoinsulinemic and die within a few weeks of birth (Leturque *et al.*, 2009). Finally, there exists the problem of the potential activation of compensatory mechanisms in genetic rodent models to counter genetic manipulations. An example of this is the sulfonylurea receptor 1 (SUR1) knock-out mouse in which

Table 1: Metabolic syndrome features at different ages in the most commonly used genetic rodent models.

Rodent model	Age (weeks)	Signs of metabolic syndrome shown by rodents				
		Obesity	Hypertension	Dyslipidaemia	Cardiovascular dysfunction	Impaired glucose tolerance
ob/ob mice	4	✓	×	×	×	×
	12	✓	×	×	×	✓
	24	✓	×	×	✓	✓
db/db mice	6	✓	×	×	×	×
	12-13	✓	×	✓	✓	✓
	20	✓	×	✓	✓	✓
ZDF rat	12–15	✓	✓	✓	✓	×
	20	✓	✓	✓	✓	×
	31–47	✓	✓	✓	✓	×
OLETF rats	8	×	×	✓	×	×
	14	×	✓	✓	×	×
	20	✓	✓	✓	×	×
	24	✓	✓	✓	×	✓
	34	✓	✓	✓	×	✓
	40	✓	✓	✓	×	✓
	60–66	✓	✓	✓	✓	✓
Goto-Kakizaki rats	4	×	×	×	×	✓
	8	×	×	✓	×	✓
	20	×	×	✓	✓	✓
	60	×	×	✓	✓	✓

Adapted from (Panchal & Brown, 2011).

pancreatic β-cell ATP-sensitive potassium channels, critical for insulin release, are defective (Seghers *et al.*, 2000). While SUR1 mutations cause hyperinsulinemic hypoglycemia in humans, SUR1 knock-out mice are normoglycemic unless stressed, exhibiting an as yet unknown compensatory mechanism.

a. Dietary models

i. High-fat diets

Of the dietary models of metabolic syndrome, high-fat diets were the first to be used in rodents, with fat representing as much as 90% of total energy (~80% by weight) (Samuels et al., 1942). More modern versions of high-fat diets typically provide a single source of fat ranging from 20-60% by weight (Varga *et al.*, 2010). Several factors, including type of fat, rodent strain, and gender influence the effectiveness of high-fat diets in generating features of metabolic syndrome. For example, when fed a 42% high-fat diet where the fat source was either lard, olive oil, coconut oil, or fish oil, rats exhibited variable physiological effects (Buettner *et al.*, 2006). Whereas lard and the two vegetable oils produced significant weight gain, fish oil led to a reduction in body weight compared to standard chow-fed rats. Moreover, hyperglycemia, hyperinsulinemia, and hypertriglyceridemia were only achieved when rats were fed olive oil, coconut oil, or lard but not fish oil.

ii. High-carbohydrate diets

High-carbohydrate rodent diets habitually consist of a single carbohydrate source, though concentrations vary extensively between studies. While all carbohydrate molecules are energetically equivalent, because they enter the glycolytic pathway at different steps, they produce variable results on whole-body metabolism (Wong et al.,

2016). Fructose, for example, bypasses the rate-limiting step of glucose to fructose-1,6-bisphosphate conversion. Instead, fructose is readily metabolized to fructose-1-phosphate by phosphofructokinase, providing a continuous source of surplus metabolic fuels. The metabolic pathways fueled by different carbohydrate sources is illustrated in **Figure 3**.

High-fructose diets substitute carbohydrates from a regular grain diet with fructose, supplied in either food or water, and represent 10-60% of the diet by weight (Lai et al., 2014). Causing disease in as little as four weeks (Hsieh et al., 2005), high-fructose diets have provided much of the evidence for the molecular mechanisms underlying hypertension, insulin resistance, and microvascular dysfunction (Tran et al., 2009). Nonetheless, while high-fructose diets generate insulin resistance, hyperglycemia, hyperinsulinemia, and hypertriglyceridemia, and hypertension in a dose-dependent manner, they fail to cause weight gain (Dai & McNeill, 1995).

Conversely, high-sucrose diets, generally consisting of 10-30% sucrose by weight (Lai et al., 2014), are capable of causing weight gain (Sweazea *et al.*, 2010) in addition to insulin resistance and hypertriglyceridemia (Santure et al., 2002; Coelho et al., 2010). However, reports on the ability of high-sucrose diets to cause hypertension are inconsistent and often require combination with other factors (e.g. use of susceptible genetic models, addition of dietary sodium, etc.) (Santure et al., 2002; Sharma et al., 2008).

iii. Combination high-fat/high-carbohydrate diets

With the aim of targeting multiple metabolic pathways and more closely reproducing human dietary patterns, rodent diets often incorporate high concentrations of both fat and carbohydrate (Panchal & Brown, 2011). As with the single-nutrient diets described

Figure 3: Metabolic pathways acted on by different carbohydrate sources as well as by fat.

(Following page) High-carbohydrate and high-fat diets exert different effects on whole body metabolism as individual macronutrients enter into distinct metabolic pathways. a) Fructose bypasses the rate-limiting step of glucose to fructose-1,6-bisphosphate conversion and is instead metabolized to fructose-1-phosphate by phosphofructokinase, providing a continuous source of surplus metabolic fuels such as pyruvate and lactate. b and c) Sucrose is converted to fructose and glucose, the latter of which is converted to glycogen via glycogenesis and broken down by the rate-limiting step of glycolysis. Furthermore, insulin is released in response to rising glucose levels, acting on adipose tissue to promote fatty acid synthesis. d) Fats undergo lipolysis, releasing fatty acids into the blood stream which are re-esterified to form triglyceride.

Adapted from (Wong *et al.*, 2016).

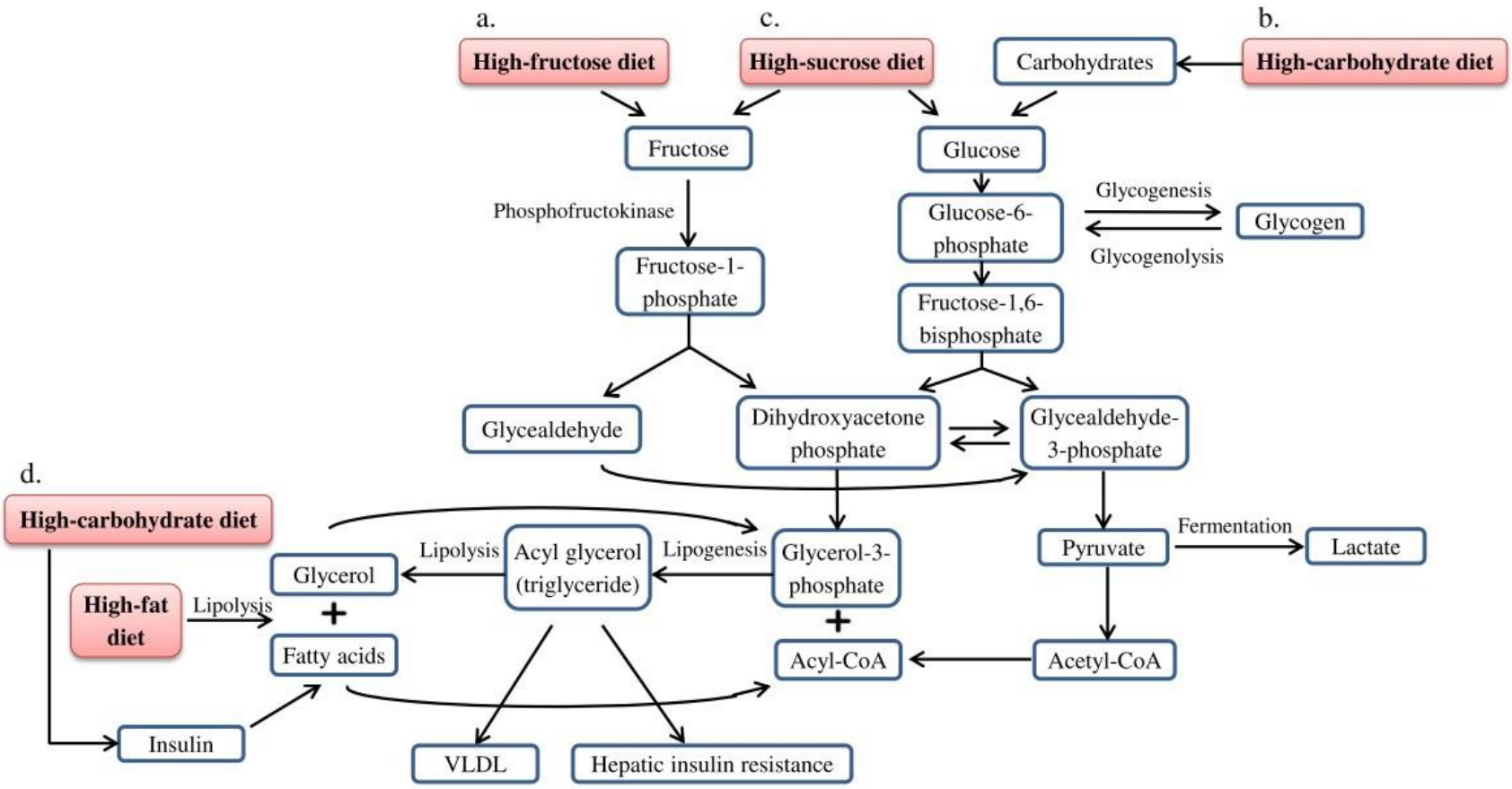
a.
c.
b.
High-fructose diet
High-sucrose diet
Carbohydrates
High-carbohydrate diet
Fructose
Glucose
Phosphofructokinase
Glucose-6-phosphate
Glycogenesis
Glycogen
Glycogenolysis
Fructose-1-phosphate
Fructose-1,6-bisphosphate
Glycealdehyde
Dihydroxyacetone phosphate
Glycealdehyde-3-phosphate
d.
High-carbohydrate diet
Lipolysis
Acyl glycerol (triglyceride)
Lipogenesis
Glycerol-3-phosphate
Pyruvate
Fermentation
Lactate
Glycerol
High-fat diet
Lipolysis
Fatty acids
Acyl-CoA
Acetyl-CoA
Insulin
VLDL
Hepatic insulin resistance

above, sugar content is typically fructose (10-60% by weight) or sucrose (10-30% by weight) while type and concentration of fat varies (20-60% by weight). This approach reliably generates features of metabolic syndrome that are more pronounced than in high-fat-only (la Fleur *et al.*, 2011) and high-carbohydrate-only (Lozano *et al.*, 2016) models. Indeed, not only do these combination diets provide nutritional fuels directed at various metabolic pathways, the joint presentation of fat with sugar also renders these diets more palatable, resulting in greater food intake (Higa *et al.*, 2014).

iv. Cafeteria diets

Notwithstanding the advantages of high-fat/high-carbohydrate diets over single-nutrient diets, they lack certain attributes of human diets that play a critical role in the development of metabolic syndrome. In particular, high-fat/high-carbohydrate diets, which are industrially manufactured and in pellet form, lack sensorial diversity, choice, and novelty, features that influence brain reward circuitry and motivation to eat (Pandit *et al.*, 2012). Cafeteria diets circumvent these problems by providing animals with a selection of high-fat and high-carbohydrate human food items. Though Cafeteria diets have long been criticized for their lack of standardization and high degree of variability between studies (Moore, 1987), they nonetheless consistently generate a metabolic syndrome phenotype with abdominal obesity, insulin resistance, and hypertriglyceridemia that is often more marked than in animals fed a high-fat diet (Sampey *et al.*, 2011; Beilharz *et al.*, 2014; Kaakoush *et al.*, 2016). Furthermore, despite each Cafeteria diet providing rodents with different human food items, relative macronutrient consumption is remarkably similar across studies (Lladó *et al.*, 1995; Shafat *et al.*, 2009; Gomez-Smith *et*

al., 2016), potentially owing to endogenous regulation mechanisms that control food self-selection (Berthoud *et al.*, 2012).

Table 2 summarizes metabolic syndrome features obtained in studies using different diets discussed in this section.

6. Statement of Research Problem Rationale and Main Objectives

Metabolic syndrome affects 21% of Canadians (Statistics Canada, 2014) and almost 35% of Americans (Aguilar *et al.*, 2015), increasing cardiovascular disease risk by 60% (Boden-Albala *et al.*, 2008). Poor lifestyle behaviours, particularly the consumption of an energy-dense, nutritionally inadequate diet and physical inactivity, are leading factors in the development of metabolic syndrome (Lim *et al.*, 2012). While features of metabolic syndrome can be improved by certain lifestyle interventions, long-term reversibility of cardiovascular damage is in question (Mozaffarian, 2016). This is concerning given that in addition to worsening cardiovascular disease risk, metabolic syndrome causes cerebrovascular dysfunction (Giannopoulos *et al.*, 2010; Tyndall *et al.*, 2016) and increases the risk of cognitive impairments (Cavalieri *et al.*, 2010).

Research advances in the field have been hampered by the use of animal models that do not accurately reflect human disease etiology and clinical presentation (Lai *et al.*, 2014). In particular, modeling the complexity of the human diet is not sufficiently prioritized (Joyner, 2014). Moreover, the great number of animal models, estimated to exceed 80, and insufficient standardization between studies has led to an accumulation of publications where little homology exists (Varga *et al.*, 2010).

To address some of these concerns, I sought to investigate the Cafeteria diet as a model of human metabolic syndrome as well as its deleterious effects on the brain. As

Table 2: Metabolic syndrome features in studies using high-fat, high-fructose, high-sucrose, combination high-fat/high-sugar, and Cafeteria diets.

(Following page) All studies listed used male rats. (+) indicates a feature was evaluated and present by the end of the experimental time course while (-) indicates that a feature was evaluated and the diet treatment group was not significantly different from the control group. (n/a) indicates that a feature was not evaluated. All metabolic syndrome features were evaluated relative to each study's chow-fed control group. Note the varied diet compositions (in terms of %kcal, source of fat, liquid or chow source of carbohydrate), diet durations, age at start of diet, and strain of rat used, contributing to large heterogeneity of phenotypes within a diet category. Also note that certain features such as blood pressure and HDL cholesterol are rarely assessed in preclinical dietary studies of metabolic syndrome.

Publication	*Diet composition (%kcal)*	*Duration of diet (age at start of diet)*	*Rat strain (males)*	**Abdominal obesity**	**↑ Triglyceride**	**↑ Blood pressure**	**↑F fasted blood glucose**	**↓ HDL cholesterol**
High-fat diet								
(Sweazea *et al.*, 2010)	60% (54% lard, 5.5% soybean)	6 wks (~6wks old)	Sprague Dawley	+	-	n/a	+	n/a
(Chen *et al.*, 2011)	49% (47.5% butter, 1.5% soybean oil)	20 wks (8wks old)	Wistar	+	-	-	-	n/a
(Buettner *et al.*, 2006)	42% (lard)	12 wks (6wks old)	Wistar	+	-	n/a	-	n/a
	42% (olive oil)			+	-	n/a	+	n/a
	42% (coconut oil)			+	+	n/a	-	n/a
	42% (fish oil)			-	-	n/a	-	n/a
(Northcott *et al.*, 2012)	36% fat (15.2% saturated, 20.8% unsaturated)	17 wks (~3wks old)	Sprague Dawley	+	n/a	+	+	n/a
(Carroll *et al.*, 2006)	32% (fat type not reported)	12 wks (~14wks old)	Sprague Dawley	+	-	-	-	-
High-fructose diet								
(Dai & McNeill, 1995)	5-20% (drinking solution)	12 wks (~6wks old)	Wistar	-	+	+	+	n/a
(Mahmoud & Elshazly, 2014)	10% (drinking solution)	12 wks (~7wks old)	Wistar	+	+	+	+	n/a
(Sanchez-Lozada *et al.*, 2007)	10% (drinking solution)	8 wks (~10wks old)	Sprague Dawley	-	-	+	-	n/a
	60% (chow)			-	-	+	-	n/a
(Katakam *et al.*, 1998)	66% (chow)	4 wks (6-10 wks old)	Sprague Dawley	-	n/a	+	-	n/a
High-sucrose diet								
(Vasanji *et al.*, 2006)	32% (drinking solution)	10 wks (5wks old)	Sprague Dawley	+	+	n/a	+	n/a
(Chen *et al.*, 2011)	30% (drinking solution)	20 wks (8wks old)	Wistar	+	+	-	+	n/a
(Sweazea *et al.*, 2010)	70% (chow)	6 wks (~6wks old)	Sprague Dawley	+	+	n/a	-	n/a

High-energy diet (combination high-fat/high-sugar)								
(Sinitskaya *et al.*, 2007)	fat: ~72% (63% lard, 8% corn oil); carbohydrate: ~18%	10 wks (~7wks old)	Sprague Dawley	+	+	n/a	-	n/a
(Chen *et al.*, 2011)	fat: 49% (47.5% butter, 1.5% soybean oil); sucrose: 30% (drinking solution)	20 wks (8wks old)	Wistar	+	+	+	+	n/a
(Fu *et al.*, 2010)	fat: ~34%; sucrose: ~14%	12 wks (9wks old)	Wistar	+	-	n/a	n/a	+
(Lozano *et al.*, 2016)	fat: 21.4%; fructose: 25% (drinking solution)	8 wks (10wks old)	Wistar	+	n/a	n/a	+	n/a
Cafeteria diet								
(Sampey *et al.*, 2011)	18 processed foods+standard chow; fat: 45-53%, carbohydrate: ~35%	10 wks (9-10wks old)	Wistar	+	n/a	n/a	-	n/a
(Beilharz *et al.*, 2014)	lard and selection of biscuits and cakes; fat: ~45%, carbohydrate: ~50%; 10% sucrose solution	3 wks (~12wks old)	Sprague Dawley	+	+	n/a	n/a	n/a
(Kaakoush *et al.*, 2016)	standard chow+lard+processed foods; fat: ~30%, carbohydrate: ~58%	16 wks (6-8wks old)	Sprague Dawley	+	n/a	n/a	-	n/a
(Gomez-Smith *et al.*, 2016)	standard chow+16 processed foods+12% sucrose solution; fat: 40%, carbohydrate: ~49%	16 wks (4wks old)	Sprague Dawley	+	+	n/a	-	+

such, the main hypothesis of my dissertation was the following: *The Cafeteria diet is an effective dietary rat model of human metabolic syndrome and its comorbidities, in particular concerning cognitive impairments, neuroinflammation and cerebrovascular dysfunction.*

To test this hypothesis, my research had three main objectives: 1) to demonstrate that the Cafeteria diet is a translationally relevant model of metabolic syndrome; 2) to investigate the effects of chronic Cafeteria diet consumption on neuroinflammation, cerebrovascular structure and function as well as on cognitive performance; 3) to query the reversibility, and therefore the severity, of these potentially negative effects by switching Cafeteria diet-fed rats to a regular chow diet.

Findings related to these three objectives are included in two manuscripts which comprise the two following chapters of my thesis. The first, titled 'A Physiological Characterization of the Cafeteria Diet Model of Metabolic Syndrome in the Rat', was published in the journal Physiology and Behavior in December 2016. The second, 'Reduced Cerebrovascular Reactivity and Increased Resting Cerebral Perfusion in Rats Exposed to a Cafeteria Diet', has been submitted to the journal *Neuroscience*.

Chapter 2 - A Physiological Characterization of the Cafeteria Diet Model of Metabolic Syndrome in the Rat

Mariana Gomez-Smith[1,6], Sudhir Karthikeyan[1,6], Matthew S. Jeffers[1,6], Rafal Janik[2,3], Lynsie A. Thomason[2], Bojana Stefanovic[2,3,6], Dale Corbett[1,4,5,6]

Physiology & Behavior, 2016 December 1; 167: 382–391.

1: Cellular and Molecular Medicine, University of Ottawa, Ottawa, ON, Canada

2: Sunnybrook Research Institute, Toronto, ON, Canada

3: Medical Biophysics, University of Toronto, Toronto, ON, Canada

4: Faculty of Medicine, Memorial University, St. John's, NL, Canada

5: Faculty of Medicine, University of Toronto, Toronto, ON, Canada

6: Canadian Partnership for Stroke Recovery, Ottawa, ON, Canada

Statement of Author Contributions

M.G.S., D.C. and M.S.J. conceived and designed the experiments. M.G.S., S.K., R.J., and L.A.T. performed the experiments. M.G.S. and M.S.J. analyzed the data. M.G.S. wrote the paper and D.C., M.S.J., and B.S. edited the paper.

Abstract

Many promising findings from pre-clinical research have failed to translate to the clinic due to their inability to incorporate human disease co-morbidity. A variety of rodent diets and feeding durations are currently used in models of human metabolic syndrome, obesity, and diabetes. One model, the Cafeteria diet, makes use of grocery store-purchased food items that more closely approximate the human ultra-processed diet than commercial high-fat or high-carbohydrate rodent diets. The present study describes the development of metabolic syndrome in rats fed a Cafeteria diet (CAF) as well as the recovery of metabolic syndrome following a healthy "lifestyle" change. In addition, we explored the effects of the Cafeteria diet on spatial learning and memory and on neuroinflammation. Three-week old male Sprague Dawley rats were fed a Cafeteria diet for three months that consisted of 16 highly palatable human food items along with standard chow and a 12% sucrose solution to mimic soda consumption. Thereafter, a sub-group of CAF rats was switched to a chow diet (SWT) for one month. Both CAF and SWT groups were compared to control rats maintained on a standard chow diet (SD). Prior to the diet switch, CAF and SWT animals developed features akin to metabolic syndrome. Both groups of rats displayed significant abdominal obesity with increased visceral adiposity, hyperinsulinemia, glucose intolerance, and dyslipidemia with elevated serum triglyceride levels and reduced HDL cholesterol. Switching to a chow diet for one month completely reversed these features in SWT animals. Although acquisition of the Barnes maze was not affected by the Cafeteria diet, these animals exhibited greater hippocampal neuroinflammation compared to both SD and SWT rats as assessed by ionized calcium-binding adapter molecule 1 (Iba1) staining. These results demonstrate

that the Cafeteria diet is very effective in creating metabolic syndrome with hippocampal inflammation in rats over a relatively short time span. This model may be of great heuristic importance in determining potential reversibility of metabolic and cerebrovascular pathologies across the lifespan and as a co-morbid factor in other disease models such as stroke.

Introduction

Cerebrovascular disease (CVD) is a significant risk factor for cognitive impairment which includes vascular dementia (Gorelick *et al.*, 2011). A constellation of metabolic abnormalities, collectively known as metabolic syndrome, has been estimated to increase the risk for CVD by 50% (Boden-Albala *et al.*, 2008). A consensus agreement by the International Diabetes Federation and the American Heart Association/National Heart, Lung and Blood Institute identifies the criteria of metabolic syndrome as: abdominal obesity, reduced HDL cholesterol, elevated triglyceride, glucose intolerance, and hypertension (Alberti *et al.*, 2009*a*). Diagnosis requires that any three out of these five criteria be present. Epidemiologically, the primary cause of metabolic syndrome is an unhealthy lifestyle, in particular a highly processed diet rich in fat, sugar, and sodium combined with physical inactivity (Park *et al.*, 2003). Many animal studies have attempted to model metabolic syndrome using high-caloric diets, though most isolate a single nutritional component (e.g. fat from lard, fructose, etc.) to study its effects. In doing so, these regimens do not fully recapitulate metabolic syndrome due to the loss of the large nutritional and sensorial diversity typical of human diets (Lai *et al.*, 2014). Moreover, despite the role of high sodium in increasing CVD risk, it is rarely included in

animal dietary models (He *et al.*, 1999). This reductionist approach in modeling human diet has hindered the translation of preclinical research to the clinic.

The role of nutritional variability on food palatability is well understood by the food industry. Complex food combinations have been extensively explored by food chemists in the development of "ultra-processed" foods and beverages, demonstrated to be at the core of the current global obesity epidemic (Pereira *et al.*, 2005). Combining high levels of fat with sugar results in greater food, and therefore caloric intake as sweet flavors render energy dense foods more palatable by masking their high fat content (Drewnowski *et al.*, 2012). Given that ultra-processed foods provide close to 60% of the caloric intake of Americans and contribute 90% of energy from added sugars (Steele *et al.*, 2016), understanding the role of this complex diet on CVD risk factors is of great importance. The closest equivalent to the human ultra-processed food diet is the Cafeteria diet which provides animals with nutritionally varied, energy dense, and highly palatable grocery store-purchased food, thereby mirroring the key obesogenic features of the human diet (Raynor & Epstein, 2001; Sørensen *et al.*, 2003).

Clinical management of metabolic syndrome recommends the adoption of a healthy lifestyle (Grundy *et al.*, 2004) which greatly reduces its peripheral features (Sleiman *et al.*, 2015). Nonetheless, it is still unclear whether CVD risk, particularly stroke incidence and mortality, can be reduced after long-term metabolic dysregulation. Clinical lifestyle modification recommendations are based on the results of retrospective or case control studies that compare healthy individuals with metabolic syndrome patients (Stamler *et al.*, 1999). A large prospective study examining the effects of adopting a healthy diet paired with moderate exercise in overweight patients with type 2 diabetes mellitus, the Look AHEAD study, failed to demonstrate reduced CVD risk after nearly ten years of

adherence to the healthy lifestyle (The Look AHEAD Research Group, 2013). Use of appropriate animal models could be extremely useful in addressing the reversibility of CVD risk following treatment of metabolic syndrome and thereby facilitate the development of new clinical interventions.

In addition to increasing CVD risk, metabolic syndrome is also a prominent risk factor for "covert" ischemic insults and dementia affecting a range of cognitive domains including memory, language, visuospatial ability, and executive function (Bokura *et al.*, 2008; Black, 2011). Cognitive impairments have been studied in rats fed standard high-fat and -carbohydrate diets using a wide variety of behavioural paradigms including, but not limited to, the radial arm maze (Greenwood & Winocur, 1990), the Morris water maze (Molteni *et al.*, 2002; Jurdak *et al.*, 2008), and conditional discrimination learning tasks (Winocur & Greenwood, 1993). These commonly used cognitive tests rely heavily on stressful aversive stimuli (e.g. water maze) or food deprivation, which are problematic for dietary studies. Given the negative effects of stress on behavioural outcome measures (Homberg, 2013), cognitive tasks that minimize these confounding factors are preferred. For example, unlike the Morris water maze, the Barnes maze relies on mildly aversive noise and light stimuli to motivate animals and thus may be useful in assessing the effects of Cafeteria diet-feeding on spatial memory.

One mechanism by which metabolic syndrome and diet have been hypothesized to play a role in cognitive decline is through chronic low-grade inflammation (Yaffe *et al.*, 2004). Indeed, nutritional signals act to maintain energetic homeostasis through vagal and humoral systems that significantly overlap with immune pathways (Hotamisligil, 2006). These nutritional and immune signals circulate systemically, reaching the brain to modify hypothalamic-controlled feeding behaviour while simultaneously influencing learning

and memory function in the hippocampus through modulators of synaptic plasticity such as BDNF. Chronic exposure to conditions of excessive caloric intake results in abnormal feeding patterns, aberrant immune responses, and cognitive deficits (Gómez-Pinilla, 2008). Within the central nervous system, resident microglia are the primary cellular target of these inflammatory signals, responding to stress signals such as chronic energy imbalance by undergoing rapid expansion and activation (Miller & Spencer, 2014). Recently, Beilharz *et al.* (Beilharz *et al.*, 2014) demonstrated that a Cafeteria diet, when combined with a 10% sucrose solution, can very quickly upregulate mRNA expression of neuroinflammatory markers such as TNFα and IL1β in the hippocampus. It remains to be demonstrated whether the Cafeteria diet can also promote microglial cell population expansion.

In light of the need for better characterization of animal models to avoid clinical translation pitfalls and wasted research resources (O'Collins *et al.*, 2006; Perrin, 2014; Bernhardt *et al.*, 2016), the goal of our study was to assess the ability of the Cafeteria diet to produce metabolic syndrome in Sprague Dawley rats as well as the degree to which these features could be reversed through switching to a healthy diet. In addition, we examined the effects of the Cafeteria diet on hippocampal spatial learning and memory using the Barnes maze as well as on neuroinflammation by quantifying microglial cell density.

Material and Methods

Animals and diets

Experimental procedures followed the guidelines established by the Canadian Council on Animal Care and were approved by the Animal Care Committee of the University of Ottawa. A total of 55 male Sprague Dawley rats (Charles River Laboratories, Montreal, Canada) were used (*n*=18 standard diet, SD; *n*=18 Cafeteria diet, CAF; and *n*=19 switch diet, SWT). Three-week old animals were pair-housed and maintained on a 12h reverse light/dark cycle (8am off/8pm on). Following one week of habituation to the animal facility (with regular handling), rats were assigned to diet groups balanced by initial body weight. CAF rats were provided with *ad libitum* access to regular chow (Teklad Global 18% Protein Rodent Diet; Harlan, Madison, WI) and a daily selection of three grocery store-purchased items from a list of 16 (**Table 3**) adapted from Sampey *et al*. (Sampey *et al.*, 2011). Cafeteria food items alternated through a list of pre-established combinations to ensure diversity and variety of foods presented. In addition, CAF animals had access to one water bottle and one bottle containing a 12% w/v sucrose solution (MP Biomedicals, Solon, OH). The control SD diet consisted of regular chow and water. SWT animals were fed the Cafeteria diet for three months after which they were switched to the SD diet for one month. Both CAF and SD rats were maintained on their respective diets for the full duration (i.e. four months) of the experiment. Food from all three diet groups was weighed on a daily basis to calculate food intake. Nutritional composition of the three diets over the course of the experiment was calculated based on values provided by the

Table 3: Cafeteria diet and standard chow nutritional information provided by manufacturers.

Food item	Manufacturer	Kcal/g	Total fat %	Saturated fat %	Trans fat %	Carbohydrate %	Protein %	Sodium (mg/g)	Cholesterol (mg/g)
standard chow #2018	Harlan Teklad	3.10	6.20	0.90	0.00	44.20	18.60	2.00	0.00
Nesquik cereal	Nestle	4.14	5.17	0.69	0.00	82.76	3.45	5.86	0.00
Joe Louis	Vachon	4.44	20.37	13.46	0.38	64.81	1.85	4.44	0.19
Chocolate chip cookies	Loblaws	5.00	26.67	14.71	0.29	56.67	10.00	3.83	0.44
Reese's peanut butter cups	Hershey	5.13	30.77	10.87	0.22	58.97	7.69	2.56	0.12
Peanut butter M&M	Mars	5.25	27.50	17.50	0.25	60.00	10.00	1.88	0.13
Butter tarts	Farmer's Market	4.00	16.47	7.06	0.00	60.00	3.53	2.47	0.47
Cheetos cheese puffs	Frito-Lay	6.00	40.00	4.00	0.40	52.00	6.00	10.40	0.00
Doritos nacho cheese	Frito-Lay	5.20	26.00	4.00	0.00	64.00	6.00	7.20	0.00
Oreo's	Christie	5.00	20.83	6.52	0.00	70.83	4.17	3.33	0.00
Vanilla wafers	Voortman	4.67	20.00	5.00	0.00	66.67	3.33	0.83	0.00
Brownies	Two-Bite	3.57	14.09	5.26	0.00	51.79	3.57	3.39	0.54
Lays original chips	Frito-Lay	5.60	36.00	4.00	0.00	54.00	6.00	4.40	0.00
Pre-cooked bacon	Maple Leaf	5.60	48.00	11.11	0.00	4.00	32.00	24.00	0.83
Blue Ribbon bologna	Schneider's	4.29	35.71	8.04	0.00	3.57	28.57	24.29	0.63
All beef hot dogs	Schneider's	2.89	23.68	9.46	0.81	7.89	10.53	9.47	0.54
Cracker Barrel cheddar cheese	Kraft	4.00	33.33	22.50	1.00	3.33	23.33	6.67	1.00

product manufacturers. One subset of 37 animals was used for metabolic syndrome profiling and Barnes maze testing while a second group of 18 animals was used for visceral and subcutaneous fat analysis using MRI.

Blood sampling and metabolic syndrome profiling

Metabolic syndrome profiling was repeated in a subset of 37 animals (n=12 SD, n=12 CAF, n=13 SWT) at two time points: immediately before switching SWT rats from the Cafeteria diet to the SD diet (three months of feeding) and again one month later (four months of feeding). Following an overnight (~16 hours) fast, blood glucose was measured using a human Contour glucometer (Bayer HealthCare LLC, Mishawaka, IN) and whole blood collected into uncoated microvettes (Sarstedt AG&Co., Numbrecht, Germany) via saphenous vein blood sampling for serum insulin, triglyceride, and cholesterol analysis. After a two-day recovery period, rats were again fasted overnight and a glucose tolerance test (GTT) was performed the next morning. Following a second two-day recovery period, rats were fasted for 6 hours in the morning prior to insulin tolerance testing (ITT). All whole blood samples were clotted for one hour, centrifuged (10min, 2000g), and serum stored at -80°C until analysis. Insulin was assessed using a rat insulin ELISA kit (Crystal Chem, Downers Grove, IL) while triglyceride and cholesterol levels were measured using colorimetric kits (Triglyceride: Cayman Chemicals, Ann Arbor, MI; Cholesterol: BioAssay Systems, Hayward, CA). For GTT testing, all animals received an injection of D-glucose *i.p.* (2g/kg, 0.25g/ml; Sigma-Aldrich, Saint-Louis, MO). Blood glucose levels were measured at 0, 15, 30, 60, and 120 minutes using a glucometer. ITT testing involved an *i.p.* injection of human recombinant insulin (0.75IU insulin/kg; Sigma-Aldrich, Saint-Louis, MO) followed by blood glucose measurements at

0, 15, 30, 60, and 120 minutes. At the experimental endpoint, abdominal circumference at point of greatest girth and body length were measured while gonadal white adipose tissue (gWAT) was dissected and weighed. BMI was calculated using the formula: weight (kg)/body length $(m)^2$.

MRI evaluation of visceral and subcutaneous fat

Repeat measurements (three and four months on the diet) of subcutaneous (SAT) and visceral (VAT) adipose tissue volumes were performed on a separate subset of 18 animals (*n*=6 SD, *n*=6 CAF, *n*=6 SWT) using a 7T BioSpec system (Bruker, Ettlingen, Germany). Rats were maintained under propofol anesthesia (45 mg/kg/hr, 10 mg/ml; PharmaScience, Montreal, Canada) following induction with 5% isoflurane. Rats received an *i.m.* injection of glycopyrrolate (0.2 mg/ml, 0.1 mg/kg; Omega, Montreal, Canada) and were reversibly intubated. A single *i.v.* injection of atracurium (10mg/ml, 1mg/kg; Sandoz, Boucherville, Canada) was given immediately prior to commencing the imaging session to reduce motion. 15 axial image slices of the abdominal region (slice gap 1mm) were acquired using the rostral extent of the kidney as a visual landmark. A T1W-RARE pulse sequence was used with a resolution of $0.4x0.4mm^2$ in plane with 2mm slice thickness and a field of view of $10x10\ cm^2$, with TR/TE of 900ms/9ms. This sequence was adapted from that of Müller *et al.* to obtain similar contrast at 7T (Müller *et al.*, 2013). A birdcage body coil was used for signal excitation. By oversampling and resampling a subset of the data (three rats, one from each diet group), it was determined that quantification of one out of every three of the 15 image slices conferred sufficient precision to accurately estimate fat volumes. Five slices from each animal were manually segmented and fat volume in cm^3 was calculated using MNI-Display software (Montreal

Neurological Institute, Montreal, Canada). Guided by threshold values, adipose tissue located within the abdominal wall was labeled as VAT and adipose tissue outside as SAT.

Barnes maze

After metabolic testing at the four-month time point, rats were trained and tested on the Barnes maze. Training occurred over the course of one day and consisted of four successive two-minute trials during which animals were taught to locate a goal box positioned below a single escape hole. At the beginning of each trial, rats were placed under a bucket located at the center of the maze. Trials began when the bucket was raised and aversive light and sound stimuli were turned on. If the animal did not locate the escape hole within the two minutes allotted, they were guided to the hole by the experimenter. All animals were able to locate the escape hole by the end of the training day. Testing began the day after training and took place over six consecutive days with two, three-minute trials per day (20 minute inter-trial interval). Three distal cues affixed to the walls of the test room allowed rats to spatially navigate the Barnes maze platform and locate the escape hole with the escape box present. Animals were randomly assigned to three distinct escape hole locations that remained unchanged throughout testing. Each testing trial proceeded in the same fashion as the training trials. Total errors, re-entry errors to previously visited holes, reference memory errors (number of incorrect holes visited), deviation (distance from escape hole on first approach), omissions (number of times escape hole avoided) and search strategy were scored manually while latency to escape, distance travelled and average velocity were measured using Ethovision tracking software (Noldus, Leesburg, VA). Rats were recorded as performing random, serial or

spatial strategies based on specific criteria adapted from O'Leary and Brown (O'Leary & Brown, 2012). A spatial strategy was used when rats went straight to the escape hole visiting only holes within ±2 of the escape box. A strategy was serial when rats visited any number of sequential holes without crossing the center of the platform. If the rat crossed the center of the platform at least once it was deemed to be a random search strategy. Experimenters performing Barnes maze testing were blind to the experimental groups.

Iba1 immunohistochemistry

Following the final session of Barnes maze testing, animals were sacrificed and hippocampal tissue from a sub-set of animals (*n*=6 SD, *n*=6 CAF, *n*=6 SWT) examined for Iba1 (Ionized calcium-Binding Adapter molecule 1) cell density. Rats were deeply anesthetized by *i.p.* administration of Euthanyl (149.5 mg/kg; Bimeda-MTC Health Inc., Cambridge, Canada) and intracardially perfused with heparinized saline followed by 4% paraformaldehyde (PFA) in phosphate-buffered saline. Brains were removed and post-fixed overnight in 4% PFA, then transferred to a 20% w/v sucrose solution in 0.1M phosphate buffer until brains sunk. Tissue throughout the dorsal hippocampus was subsequently cryosectioned and 20µm-thick serial sections were slide mounted at 200µm intervals. Following a citric acid epitope retrieval step (2.88 g/L citric acid, pH=6.0; Sigma-Aldrich, Saint-Louis, MO), tissue was incubated with anti-Iba1 primary antibody (1:1000; Wako Pure Chemical Industries, Ltd., Richmond, VA) overnight at 4°C. Sections were then incubated with a biotinylated donkey anti-rabbit antibody (1:500; Jackson ImmunoResearch Laboratories Inc., West Grove, PA, USA) for one hour at room temperature. To reveal Iba1 labeling, sections were treated with avidin-biotin peroxidase

complex (VECTASTAIN Elite; Vector Laboratories, Burlingame, CA) followed by 3,3-diaminobenzidine HRP substrate (ImmPACT DAB; Vector Laboratories, Burlingame, CA) according to manufacturer recommendations. After dehydrating and coverslipping slides, digital images of hippocampal and hypothalamic structures were acquired at 20X magnification (Aperio CS2 slide scanner; Leica Biosystems, Nussloch, Germany). Using the stereological Optical Fractionator Probe (StereoInvestigator V10.0; MicroBrightField Bioscience, Williston, VT) using parameters adapted from Marshall *et al.* (Marshall *et al.*, 2013), Iba1 cell density was independently evaluated in CA1, DG (dentate gyrus) and arcuate nucleus. A counting frame of 50 µm x 50 µm was used in all three regions. In the CA1, a sampling grid of 200 µm x 200 µm was used while in the DG and the arcuate nucleus, a sampling grid of 150 µm x 150 µm was used. Iba1 cell density was quantified in 10 hippocampal and five hypothalamic sections per animal.

Statistics

Statistics were performed using Prism software (V6, GraphPad, La Jolla, CA). Data are expressed as mean ± standard error of the mean (SEM). All analyses, except for re-entry errors, omissions and search strategy in the Barnes maze, used one- or two-way ANOVA followed by Tukey's multiple comparisons post-hoc test to determine group differences. Re-entry errors and omissions data were not normally distributed as shown by visual examination of Q-Q plots at each time point and a statistically significant result following the Shapiro Wilk test of normality. Related-samples non-parametric analysis followed by a Friedman step-wise comparison was therefore performed. Group differences in search strategy were analyzed at each individual time point using the Pearson Chi-Square test. Differences were considered significant when $p<0.05$.

Results

Greater caloric density of the Cafeteria diet due to increased energy intake from fat and carbohydrate from the 12% sucrose solution

Food intake was recorded daily throughout the experiment and data was averaged to represent monthly values. Using the manufacturers' nutritional information (**Table 3**), a detailed evaluation of feeding behavior and diet composition was performed. During the first three months of the experiment, prior to the diet switch, food intake (by weight) was not significantly different between diet groups (**Figure 4A**). Despite not observing greater food intake in rats fed the Cafeteria diet, total energy intake was increased by ~25% in comparison to SD diet-fed rats during the first two months of the diet (**Figure 4B**; CAF and SWT vs. SD $p<0.0001$), indicative of the significantly greater caloric density of the grocery store-purchased human food items. Following the diet switch at three months, food intake in SWT rats dropped by ~20% compared to pre-switch food intake and was significantly less than that of CAF and SD animals at the four month time point (**Figure 4A**; SD vs. SWT $p<0.001$, CAF vs. SWT $p<0.05$). Consequently, energy intake from food in the SWT group dropped significantly by ~33% relative to CAF animals (**Figure 4B**; $p<0.0001$) and by ~21% relative to SD animals (**Figure 4B**; $p<0.01$). Not typically reported in studies using obesogenic diets, sodium intake was increased two-fold in the CAF and SWT diet rats relative to the SD diet animals during the first three months (**Figure 4C**; CAF and SWT vs. SD $p<0.001$ at both time points). The Cafeteria diet was energetically enriched in fat, which represented ~40% of kcal consumed (**Figure 4D**). Saturated fat, in particular, represented ~13% of total caloric

Figure 4: Cafeteria diet feeding leads to greater energy intake, primarily from fat and sucrose in drinking water.

(Following page) (A) Daily average food intake of chow and Cafeteria diet food items (in grams) of SD, CAF, and SWT rats throughout the four month duration of the experiment. (B) Daily average energy intake, in kcal. (C) Daily average sodium intake, in mg. Monthly nutritional caloric breakdown of the (D) CAF, (E) SWT, and (F) SD diets. Letters indicate a significant difference following pair-wise comparisons ($p < 0.05$; b: SD vs. SWT, c: CAF vs. SWT). n = 18 SD, n = 18 CAF, n = 19 SWT. Values are mean ± SEM.

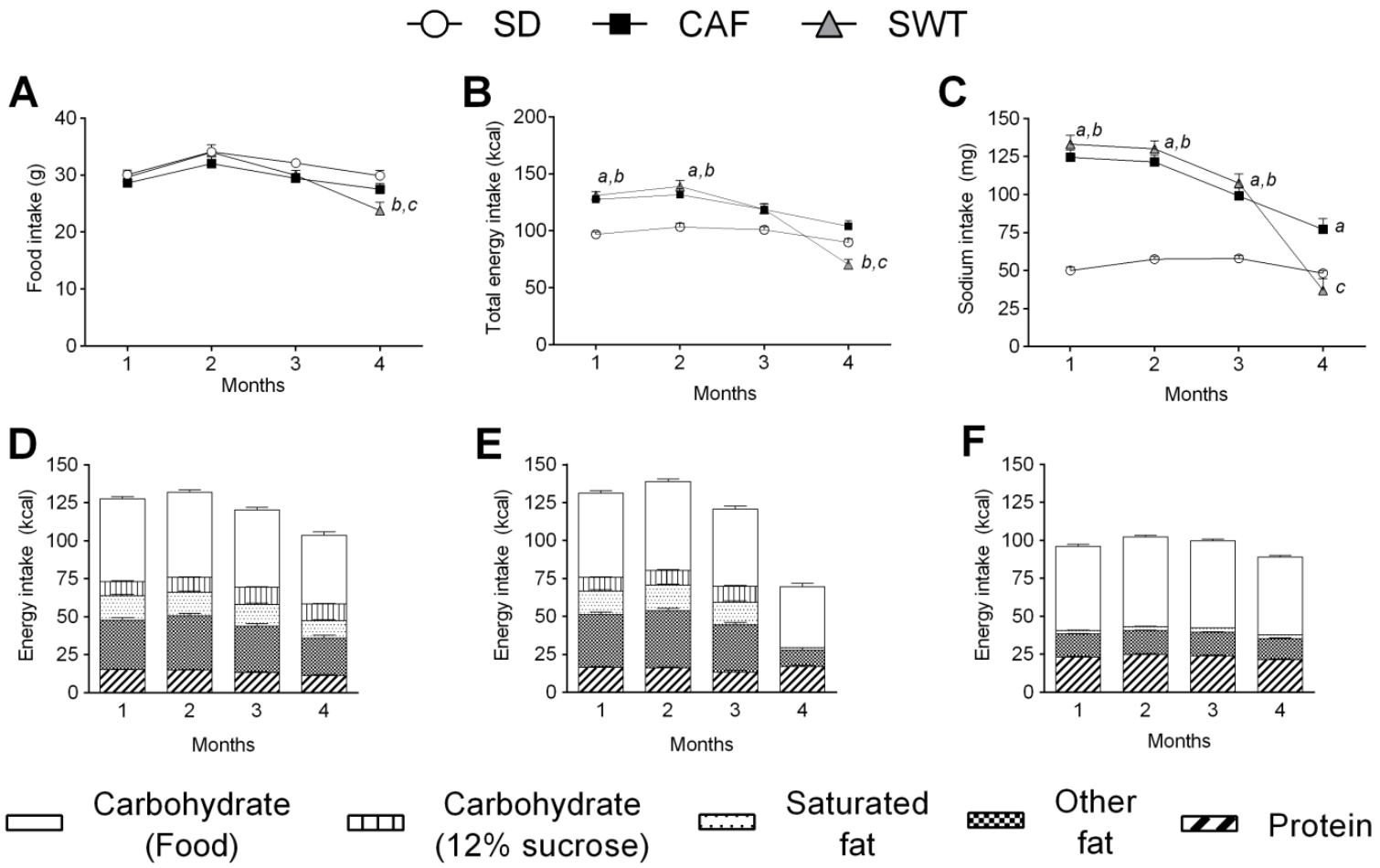
SD
CAF
SWT
A
Food intake (g)
Months
b,c
B
Total energy intake (kcal)
a,b
a,b
b,c
C
Sodium intake (mg)
a,b
a,b
a,b
a
c
D
Energy intake (kcal)
E
F
Carbohydrate (Food)
Carbohydrate (12% sucrose)
Saturated fat
Other fat
Protein

intake of CAF rats, with ~42% of kcal from food and the remainder (~7%) from the sucrose solution (**Figure 4D**). Protein contributed ~11% of the energy consumed by CAF rats. These values were the same in SWT rats (**Figure 4E**) in the three months preceding the diet switch. As expected, during the month following the diet switch, the relative nutritional intake of SWT rats was identical to that of SD (**Figure 4F**). That is, the SD diet was comprised of 18% kcal from fat (2.6% from saturated fat), 57% from carbohydrate, and 24% from protein (**Figure 4F**). Compared to the SD diet, the Cafeteria diet was significantly elevated in fat ($p<0.0001$ at both time points). Moreover, CAF rats consumed more energy from carbohydrate ($p<0.0001$ at both time points) than SD rats, though this increase came exclusively from the 12% sucrose solution. Indeed, there were no statistically significant differences between SD and CAF rats in food carbohydrate intake throughout the duration of the experiment.

Increased visceral obesity caused by the Cafeteria diet with rapid body weight stabilization following diet switch

The increased caloric density of the Cafeteria diet led to significant weight gain in CAF and SWT animals compared to SD after 11 ($p<0.05$) and 10 ($p<0.05$) weeks, respectively, on the diet. While CAF animals continued to gain weight compared to SD animals, the body weight of SWT rats plateaued immediately after the diet switch and was no longer different from that of SD animals by week 14, only two weeks after the switch (**Figure 5A**). Prior to the diet switch, structural MR imaging of the abdomen showed that, relative to SD animals, SAT (**Figure 5B**) volumes were significantly elevated in SWT ($p<0.05$) animals. Furthermore, VAT volumes (**Figure 5C**) were

Figure 5: CAF and SWT animals have greater central adiposity than SD chow-fed animals, which resolves with one month of SD feeding.

(Following page) (A) Body weight progression of SD, CAF, and SWT animals over four months. (B) Subcutaneous and (C) visceral adipose tissue volumes at three and four months on the diet. (D) Percent change in SAT and VAT volumes between the 3- and 4-month time point. (E) Representative T1W RARE axial slices of SD, CAF, and SWT animals after four months on the diet. Letters indicate a significant difference following pair-wise comparisons ($p < 0.05$; a: SD vs. CAF, b: SD vs. SWT, c: CAF vs. SWT). $n = 6$ SD, $n = 6$ CAF, $n = 6$ SWT. Values are mean ± SEM.

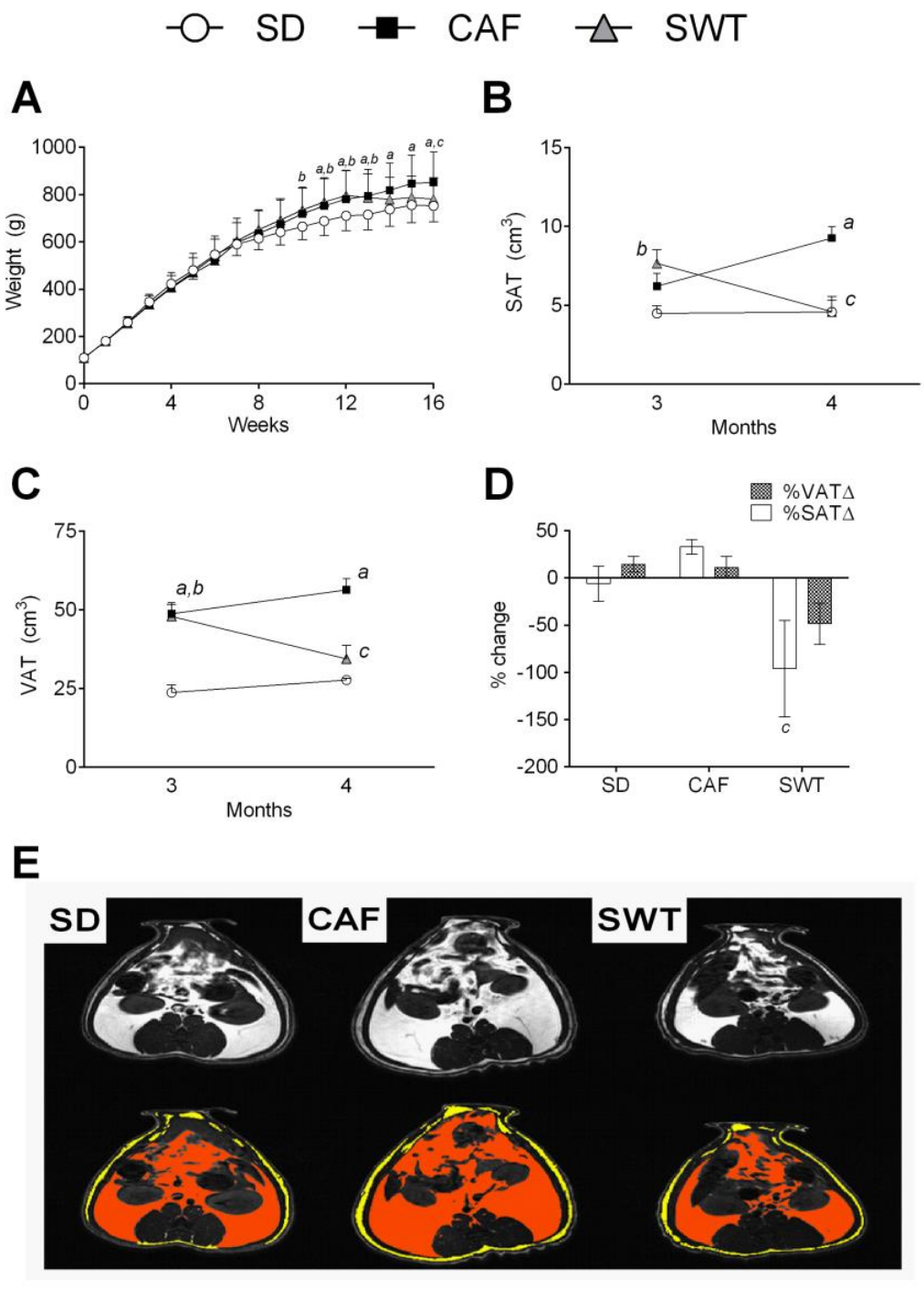
SD
CAF
SWT
A
Weight (g)
Weeks
B
SAT (cm3)
Months
C
VAT (cm3)
Months
D
%VATΔ
%SATΔ
% change
SD
CAF
SWT
E
SD
CAF
SWT

significantly elevated and nearly double that of SD animals in both CAF ($p<0.001$) and SWT ($p<0.001$) animals. One month after the diet switch, SAT volume in SWT rats decreased to levels of SD rats and was significantly lower than that of CAF rats ($p<0.001$), while the SAT volume of CAF rats continued to increase, exceeding the levels of SD rats ($p<0.0001$). After the diet switch, the VAT volume of SWT rats was significantly reduced compared to CAF rats ($p<0.001$) and was indistinguishable from that of SD rats. The VAT of CAF rats, on the other hand, continued to increase and remained elevated compared to the VAT of the SD group ($p<0.0001$). Interestingly, examination of the %SAT and %VAT change between the two time points (**Figure 5D**) revealed that the SAT volume of SWT rats decreased twice as much as their VAT volume following the diet switch. This drop was significant ($p<0.01$) relative to the %SAT change of CAF animals between the 3 and 4-month time points. A representative image of the median slice of the abdominal cavities of SD, CAF, and SWT animals at the final time point is shown in **Figure 5E**. Data collected from animals at sacrifice, including measures of abdominal circumference (**Figure 6A**), BMI (**Figure 6B**) and gonadal white adipose tissue (gWAT, **Figure 6C**) paralleled the changes observed with the imaging data. The abdominal circumferences of CAF animals were significantly larger than those of SD animals ($p<0.05$) though not of SWT animals. As body length was identical in all three groups (SD: 29.6±0.3cm, CAF: 29.5±0.3cm, SWT: 29.6±0.3cm), increased BMI of CAF ($p<0.05$) and SWT ($p<0.01$) rats relative to that of SD rats reflected the increase in abdominal circumference. The gWAT depots of CAF animals were significantly larger than those of SD ($p<0.01$) but also of SWT ($p<0.05$) rats. In all three measures, SWT animals were not different from SD at the time of sacrifice.

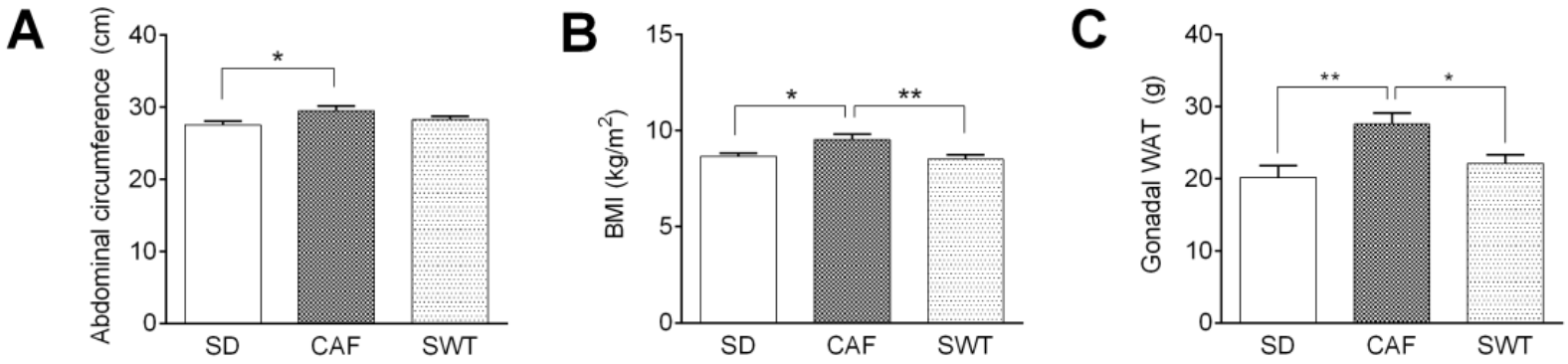

Figure 6: Abdominal circumference, BMI and gonadal white adipose tissue are all sensitive measures of increased central adiposity in CAF animals.

(A) Abdominal circumference, (B) BMI and (C) weight of gonadal fat pads of SD, CAF, and SWT animals at sacrifice. * and ** indicate significant differences following pairwise comparisons (*: $p<0.05$, **: $p<0.01$). n=12 SD, n=12 CAF, n=13 SWT. Values are mean ± SEM.

Cafeteria diet-induced hyperinsulinemia and glucose intolerance are both reversible

Blood was sampled after overnight fasting at three and four months on the diet. Glucose (**Figure 7A**) and insulin (**Figure 7B**) were measured at both time points. Despite no increase in fasted blood glucose in the CAF rats relative to that in SD animals, insulin serum levels were significantly elevated and more than doubled at both time points in CAF animals (3 months: $p<0.01$, 4 months: $p<0.001$). Serum insulin levels in SWT animals dropped to those of SD animals after the diet switch and were significantly lower than those of CAF rats ($p<0.01$). Prior to the diet switch, glucose tolerance testing showed impaired glucose tolerance in CAF rats (**Figure 7C**) as both CAF and SWT groups' glucose levels were significantly elevated above SD at the 60-minute ($p<0.01$) and 120-minute (SD vs. CAF: $p<0.001$, SD vs. SWT: $p<0.05$) time points. One month after the diet switch, glucose tolerance in CAF animals continued to worsen (**Figure 7D**), with significantly elevated glucose levels in CAF rats relative to those of SD rats as early as the 30-minute ($p<0.05$) time point. Intriguingly, glucose tolerance in SWT animals was indistinguishable from that of SD animals and significantly improved over CAF animals' glucose tolerance at the 30- ($p<0.001$), 60- ($p<0.01$), and 120- ($p<0.01$) minute time points (**Figure 7D**). However, insulin tolerance testing did not reveal any diet group differences in terms of the rats' response to a discrete insulin *i.p.* injection (**Figure 7E,F**), indicating that CAF animals maintained an intact compensatory adrenal and pituitary response to insulin (Pasquali *et al.*, 2006).

Cafeteria diet-induced dyslipidemia is also reversible

CAF rats were dyslipidemic after four months on the diet with a two-fold increase in serum triglyceride relative to that of SD (**Figure 8A**; $p<0.01$). Despite not being

Figure 7: Cafeteria diet-feeding causes hyperinsulinemia and impaired glucose tolerance but does not elevate fasted blood glucose.

(Following page) (A) Fasted blood glucose and (B) serum insulin concentrations in SD, CAF, and SWT animals at three and four months on the diet. GTT blood glucose levels at (C) three and (D) four months on the diet. ITT blood glucose levels at (E) three and (F) four months on the diet. Letters indicate a significant difference following pair-wise comparisons ($p < 0.05$; a: SD vs. CAF, b: SD vs. SWT, c: CAF vs. SWT). n = 12 SD, n = 12 CAF, n = 13 SWT. Values are mean ± SEM.

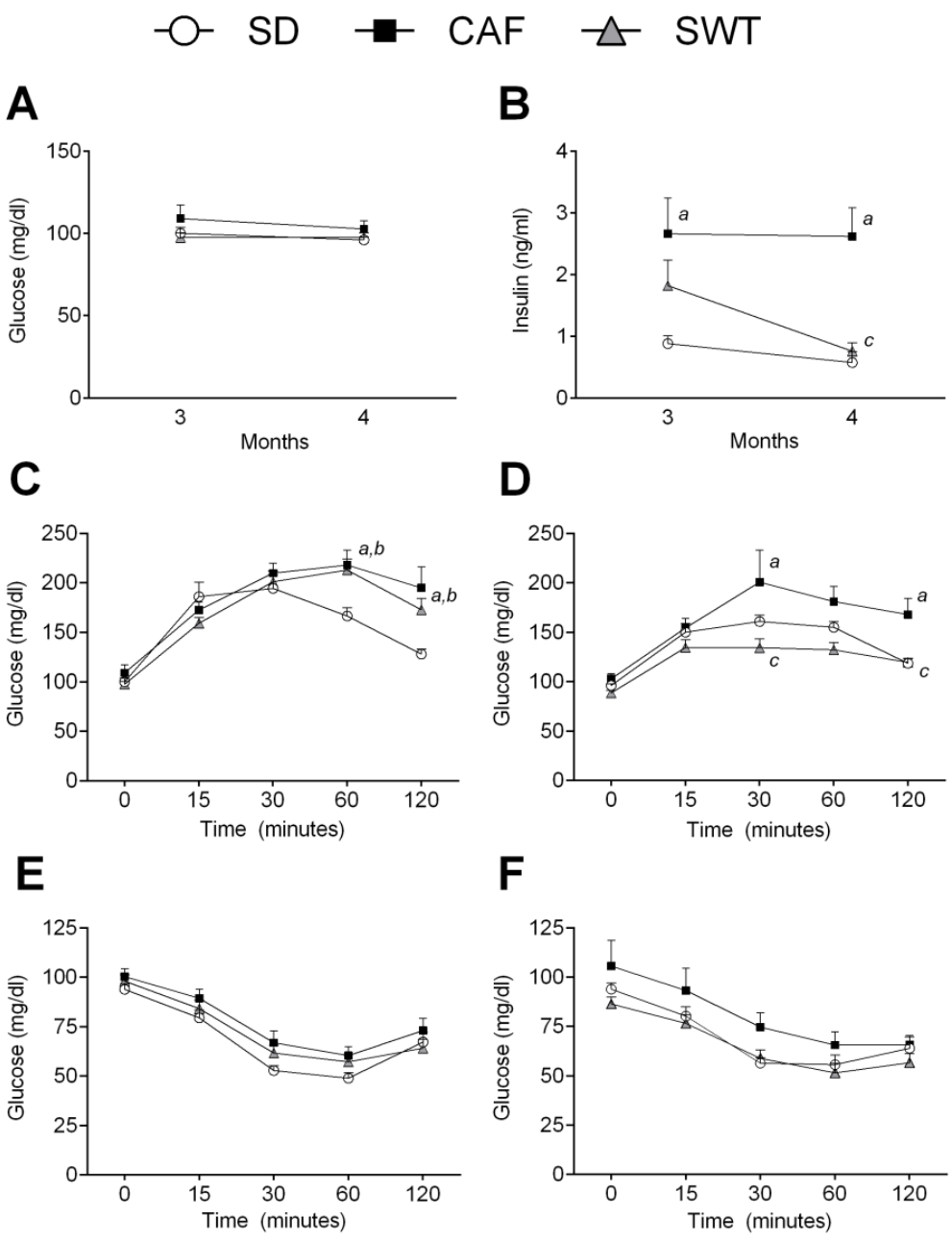
SD
CAF
SWT
A
Glucose (mg/dl)
150
100
50
0
3
4
Months
B
Insulin (ng/ml)
4
3
2
1
0
a
a
c
3
4
Months
C
Glucose (mg/dl)
250
200
150
100
50
0
a,b
a,b
0
15
30
60
120
Time (minutes)
D
Glucose (mg/dl)
250
200
150
100
50
0
a
a
c
c
0
15
30
60
120
Time (minutes)
E
Glucose (mg/dl)
125
100
75
50
25
0
0
15
30
60
120
Time (minutes)
F
Glucose (mg/dl)
125
100
75
50
25
0
0
15
30
60
120
Time (minutes)

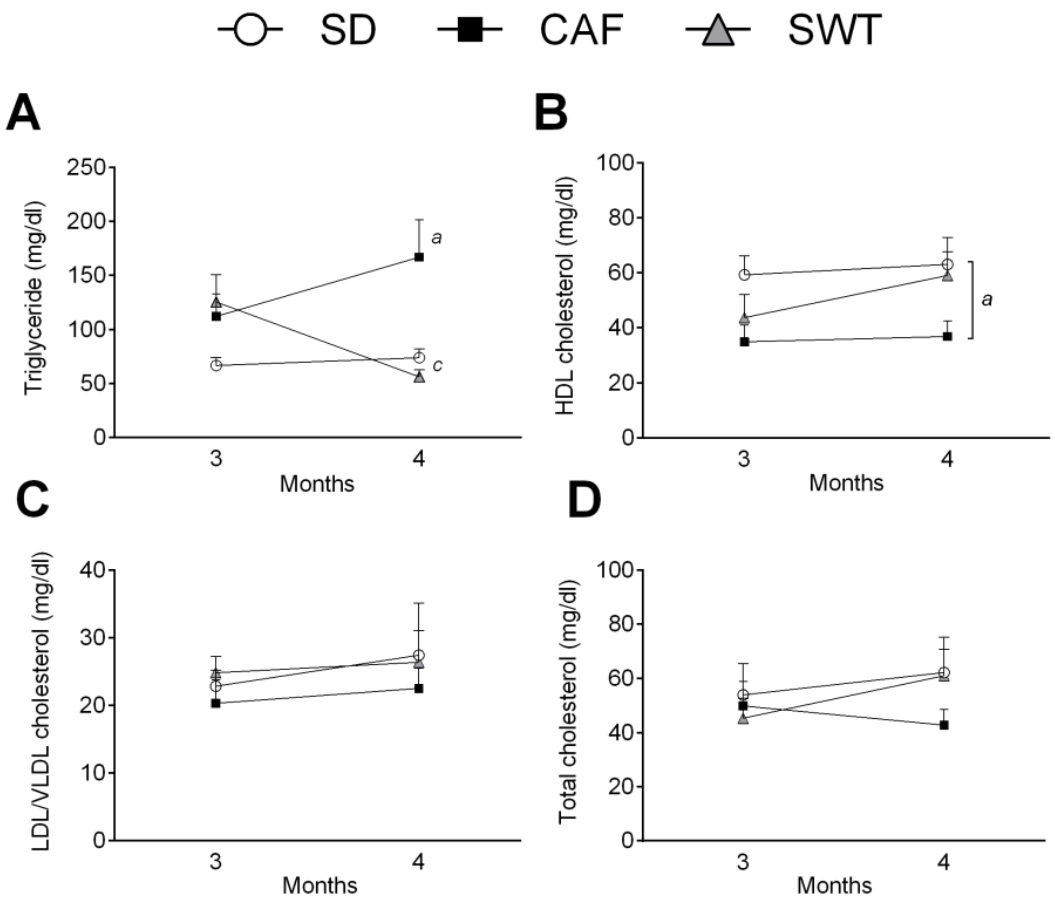

Figure 8: Cafeteria diet causes dyslipidemia.

(A) Serum triglyceride, (B) HDL cholesterol, (C) LDL/ VLDL cholesterol and (D) total cholesterol in SD, CAF, and SWT animals at three and four months on the diet. Letters indicate a significant main effect of diet (HDL cholesterol) or a significant difference following pair-wise comparisons ($p < 0.05$; a: SD vs. CAF, b: SD vs. SWT, c: CAF vs. SWT). n = 12 SD, n = 12 CAF, n = 13 SWT. Values are mean ± SEM.

significantly elevated at three months, serum triglyceride of SWT animals was indistinguishable from SD rats and significantly lower than the CAF group ($p<0.001$) at four months. A main effect of diet was detected between SD and CAF animals regarding HDL cholesterol, with CAF animals exhibiting significantly lower HDL levels than SD animals when data was collapsed across the two time points (**Figure 8B**; $p<0.05$). HDL cholesterol in SWT animals was not significantly different from either of the other two diet groups though there was a clear visible trend for recovery of HDL levels over time (**Figure 8B**). There was no significant effect of either time or diet on either LDL/VLDL cholesterol (**Figure 8C**) or total cholesterol (**Figure 8D**) levels.

Spatial learning and memory in the Barnes maze is not impaired by Cafeteria diet

After CAF rats had been on the diet for four months and SWT animals had been returned to SD chow for one month, spatial learning and memory were tested in the Barnes maze. Latency (**Figure 9A**), distance travelled (**Figure 9B**), and velocity (**Figure 9C**) were examined. No significant effects were detected for any of these outcome measures. The same was true of total errors, reference memory errors, deviation, re-entry errors, omissions (**Figure 10**), and search strategy (**Figure 11**).

Reversible elevated inflammatory response in the hippocampus of CAF rats

After four months on their respective diets, Iba1 cell density was significantly elevated in the CA1 hippocampal region of CAF rats compared to SD rats (**Figure 12A**, $p<0.05$). In SWT animals, Iba1 cell density in the CA1 was not different from that of the control SD group. A trend towards increased Iba1 cell density was also observed in CAF DG (**Figure 12B**), but was not statistically significant. In the arcuate nucleus of the

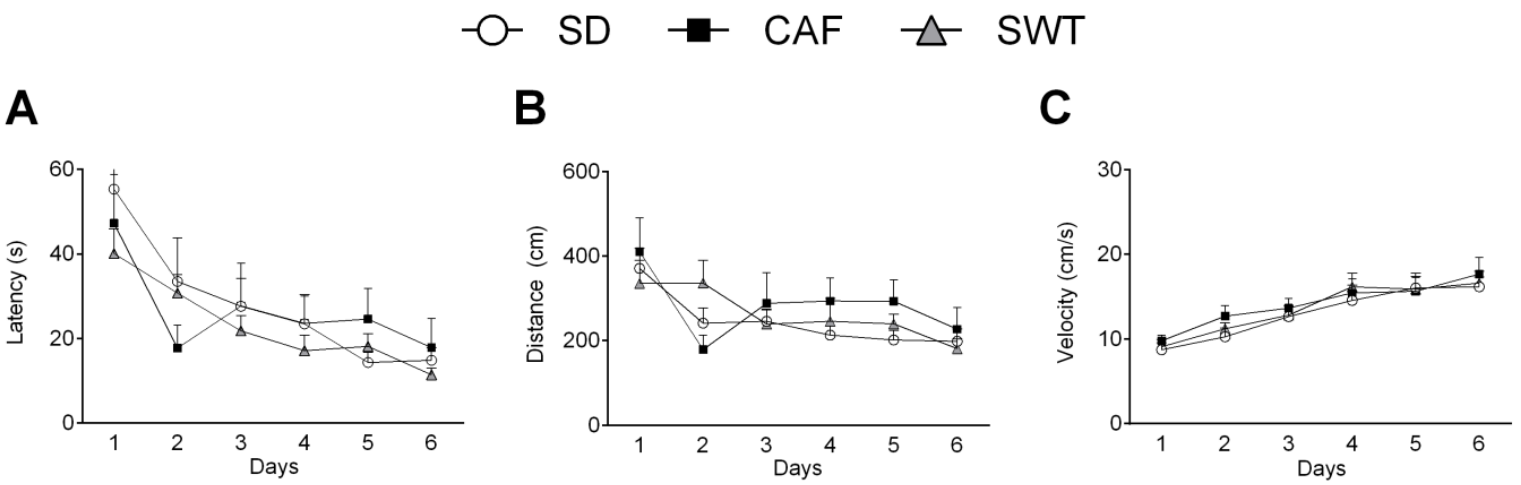

Figure 9: Cafeteria diet does not cause spatial learning and memory deficits as assessed using the Barnes maze.

(A) Latency to escape, (B) distance traveled and (C) velocity traveled by SD, CAF, and SWT rats in the Barnes maze after four months on the diet. n = 12 SD, n = 12 CAF, n = 13 SWT. Values are mean ± SEM.

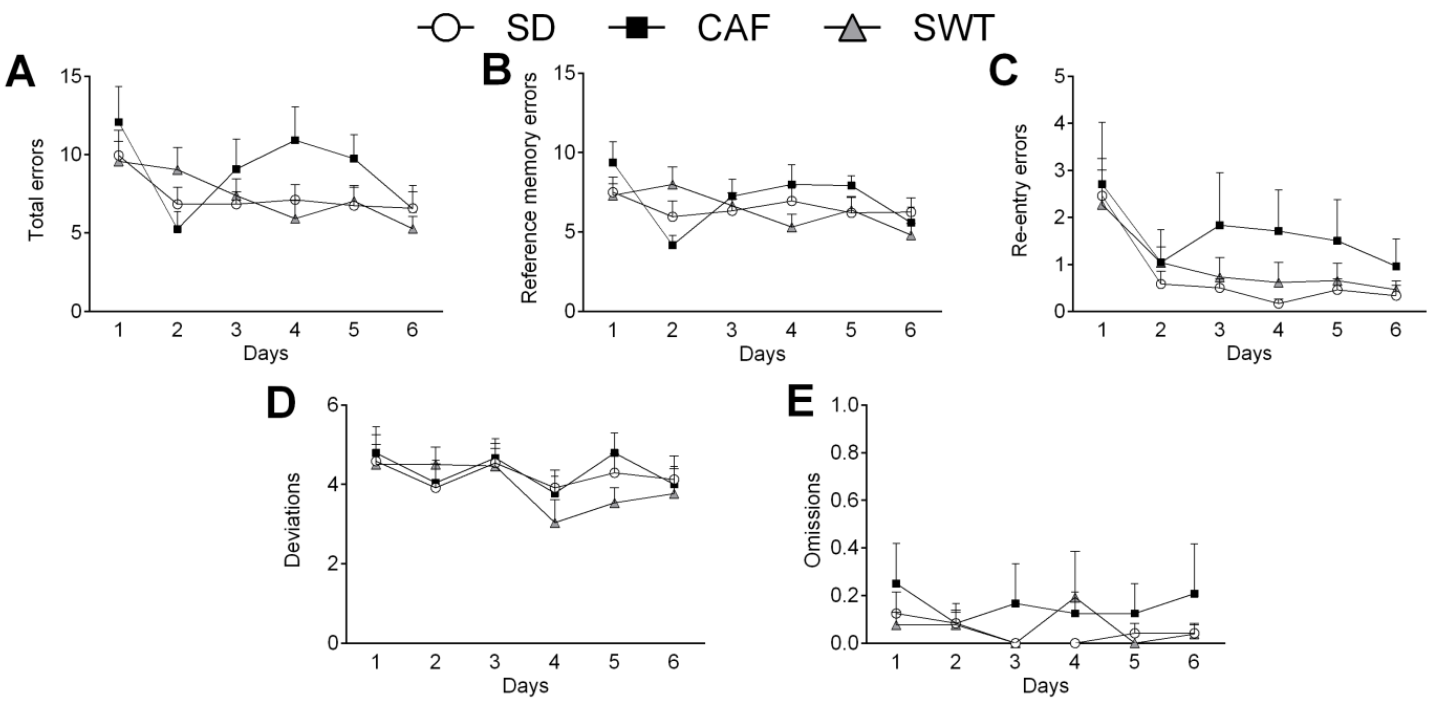

Figure 10: Errors, omissions and deviation in the Barnes maze task.

(A) Total errors, (B) re-entry errors, (C) reference memory errors, (D) deviation and (E) omissions of SD, CAF, and SWT rats over the six days of testing on the Barnes maze. There was no effect of diet on any of these measures. n=12 SD, n=12 CAF, n=13 SWT. Values are mean ± SEM.

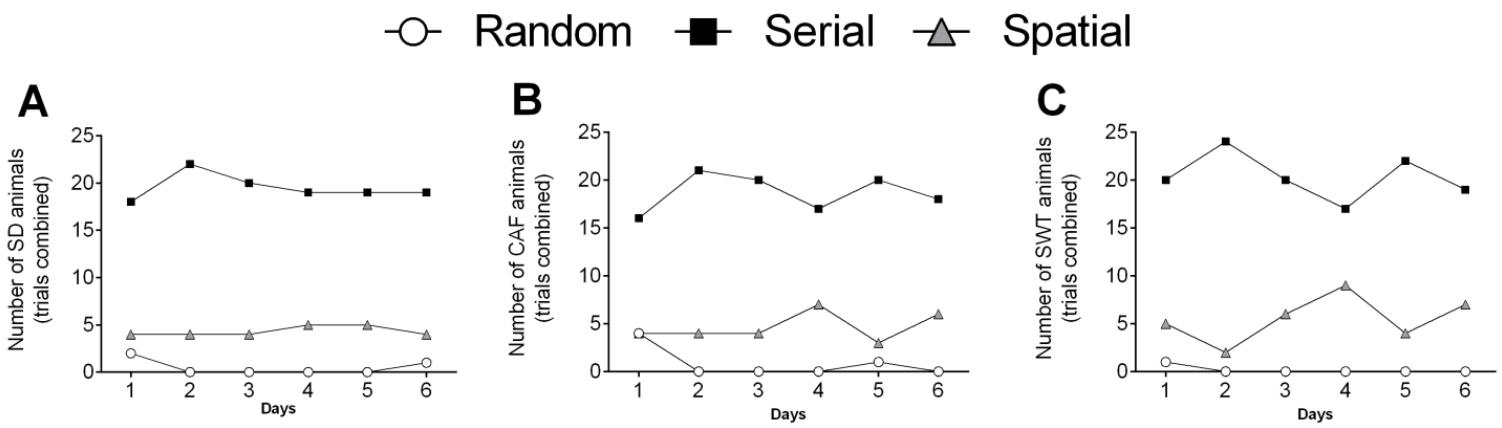

Figure 11: Search strategy in the Barnes maze.

Random, serial and spatial search strategy over the course of the six days of testing in (A) SD, (B) CAF and (C) SWT rats. Values represent total number of animals performing a particular strategy with data from the two daily trials combined. Pearson Chi-Square analysis revealed no effect of diet at any individual time point. n=12 SD, n=12 CAF, n=13 SWT.

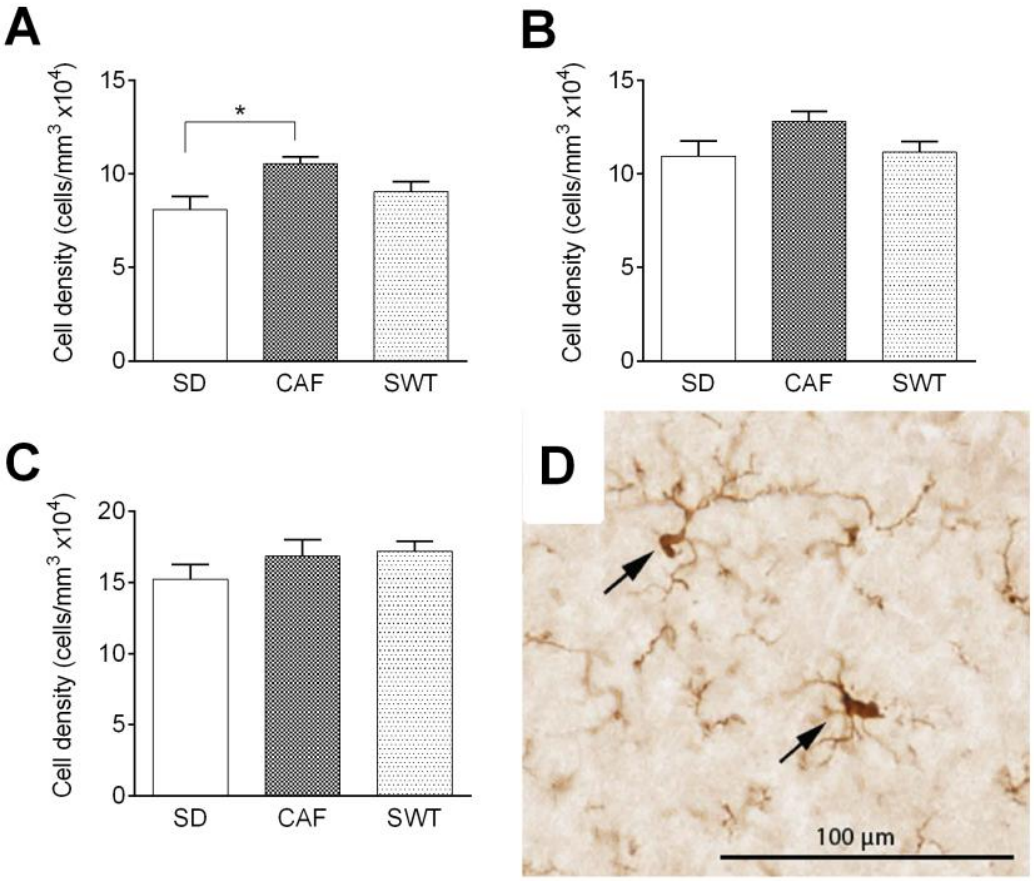

Figure 12: Cafeteria diet increases Iba1 cell density in the hippocampus which returns to control levels after one month of chow diet.

Iba1 cell density in the (A) CA1 and (B) DG regions of the hippocampus in SD, CAF, and SWT rats after four months on the diet. (C) Iba1 cell density in the arcuate nucleus of the hypothalamus. (D) Representative image of Iba1+ microglia cells (arrowheads) in the CA1. * indicates a significant difference following pairwise comparisons (*: $p < 0.05$). n = 12 SD, n = 12 CAF, n = 13 SWT. Values are mean ± SEM.

hypothalamus, there was no effect of diet on microglial cell density (**Figure 12C**). A representative image of hippocampal Iba1+ stained microglia is shown in **Figure 12D**.

Discussion

The high global incidence of CVD is a pressing problem within countries with aging populations (Roth et al., 2015). Metabolic syndrome contributes to CVD and represents a potentially important target for lowering CVD incidence. However, it is not known whether adopting a healthy lifestyle that effectively reduces metabolic syndrome features in humans translates to lower CVD risk over time (Dutton & Lewis, 2015). In this study, we investigated whether a diet more similar to the human ultra-processed diet than conventional rodent laboratory diets could recapitulate human metabolic syndrome in rats. Furthermore, we assessed the degree to which metabolic syndrome features could be reversed after transferring CAF rats to a healthy diet, in much the same way that adoption of a healthy lifestyle is recommended for clinical management of metabolic syndrome in patients. We show that three months of Cafeteria diet produced metabolic syndrome in rats by causing abdominal obesity, hyperinsulinemia, glucose intolerance, and dyslipidemia. Interestingly, a single month of switching CAF rats to a standard chow diet completely reversed the metabolic syndrome features.

By weighing food intake on a daily basis throughout the experiment, we were able to accurately describe the nutritional composition of the Cafeteria diet. Despite consuming 16 different grocery store-purchased human food items in addition to standard chow and drinking a 12% sucrose solution, relative intake of fat, carbohydrate, and protein was stable throughout the four months of Cafeteria diet-feeding. Sodium intake by CAF rats, on the other hand, appeared to decline somewhat during the third and fourth month.

While energy density of individual Cafeteria diet food items was similar, sodium content was quite heterogeneous (**Table 3**) resulting in greater difficulty to maintain constant levels of sodium in the Cafeteria diet. Conscientious use of the Cafeteria diet is a reliable method of generating human-like metabolic syndrome in rodents though attention must be payed to presenting equal proportions of macronutrients over time. Food intake prior to the diet switch was identical between the three diet groups. This supports previous results showing that rats prefer the more palatable Cafeteria diet to a traditional high-fat diet as rats fed the latter typically show a significant drop in food intake compared to control chow animals (Sampey *et al.*, 2011; Higa *et al.*, 2014). In addition, we observed a dramatic drop in food intake immediately following the diet switch, again confirming the results of others (Rogers, 1985; South *et al.*, 2014). Rogers (Rogers, 1985) postulated that this phenomenon is due to a negative contrast effect whereby animals receiving a highly palatable, and thus salient, food reward drop to below control levels of food intake when the quality of the food reward decreases.

The Cafeteria diet caused rats to become hyperinsulinemic with reduced insulin sensitivity as rats remained hyperglycemic two hours following a glucose challenge. Despite this, CAF rats were normoglycemic in the fasting state and did not exhibit impairments with the insulin tolerance test. However, it is important to note that the insulin tolerance test is reputed to be less sensitive than the glucose tolerance test in detecting insulin resistance (Hermans *et al.*, 1999). These alterations in glucose metabolism demonstrate that three months of Cafeteria diet-feeding is capable of generating an early, pre-diabetic, condition (Saisho, 2014). It is commonly thought that insulin resistance underlies dyslipidemia (Miranda *et al.*, 2005) which corresponds to our findings of hypertriglyceridemia and reduced HDL cholesterol in CAF rats. Furthermore,

abdominal obesity, more specifically visceral adiposity, is hypothesized to cause insulin resistance through release of free fatty acids into the portal vein supplying the liver (Bergman *et al.*, 2006) coupled with systemic release of inflammatory cytokines (Lumeng & Saltiel, 2011; Samuel & Shulman, 2012). Conversely, according to the lipid overflow-ectopic fat model, insulin resistance can itself potentiate lipid storage in visceral adipose tissue (VAT) at the expense of subcutaneous adipose tissue (SAT) (Després & Lemieux, 2006).

Given the strong correlation between CVD and increased visceral fat deposition (Kaess *et al.*, 2012), it is imperative to directly assess rodent abdominal obesity when describing metabolic syndrome in addition to body weight measurements. Imaging techniques are preferred as they allow for repeated measurements and evaluation of multiple tissue types (Müller *et al.*, 2013). Our study is the first to use MRI in CAF rats to evaluate both VAT and SAT volumes. A recent report on a three-month traditional high-fat diet showed increases in percent SAT (%SATΔ) and VAT (%VATΔ) changes similar to those seen in our CAF rats (Kn *et al.*, 2014). However, despite similar degrees of caloric reduction during a subsequent one-month period, we observed dramatically different effects on %SATΔ and %VATΔ in SWT rats. By restricting the kcal in the high-fat diet by 30% without changing the nutritional composition, Kn *et al.* reported a surprising increase in %SATΔ (+20%). This increase was nonetheless blunted compared to the +42% increase in control rats maintained on the high-fat diet, along with a stabilization of %VATΔ (-2%). In our study, switching rats from the CAF to the SD chow diet resulted in a ~40% drop in energy consumption. Consequently, we observed a dramatic decrease in both SAT (-96%) and VAT (-49%). The difference between our observations and those of others could be due to either 1) the reduction in food intake

following the diet switch owing to the lower palatability of the standard chow diet or due to 2) the transition to a diet with a different nutritional composition. In addition, the two-fold greater decrease in SAT rather than VAT volume is surprising given that VAT is preferentially decreased in human metabolic syndrome patients via diet, exercise or pharmaceutical interventions (Chaston & Dixon, 2008). Considering the lipid overflow-ectopic fat model whereby insulin resistance in SAT tissue leads to increased lipid storage in VAT, the degree of insulin resistance and glucose tolerance may play a key role in regulating the VAT/SAT ratio. The early stage of insulin resistance achieved in our Cafeteria diet model may explain the greater weight loss in SAT tissue. Moreover, clinical guidelines recommend gradual weight loss with a daily caloric reduction of 500-1000 kcal/day from usual intake to avoid triggering biological pathways intended to prevent starvation (NHLBI Obesity Education Initiative Expert Panel, 2000). The extent of decrease in energy consumption in the clinical setting is therefore less than what was achieved in our rodent study and may participate in explaining the difference in weight loss profile between rats and humans.

In addition to these physiological findings, we report that four months of Cafeteria diet feeding does not cause spatial learning and memory deficits as assessed by the Barnes maze. We specifically chose this test as it is one of the few cognitive tasks that does not rely on food restriction. Given our findings that one month of switching rats to a standard diet is sufficient to abolish features of metabolic syndrome, the decision to use food restriction to motivate rodent performance is an important one. This is of particular importance when conducting studies using dietary models. Though the Morris water maze also does not use food restriction to motivate performance, it causes significantly greater degrees of stress which can also act as a confounding factor on behavioural

outcome measures (Harrison *et al.*, 2009). Indeed, highly stressful stimuli including exposure to the water maze are rather discordant with human research methods that typically use positive rewards in learning tasks (Homberg, 2013). This mismatch may explain conflicting reports of the effects of diet on stress and anxiety outcome measures (Prasad & Prasad, 1996; Buchenauer *et al.*, 2009; Maniam & Morris, 2010; Sharma & Fulton, 2012).

Despite the absence of diet-induced spatial and learning memory deficits in CAF rats in the Barnes maze, an increase in microglial Iba1 cell density in the CA1 region was detected after only four months on the diet. This indicated that hippocampal neuroinflammation is not sufficient to induce cognitive impairment. In a mouse model using a Cafeteria diet without a sucrose solution, Auer *et al.* (Auer *et al.*, 2015) were unable to detect changes in the hippocampal Iba1+ microglial cell population. In contrast, a study comparing Cafeteria diet-fed rats presented with or without a 10% sucrose solution, showed that the sucrose solution was required to upregulate gene expression of inflammatory markers (Beilharz *et al.*, 2014). These findings suggest that increased carbohydrate intake through consumption of sugar may be a key contributing factor to metabolic syndrome-induced neuropathology. We also demonstrated that Iba1 cell density was not increased in SWT rats. It is possible that the Cafeteria diet-induced hippocampal inflammatory microenvironment may be sufficiently recovered after a single month of standard chow diet, limiting proliferation-promoting signals. Indeed, microglial cell numbers in the hippocampus can normalize within weeks following a neurological insult (Ladeby *et al.*, 2005). We did not detect increased microglial cell density in the arcuate nucleus as reported in mice fed high-fat diets (Jeon *et al.*, 2012; Thaler *et al.*, 2012; Gao *et al.*, 2014). This may be due to a species difference or

differences in the type of dietary fat. Indeed, the diets used in the mouse studies were comprised of 60% kcal from lard while the Cafeteria diet contained 40% kcal from fat derived from various sources. Valdearcos *et al.* demonstrated that it is specifically saturated lipid species which accumulate within the hypothalamus to trigger an inflammatory response (Valdearcos *et al.*, 2014). Our findings suggest that hippocampal inflammation occurs independently of inflammation in the hypothalamus with an important role played by the type and concentration of dietary fat.

Conclusions

There is growing concern with the failure of basic research results not translating to the clinic, particularly in the field of stroke (Endres *et al.*, 2008; Philip *et al.*, 2009; Kahle & Bix, 2012). One key recommendation arising from international advisory groups is the use of more clinically relevant animal models that incorporate human disease co-morbidities (Carmichael, 2005; Krakauer *et al.*, 2012; Corbett *et al.*, 2015). To address these concerns, we used a human diet of ultra-processed foods and demonstrated that metabolic syndrome develops in as little as three months in Sprague Dawley rats. Furthermore, a "heathy lifestyle" intervention that involves switch to a standard chow diet for one month completely reverses these features. It remains to be seen whether these features could be reversed following longer Cafeteria diet exposures, particularly in animals maintained into middle or early old age. Similarly, longer exposure to the Cafeteria diet may predispose animals to cognitive impairments particularly when more challenging tests are employed. An important finding was that even short term Cafeteria diet exposure induced a pro-inflammatory state, an effect that may be especially deleterious with advancing age or coupled with injury such as stroke. Taken together, the

metabolic syndrome model described herein has great utility for providing a rapid means for inducing prominent CVD co-morbidity factors into animal models of disease including stroke and dementia.

Acknowledgments

The authors would like to thank Dr. Jessica Livingston-Thomas, Dr. Carine Nguemeni, Evelyn Lake, and Adrienne Dorr for invaluable technical support, advice, and help with animal experiments.

Competing interests

The authors declare no conflict of interest.

Funding

D.C. supported this work with grants from the Canadian Institutes of Health Research [grant number 102534], the Canadian Consortium on Neurodegeneration in Aging, and the Canadian Vascular Network. M.G.S received funding from the Heart and Stroke Foundation of Canada [Focus on Stroke doctoral scholarship] and the Canadian Partnership for Stroke Recovery.

Chapter 3 - Reduced Cerebrovascular Reactivity and Increased Resting Cerebral Perfusion in Rats Exposed to a Cafeteria Diet

Mariana Gomez-Smith [a,f], Rafal Janik [b,c], Evelyn M. Lake [b,c], Lynsie A. M. Thomason [b], Conner Adams [b,c], Matthew S. Jeffers [a,f], Bojana Stefanovic [b,c,f], Dale Corbett [a,d,e,f]

Submitted to *Neuroscience*, April 20th, 2017

a: Cellular and Molecular Medicine, University of Ottawa, Ottawa, ON, Canada

b: Sunnybrook Research Institute, Toronto, ON, Canada

c: Medical Biophysics, University of Toronto, Toronto, ON, Canada

d: Faculty of Medicine, Memorial University, St. John's, NL, Canada

e: Faculty of Medicine, University of Toronto, Toronto, ON, Canada

f: Canadian Partnership for Stroke Recovery, Ottawa, ON, Canada

Statement of Author Contributions

M.G.S., R.J., D.C., and B.S. conceived and designed the experiments. M.G.S., R.J., and L.A.T. performed the experiments. M.G.S., R.J., E.M.L., C.A., and M.S.J. analyzed the data. M.G.S. wrote the paper and D.C., M.S.J. ,and B.S. edited the paper.

Abstract

To better understand the effects of a diet high in fat, sugar, and sodium on cerebrovascular function, Sprague Dawley rats were chronically exposed to a Cafeteria diet. Resting cerebral perfusion and cerebrovascular reactivity were quantified using continuous arterial spin labeling (CASL) magnetic resonance imaging (MRI). In addition, structural changes to the cerebrovasculature and susceptibility to ischemic lesion were examined. Compared to control animals fed standard chow (SD), Cafeteria diet rats (CAF) exhibited increased resting brain perfusion and reduced cerebrovascular reactivity in response to 10% inspired CO_2 challenges in the cortex and in the hippocampus. CAF rats switched to chow for one month (SWT) partially improved resting perfusion in both regions and cerebrovascular reactivity in the hippocampus. However, the diet switch did not improve cerebrovascular reactivity in the cortex. These changes were not accompanied by alterations in the structural integrity of the cerebral microvasculature, examined using rat endothelial cell antigen-1 (RECA-1) and immunoglobulin G (IgG) immunostaining. Also, the extent of tissue damage induced by endothelin-1 injection into sensorimotor cortex was not affected by the Cafeteria diet. These results demonstrate that short-term consumption of an ultra-processed diet reduces cerebrovascular reactivity. This effect persists after dietary normalization despite recovery of peripheral symptomatology.

Introduction

Metabolic syndrome affects 20-40% of the world population and is increasing in prevalence (Batsis *et al.*, 2007). It is defined as the combination of any three of the

following five characteristics: abdominal obesity, reduced high-density lipoprotein (HDL) cholesterol, elevated triglycerides, raised fasted blood glucose, and hypertension (Alberti *et al.*, 2009*b*). Despite the ability of dietary interventions to correct peripheral features of metabolic syndrome (Salas-Salvadó *et al.*, 2011; The Look AHEAD Research Group, 2014), cardiovascular mortality risk is often not improved (Mozaffarian, 2016), begging the question of whether chronic consumption of a diet high in fat, sugar, and sodium can cause irreparable damage to the vasculature.

Whereas peripheral vascular dysfunction has been thoroughly described in individuals with metabolic syndrome (Limberg *et al.*, 2013; Walther *et al.*, 2015; Shimabukuro *et al.*, 2016), limited reports exist regarding its effects on the cerebrovasculature. Nonetheless, some results suggest that metabolic syndrome also impairs cerebrovascular hemodynamics. In a retrospective study, Giannopoulos *et al.* analyzed transcranial Doppler data from metabolic syndrome patients with atherosclerotic disease and found a significant correlation between reduced cerebrovascular reactivity to hypercapnia and metabolic syndrome (Giannopoulos *et al.*, 2010). These results were further confirmed in a more recent prospective study (Tyndall *et al.*, 2016). In rats fed a high-fat diet, a similar reduction in functional hyperemia upon whisker stimulation was observed using laser Doppler imaging (Li *et al.*, 2013).

Although transcranial Doppler offers certain advantages over other imaging techniques, it is limited to measuring blood velocity in major cerebral arteries that supply pial vessels (Sorond *et al.*, 2010). In contrast, magnetic resonance imaging (MRI) allows for the evaluation of cerebral blood flow (CBF) throughout the brain. Arterial spin labeling (ASL) is particularly useful as it quantifies CBF by non-invasive generation of

an endogenous tracer through magnetic labeling of blood water in the carotids (Borogovac & Asllani, 2012).

A deterioration in cerebrovascular hemodynamics is often accompanied by changes in vessel structure and vascular network architecture, such as the thickening of arteriolar walls that occurs in hypertension (Rizzoni *et al.*, 2009) and the increase in aberrant angiogenesis of the diabetic brain (Prakash *et al.*, 2013*a*). These structural changes, which result from shear stress and hypoxia, are accompanied by damage to vascular cell layers that cause endothelial cell death (Ergul *et al.*, 2014), microvessel rarefication (Sokolova *et al.*, 1985), and increased blood-brain barrier permeability (Li *et al.*, 2010). Such aberrant changes in vessel structure, coupled with a reduction in cerebrovascular reactivity, increase tissue damage and worsen functional outcomes following stroke in animal models (Li *et al.*, 2013; Prakash *et al.*, 2013*b*).

Our understanding of the cerebrovasculature has been greatly enhanced by the use of animal models. However, rodent studies often utilize genetically engineered strains to mimic human disease (Russell & Proctor, 2006). Genetic mutations alone rarely cause overt disease in humans whereas in metabolic syndrome and related disorders, diets comprised of ultra-processed foods high in fat, sugar, and sodium, combined with a sedentary lifestyle, play a much greater role (Groop, 2000). Consumption of ultra-processed foods, which are food items comprised almost exclusively of processed substances refined from whole foods, has greatly increased in industrialized nations since the 1980s (Monteiro *et al.*, 2013). Unfortunately, common commercial rodent diets focus on isolated nutrients and rarely recapitulate the full gamut of human metabolic syndrome features (Lai *et al.*, 2014). The Cafeteria diet, on the other hand, provides animals with a varied selection of human grocery store, ultra-processed foods and more accurately

reflects human disease co-morbidities (Sampey *et al.*, 2011; Higa *et al.*, 2014). We have previously shown that a Cafeteria diet is capable of generating metabolic syndrome in rats, with increased visceral adiposity, dyslipidemia, and insulin resistance (Gomez-Smith *et al.*, 2016). In addition to these peripheral effects, inflammation was also increased in the hippocampus of Cafeteria diet-fed rats. Notably, the metabolic perturbations and hippocampal neuroinflammation were fully resolved by switching animals to a healthy standard chow diet for one month.

To date, cerebrovascular hemodynamics and microvascular structure have not been studied in the Cafeteria diet model of metabolic syndrome despite the clear link between ultra-processed diets and cardiovascular disease risk (Malik *et al.*, 2010). In the current study, we investigated cerebrovascular reactivity to hypercapnia in an established rat model of metabolic syndrome using continuous arterial spin labeling (CASL), a highly sensitive and non-invasive imaging method to evaluate CBF. To further complement these measurements, we examined the structure of the cerebral microvasculature, including vessel area, integrity of the blood-brain barrier (BBB), and susceptibility to an ischemic insult. Cafeteria diet-fed rats were compared to both standard chow-fed rats and rats switched from the Cafeteria to a standard chow diet.

Experimental Procedures

Animals and Diets

Animal procedures followed the guidelines established by the Canadian Council on Animal Care and were approved by the Animal Care Committees of the University of Ottawa and the Sunnybrook Research Institute. Experiments have been reported

following the ARRIVE guidelines. Three-week-old male Sprague Dawley rats (Charles River Laboratories, Montreal, Canada) were used for all experiments. Rats were pair-housed and maintained on a 12-hour reverse light/dark cycle (8 am off/8 pm on). One week after habituation to the facility, rats were randomly assigned to a Standard (SD), Cafeteria (CAF), or Switch (SWT) diet as previously described. Briefly, SD rats had *ad libitum* access to regular chow (Teklad Global 18% Protein Rodent Diet; Harlan, Madison, WI) and drinking water. CAF rats had *ad libitum* access to regular chow and drinking water in addition to a daily selection of three grocery store-purchased food items from a menu of 16 items (**Table 4**) as well as a 12% w/v sucrose drinking solution (MP Biomedicals, Solon, OH). Grocery store items alternated through a list of pre-established food combinations to ensure diversity of foods presented. SWT rats were provided the Cafeteria diet for three months after which they were switched to the regular chow and water-only SD diet for an additional month (Gomez-Smith *et al.*, 2016).

Magnetic Resonance Imaging

Animal preparation

Rats used for imaging were transferred from the University of Ottawa to the Sunnybrook Research Institute in Toronto two weeks prior to imaging to allow for habituation to the new facility. Eighteen rats (6 SD, 6 CAF, 6 SWT) were imaged twice, the first time after three months on the diet (immediately prior to the diet switch) and again after four months on the diet (one month after the diet switch). Since SWT rats were not treated differently from CAF animals at the three-month time point, their imaging data were combined. Data from one SD rat at the three-month time point and two rats (1 SD, 1 CAF) at the four-month time point were not included due to equipment

Table 4: List of food items comprising the Cafeteria diet. Kcal/g were provided by manufacturers.

Food item	Manufacturer	Kcal/g
standard chow #2018	Harlan Teklad	3.10
All beef hot dogs	Schneider's	2.89
Blue Ribbon bologna	Schneider's	4.29
Brownies	Two-Bite	3.57
Butter tarts	Farmer's Market	4.00
Cheetos cheese puffs	Frito-Lay	6.00
Chocolate chip cookies	Loblaws	5.00
Cracker Barrel cheddar cheese	Kraft	4.00
Doritos nacho cheese	Frito-Lay	5.20
Joe Louis	Vachon	4.44
Lays original chips	Frito-Lay	5.60
Nesquik cereal	Nestle	4.14
Oreo's	Christie	5.00
Peanut butter M&M	Mars	5.25
Pre-cooked bacon	Maple Leaf	5.60
Reese's peanut butter cups	Hershey	5.13
Vanilla wafers	Voortman	4.67

failure during imaging. One SWT rat died prior to the four-month imaging session. Two rats (1 SD, 1 CAF) died during the four-month imaging session. Data were thus collected in 5 SD, 6 CAF, and 6 SWT rats at 3 months and in 4 SD, 4 CAF, and 5 SWT rats at 4 months. Based on the effect sizes that we obtained with the present N, we achieved a power level greater than 99%. The sample size was therefore deemed sufficient.

In preparation for imaging, rats were induced with 5% isoflurane and subsequently switched to *i.v.* propofol (45 mg/kg/hr, 10 mg/ml; PharmaScience, Montreal, Canada). Animals received an *i.m.* injection of glycopyrrolate (0.2 mg/ml, 0.1 mg/kg; Omega, Montreal, Canada) to reduce airway secretions. They were subsequently intubated and mechanically ventilated using a small animal ventilator (CWE Inc., Ardmore, PA) with a gas mixture of 70% nitrogen and 30% oxygen. To reduce motion, rats received a single *i.v.* injection of atracurium (10 mg/ml, 1 mg/kg; Sandoz, Boucherville, Canada) immediately prior to imaging. Physiological parameters, including heart rate, oxygen saturation, core temperature, transcutaneous partial pressure of CO_2 ($tcPCO_2$) and end tidal CO_2 were monitored throughout the experiment (Biopac Systems Inc., Montreal, Canada; MouseOx, Starr Life Sciences Corp., Oakmont, PA; TCM4 monitor, Radiometer, London, Canada; MicroCapStar CO_2 monitor, CWE Incorporated, Ardmore, PA). At the three-month time point, ten rats (2 SD, 4 CAF, 4 SWT) were ventilated with the aforementioned gas mixture via a programmable GSM-3 gas mixer (CWE Inc., Ardmore, PA); in the other eight rats the gas mixture was adjusted manually using a flow regulator due to equipment unavailability. At four months, the gas mixer was used with all animals. Following each imaging session, rats were carefully extubated, closely monitored on a heating blanket during recovery, and administered *s.q.* buprenorphine (0.3

mg/ml, 0.1 mg/kg; Reckitt Benckiser Healthcare, Hull, UK) in saline for pain management.

Data acquisition

Imaging was performed using a 7T BioSpec 70/30 USR system (Bruker, Ettlingen, Germany), equipped with a 20 cm inner diameter gradient set (200 mT/m). A birdcage body coil and a quadrature receive-only coil were used for signal excitation and signal reception, respectively. Rats were positioned with their heads immobilized on a custom head holder. Manual shimming was performed before all experiments. Structural images were acquired using a T2-weighted rapid acquisition with relaxation enhancement (RARE) sequence. Twenty-five 0.5-mm thick coronal slices were acquired with in-plane spatial resolution of 0.1 x 0.1 mm^2, field of view (FOV) of 12.8 x 25.6 mm^2, 128 x 256 matrix, 5500 ms repetition time (TR) and 47 ms echo time(TE), and RARE factor 8. For CASL experiments, tri-pilot images guided the identification of cortical and hippocampal regions of interest (ROI). Anatomical landmarks, derived from the Paxinos and Watson Rat Brain Atlas (Paxinos & Watson, 2007), were used to place a total of three 1.5 mm thick coronal slices along the anterior-posterior (AP) axis. One slice comprising somatosensory, motor, and cingulate cortex (Cx) was positioned at approximately +1 mm AP relative to Bregma. A slice package containing two slices with an inter-slice distance of 0.5 mm was placed to span the rostral and caudal regions of the hippocampus (Hc), corresponding approximately to -3 mm and -5 mm AP relative to Bregma. The labeling plane was positioned perpendicular to the carotid arteries to optimize the inversion efficiency. Labeling was achieved by applying a 1.5 second RF pulse (1.2 W) in the presence of a 10 mT/m longitudinal gradient, approximately 30 mm posterior from isocenter. 540 pairs of interleaved tag and control echo planar images (EPI) were

acquired with a TR/TE of 2000 ms/12.3 ms, a nominal in-plane spatial resolution of 0.25 x 0.25 mm^2, and an FOV of 20 x 20 mm^2, for a total scan time of 36 minutes. Seven 5-minute hypercapnic challenges were acquired comprising one minute of 10% fractional concentration of inspired CO_2 ($FiCO_2$) followed by four minutes of 0% $FiCO_2$.

Data processing

The CASL data were motion corrected using the 3dvolreg Analysis of Functional NeuroImages (AFNI) program (Cox & Jesmanowicz, 1999). EPI frames exhibiting greater than 0.5 mm of translation in any direction were removed from further analysis. Each slice from the EPI readout was registered to T2 structural images by full affine registration using MNI-Display software (Montreal Neurological Institute, Montreal, Canada), manually identifying a minimum of 20 anatomical landmarks per slice. Thereafter, white matter and ventricles were segmented in MNI-Display using signal intensity thresholds. ROI masks were manually delineated in Matlab (Mathworks, Natick, MA) and data were blurred within ROI masks using the 3dBlurInMask AFNI program. A boxcar function alternating between 0 and 1 modeled the tag-control time series while perfusion responses to hypercapnia were modeled by convolving the boxcar function with a gamma variate function using the 3dDeconvolve AFNI program. The latter was obtained with the AFNI waver program by convolving an idealized hemodynamic response function with CO_2 stimulus onset times as determined by end tidal CO_2 measurements. To control for multiple comparisons, a cluster correction was performed with a voxelwise significance threshold of p=0.05. Cluster size was determined using the 3dClustSim AFNI program (Cox & Jesmanowicz, 1999) with a clusterwise α of 0.05. Perfusion measurements were expressed in relative units (percentages), with ASL signal change between labelled and control frames being a direct estimate of tissue perfusion

(scaled by the tissue longitudinal relaxation time constant, inversion efficiency, and blood-brain partition coefficient) (Chugh *et al.*, 2012).

Histological Analysis

Animals

A separate group of 30 rats were used for the histological study. Twelve rats (6 SD, 6 CAF) underwent endothelin-1 stroke surgery after three months on the diet and were sacrificed one week after stroke. The remaining eighteen control rats (6 SD, 6 CAF, 6 SWT) did not undergo stroke surgery and were sacrificed at four months, with the diet switch occurring after three months.

Endothelin-1 stroke induction

Endothelin-1 stroke surgery was conducted as previously described (Nguemeni *et al.*, 2015). Rats were induced (5%) and maintained (1.5-2%) on isoflurane anesthesia. The skull was carefully exposed and two burr holes were made at stereotaxic coordinates +2.0 mm and +0.0 mm AP relative to Bregma and ±2.5 mm medial-lateral (ML). Both injections were performed in the same hemisphere. The injected hemisphere was contralateral to the limb with highest reaching performance as determined following training on the Montoya staircase prior to stroke, methods which are described elsewhere (Jeffers *et al.*, 2014). Two 2µl endothelin-1 injections (400pmol/µl in sterile water; Calbiochem, San Diego, CA) were slowly injected at a depth of 1.7 mm from the surface of the dura at each cortical site. After injections, the scalp was sutured and topical bupivacaine applied (2%, 0.2ml; Chiron, Guelph, Canada). Animals were placed in an incubator to maintain body temperature at 37°C during recovery, given a single *s.q.*

injection of buprenorphine (0.05 mg/kg; Reckitt Benckiser Pharmaceuticals Inc., Richmond, USA) and then returned to their home cage.

Tissue preparation

Animals were deeply anesthetized by *i.p.* administration of Euthanyl (149.5 mg/kg, Bimeda-MTC Health Inc., Cambridge, Canada) and intracardially perfused with heparinized saline followed by 4% paraformaldehyde (PFA) in phosphate-buffered saline (PBS). Brains were removed and post-fixed overnight in 4% PFA, then transferred to a 20% w/v sucrose solution in 0.1 M phosphate buffer until brains were saturated. Frozen 20 µm and 50 µm coronal sections were cut at 200 µm intervals. 20 µm sections were immediately slide-mounted while 50 µm sections were collected for free-floating histology. In rats that did not undergo stroke surgery, tissue spanning the prefrontal cortex to the caudal extent of the hippocampus was collected; in rats with stroke, tissue was collected throughout the injury.

Infarct volume assessment

Tissue was stained with haematoxylin and eosin (H&E) and 10 sections throughout the infarct were visualized at 20X magnification with a Leica DMR microscope (Leica Microsystems, Germany). Using StereoInvestigator software (StereoInvestigator® V10.0 MicroBrightField Bioscience, Williston, VT), intact tissue in both hemispheres was manually traced by an experimenter that was blinded to the diet group. Infarct volume in mm^3 was calculated as $\sum$[(area of contralesional tissue – area of undamaged ipsilesional tissue) x distance between sections x thickness of sections] (Nguemeni *et al.*, 2015).

RECA-1 staining and vessel area quantification

50 µm free-floating sections spaced every 2400 µm were isolated in control and stroke rats. In control rats, three consecutive sections were evaluated for cortical vessel area (approximate AP coordinates: +2.4 mm, 0 mm and -2.4 mm). For hippocampal vessel area, two sections (approximate AP coordinates: -2.4 mm and -4.8 mm) were analyzed. In stroked rats, three consecutive sections equally spaced throughout the infarct were used. Tissue was stained overnight at 4°C with the anti-rat endothelial cell antigen-1 (RECA-1) mouse monoclonal antibody (1:200; Abcam, Toronto, Canada). After washing in PBS, a biotinylated goat anti-mouse secondary antibody was applied for one hour at room temperature (1:400; Jackson ImmunoResearch, West Grove, PA). Stain was amplified using the Vectastain ABC avidin-biotin kit (Vector Laboratories, Burlingame, CA) and visualized with ImmPACT DAB substrate (Vector Laboratories, Burlingame, CA) after which sections were slide mounted. High resolution images of individual sections were collected with the Virtual Tissue function of StereoInvestigator software at 10X magnification. The area fraction fractionator probe in StereoInvestigator was used to estimate vessel area using parameters taken from Wälchli *et al.* (100 µm x 100 µm counting frame, 200 µm x 200 µm grid spacing and 8 µm spacing between grid points) (Wälchli *et al.*, 2015). Vessel area was quantified by an experimenter that was blinded to the diet group. Cortical vessel area in control brains was evaluated in six rectangular ROI (800 µm x 500 µm) per section, positioned in symmetrical locations in the left and right hemispheres extending laterally from the midline. Hippocampal vessel area in these same animals was evaluated in the entire dentate gyrus (DG) and the cornu ammonis sub-fields CA3 and CA1, from left and right hemispheres. In rats with stroke, six rectangular ROI (800 µm x 500 µm) per section were evaluated, three per hemisphere. In the ipsilateral

hemisphere, ROI were placed immediately next to infarcted tissue. Three ROI were placed in the contralateral tissue in homologous locations.

IgG staining and evaluation of BBB integrity

Methods were adapted from Yi *et al.* (Yi *et al.*, 2012) and Marcon *et al.* (Marcon *et al.*, 2009). A series of slide-mounted 20 µm sections from control rats was incubated overnight at 4°C with donkey anti-rat biotin-conjugated immunoglobulin G (IgG) antibody (1:250; Jackson ImmunoResearch Laboratories Inc., West Grove, PA). Vectastain ABC avidin-biotin and ImmPACT DAB were used to amplify and visualize IgG staining. Eight 200 µm-spaced sections containing hypothalamic arcuate nucleus and eight hippocampal sections, at 400 µm intervals, were identified and evaluated by an experimenter blinded to the diet group. In sections containing arcuate nucleus, IgG-stained tissue surrounding the third ventricle was traced and IgG extravasation volume calculated as: ∑(area of IgG staining x distance between sections x thickness of sections). In hippocampal sections, tissue in both hippocampus and cortex was inspected for perivascular IgG staining, indicative of extravasation of blood proteins, as demonstrated by others (Rigau *et al.*, 2007; Jalal *et al.*, 2012).

Statistical Analysis

Voxelwise MRI datasets, effect of method of CO_2 delivery on resting perfusion, and cerebrovascular reactivity were analyzed using linear mixed effects modeling with the restricted maximum likelihood (REML) method in IBM SPSS Statistics (v.23, IBM Corp., Armonk, NY). Diet was treated as a fixed effect while animals were considered random effects. The Bonferroni correction was used to adjust for multiple comparisons and data are presented as estimated marginal means ± standard error of the mean (SEM).

Analysis of physiological parameters during the imaging experiment was performed using univariate analysis of variance followed by Tukey's post-hoc tests in IBM SPSS Statistics software. Data are represented as mean ± SEM. Histological data analysis was performed using Prism software (V6, GraphPad, La Jolla, CA). All analyses used paired t-tests or univariate analysis of variance followed by Tukey's multiple comparisons post-hoc test for pairwise comparisons. Histological data are expressed as mean ± SEM. Statistical significance was taken at $p<0.05$ in all experiments.

Results

The Cafeteria Diet Increased Weight Gain

Body weight of rats used for the MRI study was recorded at weekly intervals throughout the experiment. The increased caloric density of the Cafeteria diet food items (**Table 4**) caused CAF and SWT rats to consume more kcal per day than SD rats (**Table 5**). This resulted in significant weight gain in rats that consumed the Cafeteria diet. Indeed, as early as nine weeks after the start of the diet, CAF (862 g ±27 g, $p<0.01$) and SWT (844 g ±24 g, $p<0.05$) rats were significantly heavier than SD (724 g ±28 g) rats (**Figure 13**). Immediately after the diet switch at 12 weeks, the body weight of SWT rats declined and subsequently plateaued. By week 14, SWT rats were similar to SD rats. Cafeteria diet rats continued to gain weight until the experimental end point; by 16 weeks, CAF rats (928 g ±23 g) were considerably heavier than SD rats (759 g ±25 g, $p<0.001$).

Table 5: Daily kcal intake (food and 12% sucrose solution) pre- and post- diet switch. Data represent mean ± SEM. Statistical differences were determined using the Student t-test on pre-diet switch data and one-way ANOVA on post-diet switch data. Rats fed the Cafeteria diet consumed significantly more daily kcal than SD rats prior to the diet switch (**: $p < 0.01$) while there was no significant effect of diet after the diet switch.

	Pre-diet switch	**Post-diet switch**
SD	103.6 ± 4.1	84.0 ± 7.6
CAF	124.7 ± 3.6**	97.1 ± 3.2
SWT		55.9 ± 9.3

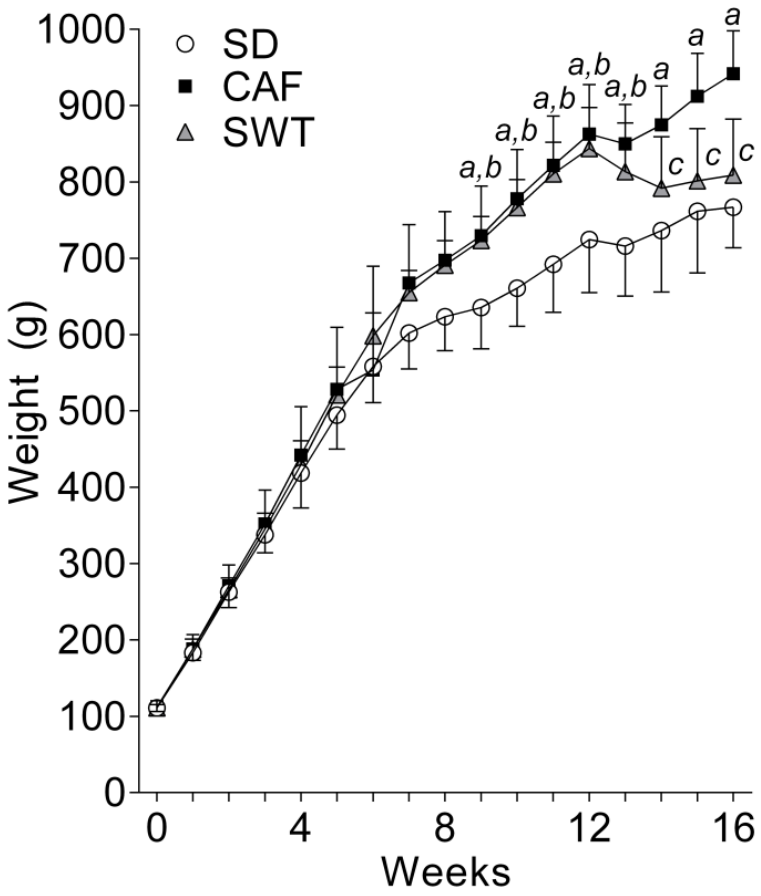

Figure 13: The Cafeteria diet caused weight gain that was reversed with a switch to standard chow.

Letters indicate a significant difference following pair-wise comparisons ($p<0.05$; a: SD vs. CAF, b: SD vs. SWT, c: CAF vs. SWT). Values are mean ± SEM.

Increased Resting Perfusion and Reduced Cerebrovascular Reactivity in CAF Rats with Only Partial Recovery After a Switch to Standard Chow

Immediately before and one month following a switch to standard chow, SD, CAF, and SWT rats underwent MRI to evaluate brain hemodynamics. These time points were based on our previous findings that three months of Cafeteria diet consumption caused metabolic syndrome (e.g. abdominal obesity, dyslipidemia, etc.). Furthermore, we had shown that switching CAF rats to standard chow for four weeks was sufficient to resolve these features (Gomez-Smith *et al.*, 2016).

Baseline core temperature, oxygen saturation, and $tcPCO_2$ immediately prior to commencing CO_2 challenges were not different between time points or between diets at each time point (**Table 6**). Moreover, all rats were normocapnic with $tcPCO_2$ not exceeding 45 mmHg prior to imaging. During CO_2 challenges, maximum $tcPCO_2$ and range of $tcPCO_2$ achieved were not different between diet groups at either time point. However, both maximum $tcPCO_2$ ($p<0.01$) and $tcPCO_2$ range ($p<0.05$) were significantly higher at the three-month time point, regardless of diet, as a result of the different methods of CO_2 delivery. This difference may explain the significant main effect of time that was revealed for resting perfusion ($p<0.001$) and perfusion response ($p<0.001$), necessitating an independent analysis at each time point.

The Cafeteria diet led to an overall increase in resting brain perfusion at both time points (**Figure 14**), expressed in relative units as per cent CBF. At three months (**Figure 14A**), CAF rats exhibited ~15% higher resting perfusion in the cortex (1.44% ±0.02%, $p<0.001$) and ~38% higher resting perfusion in the hippocampus (2.29% ±0.03%, $p<0.001$) compared to SD control rats (Cx: 1.25% ±0.04%; Hc: 1.66% ±0.04%). One month later (**Figure 14B**), resting perfusion in CAF rats was also elevated in comparison

Table 6: Summary of physiological parameters at baseline and during CO_2 challenges in the MRI experiment.

Data represent mean ± SEM. *a* and *b* represent groups that are significantly different from each other ($p<0.05$). Max $tcPCO_2$ and $tcPCO_2$ range were significantly elevated at the three-month time point but core temperature, baseline oxygen saturation, and baseline $tcPCO_2$ were not. There was no effect of diet on any physiological parameter at either time point.

	3 months		4 months		
	SD	**CAF**	**SD**	**CAF**	**SWT**
Core temperature (°C)	36.6 ± 0.4	36.4 ± 0.3	36.4 ± 0.4	35.8 ± 0.3	35.9 ± 0.2
Baseline oxygen saturation (%)	97.6 ± 0.6	98.2 ± 0.4	98.8 ± 0.2	98.7 ± 0.5	98.9 ± 0.3
Baseline $tcPCO_2$ (mmHg)	39.3 ± 2.7	42.7 ± 1.7	41.8 ± 4.2	42.6 ± 2.7	37.8 ± 2.6
Max $tcPCO_2$ (mmHg)	54.3 ± 2.0[a]	55.7 ± 2.2[a]	49.6 ± 3.9[b]	51.4 ± 3.2[b]	46.8 ± 2.1[b]
$tcPCO_2$ range (mmHg)	15.0 ± 3.6[a]	13.0 ± 1.2[a]	7.8 ± 0.4[b]	8.8 ± 1.1[b]	8.4 ± 0.7[b]

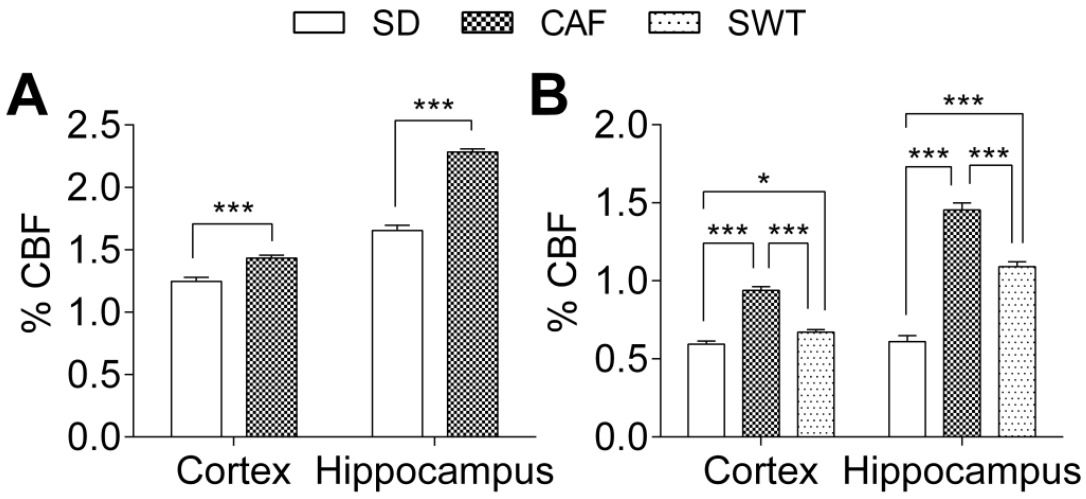

Figure 14: Resting perfusion increased in Cafeteria diet-fed rats.

Resting perfusion at (A) three and (B) four months on the SD, CAF, and SWT diets in both the cortex and the hippocampus. Values are estimated marginal means ± SEM. Linear mixed model analysis was performed independently on data from each time point. Significant differences following pairwise comparisons were as follows: * $p<0.05$, *** $p<0.001$.

to SD rats, with ~58% higher resting perfusion in the cortex (0.94% ±0.04%, $p<0.001$) and ~138% higher resting perfusion in the hippocampus (1.46% ±0.05%, $p<0.001$) compared to SD rats (Cx: 0.6% ±0.04%, Hc: 0.61% ±0.04%). The diet switch decreased resting perfusion (**Figure 14B**) by ~25% in both ROI (Cx: 0.67 ±0.03%, $p<0.001$; Hc: 1.09 ±0.03%, $p<0.001$) relative to CAF levels. Nonetheless, resting perfusion in SWT rats remained significantly elevated compared to SD in the cortex ($p<0.05$) and in the hippocampus ($p<0.001$).

Perfusion increase to CO_2 challenges, an indicator of cerebrovascular reactivity, was expressed as change in per cent CBF. At both time points and in both ROI, cerebrovascular reactivity to hypercapnia was blunted in CAF rats compared to SD (**Figure 15**). At three months (**Figure 15A**), the cortical (98% ±1.8%, $p<0.001$) and hippocampal (42.1%±0.7%, $p<0.001$) vasculature of CAF rats were ~27% and ~37% less responsive, respectively, than the vasculature of SD rats (Cx: 134.2% ±2.7%, Hc: 66.5% ±1.1%). At four months (**Figure 15B**), CAF cortical (178.9% ±22.8%, $p<0.001$) and hippocampal (57.4% ±7.7%, $p<0.001$) perfusion increases to CO_2 were smaller by ~37% and ~47%, respectively, than those of SD (Cx: 284.6% ±19.9%, Hc: 107.6% ±6.1%). While the diet switch intervention partially normalized resting perfusion, this was not the case for cerebrovascular reactivity to CO_2. Indeed, CBF increase to hypercapnia in the cortex was not statistically different between CAF (178.9% ±22.8%) and SWT (182.3% ±17.7%) rats one month after the switch to the chow diet, remaining significantly lower than that of SD ($p<0.001$). Cerebrovascular reactivity in SWT rats in the hippocampus (84% ±4.9%, $p<0.01$) improved significantly by ~46% from CAF levels yet remained depressed by ~21% compared to SD (**Figure 15B**). Representative perfusion response

Figure 15: Perfusion response to hypercapnia decreased in Cafeteria diet-fed rats.

(Following page) Perfusion response to hypercapnia expressed in terms of change in CBF at (A) three and (B) four months. Values are estimated marginal means ± SEM. Linear mixed model analysis was performed independently on data from each time point. Significant differences following pairwise comparisons were as follows: ** $p<0.01$, *** $p<0.001$. Representative perfusion response and time course data during CO_2 challenges at the 3-month imaging time point are shown for a (C) SD and for a (D) CAF rat. (Left) The perfusion response map is color-coded to represent magnitude of regional changes in perfusion. (Right) ASL signal time courses represent mean cortical CBF, averaged across the seven CO_2 challenges, with the grey shaded region corresponding to the standard deviation from the mean CBF. The orange bars indicate the period of hypercapnic gas mixture delivery by the GSM-3 gas mixer.

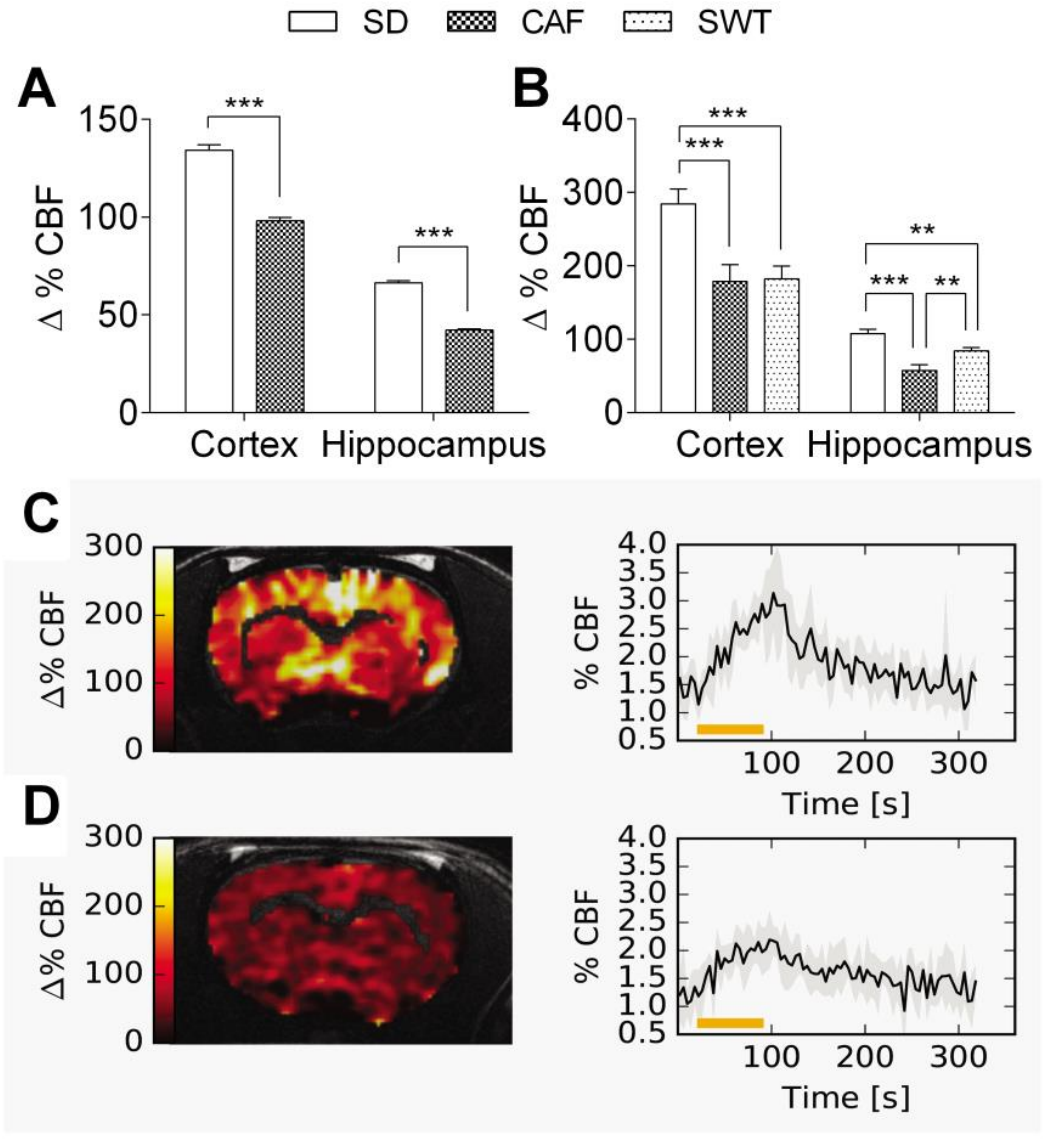
SD
CAF
SWT
A
Δ % CBF
150
100
50
0
***
***
Cortex
Hippocampus
B
Δ % CBF
400
300
200
100
0
***
***
**
***
**
Cortex
Hippocampus
C
Δ% CBF
300
200
100
0
% CBF
4.0
3.5
3.0
2.5
2.0
1.5
1.0
0.5
100
200
300
Time [s]
D
Δ% CBF
300
200
100
0
% CBF
4.0
3.5
3.0
2.5
2.0
1.5
1.0
0.5
100
200
300
Time [s]

data and corresponding ASL signal time courses during CO_2 challenges are shown for an SD (**Figure 15C**) and a CAF (**Figure 15D**) rat, highlighting the reduction in cerebrovascular reactivity following Cafeteria diet feeding.

At the three-month time point, the effect of gas delivery method on resting perfusion and cerebrovascular reactivity was examined. Within both SD and CAF cohorts as well as in both ROI, there was a significant effect of gas delivery method on hemodynamic outcome measures ($p<0.01$ for all comparisons, **Table 7**). Nevertheless, statistical comparisons made within groups of rats receiving the same method of gas delivery showed that the main effect of the Cafeteria diet, i.e. increased resting perfusion and reduced cerebrovascular responsiveness in CAF rats, was maintained with significant differences between SD and CAF rats under both sets of gas delivery conditions ($p<0.01$ for all comparisons). Moreover, fundamental physiological parameters modified by the hypercapnic challenge, namely oxygen saturation and CO_2 tension, were not significantly affected by the method of gas delivery (**Table 8**).

Effects of Cafeteria Diet on Vessel Area, Cortical Infarct Volume and Vessel Wall Integrity

The hemodynamic effects of the Cafeteria diet were not accompanied by structural changes in cerebral blood vessels. Stereological quantification of RECA-1-stained tissue (**Figure 16A,B**) revealed that cortical (**Figure 16C**) and hippocampal (**Figure 16D**) vessel area were unaffected by four months of Cafeteria diet-feeding. The Cafeteria diet also did not impact vessel area consequent to ischemic strokes (**Figure 16E**) nor did it worsen infarct volume (**Figure 16F**). A representative image showing the maximal extent of stroke injury is shown in **Figure 16G**. Finally, BBB integrity was assessed in the

Table 7: Effect of method of gas delivery on resting perfusion and cerebrovascular reactivity at the three-month time point.

All comparisons between groups based on diet, ROI, or method of gas delivery were statistically significant ($p<0.01$). Nonetheless, the main effect of the Cafeteria diet on both resting perfusion and cerebrovascular reactivity was constant regardless of method of gas delivery.

		Without gas mixer		**With gas mixer**	
		SD (n=4)	**CAF (n=4)**	**SD (n=2)**	**CAF (n=8)**
Resting perfusion	Cortex	1.31 ± 0.04	1.79 ± 0.04	1.03 ± 0.07	1.24 ± 0.03
CBF (%)	Hippocampus	1.74 ± 0.04	2.48 ± 0.04	1.33 ± 0.1	2.19 ± 0.03
Cerebrovascular	Cortex	121.7 ± 2.3	89.0 ± 2.3	179.0 ± 6.7	103.3 ± 2.6
reactivity					
Δ CBF (%)	Hippocampus	64.8 ± 1.2	45.3 ± 1.0	73.3 ± 2.3	40.1 ± 0.9

Table 8: Fundamental physiological parameters modified by the hypercapnic challenge.

Oxygen saturation and CO_2 tension were not significantly affected by the method of gas delivery. † indicates that measurements were acquired in only one animal.

	no gas mixer		**gas mixer**	
	SD (n=4)	**CAF (n=4)**	**SD (n=2)**	**CAF (n=8)**
Baseline oxygen saturation (%)	98.5 ±0.3	98.5 ±0.8	96.4 ±0.6	98.1 ±0.2
Baseline tcPCO$_2$ (mmHg)	37.5 ±3.5	42.75 ±2.8	43 †	42.7 ±2.3
Max tcPCO$_2$ during CO$_2$ challenges (mmHg)	56 ±2.0	59 ±3.4	51 †	53.5 ±2.6

Figure 16: Vessel area and infarct volume not altered by diet.

(Following page) (A) Representative image of RECA-1-stained tissue used for stereological quantification of vessel area. Shown are an 800 µm x 500 µm ROI sampling site (red), the 200 µm x 200 µm sampling grid (black), and 100 µm x 100 µm counting frames (green). (B) A magnified image of a single counting frame; diamonds indicating Cavalieri grid points that overlap with RECA-1-stained vessels. (C) Cortical and (D) hippocampal vessel area in RECA-1-stained tissue from SD, CAF, and SWT animals at four months on the diet. (E) Contralesional and perilesional vessel area in stroke tissue. (F) Infarct volume in SD and CAF rats that underwent focal ischemia. Values are mean ± SEM. (G) H&E-stained section showing maximal injury from a representative SD rat one week after ET-1 stroke induction. The border between intact and infarcted tissue is outlined in white. (H) Hypothalamic IgG extravasation volume in SD, CAF, and SWT animals at four months on the diet. Values are mean ± SEM. (I) Representative image of IgG staining in the arcuate nucleus of a rat in proximity to the third ventricle.

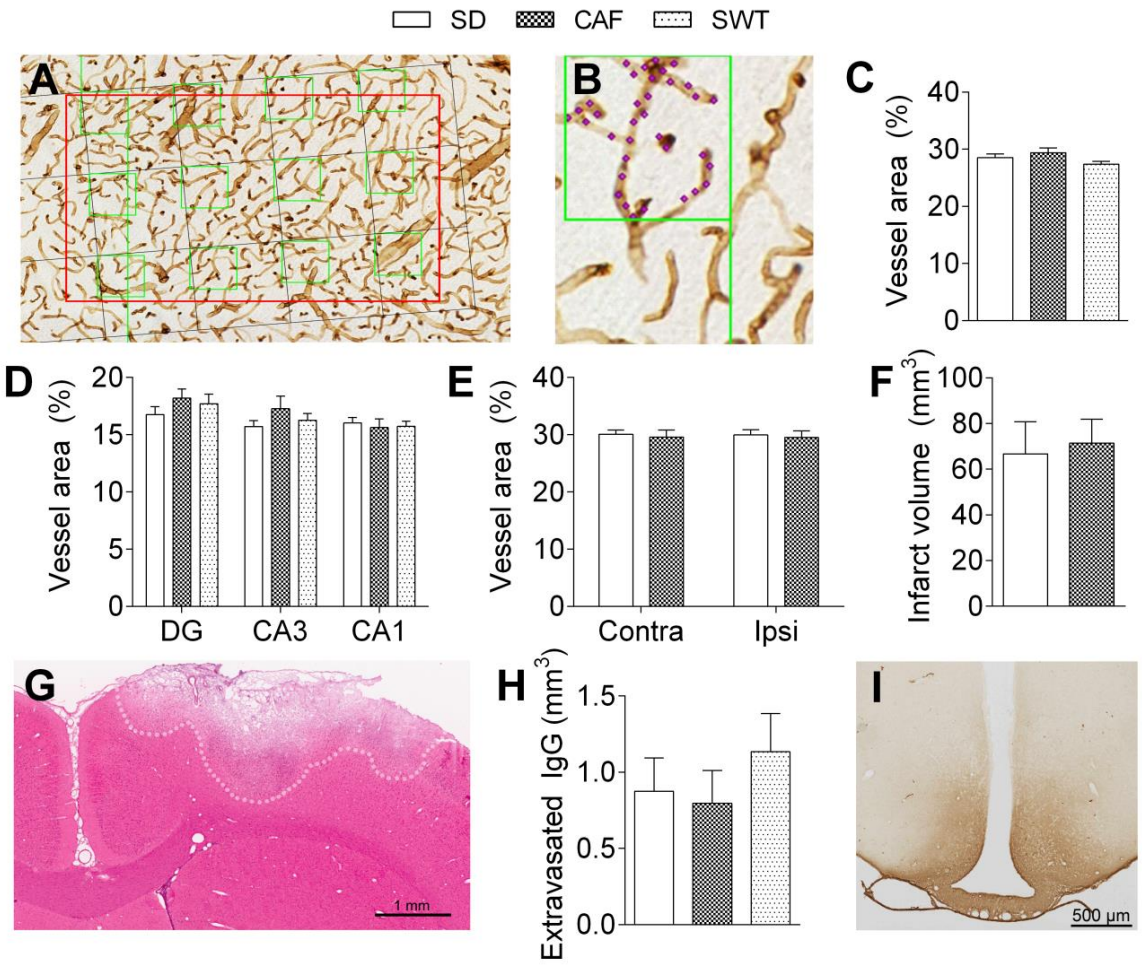
SD
CAF
SWT
A
B
C
Vessel area (%)
40
30
20
10
0
D
Vessel area (%)
20
15
10
5
0
DG
CA3
CA1
E
Vessel area (%)
40
30
20
10
0
Contra
Ipsi
F
Infarct volume (mm3)
100
80
60
40
20
0
G
1 mm
H
Extravasated IgG (mm3)
1.5
1.0
0.5
0.0
I
500 µm

cortex, hippocampus as well as in the arcuate nucleus in SD, CAF, and SWT brains in the absence of endothelin-1 stroke. Serial sections taken throughout these structures were inspected for IgG extravasation. In the cortex and hippocampus, perivascular IgG staining was effectively absent in all three diet groups (data not shown), while in the arcuate nucleus, IgG extravasation volume was small and not different between diet groups (**Figure 16H**). A representative image of IgG-stained arcuate nucleus is shown in **Figure 16I**.

Discussion

In the present study, we examined the effect of an ultra-processed Cafeteria diet on cerebral hemodynamics and microvascular structure in a rat model of metabolic syndrome. Furthermore, we tested the potential of a subsequent healthy diet intervention to recover the cerebrovascular changes induced by the Cafeteria diet. Consistent with our previous study (Gomez-Smith *et al.*, 2016), three months of Cafeteria diet-feeding caused CAF rats to gain significantly more weight than SD chow-fed rats. Our MRI results showed that the Cafeteria diet led to resting hyperperfusion in the brain regions under study while simultaneously contributing to reduced cerebrovascular reactivity to hypercapnia. Switching to the chow diet only partially recovered these effects. However, these functional changes in cerebrovascular hemodynamics were not accompanied by alterations in the structure of the cerebrovasculature.

Our resting perfusion results are interesting as hypoperfusion has been reported in patients with metabolic syndrome (Birdsill *et al.*, 2013) and insulin resistance (Rusinek *et al.*, 2015) as well as in type 1 (van Golen *et al.*, 2013) and type 2 diabetics (Last *et al.*, 2007), while other studies have failed to show a change in resting perfusion in type 2 diabetes (Tiehuis *et al.*, 2008; Rusinek *et al.*, 2015). Mice with streptozotocin-induced

type 1 diabetes, on the other hand, exhibit elevated blood flow velocity (Tennant & Brown, 2013). This would suggest that hyperglycemia alone is not sufficient to induce hypoperfusion which may instead critically depend on the duration of metabolic dysfunction and increased age of human subjects. Indeed, age itself is a key driving force in the development of hypoperfusion (Liu *et al.*, 2012). Experimental models that allow for the examination of the initial signs of pathology are therefore of great value in determining the direct effects of metabolic dysfunction on cerebral hemodynamics. Additionally, elevated cerebral metabolic rate or diet-induced blood acidosis in Cafeteria diet-fed rats may cause increased vasodilation in the resting state, potentially explaining the observed resting perfusion results (Cipolla, 2009; Williams *et al.*, 2016*b*). Future experiments investigating the rate of cerebral glucose metabolism, via magnetic resonance spectroscopy imaging of deoxyglucose uptake (Nasrallah *et al.*, 2013), or the blood chemistry of Cafeteria diet-fed rats would be of interest.

CASL imaging revealed an overall decrease in cerebrovascular reactivity to hypercapnia in CAF rats which is largely in agreement with human (Giannopoulos *et al.*, 2010; Tyndall *et al.*, 2016) and rodent (Li et al., 2013) studies performed using laser Doppler imaging. Nonetheless, we are the first to report reduced cerebrovascular reactivity to hypercapnia in a rodent model of metabolic syndrome using MRI which allows for the examination of blood flow in deeper brain structures. Our present data indicate that the decrease in cerebrovascular reactivity in Cafeteria diet-fed rats is likely the result of a reduction in functional responsiveness of the cerebrovasculature to hypercapnia rather than of a decrease in dilatory reserve consequent to the elevation in resting perfusion. Indeed, while SWT cortical resting perfusion recovered almost to SD levels after the transition to chow, the perfusion response of these rats to hypercapnia

remained significantly impaired relative to SD animals and commensurate with that of rats that continued on the Cafeteria diet.

The Cafeteria diet-induced alterations in cerebral hemodynamics do not correlate with global changes in microvascular structure as we did not observe an effect of diet on vessel area or on BBB integrity. Herein, no vessel growth was observed in RECA-1 stained tissue following exposure to either the Cafeteria diet alone or the combination of Cafeteria diet with ischemia induced by direct cortical microinjection of endothelin-1. Similar findings have been observed in the streptozotocin mouse model of type 1 diabetes using the photothrombotic stroke model (Tennant & Brown, 2013; Reeson *et al.*, 2015). However, in two genetic models of type 2 diabetes, the Goto-Kakizaki rat and the db/db leptin receptor mutant mouse, angiogenesis is greatly increased in the absence of stroke (Prakash *et al.*, 2013*a*) and new vessels remain largely unperfused and regress following middle cerebral artery occlusion (Prakash *et al.*, 2013*b*). These divergent findings among rodent species and strains using different stroke models supports the need for the examination of vascular structure in different conditions. In addition to these findings regarding vessel area, examination of IgG extravasation revealed that the BBB remained intact in the hippocampus and the arcuate nucleus of CAF rats. In contrast, several studies have demonstrated a role for high-fat diets in the loss of BBB integrity in these structures with degradation of endothelial tight junctions (Davidson *et al.*, 2012; Freeman & Granholm, 2012; Yi *et al.*, 2012). The discrepancy in our findings and those of others may relate to the considerably higher concentration of dietary saturated fat used in these studies as saturated fat is uniquely capable of increasing BBB leakage compared to other lipid species (Takechi *et al.*, 2013).

A number of mechanisms may explain the observed effects of the Cafeteria diet on cerebral hemodynamics. Factors including impaired endothelium-dependent vasodilation (Tziomalos *et al.*, 2010), pericyte regulation of capillary contractility (Prakash *et al.*, 2012), alterations in neurotransmitter production (Auer *et al.*, 2015), neuron-astrocyte interactions (Zheng *et al.*, 2017), and changes in concentration of arachidonic acid brain metabolites (Sharma *et al.*, 2012) may contribute to the Cafeteria diet-induced reduction in cerebrovascular reactivity, as diet and metabolic conditions such as diabetes significantly alter each of these factors. Additional experiments are required to determine the specific mechanisms underlying the effects of the Cafeteria diet on cerebrovascular hemodynamics. Further, investigation of sub-region differences in the cortical perfusion response to hypercapnia is warranted. Indeed, in humans with significant cardiovascular disease risk factors, cerebrovascular reactivity is reduced in the cingulate cortex relative to the sensorimotor cortex (Haight *et al.*, 2015). This analysis was precluded in the current study due to the limited coverage of the CASL acquisition and its low sensitivity.

Taken together, we have shown that the Cafeteria diet model of metabolic syndrome increases resting cerebral perfusion and attenuates cerebrovascular reactivity to hypercapnia in the cortex and hippocampus. Moreover, while switching rats to a healthy diet recovers peripheral features of metabolic syndrome (Gomez-Smith *et al.*, 2016), it only partially improves cerebrovascular reactivity. This is the first study to use CASL MRI to examine perfusion in a clinically relevant rodent model of metabolic syndrome. Our results provide evidence for the role of ultra-processed foods in reducing cerebrovascular reserve capacity, a critical function in healthy neurovascular coupling and cognition.

Acknowledgments

The authors would like to thank Margaret Koletar for invaluable technical support, advice and help with experiments.

Conflict of Interest

The Author(s) declare(s) that there is no conflict of interest.

Funding

This work was supported by the Canadian Institutes of Health Research [grant number 102534 to D.C.], the Canadian Consortium on Neurodegeneration and Aging, the Canadian Vascular Network, the Heart and Stroke Foundation of Canada [Focus on Stroke doctoral scholarship to M.G.S.], and the Canadian Partnership for Stroke Recovery.

Chapter 4 - General Discussion

1. Summary

Animal models of metabolic syndrome have greatly contributed to understanding disease pathophysiology including its detrimental effects on the brain (Varga *et al.*, 2010). The growing understanding of the important role played by dietary patterns, nutrient combinations, and ultra-processed foods in the development of metabolic syndrome (Mozaffarian, 2016) have caused a renewed interest in complex rodent diets such as the Cafeteria diet (Barrett *et al.*, 2016). However, despite being used for decades to study metabolic disruption (Sclafani & Springer, 1976) and feeding behavior (Sclafani, 1987), Cafeteria diets have received criticism because of their variable nutritional composition (Moore, 1987; Lai *et al.*, 2014). For that reason, the first goal of my thesis was to demonstrate that the Cafeteria diet is a translationally relevant model of metabolic syndrome by undertaking a detailed characterization of the diet's nutritional composition and by assessing its ability to generate metabolic syndrome features. Data to this effect was presented in Chapter 2 of my thesis.

The collective cluster of metabolic syndrome features increases cardiovascular disease risk by 60% and has a greater impact on disease causation than any of its individual components in isolation (Boden-Albala *et al.*, 2008). Moreover, individuals with metabolic syndrome are more likely to develop cognitive deficits later in life (Yaffe *et al.*, 2004). This enhanced disease risk is the result of pathological changes affecting the cerebrovasculature and brain parenchyma resulting from chronic low-grade inflammation and oxidative stress caused by surplus metabolic fuels (Yates *et al.*, 2012). To determine whether the Cafeteria diet produces common metabolic syndrome comorbidities, the

second goal of my thesis was to investigate the effects of chronic Cafeteria diet consumption on cognitive performance, neuroinflammation, as well as on cerebrovascular structure and function. These results were described in Chapters 2 and 3 of my thesis.

While a nutritionally balanced diet, in combination with regular exercise, can improve metabolic syndrome features (Mozaffarian, 2016), it is less clear to what extent cerebrovascular and other central nervous system-related effects are reversible. The third goal of my thesis was therefore to determine whether certain biological processes are more recalcitrant to dietary reversal than others by testing a diet 'switch' group of rats alongside SD control and Cafeteria diet-fed CAF rats. This SWT group of rats was used in experiments in Chapters 2 and 3 of my thesis.

2. Principal Findings and Scientific Impact

a. The Cafeteria diet is a translationally relevant model of human diet

Daily recording of food intake determined that, on average, Cafeteria diet-fed rats consumed ~40% of total energy from fat, ~49% from carbohydrate and ~11% from protein despite being provided *ad libitum* access to a combination of 16 ultra-processed human food items, standard chow, and a 12% sucrose solution. Moreover, these relative proportions remained constant over the course of the four months of the experiment. In comparison, according to the 2004 Canadian Community Health Survey (CCHS), the average adult Canadian consumed between 30.5% to 32.2% of energy from fat, which varied based on age and gender (Health Canada & Statistics Canada, 2004). Similarly, 47.3% to 55.5% of energy came from carbohydrates while 14.0% to 17.0% of energy was from protein.

It is challenging to directly compare our results with those of the CCHS due to the inherent difference in nature of the two data collection methods. Indeed, owing to the survey format of the CCHS, it has been estimated that energy intake was under-reported by ~10% (Garriguet, 2008). Moreover, the data from the CCHS is out of date. Given the modest reduction in energetic intake seen in the United States between 2004 and 2010 (Ng *et al.*, 2014), more recent Canadian data would be of great value. Nonetheless, we can see that the voluntary feeding pattern of Cafeteria diet rats is approximately in line with that of the average Canadian. This is particularly true in regards to carbohydrate preference, though CAF rats are biased towards greater fat intake at the expense of protein. Additional analysis of the feeding patterns of Cafeteria diet-fed rats (data not shown) revealed that the relative intake by weight of standard chow (~35%) and ultra-processed food items (~65%) as well as sucrose solution (~20 ml/animal/day) was constant across time points. Furthermore, the amount consumed of a given Cafeteria food item also varied little between feeding sessions across the four months of the experiment. This would indicate that consistent feeding behaviour can be obtained when using the Cafeteria diet.

b. The Cafeteria diet is an effective model of metabolic syndrome

The Cafeteria diet led to the development of features akin to human metabolic syndrome as per the 2009 harmonized definition (Alberti *et al.*, 2009*a*). Indeed, after three months of Cafeteria diet feeding, CAF rats were significantly different from SD chow-fed rats on three of the five essential components: abdominal obesity, low HDL cholesterol, and raised triglyceride. CAF rats were also insulin resistant, exhibiting hyperinsulinemia and glucose intolerance, indicative of a pre-diabetic state (Brownlee,

2001). Of interest, the combination of these three particular metabolic syndrome features is also the most common among Canadians, representing ~30% of all cases (Riediger & Clara, 2011).

Despite exhibiting most metabolic syndrome features after three months on the diet, Cafeteria diet-fed rats were likely not hypertensive at this time point. In an additional study that I performed involving a small cohort of animals (N=2 SD, 3 CAF), rats were chronically implanted with telemetry probes for one month, recording cardiovascular parameters on an hourly basis. Mean values are summarized in **Appendix 1**. Briefly, systolic blood pressure was not different between rats of either diet and diastolic and mean arterial pressure were both significantly reduced in CAF rats. In addition, CAF rats exhibited raised heart rate and pulse pressure compared to SD. Though CAF rats were not hypertensive, these results indicate a possible pre-hypertensive state. Indeed, hypertension is a product of both cardiac output and systemic vascular resistance, with the contribution of each changing over time (Johnson *et al.*, 2015). In individuals with pre-hypertension, heart rate and cardiac output are elevated while peripheral vascular resistance is normal. Over time, this increased cardiac activity causes the walls of large elastic arteries to deteriorate, increasing vascular resistance (Fox & Ferrari, 2011). It is therefore probable that long-term exposure to the Cafeteria diet might eventually result in hypertension.

Taken together, these findings support the use of the Cafeteria diet as an effective and translationally relevant model of metabolic syndrome that closely approximates human symptomatology and dietary patterns.

c. The Cafeteria diet does not cause deficits in spatial learning and memory as assessed with the Barnes maze

Because metabolic syndrome is a significant risk factor for cognitive impairment (Yaffe et al., 2004), I sought to investigate whether the Cafeteria diet negatively affects cognition. In particular, I was interested in examining spatial learning and memory, a domain that is especially vulnerable to the effects of diet in rodents (Kanoski & Davidson, 2010; Beilharz *et al.*, 2014). I chose to assess rats' ability to learn the Barnes maze rather than other common spatial orientation tasks using radial arm or T mazes in order to avoid confounding factors related to the increased stress associated with long-term food deprivation (Homberg, 2013) or the differential priming effect of palatable foods versus chow on food approach behaviours (Liu et al., 2016). Despite the ability of the Cafeteria diet to induce metabolic syndrome, I did not observe a significant effect of diet on any of the evaluated outcome measures in the Barnes maze. These included: total errors committed in search of the escape box, re-entry errors to previously visited holes, reference memory errors by visiting incorrect holes, deviation distance from the escape box on first approach, number of escape hole omissions, as well as spatial, serial, or random search strategies.

To the best of my knowledge, ours is the first study to assess spatial learning and memory using the Barnes maze in Cafeteria diet-fed Sprague Dawley rats. Moreover, only one other study of Sprague Dawley rats fed a high-energy diet has used a similar Barnes maze paradigm (Hsu et al., 2015). In the latter, consumption of either a sucrose or high-fructose corn syrup solution for 30 days impaired learning in adolescent rats. However, adult rats provided either sweetened beverage for the same amount of time were not impaired. This greater susceptibility of adolescent rodents to diet-dependent

learning impairments has been observed by others (Boitard et al., 2012; Valladolid-Acebes et al., 2013). Furthermore, juvenile rodents also exhibit a greater vulnerability to diet-induced obesity than adults (de Castro et al., 2013). It was for this reason that I was motivated to start the Cafeteria diet in four week-old rats.

Other rodent models of metabolic syndrome using adult animals have failed to show impairments in learning to navigate the Barnes maze. Otsuka Long-Evans Tokushima Fatty (OLETF) rats, pre-diabetic at 20 weeks of age and transitioning to overt type 2 diabetes by 40 weeks, did not show a reduced ability to learn the Barnes maze at either time point (Olver et al., 2017). Likewise, two mouse strains, C57Bl/6 and Swiss Webster mice, fed a 60% high-fat diet for eight weeks were not impaired in acquisition of the Barnes maze task (Anderson et al., 2014). It is likely that the Barnes maze is not sufficiently sensitive to detect subtle spatial cognitive deficits in adult rodents caused by high-energy diets. Indeed, tasks in which animals commit few errors early in acquisition, as is the case with the Barnes maze (~5 errors after 6 trials), offer a limited range of possible scores from which it is possible to determine significant main effects (Vorhees & Williams, 2014).

Future experiments employing a battery of behavioural tasks would therefore be warranted to further query the impact of the Cafeteria diet on cognitive ability. One such task, the Morris water maze, was not readily available for use with rats in our behaviour core facility. Nonetheless, it has revealed itself to be sufficiently sensitive in detecting interesting, yet discrepant, findings regarding hippocampal-dependent spatial memory in rodent studies using different energy-dense diets (Greenwood & Winocur, 1990; Molteni *et al.*, 2002; Arvanitidis *et al.*, 2009). While the aversive conditions of the Morris water maze are significantly greater than in the Barnes maze (Harrison et al., 2009), mild

cognitive impairments may only be revealed with the presence of an additional load of stress. Another candidate, the attention set-shift task, may be of interest as it is a sensitive measure of executive function (Cordova et al., 2014). A combination of tasks such as these that target a variety of neural substrates and that do not rely heavily on food deprivation or food reward would help to clarify the impact of ultra-processed foods on cognition.

d. The Cafeteria diet causes hippocampal inflammation but does not affect microvessel density or vessel integrity

High-energy diets and metabolic syndrome are inexorably associated with systemic inflammation in humans (Hotamisligil, 2006; Després, 2012). Moreover, there is mounting evidence from animal studies for a similar role in neuroinflammation, characterized in part by increased microglial proliferation (Miller & Spencer, 2014). Consequently, examination of the ability of the Cafeteria diet to induce neuroinflammation was warranted. To this end, I used stereology to quantify microglial density in the hippocampus and the hypothalamus, regions where increased neuroinflammation has been detected in other rodent models of metabolic syndrome (Beilharz *et al.*, 2014; Valdearcos *et al.*, 2014; Bocarsly *et al.*, 2015).

Microglial density was increased in the hippocampal CA1 region of CAF rats, confirming that the Cafeteria diet produces neuroinflammation. While more highly ramified microglia have been observed in the hippocampi of high-fat fed rats (Bocarsly *et al.*, 2015) and inflammatory markers were elevated in hippocampal mRNA extracts of Cafeteria diet-fed rats (Beilharz *et al.*, 2014), to the best of my knowledge my study is the first to show increased hippocampal microglial proliferation in a dietary model of

metabolic syndrome. As microglial proliferation represents an early functional state in the sequence of microglial activation (Gomez-Nicola & Perry, 2015), future experiments to more completely characterize morphological changes would be merited. Indeed, identification of the graded state of microglial activation via the use of multiple histological markers would help to distinguish between activated microglia that exert a beneficial homeostatic role and cytotoxic microglia with the potential to contribute to neurodegeneration (Marshall *et al.*, 2013).

Though microglial proliferation has been observed in the hypothalamus of high-fat fed rats (Thaler *et al.*, 2012; Berkseth *et al.*, 2014; Valdearcos *et al.*, 2014), I did not observe an effect of diet on microglial density in the arcuate nucleus. The disparity between our findings and those of others may result from species differences or the type and concentration of fat used in the different diets. Indeed, a high concentration (60%) saturated but not monounsaturated fat diet induced hypothalamic microglial proliferation in gavage-fed mice (Valdearcos et al., 2014). In contrast, saturated fat represented only ~13% of total calories in our Cafeteria diet and total fat content was comprised of various fat types. This dose was potentially insufficient to cause microglial proliferation in the hypothalamus of CAF rats. Moreover, our divergent findings in the hippocampus and hypothalamus may follow from region-specific mechanisms related to the uptake and metabolism of specific lipid sub-types which vary between brain regions (Valdearcos *et al.*, 2014).

After confirming that the Cafeteria diet causes neuroinflammation, I investigated its impact on microvessel structure and integrity given that the cerebrovasculature, central to healthy brain perfusion and cognitive performance, is a key target of inflammatory insults (Gorelick *et al.*, 2011). To assess general vessel viability, I quantified microvessel density

in naïve SD, CAF, and SWT brains as well as after an ischemic challenge by way of endothelin-1 injections to the cortex. In addition, I evaluated BBB integrity by measuring IgG extravasation in the hippocampus and the hypothalamus. The Cafeteria diet did not produce significantly different results from those of SD control rats on any of these measures.

Contrasting these results with those of others helps to shed light on the specific pathologies that underlie changes to the cerebrovasculature while also revealing the critical importance in the choice of metabolic syndrome model. Contrary to my findings regarding vessel density prior to and following stroke, two genetic rodent models of type 2 diabetes, the Goto-Kakizaki rat and the db/db mouse, exhibit increased baseline vessel density with concomitant vulnerability to an ischemic challenge (Prakash *et al.*, 2013*b*). Glucose homeostatic dysregulation is critically important as these effects are completely abrogated in Goto-Kakizaki rats treated with metformin (Prakash *et al.*, 2013*a*, 2013*b*). While Cafeteria diet rats are insulin resistant they are not hyperglycemic, suggesting a critical role for hyperglycemia in aberrant angiogenesis. Nevertheless, STZ-induced type 1 diabetic mice with severe hyperglycemia do not exhibit increased vessel density (Tennant & Brown, 2013). Rodent genetic background may therefore be a critical factor in potentiating structural changes within the microvasculature.

The animal literature supports a role for diet and metabolic disruption in the disruption of the BBB. Naïve rats fed a high-fat/high-carbohydrate diet similar in general macronutrient composition to the Cafeteria diet exhibit increased BBB permeability with greater sodium fluorescein extrusion in the hippocampus and pre-frontal cortex (Davidson *et al.*, 2012). Similarly, rats fed a high-fat and 2% cholesterol diet show a change in expression of tight junction proteins around hippocampal and cortical

microvessels (Freeman & Granholm, 2012). Moreover, STZ-induced type 1 diabetes in rats increases generalized perfusion of 14C sucrose, further indicating a breakdown of BBB tight junctions (Hawkins *et al.*, 2007). Analogous findings are observed in the hypothalamus of mice fed a 58% high-fat diet, with increased IgG accumulation in the arcuate nucleus (Yi *et al.*, 2012). In addition, IgG has been observed within proliferating microglia in the arcuate nucleus, supposedly as the IgG molecule is actively phagocytosed by these scavenger cells (Gao *et al.*, 2014). Our negative findings are difficult to interpret in the absence of comparable studies using a Cafeteria diet. Complementary histological experiments, involving Evans blue or fluorescein infusion prior to sacrifice, or the examination of tight junction protein expression would be called for to conclusively determine whether the Cafeteria diet does or does not have an effect on BBB integrity.

e. The Cafeteria diet impairs vascular hemodynamics by increasing resting perfusion and reducing cerebrovascular reactivity

While our choice of dietary metabolic syndrome model or experimental technique may explain the absence of manifest structural changes affecting the cerebrovasculature, it is quite possible that longer exposure to the Cafeteria diet may have induced pathological structural changes. Nonetheless, absence of structural alterations does not preclude functional cerebrovascular deficits. Therefore, using CASL MRI, a sensitive and non-invasive imaging technique, I examined resting perfusion and cerebrovascular reactivity to a CO_2 challenge in both the hippocampus and cortex. In both regions, while the Cafeteria diet caused rats to exhibit raised resting perfusion relative to control rats, cerebrovascular reactivity to the potent vasodilator was significantly reduced.

The resting perfusion findings are in contrast to predictions from the human literature. Studies of subjects with varying degrees of metabolic dysfunction, including insulin resistance (Baker et al., 2011; Rusinek et al., 2015), type 2 diabetes (Last et al., 2007), obesity (Willeumier et al., 2011), and metabolic syndrome (Birdsill et al., 2013) have all shown lower resting perfusion compared to healthy controls. While low resting perfusion may result from vascular dysfunction, it may also be a consequence of global or regional brain atrophy (Sabri et al., 2000). Indeed, a smaller brain has diminished energetic, and therefore blood flow, requirements (Wardlaw et al., 2003). As brain atrophy is the ultimate outcome of large-scale neuronal senescence and cell loss (Dorszewska, 2013), it represents a later stage in neuropathology. Elevated resting perfusion in our Cafeteria diet model may instead reflect early functional vascular dysfunction preceding brain atrophy, vascular structural changes, and cognitive impairment. Though limited evidence regarding resting perfusion exists in animal models, a study examining STZ-induced type 1 diabetic mice appears to confirm our findings, showing an elevation in blood flow velocity (Tennant & Brown, 2013).

On the other hand, the observation of reduced cerebrovascular reactivity to CO_2 challenges in Cafeteria diet-fed rats was not surprising as both human studies of metabolic syndrome (Giannopoulos et al., 2010; Tyndall et al., 2016) and studies of rats fed a high-fat diet (Li et al., 2013) have reported similar findings. Nonetheless, the joint observation of increased resting perfusion and decreased cerebrovascular reactivity was unexpected. Indeed, reduced vascular reactivity is typically associated with a decreased capacity for vasodilation, leading to increased vessel resistance and consequently to low CBF (Cipolla, 2009). In the absence of comparable studies examining both resting

perfusion and cerebrovascular reactivity in younger individuals, insight may be gained from other disease states.

Similar findings of raised resting perfusion and decreased cerebrovascular reactivity have been seen in patients with MELAS syndrome (mitochondrial encephalomyopathy, lactic acidosis, and stroke-like episodes), a genetic disorder characterized by mitochondrial dysfunction (Rodan et al., 2015). In MELAS patients, mitochondria overproduce lactic acid, causing lactic acidosis. This is thought to increase resting perfusion based on the high responsiveness of CBF autoregulatory mechanisms to small changes in pH. In fact, a small drop in pH from 7.4 to 7.0 causes notable vasodilation through a shift in smooth muscle cell calcium channel activity (Dabertrand et al., 2012). Of interest to my study, overfeeding of a 'Western' diet also causes pH to decrease to the lower end of the physiological range (Williams *et al.*, 2016*a*). Consequently, raised resting CBF in our Cafeteria diet model may result from chronic vasodilation caused by diet-induced blood acidosis. Furthermore, this phenomenon may contribute to the reduction in cerebrovascular reactivity in CAF rats as additional vasodilation in response to CO_2 may be restricted due to a reduced range in vessel dilatory capacity (Bright et al., 2011). However, given our findings in SWT rats whereby cortical cerebrovascular reactivity remained impaired while resting perfusion recovered almost to SD levels after the transition to chow, mechanisms other than a reduction in dilatory reserve may be at play.

f. The pathophysiological effects of the Cafeteria diet are not fully reversible

In conjunction with most of the studies presented in this thesis, SD and CAF rats were compared to SWT rats that underwent a switch from the Cafeteria diet to chow for one

month. This was done in order to evaluate the degree of reversibility of different pathologies. The diet switch allowed complete recovery of all metabolic syndrome features and also decreased neuroinflammation in the hippocampus. Furthermore, resting perfusion returned to SD levels after one month of diet switch. However, cerebrovascular reactivity to CO_2 in the hippocampus was only partially improved while no improvement was seen in the cortex of SWT rats, remaining significantly blunted compared to SD rats.

Regarding cerebrovascular reactivity, the greater vulnerability of the cortex compared to the hippocampus is curious given that CA1 neurons are particularly vulnerable to hypoxic ischemic insult (Langdon *et al.*, 2008). While the comparatively lower microvessel density in the CA1 may be partly responsible (Cavaglia et al., 2001), different intracellular properties of neurons in each region likely play a greater role (Zhu *et al.*, 2012). Instead, the manner in which blood is supplied to each region might hold an important clue. Indeed, the hippocampus is directly supplied by a large caliber vessel, the longitudinal hippocampal artery (Coyle, 1976), while the cortex is fed by smaller caliber penetrating arterioles (Cavaglia et al., 2001). The latter are considered a 'bottleneck' in cortical perfusion as occlusion of an individual vessel is capable of significantly reducing local blood flow and inducing behavioural deficits (Shih et al., 2013).

The complete reversal of metabolic syndrome features following one month of switch to chow was to be expected given the findings of other animal studies (Parekh *et al.*, 1998; Berkseth *et al.*, 2014; Littlejohns *et al.*, 2014). Moreover, the maintenance of cerebrovascular impairments despite recovery of metabolic syndrome features parallels the findings of human lifestyle interventions using low-fat diets (Howard *et al.*, 2006; The Look AHEAD Research Group, 2014). Nonetheless, this finding is not unique to the cerebrovasculature. Indeed, Littlejohn *et al.* observed the maintenance of cardiomyocyte

contractility deficits subsequent to the consumption of a high-fat diet despite switching mice to regular chow for four to six weeks (Littlejohns *et al.*, 2014). An extrapolation could be made that the molecular mechanisms regulating cardiomyocyte contractility affected by high-fat diet may be similar to those affecting the cerebrovasculature, perhaps at the level of the smooth muscle cell layer.

3. Conclusions and Future Directions

Taken together, the results presented in this thesis support the use of the Cafeteria diet as an effective and highly relevant model of metabolic syndrome. Rats fed the diet for three months develop several features of metabolic syndrome, including abdominal obesity, dyslipidemia, and insulin resistance. In addition, Cafeteria diet-fed rats exhibit hippocampal inflammation and changes to cerebrovascular hemodynamics characterized by elevated resting perfusion and decreased cerebrovascular reactivity to a vasodilator. Moreover, the persistent cortical deficits in cerebrovascular reactivity may serve as a potential early target for clinical interventions to minimize eventual cognitive impairments.

Several aspects of the research presented in this thesis would benefit from further investigation to validate specific hypotheses. Conducting experiments in rats fed the Cafeteria diet for a longer duration (e.g. 12-16 months) would aid in determining whether hypertension or vascular structural changes would occur with a greater degree of metabolic pathology. Moreover, a longer diet duration could be useful in determining whether Cafeteria diet rats eventually develop resting hypoperfusion in line with the human evidence. In addition, a diet switch of longer duration would inform the important question as to whether cerebrovascular reactivity in the cortex can eventually be

normalized or whether abnormalities are permanent. Regarding cognitive deficits and behavioural testing, employing a battery of more sensitive tests in animals maintained on the Cafeteria diet into middle or early old age may be much more revealing of spatial learning and memory deficits. Also, further histological studies aimed at elucidating the graded state of microglial activation would be useful in determining whether neuroinflammation caused by the Cafeteria diet is beneficial perhaps initially, but with longer exposure becomes cytotoxic. Finally, the use of additional histological techniques to evaluate BBB permeability would be warranted to conclusively determine the effect of the Cafeteria diet on vascular integrity.

In addition to these potential future studies, the important discoveries made in the last few years regarding the interaction between diet and the gut microbiome (Turnbaugh *et al.*, 2009*b*) as well as their relationship to cardio-metabolic disease (Vinjé *et al.*, 2014) and brain dysfunction (Noble *et al.*, 2017) warrant investigation in the context of our Cafeteria diet model. Recently, Beilharz *et al.* demonstrated that a Cafeteria diet dramatically alters the composition of the gut microbiome compared to that of chow-fed Sprague Dawley rats (Beilharz *et al.*, 2017). Furthermore, probiotic treatment prevented Cafeteria diet-induced hippocampal-dependent deficits in spatial memory in a novel place task. Stemming from these findings, it would be interesting to test whether a similar probiotic treatment could recover the Cafeteria diet-induced cerebrovascular hemodynamic dysfunction described in our experiments. In particular, this experiment is relevant as comparatively little is known regarding the connection between gut dysbiosis and cerebrovascular function (Talmor-Barkan & Kornowski, 2017). Nonetheless, evidence from another recent study suggests that such a connection does exist as butyrate

treatment in high-fat diet-fed low-density-lipoprotein receptor knockout mice fully recovers impairments in cerebrovascular perfusion (Arnoldussen *et al.*, 2017).

In conclusion, several novel findings presented in my thesis, in particular the reversible increase in microglial hippocampal proliferation in rats fed a high-energy Cafeteria diet and the irreversible impairment of cerebrovascular reactivity in cortical tissue, are notable and are an exciting addition to the body of literature regarding the role of ultra-processed foods on the cerebrovasculature.

References

Aguilar M, Bhuket T, Torres S, Liu B & Wong RJ (2015). Prevalence of the metabolic syndrome in the United States, 2003-2012. *JAMA* **313,** 1973–1974.

Alberti KGMM, Eckel RH, Grundy SM, Zimmet PZ, Cleeman JI, Donato KA, Fruchart J-C, James WPT, Loria CM & Smith SC (2009*a*). Harmonizing the Metabolic Syndrome. *Circulation* **120,** 1640–1645.

Alberti KGMM, Eckel RH, Grundy SM, Zimmet PZ, Cleeman JI, Donato KA, Fruchart J-C, James WPT, Loria CM & Smith SC (2009*b*). Harmonizing the metabolic syndrome: A joint interim statement of the International Diabetes Federation task force on epidemiology and prevention; National Heart, Lung, and Blood Institute; American Heart Association; World Heart Federation; International. *Circulation* **120,** 1640–1645.

Alberti KGMM & Zimmet P (1998). Definition, diagnosis and classification of diabetes mellitus and its complications. Part 1: diagnosis and classification of diabetes mellitus. Provisional report of a WHO consultation. *Diabet Med* **15,** 539–553.

Alberti KGMM, Zimmet P, Shaw J & IDF Epidemiology Task Force Consensus Group (2005). The metabolic syndrome - A new worldwide definition. *Lancet* **366,** 1059–1062.

Aleixandre de Artiñano A & Miguel Castro M (2009). Experimental rat models to study the metabolic syndrome. *Br J Nutr* **102,** 1246–1253.

Almiron-Roig E & Drewnowski A (2003). Hunger, thirst, and energy intakes following consumption of caloric beverages. *Physiol Behav* **79,** 767–773.

Anderson NJ, King MR, Delbruck L & Jolivalt CG (2014). Role of insulin signaling

impairment, adiponectin and dyslipidemia in peripheral and central neuropathy in mice. *Dis Model Mech* **7,** 625–633.

Antonopoulos AS, Oikonomou EK, Antoniades C & Tousoulis D (2016). From the BMI paradox to the obesity paradox: the obesity-mortality association in coronary heart disease. *Obes Rev* **10,** 989–1000.

Arnoldussen IAC, Wiesmann M, Pelgrim CE, Wielemaker EM, van Duyvenvoorde W, Amaral-Santos PL, Verschuren L, Keijser BJF, Heerschap A, Kleemann R, Wielinga PY & Kiliaan AJ (2017). Butyrate restores HFD-induced adaptations in brain function and metabolism in mid-adult obese mice. *Int J Obes* **41,** 935–944.

Arvanitidis AP, Corbett D & Colbourne F (2009). A high fat diet does not exacerbate CA1 injury and cognitive deficits following global ischemia in rats. *Brain Res* **1252,** 192–200.

Attuquayefio T, Stevenson RJ, Boakes RA, Oaten MJ, Yeomans MR, Mahmut M & Francis HM (2016). A high-fat high-sugar diet predicts poorer hippocampal-related memory and a reduced ability to suppress wanting under satiety. *J Exp Psychol Anim Learn Cogn* **42,** 415–428.

Auer MK, Sack M, Lenz JN, Jakovcevski M, Biedermann S V, Falfán-Melgoza C, Deussing J, Steinle J, Bielohuby M, Bidlingmaier M, Pfister F, Stalla GK, Ende G, Weber-Fahr W, Fuss J & Gass P (2015). Effects of a high-caloric diet and physical exercise on brain metabolite levels: a combined proton MRS and histologic study. *J Cereb Blood Flow Metab* **35,** 554–564.

Avena NM, Rada P & Hoebel BG (2008). Evidence for sugar addiction: behavioral and neurochemical effects of intermittent, excessive sugar intake. *Neurosci Biobehav Rev* **32,** 20–39.

Baker LD, Cross DJ, Minoshima S, Belongia D, Watson GS & Craft S (2011). Insulin resistance and Alzheimer-like reductions in regional cerebral glucose metabolism for cognitively normal adults with prediabetes or early type 2 diabetes. *Arch Neurol* **68,** 51–57.

Barrett P, Mercer JG & Morgan PJ (2016). Preclinical models for obesity research. *Dis Model Mech* **9,** 1245–1255.

Batsis JA, Nieto-Martinez RE & Lopez-Jimenez F (2007). Metabolic syndrome: from global epidemiology to individualized medicine. *Clin Pharmacol Ther* **82,** 509–524.

Beilharz JE, Kaakoush N, Maniam J & Morris MJ (2017). Cafeteria diet and probiotic therapy: cross talk among memory, neuroplasticity, serotonin receptors and gut microbiota in the rat. *Mol Psychiatry*.

Beilharz JE, Maniam J & Morris MJ (2014). Short exposure to a diet rich in both fat and sugar or sugar alone impairs place, but not object recognition memory in rats. *Brain Behav Immun* **37,** 134–141.

Bergman RN, Kim SP, Catalano KJ, Hsu IR, Chiu JD, Kabir M, Hucking K & Ader M (2006). Why visceral fat is bad: mechanisms of the metabolic syndrome. *Obesity* **14,** 16S–19S.

Berkseth KE, Guyenet SJ, Melhorn SJ, Lee D, Thaler JP, Schur EA & Schwartz MW (2014). Hypothalamic gliosis associated with high-fat diet feeding is reversible in mice: a combined immunohistochemical and magnetic resonance imaging study. *Endocrinology* **155,** 2858–2867.

Bernhardt J, Borschmann K, Boyd L, Carmichael ST, Corbett D, Cramer SC, Hoffmann T, Kwakkel G, Savitz SI, Saposnik G, Walker M & Ward N (2016). Moving rehabilitation research forward: developing consensus statements for rehabilitation

and recovery research. *Int J Stroke* **11,** 454–458.

Berthoud H-R, Münzberg H, Richards BK & Morrison CD (2012). Neural and metabolic regulation of macronutrient intake and selection. *Proc Nutr Soc* **71,** 390–400.

Bettcher BM & Kramer JH (2014). Longitudinal inflammation, cognitive decline, and Alzheimer's disease: a mini-review. *Clin Pharmacol Ther* **96,** 464–469.

Birdsill AC, Carlsson CM, Willette AA, Okonkwo OC, Johnson SC, Xu G, Oh JM, Gallagher CL, Koscik RL, Jonaitis EM, Hermann BP, LaRue A, Rowley HA, Asthana S, Sager MA & Bendlin BB (2013). Low cerebral blood flow is associated with lower memory function in metabolic syndrome. *Obesity* **21,** 1313–1320.

Black SE (2011). Vascular cognitive impairment: epidemiology, subtypes, diagnosis and management. *J R Coll Physicians Edinb* **41,** 49–56.

Bocarsly ME, Fasolino M, Kane GA, LaMarca EA, Kirschen GW, Karatsoreos IN, McEwen BS & Gould E (2015). Obesity diminishes synaptic markers, alters microglial morphology, and impairs cognitive function. *PNAS* **112,** 15731–15736.

Boden-Albala B, Sacco RL, Lee H-S, Grahame-Clarke C, Rundek T, Elkind M V, Wright C, Giardina E-G V, DiTullio MR, Homma S & Paik MC (2008). Metabolic syndrome and ischemic stroke risk: Northern Manhattan Study. *Stroke* **39,** 30–35.

Boitard C, Etchamendy N, Sauvant J, Aubert A, Tronel S, Marighetto A, Layé S & Ferreira G (2012). Juvenile, but not adult exposure to high-fat diet impairs relational memory and hippocampal neurogenesis in mice. *Hippocampus* **22,** 2095–2100.

Bokura H, Yamaguchi S, Iijima K, Nagai A & Oguro H (2008). Metabolic syndrome is associated with silent ischemic brain lesions. *Stroke* **39,** 1607–1609.

Bonora E, Kiechl S, Willeit J, Oberhollenzer F, Egger G, Targher G, Alberiche M, Bonadonna RC & Muggeo M (1998). Prevalence of insulin resistance in metabolic

disorders: The Bruneck Study. *Diabetes* **47,** 1643–1649.

Borogovac A & Asllani I (2012). Arterial Spin Labeling (ASL) fMRI: advantages, theoretical constraints and experimental challenges in neurosciences. *Int J Biomed Imaging* **2012,** 1–13.

Braniste V, Al-Asmakh M, Kowal C, Anuar F, Abbaspour A, Tóth M, Korecka A, Bakocevic N, Ng LG, Kundu P, Gulyás B, Halldin C, Hultenby K, Nilsson H, Hebert H, Volpe BT, Diamond B & Pettersson S (2014). The gut microbiota influences blood-brain barrier permeability in mice. *Sci Transl Med* **6,** 1–11.

Bray GA (1985). Complications of obesity. *Ann Intern Med* **103,** 1052–1062.

Bright MG, Donahue MJ, Duyn JH, Jezzard P & Bulte DP (2011). The effect of basal vasodilation on hypercapnic and hypocapnic reactivity measured using magnetic resonance imaging. *J Cereb Blood Flow Metab* **31,** 426–438.

Brownlee M (2001). Biochemistry and molecular cell biology of diabetic complications. *Nature* **414,** 813–820.

Bruce-Keller AJ, Salbaum JM, Luo M, Blanchard E, Taylor CM, Welsh DA & Berthoud H-R (2015). Obese-type Gut Microbiota Induce Neurobehavioral Changes in the Absence of Obesity. *Biol Psychiatry* **77,** 607–615.

Buchenauer T, Behrendt P, Bode FJ, Horn R, Brabant G, Stephan M & Nave H (2009). Diet-induced obesity alters behavior as well as serum levels of corticosterone in F344 rats. *Physiol Behav* **98,** 563–569.

Buettner R, Parhofer KG, Woenckhaus M, Wrede CE, Kunz-Schughart LA, Schölmerich J & Bollheimer LC (2006). Defining high-fat-diet rat models: metabolic and molecular effects of different fat types. *J Mol Endocrinol* **36,** 485–501.

Canada S (2015). Directly measured physical activity in adults, 2012 and 2013. *Fact*

Sheet Cat #82-625-X. Available at: http://www.statcan.gc.ca/pub/82-625-x/2015001/article/14135-eng.htm.

Canfora EE, Jocken JW & Blaak EE (2015). Short-chain fatty acids in control of body weight and insulin sensitivity. *Nat Rev Endocrinol* **11,** 577–591.

Carmichael ST (2005). Rodent models of focal stroke: size, mechanism, and purpose. *NeuroRx* **2,** 396–409.

Carroll JF, Zenebe WJ & Strange TB (2006). Cardiovascular Function in a Rat Model of Diet-Induced Obesity. *Hypertension* **48,** 65–72.

de Castro UGM, dos Santos RAS, Silva ME, de Lima WG, Campagnole-Santos MJ & Alzamora AC (2013). Age-dependent effect of high-fructose and high-fat diets on lipid metabolism and lipid accumulation in liver and kidney of rats. *Lipids Health Dis* **12,** 1–11.

Cavaglia M, Dombrowski SM, Drazba J, Vasanji A, Bokesch PM & Janigro D (2001). Regional variation in brain capillary density and vascular response to ischemia. *Brain Res* **910,** 81–93.

Cavalieri M, Ropele S, Petrovic K, Pluta-Fuerst A, Homayoon N, Enzinger C, Grazer A, Katschnig P, Schwingenschuh P, Berghold A & Schmidt R (2010). Metabolic syndrome, brain magnetic resonance imaging, and cognition. *Diabetes Care* **33,** 2489–2495.

Chaston TB & Dixon JB (2008). Factors associated with percent change in visceral versus subcutaneous abdominal fat during weight loss: findings from a systematic review. *Int J Obes* **32,** 619–628.

Chen GC, Huang CY, Chang MY, Chen CH, Chen SW, Huang CJ & Chao PM (2011). Two unhealthy dietary habits featuring a high fat content and a sucrose-containing

beverage intake, alone or in combination, on inducing metabolic syndrome in Wistar rats and C57BL/6J mice. *Metabolism* **60,** 155–164.

Chugh BP, Bishop J, Zhou Y-Q, Wu J, Henkelman RM & Sled JG (2012). Robust method for 3D arterial spin labeling in mice. *Magn Reson Med* **68,** 98–106.

Cipolla MJ (2009). *The Cerebral Circulation*ed. Granger DN & Granger J. Morgan & Claypool Life Sciences.

Clément K, Vaisse C, Lahlou N, Cabrol S, Pelloux V, Cassuto D, Gourmelan M, Dina C, Chambaz J, Lacorte J-M, Basdevant A, Bougnères P, Lebouc Y, Froguel P & Guy-Grand B (1998). A mutation in the human leptin receptor gene causes obesity and pituitary dysfunction. *Nature* **392,** 398–401.

Coelho MS, Lopes KL, Freitas R de A, de Oliveira-Sales EB, Bergasmaschi CT, Campos RR, Casarini DE, Carmona AK, Araújo M da S, Heimann JC & Dolnikoff MS (2010). High sucrose intake in rats is associated with increased ACE2 and angiotensin-(1–7) levels in the adipose tissue. *Regul Pept* **162,** 61–67.

Corbett D, Jeffers M, Nguemeni C, Gomez-Smith M & Livingston-Thomas J (2015). Lost in translation: rethinking approaches to stroke recovery. *Prog Brain Res* **218,** 413–434.

Cordova CA, Jackson D, Langdon KD, Hewlett KA & Corbett D (2014). Impaired executive function following ischemic stroke in the rat medial prefrontal cortex. *Behav Brain Res* **258,** 106–111.

Cox RW & Jesmanowicz A (1999). Real-time 3D image registration for functional MRI. *Magn Reson Med* **42,** 1014–1018.

Coyle P (1976). Vascular patterns of the rat hippocampal formation. *Exp Neurol* **52,** 447–458.

Crichton GE, Elias MF, Davey A & Alkerwi A (2014). Cardiovascular health and cognitive function: the Maine-Syracuse Longitudinal Study ed. Ikram MA. *PLoS One* **9,** e89317.

Dabertrand F, Nelson MT & Brayden JE (2012). Acidosis dilates brain parenchymal arterioles by conversion of calcium waves to sparks to activate BK Channels. *Circ Res* **110,** 285–294.

Dai S & McNeill JH (1995). Fructose-induced hypertension in rats is concentration- and duration-dependent. *J Pharmacol Toxicol Methods* **33,** 101–107.

Danforth E (2000). Failure of adipocyte differentiation causes type II diabetes mellitus? *Nat Genet* **26,** 13–13.

Davidson TL, Kanoski SE, Walls EK & Jarrard LE (2005). Memory inhibition and energy regulation. *Physiol Behav* **86,** 731–746.

Davidson TL, Monnot A, Neal AU, Martin AA, Horton JJ & Zheng W (2012). The effects of a high-energy diet on hippocampal-dependent discrimination performance and blood-brain barrier integrity differ for diet-induced obese and diet-resistant rats. *Physiol Behav* **107,** 26–33.

Després J-P (2012). Abdominal obesity and cardiovascular disease: is inflammation the missing link? *Can J Cardiol* **28,** 642–652.

Després J-P & Lemieux I (2006). Abdominal obesity and metabolic syndrome. *Nature* **444,** 881–887.

Dorszewska J (2013). Cell biology of normal brain aging: synaptic plasticity–cell death. *Aging Clin Exp Res* **25,** 25–34.

Drewnowski A, Mennella JA, Johnson SL & Bellisle F (2012). Sweetness and food preference. *J Nutr* **142,** 1142S–1148S.

Dutton GR & Lewis CE (2015). The Look AHEAD Trial: implications for lifestyle intervention in type 2 diabetes mellitus. *Prog Cardiovasc Dis* **58,** 69–75.

Endres M, Engelhardt B, Koistinaho J, Lindvall O, Meairs S, Mohr JP, Planas A, Rothwell N, Schwaninger M, Schwab ME, Vivien D, Wieloch T & Dirnagl U (2008). Improving outcome after stroke: overcoming the translational roadblock. *Cerebrovasc Dis* **25,** 268–278.

Ergul A, Abdelsaid M, Fouda AY & Fagan SC (2014). Cerebral neovascularization in diabetes: implications for stroke recovery and beyond. *J Cereb Blood Flow Metab* **34,** 553–563.

Erny D et al. (2015). Host microbiota constantly control maturation and function of microglia in the CNS. *Nat Neurosci* **18,** 965–977.

Eskelinen MH, Ngandu T, Helkala E, Tuomilehto J, Nissinen A, Soininen H & Kivipelto M (2008). Fat intake at midlife and cognitive impairment later in life: a population-based CAIDE study. *Int J Geriatr Psychiatry* **23,** 741–747.

Estruch R, Ros E, Salas-Salvadó J, Covas M-I, Corella D, Arós F, Gómez-Gracia E, Ruiz-Gutiérrez V, Fiol M, Lapetra J, Lamuela-Raventos RM, Serra-Majem L, Pintó X, Basora J, Muñoz MA, Sorlí J V., Martínez JA & Martínez-González MA (2013). Primary Prevention of Cardiovascular Disease with a Mediterranean Diet. *N Engl J Med* **368,** 1279–1290.

Expert Panel on Detection Evaluation and Treatment of High Blood Cholesterol in Adults. (2001). Executive summary of the third report of the National Cholesterol Education Program (NCEP) expert panel on Detection, Evaluation, And Treatment of High Blood Cholesterol In Adults (Adult Treatment Panel III). *JAMA* **285,** 2486–2497.

Flegal KM, Carroll MD, Kuczmarski RJ & Johnson CL (1998). Overweight and obesity in the United States: prevalence and trends, 1960-1994. *Int J Obes* **22,** 39–47.

la Fleur SE, Luijendijk MCM, van Rozen a J, Kalsbeek A & Adan R a H (2011). A free-choice high-fat high-sugar diet induces glucose intolerance and insulin unresponsiveness to a glucose load not explained by obesity. *Int J Obes* **35,** 595–604.

Fox KM & Ferrari R (2011). Heart rate: a forgotten link in coronary artery disease? *Nat Rev Cardiol* **8,** 369–379.

Freeman LR & Granholm A-CE (2012). Vascular changes in rat hippocampus following a high saturated fat and cholesterol diet. *J Cereb Blood Flow Metab* **32,** 643–653.

Fu J -h., Sun H -s., Wang Y, Zheng W -q., Shi Z -y. & Wang Q -j. (2010). The Effects of a Fat- and Sugar-Enriched Diet and Chronic Stress on Nonalcoholic Fatty Liver Disease in Male Wistar Rats. *Dig Dis Sci* **55,** 2227–2236.

Gao Y, Ottaway N, Schriever SC, Legutko B, Garcia-Caceres C, de la Fuente E, Mergen C, Bour S, Thaler JP, Seeley RJ, Filosa J, Stern JE, Perez-Tilve D, Schwartz MW, Tschop MH & Yi CX (2014). Hormones and diet, but not body weight, control hypothalamic microglial activity. *Glia* **62,** 17–25.

Garriguet D (2008). Under-reporting of energy intake in the Canadian Community Health Survey. *Heal reports* **19,** 37–45.

Giannopoulos S, Boden-Albala B, Choi JH, Carrera E, Doyle M, Perez T & Marshall RS (2010). Metabolic syndrome and cerebral vasomotor reactivity. *Eur J Neurol* **17,** 1457–1462.

Gibbs J, Young RC & Smith GP (1973). Cholecystokinin decreases food intake in rats. *J Comp Physiol Psychol* **84,** 488–495.

van Golen LW, Huisman MC, Ijzerman RG, Hoetjes NJ, Schwarte LA, Lammertsma AA & Diamant M (2013). Cerebral blood flow and glucose metabolism measured with positron emission tomography are decreased in human type 1 diabetes. *Diabetes* **62,** 2898–2904.

Gomez-Nicola D & Perry VH (2015). Microglial dynamics and role in the healthy and diseased brain: a paradigm of functional plasticity. *Neurosci* **21,** 169–184.

Gómez-Pinilla F (2008). Brain foods: the effects of nutrients on brain function. *Nat Rev Neurosci* **9,** 568–578.

Gomez-Smith M, Karthikeyan S, Jeffers MS, Janik R, Thomason LA, Stefanovic B & Corbett D (2016). A physiological characterization of the Cafeteria diet model of metabolic syndrome in the rat. *Physiol Behav* **167,** 382–391.

Gorelick PB et al. (2011). Vascular contributions to cognitive impairment and dementia: a statement for healthcare professionals from the American Heart Association/American Stroke Association. *Stroke* **42,** 2672–2713.

Greenwood CE & Winocur G (1990). Learning and memory impairment in rats fed a high saturated fat diet. *Behav Neural Biol* **53,** 74–87.

Groop L (2000). Genetics of the metabolic syndrome. *Br J Nutr* **83 Suppl 1,** S39-48.

Grundy SM, Brewer HB, Cleeman JI, Smith SC & Lenfant C (2004). Definition of metabolic syndrome: report of the National Heart, Lung, and Blood Institute/American Heart Association conference on scientific issues related to definition. In *Circulation*, pp. 433–438.

Gustafson B, Hedjazifar S, Gogg S, Hammarstedt A & Smith U (2015). Insulin resistance and impaired adipogenesis. *Trends Endocrinol Metab* **26,** 193–200.

Haight TJ, Bryan RN, Erus G, Davatzikos C, Jacobs DR, D'Esposito M, Lewis CE &

Launer LJ (2015). Vascular risk factors, cerebrovascular reactivity, and the default-mode brain network. *Neuroimage* **115,** 7–16.

Hainsworth AH & Markus HS (2008). Do in vivo experimental models reflect human cerebral small vessel disease? A systematic review. *J Cereb Blood Flow Metab* **28,** 1877–1891.

Haller H (1977). Epidemiology and associated risk factors of hyperlipoproteinemia. *Zeitschrift für die gesamte Inn Medizin und ihre Grenzgebiete* **32,** 124–128.

Harrison FE, Hosseini AH & McDonald MP (2009). Endogenous anxiety and stress responses in water maze and Barnes maze spatial memory tasks. *Behav Brain Res* **198,** 247–251.

Hawkins BT, Ocheltree SM, Norwood KM & Egleton RD (2007). Decreased blood-brain barrier permeability to fluorescein in streptozotocin-treated rats. *Neurosci Lett* **411,** 1–5.

He J, Ogden LG, Vupputuri S, Bazzano LA, Loria C & Whelton PK (1999). Dietary sodium intake and subsequent risk of cardiovascular disease in overweight adults. *JAMA* **282,** 2027–2034.

Health Canada & Statistics Canada (2004). *Canadian Community Health Survey Cycle 2.2, Nutrition*.

Hermans MP, Levy JC, Morris RJ & Turner RC (1999). Comparison of insulin sensitivity tests across a range of glucose tolerance from normal to diabetes. *Diabetologia* **42,** 678–687.

Heyward FD, Walton RG, Carle MS, Coleman MA, Garvey WT & Sweatt JD (2012). Adult mice maintained on a high-fat diet exhibit object location memory deficits and reduced hippocampal SIRT1 gene expression. *Neurobiol Learn Mem* **98,** 25–32.

Higa TS, Spinola A V., Fonseca-Alaniz MH & Evangelista FS (2014). Comparison between cafeteria and high-fat diets in the induction of metabolic dysfunction in mice. *Int J Physiol Pathophysiol Pharmacol* **6,** 47–54.

Hills S, Balkau B, Coppack SW, Dekker JM, Mari A, Natali A, Walker M & Ferrannini E (1999). The EGIR-RISC STUDY (The European group for the study of insulin resistance: relationship between insulin sensitivity and cardiovascular disease risk): I. Methodology and objectives. *Diabetologia* **47,** 566–570.

Homberg JR (2013). Measuring behaviour in rodents: towards translational neuropsychiatric research. *Behav Brain Res* **236,** 295–306.

Hoogland ICM, Houbolt C, van Westerloo DJ, van Gool WA & van de Beek D (2015). Systemic inflammation and microglial activation: systematic review of animal experiments. *J Neuroinflammation* **12,** 1–13.

Hotamisligil GS (2006). Inflammation and metabolic disorders. *Nature* **444,** 860–867.

Howard B V. et al. (2006). Low-fat dietary pattern and risk of cardiovascular disease. *JAMA* **295,** 655–666.

Hsieh P-S, Tai Y-H, Loh C-H, Shih K-C, Cheng W-T & Chu C-H (2005). Functional interaction of AT1 and AT2 receptors in fructose-induced insulin resistance and hypertension in rats. *Metabolism* **54,** 157–164.

Hsu TM, Konanur VR, Taing L, Usui R, Kayser BD, Goran MI & Kanoski SE (2015). Effects of sucrose and high fructose corn syrup consumption on spatial memory function and hippocampal neuroinflammation in adolescent rats. *Hippocampus* **25,** 227–239.

Iadecola C (2013). The pathobiology of vascular dementia. *Neuron* **80,** 844–866.

Jalal FY, Yang Y, Thompson J, Lopez AC & Rosenberg GA (2012). Myelin loss

associated with neuroinflammation in hypertensive rats. *Stroke* **43,** 1115–1122.

Jeffers MS, Hoyles A, Morshead C & Corbett D (2014). Epidermal growth factor and erythropoietin infusion accelerate functional recovery in combination with rehabilitation. *Stroke* **45,** 1856–1858.

Jeon BT, Jeong EA, Shin HJ, Lee Y, Lee DH, Kim HJ, Kang SS, Cho GJ, Choi WS & Roh GS (2012). Resveratrol attenuates obesity-associated peripheral and central inflammation and improves memory deficit in mice fed a high-fat diet. *Diabetes* **61,** 1444–1454.

Johnson RJ, Lanaspa MA, Gabriela Sánchez-Lozada L & Rodriguez-Iturbe B (2015). The discovery of hypertension: evolving views on the role of the kidneys, and current hot topics. *Am J Physiol - Ren Physiol* **308,** F167–F178.

Joyner MJ (2014). Rethinking animal models and human obesity. *Physiology* **29,** 384–385.

Joyner MJ & Green DJ (2009). Exercise protects the cardiovascular system: effects beyond traditional risk factors. *J Physiol* **587,** 5551–5558.

Jurdak N, Lichtenstein AH & Kanarek RB (2008). Diet-induced obesity and spatial cognition in young male rats. *Nutr Neurosci* **11,** 48–54.

Kaakoush NO, Martire SI, Raipuria M, Mitchell HM, Nielsen S, Westbrook RF & Morris MJ (2016). Alternating or continuous exposure to cafeteria diet leads to similar shifts in gut microbiota compared to chow diet. *Mol Nutr Food Res* **0,** 1–9.

Kaess BM, Pedley A, Massaro JM, Murabito J, Hoffmann U & Fox CS (2012). The ratio of visceral to subcutaneous fat, a metric of body fat distribution, is a unique correlate of cardiometabolic risk. *Diabetologia* **55,** 2622–2630.

Kahle MP & Bix GJ (2012). Successfully climbing the "STAIRS": surmounting failed

translation of experimental ischemic stroke treatments. *Stroke Res Treat* **2012,** 1–8.

Kanoski SE & Davidson TL (2010). Different patterns of memory impairments accompany short- and longer-term maintenance on a high-energy diet. *J Exp Psychol Anim Behav Process* **36,** 313–319.

Katakam P, Snipes J, Steed M & Busija D (2012). Insulin-induced generation of reactive oxygen species and uncoupling of nitric oxide synthase underlie the cerebrovascular insulin resistance in obese rats. *J Cereb Blood Flow Metab* **32,** 792–804.

Katakam P V, Ujhelyi MR, Hoenig ME & Miller AW (1998). Endothelial dysfunction precedes hypertension in diet-induced insulin resistance. *Am J Physiol* **275,** R788-92.

Kearns CE, Schmidt LA & Glantz SA (2016). Sugar industry and coronary heart disease research. *JAMA Intern Med* **176,** 1680–1685.

Keys A, Aravanis C, Buchem FSP Van, Blackburn H, Buzina R, Djordjevic BS, Dontas AS, Fidanza F, Karvonen MJ, Kimura N, Menotti A, Nedeljkovic S, Puddu V, Punsar S & Taylor HL (1981). The diet and all-causes death rate in the Seven Countries Study. *Lancet* **318,** 58–61.

Keys A, Menotti A, Karvonen MJ, Aravanis C, Blackburn H, Buzina R, Djordjevic BS, Dontas AS, Fidanza F, Keys MH, Kromhout D, Nedeljkovic S, Punsar S, Seccareccia F & Toshima H (1986). The diet and 15-year death rate in the Seven Countries Study. *Am J Epidemiol* **124,** 903–915.

Kn BP, Gopalan V, Lee SS & Velan SS (2014). Quantification of abdominal fat depots in rats and mice during obesity and weight loss interventions. *PLoS One* **9,** e108979.

Komaroff AL, E VN, F H, J Y, PJ T & LM K (2017). The Microbiome and Risk for Obesity and Diabetes. *JAMA* **317,** 355–356.

Krakauer JW, Carmichael ST, Corbett D & Wittenberg GF (2012). Getting neurorehabilitation right: what can be learned from animal models? *Neurorehabil Neural Repair* **26,** 923–931.

Kylin E (1923). Studien über das Hypertonie-Hyperglykämie-Hyperurikämiesyndrom. *Zentralblatt für Inn Medizin* **7,** 105–127.

Ladeby R, Wirenfeldt M, Garcia-Ovejero D, Fenger C, Dissing-Olesen L, Dalmau I & Finsen B (2005). Microglial cell population dynamics in the injured adult central nervous system. *Brain Res Brain Res Rev* **48,** 196–206.

Lai M, Chandrasekera PC & Barnard ND (2014). You are what you eat, or are you? The challenges of translating high-fat-fed rodents to human obesity and diabetes. *Nutr Diabetes* **4,** e135.

Langdon KD, Granter-Button S & Corbett D (2008). Persistent behavioral impairments and neuroinflammation following global ischemia in the rat. *Eur J Neurosci* **28,** 2310–2318.

Last D, Alsop DC, Abduljalil AM, Marquis RP, De Bazelaire C, Hu K, Cavallerano J & Novak V (2007). Global and regional effects of type 2 diabetes on brain tissue volumes and cerebral vasoreactivity. *Diabetes Care* **30,** 1193–1199.

Lavie CJ, de Schutter A & Milani R V. (2014). Healthy obese versus unhealthy lean: the obesity paradox. *Nat Rev Endocrinol* **11,** 55–62.

Lemieux I (2004). Energy partitioning in gluteal-femoral fat: does the metabolic fate of triglycerides affect coronary heart disease risk? *Arterioscler Thromb Vasc Biol* **24,** 795–797.

Leturque A, Brot-Laroche E & Gall M Le (2009). GLUT2 mutations, translocation, and receptor function in diet sugar managing. *Am J Physiol - Endocrinol Metab* **296,**

E985–E992.

Li W, Prakash R, Chawla D, Du W, Didion SP, Filosa J a, Zhang Q, Brann DW, Lima V V, Tostes RC & Ergul A (2013). Early effects of high-fat diet on neurovascular function and focal ischemic brain injury. *Am J Physiol Regul Integr Comp Physiol* **304,** R1001-1008.

Li W, Prakash R, Kelly-Cobbs AI, Ogbi S, Kozak A, El-Remessy AB, Schreihofer DA, Fagan SC & Ergul A (2010). Adaptive cerebral neovascularization in a model of type 2 diabetes: relevance to focal cerebral ischemia. *Diabetes* **59,** 228–235.

Li Y, Hruby A, Bernstein AM, Ley SH, Wang DD, Chiuve SE, Sampson L, Rexrode KM, Rimm EB, Willett WC & Hu FB (2015). Saturated fats compared with unsaturated fats and sources of carbohydrates in relation to risk of coronary heart disease. *J Am Coll Cardiol* **66,** 1538–1548.

Lim SS et al. (2012). A comparative risk assessment of burden of disease and injury attributable to 67 risk factors and risk factor clusters in 21 regions, 1990–2010: a systematic analysis for the Global Burden of Disease Study 2010. *Lancet* **380,** 2224–2260.

Limberg JK, Harrell JW, Johansson RE, Eldridge MW, Proctor LT, Sebranek JJ & Schrage WG (2013). Microvascular function in younger adults with obesity and metabolic syndrome: role of oxidative stress. *Am J Physiol Heart Circ Physiol* **305,** H1230–H1237.

Littlejohns B, Lin H, Angelin GD, Halestrap AP & Suleiman MS (2014). Switching back to normal diet following high-fat diet feeding reduces cardiac vulnerability to ischaemia and reperfusion injury. *Cell Physiol Biochem* **34,** 1090–1100.

Liu S, Globa AK, Mills F, Naef L, Qiao M, Bamji SX & Borgland SL (2016).

Consumption of palatable food primes food approach behavior by rapidly increasing synaptic density in the VTA. *Proc Natl Acad Sci* **113,** 2520–2525.

Liu Y, Zhu X, Feinberg D, Guenther M, Gregori J, Weiner MW & Schuff N (2012). Arterial spin labeling MRI study of age and gender effects on brain perfusion hemodynamics. *Magn Reson Med* **68,** 912–922.

Lladó I, Picó C, Palou A & Pons A (1995). Protein and amino acid intake in cafeteria fed obese rats. *Physiol Behav* **58,** 513–519.

Lozano I, Van der Werf R, Bietiger W, Seyfritz E, Peronet C, Pinget M, Jeandidier N, Maillard E, Marchioni E, Sigrist S & Dal S (2016). High-fructose and high-fat diet-induced disorders in rats: impact on diabetes risk, hepatic and vascular complications. *Nutr Metab (Lond)* **13,** 1–13.

Lumeng CN & Saltiel AR (2011). Inflammatory links between obesity and metabolic disease. *J Clin Invest* **121,** 2111–2117.

Mahmoud AAA & Elshazly SM (2014). Ursodeoxycholic acid ameliorates fructose-induced metabolic syndrome in rats ed. Alisi A. *PLoS One* **9,** 1–8.

Malik VS, Popkin BM, Bray GA, Després J-P & Hu FB (2010). Sugar-sweetened beverages, obesity, type 2 diabetes mellitus, and cardiovascular disease risk. *Circulation* **121,** 1356–1364.

Malik VS, Willett WC & Hu FB (2008). Sugar-sweetened beverages and BMI in children and adolescents: reanalyses of a meta-analysis. *Am J Clin Nutr* **89,** 438–439.

Maniam J & Morris MJ (2010). Palatable cafeteria diet ameliorates anxiety and depression-like symptoms following an adverse early environment. *Psychoneuroendocrinology* **35,** 717–728.

Marcon J, Gagliardi B, Balosso S, Maroso M, Noé F, Morin M, Lerner-Natoli M,

Vezzani A & Ravizza T (2009). Age-dependent vascular changes induced by status epilepticus in rat forebrain: implications for epileptogenesis. *Neurobiol Dis* **34,** 121–132.

Marshall SA, McClain JA, Kelso ML, Hopkins DM, Pauly JR & Nixon K (2013). Microglial activation is not equivalent to neuroinflammation in alcohol-induced neurodegeneration: The importance of microglia phenotype. *Neurobiol Dis* **54,** 239–251.

Mather KJ, Steinberg HO & Baron AD (2013). Insulin resistance in the vasculature. *J Clin Invest* **123,** 1003–1004.

Micha R & Mozaffarian D (2010). Saturated fat and cardiometabolic risk factors, coronary heart disease, stroke, and diabetes: a fresh look at the evidence. *Lipids* **45,** 893–905.

Miller AA & Spencer SJ (2014). Obesity and neuroinflammation: a pathway to cognitive impairment. *Brain Behav Immun* **42,** 10–21.

Miranda PJ, DeFronzo RA, Califf RM & Guyton JR (2005). Metabolic syndrome: Definition, pathophysiology, and mechanisms. *Am Heart J* **149,** 33–45.

Molteni R, Barnard RJ, Ying Z, Roberts CK & Gómez-Pinilla F (2002). A high-fat, refined sugar diet reduces hippocampal brain-derived neurotrophic factor, neuronal plasticity, and learning. *Neuroscience* **112,** 803–814.

Monteiro CA, Moubarac J-C, Cannon G, Ng SW & Popkin B (2013). Ultra-processed products are becoming dominant in the global food system. *Obes Rev* **14,** 21–28.

Moore BJ (1987). The cafeteria diet-an inappropriate tool for studies of thermogenesis. *J Nutr* **117,** 227–231.

Mozaffarian D (2016). Dietary and policy priorities for cardiovascular disease, diabetes,

and obesity: a comprehensive review. *Circulation* **133,** 187–225.

Mozaffarian D (2017). Foods, obesity, and diabetes—are all calories created equal? *Nutr Rev* **75,** 19–31.

Mozaffarian D, Hao T, Rimm EB, Willett WC & Hu FB (2011). Changes in diet and lifestyle and long-term weight gain in women and men. *N Engl J Med* **364,** 2392–2404.

Müller HP, Niessen HG, Kaulisch T, Ludolph AC, Kassubek J & Stiller D (2013). MRI allows for longitudinal quantitative analysis of body fat composition in rats: an analysis of sibutramine-associated changes at the group level. *Magn Reson Imaging* **31,** 1150–1155.

Nasrallah FA, Pagès G, Kuchel PW, Golay X & Chuang K-H (2013). Imaging brain deoxyglucose uptake and metabolism by glucoCEST MRI. *J Cereb blood flow Metab* **33,** 1270–1278.

Neel J V. (1962). Diabetes mellitus: a “thrifty” genotype rendered detrimental by “progress”? *Am J Hum Genet* **14,** 353–362.

Neufer PD et al. (2015). Understanding the cellular and molecular mechanisms of physical activity-induced health benefits. *Cell Metab* **22,** 4–11.

Ng SW, Slining MM & Popkin BM (2014). Turning point for US diets? Recessionary effects or behavioral shifts in foods purchased and consumed. *Am J Clin Nutr* **99,** 609–616.

Nguemeni C, Gomez-Smith M, Jeffers MS, Schuch CP & Corbett D (2015). Time course of neuronal death following endothelin-1 induced focal ischemia in rats. *J Neurosci Methods* **242,** 72–76.

NHLBI Obesity Education Initiative Expert Panel (2000). *The practical guide:*

Identification, evaluation and treatment of overweight and obesity in adults.

Noble EE, Hsu TM & Kanoski SE (2017). Gut to brain dysbiosis: mechanisms linking Western Diet consumption, the microbiome, and cognitive impairment. *Front Behav Neurosci* **11,** 1–10.

Northcott CA, Fink GD, Garver H, Haywood JR, Laimon-Thomson EL, McClain JL, Pires PW, Rainey WE, Rigsby CS & Dorrance AM (2012). The development of hypertension and hyperaldosteronism in a rodent model of life-long obesity. *Endocrinology* **153,** 1764–1773.

O'Collins VE, Macleod MR, Donnan GA, Horky LL, Van Der Worp BH & Howells DW (2006). 1,026 Experimental treatments in acute stroke. *Ann Neurol* **59,** 467–477.

O'Leary TP & Brown RE (2012). The effects of apparatus design and test procedure on learning and memory performance of C57BL/6J mice on the Barnes maze. *J Neurosci Methods* **203,** 315–324.

Obermeier B, Daneman R & Ransohoff RM (2013). Development, maintenance and disruption of the blood-brain barrier. *Nat Med* **19,** 1584–1596.

Oldendorf WH, Cornford ME & Brown WJ (1977). The large apparent work capability of the blood-brain barrier: a study of the mitochondrial content of capillary endothelial cells in brain and other tissues of the rat. *Ann Neurol* **1,** 409–417.

Olver TD, McDonald MW, Klakotskaia D, Richardson RA, Jasperse JL, Melling CWJ, Schachtman TR, Yang HT, Emter CA & Laughlin MH (2017). A chronic physical activity treatment in obese rats normalizes the contributions of ET-1 and NO to insulin-mediated posterior cerebral artery vasodilation. *J Appl Physiol*Epub ahead of press.

Opie RS, Ralston RA & Walker KZ (2013). Adherence to a Mediterranean-style diet can

slow the rate of cognitive decline and decrease the risk of dementia: a systematic review. *Nutr Diet* **70,** 206–217.

Ortega FB, Lee DC, Katzmarzyk PT, Ruiz JR, Sui X, Church TS & Blair SN (2013). The intriguing metabolically healthy but obese phenotype: Cardiovascular prognosis and role of fitness. *Eur Heart J* **34,** 389–397.

Palmer C, Bik EM, DiGiulio DB, Relman DA & Brown PO (2007). Development of the Human Infant Intestinal Microbiota ed. Ruan Y. *PLoS Biol* **5,** e177.

Panchal SK & Brown L (2011). Rodent models for metabolic syndrome research. *J Biomed Biotechnol* **2011,** 1–14.

Pandit R, Mercer JG, Overduin J, la Fleur SE & Adan RAH (2012). Dietary factors affect food reward and motivation to eat. *Obes Facts* **5,** 221–242.

Paracchini V, Pedotti P & Taioli E (2005). Genetics of leptin and obesity: a HuGE review. *Am J Epidemiol* **162,** 101–114.

Parekh P, Petro A, Tiller J, Feinglos M & Surwit R (1998). Reversal of diet-induced obesity and diabetes in C57BL/6J mice. *Metabolism* **47,** 1089–1096.

Park Y-W, Zhu S, Palaniappan L, Heshka S, Carnethon MR & Heymsfield SB (2003). The metabolic syndrome: prevalence and associated risk factor findings in the US population from the Third National Health and Nutrition Examination Survey, 1988-1994. *Arch Intern Med* **163,** 427–436.

Pasquali R, Vicennati V, Cacciari M & Pagotto U (2006). The hypothalamic-pituitary-adrenal axis activity in obesity and the metabolic syndrome. *Ann N Y Acad Sci* **1083,** 111–128.

Paxinos G & Watson C (2007). *The Rat Brain in Stereotaxic Coordinates*, 6th ed. Academic Press.

Pereira MA, Kartashov AI, Ebbeling CB, Van Horn L, Slattery ML, Jacobs PDR & Ludwig DS (2005). Fast-food habits, weight gain, and insulin resistance (the CARDIA study): 15-year prospective analysis. *Lancet* **365,** 36–42.

Perrin S (2014). Make mouse studies work. *Nature* **507,** 423.

Philip M, Benatar M, Fisher M & Savitz SI (2009). Methodological quality of animal studies of neuroprotective agents currently in phase II/III acute ischemic stroke trials. *Stroke* **40,** 577–581.

Pouliot MC, Després JP, Moorjani S, Lupien PJ, Tremblay A, Nadeau A & Bouchard C (1991). Regional variation in adipose tissue lipoprotein lipase activity: association with plasma high density lipoprotein levels. *Eur J Clin Invest* **21,** 398–405.

Prakash R, Johnson M, Fagan SC & Ergul A (2013*a*). Cerebral neovascularization and remodeling patterns in two different models of type 2 diabetes. *PLoS One* **8,** e56264.

Prakash R, Li W, Qu Z, Johnson MA, Fagan SC & Ergul A (2013*b*). Vascularization pattern after ischemic stroke is different in control versus diabetic rats relevance to stroke recovery. *Stroke* **44,** 2875–2882.

Prakash R, Somanath PR, El-Remessy AB, Kelly-Cobbs A, Stern JE, Dore-Duffy P, Johnson M, Fagan SC & Ergul A (2012). Enhanced cerebral but not peripheral angiogenesis in the Goto-Kakizaki model of type 2 diabetes involves VEGF and peroxynitrite signaling. *Diabetes* **61,** 1533–1542.

Prasad A & Prasad C (1996). Short-term consumption of a diet rich in fat decreases anxiety response in adult male rats. *Physiol Behav* **60,** 1039–1042.

Public Health Agency of Canada (2011). *Tracking Heart Disease and Stroke in Canada - Stroke Highlights 2011*.

Raynor HA & Epstein LH (2001). Dietary variety, energy regulation, and obesity.

Psychol Bull **127,** 325–341.

Reaven GM (1988). Role of insulin resistance in human disease. *Diabetes* **37,** 1595–1607.

Reaven GM (2006). The metabolic syndrome: is this diagnosis necessary? *Am J Clin Nutr* **83,** 1237–1247.

Reeson P, Tennant KA, Gerrow K, Wang J, Weiser Novak S, Thompson K, Lockhart K-L, Holmes A, Nahirney PC & Brown CE (2015). Delayed inhibition of VEGF signaling after stroke attenuates blood-brain barrier breakdown and improves functional recovery in a comorbidity-dependent manner. *J Neurosci* **35,** 5128–5143.

Riediger ND & Clara I (2011). Prevalence of metabolic syndrome in the Canadian adult population. *CMAJ* **183,** E1127–E1134.

Rigau V, Morin M, Rousset M-C, de Bock F, Lebrun A, Coubes P, Picot M-C, Baldy-Moulinier M, Bockaert J, Crespel A & Lerner-Natoli M (2007). Angiogenesis is associated with blood-brain barrier permeability in temporal lobe epilepsy. *Brain* **130,** 1942–1956.

Rizzoni D, De Ciuceis C, Porteri E, Paiardi S, Boari GE, Mortini P, Cornali C, Cenzato M, Rodella LF, Borsani E, Rizzardi N, Platto C, Rezzani R & Rosei EA (2009). Altered structure of small cerebral arteries in patients with essential hypertension. *J Hypertens* **27,** 838–845.

Rodan LH, Poublanc J, Fisher JA, Sobczyk O, Wong T, Hlasny E, Mikulis D & Tein I (2015). Cerebral hyperperfusion and decreased cerebrovascular reactivity correlate with neurologic disease severity in MELAS. *Mitochondrion* **22,** 66–74.

Rogers PJ (1985). Returning “cafeteria-fed” rats to a chow diet: negative contrast and effects of obesity on feeding behaviour. *Physiol Behav* **35,** 493–499.

Roth GA, Forouzanfar MH, Moran AE, Barber R, Nguyen G, Feigin VL, Naghavi M, Mensah GA & Murray CJL (2015). Demographic and epidemiologic drivers of global cardiovascular mortality. *N Engl J Med* **372,** 1333–1341.

Rusinek H, Ha J, Yau PL, Storey P, Tirsi A, Tsui WH, Frosch O, Azova S & Convit A (2015). Cerebral perfusion in insulin resistance and type 2 diabetes. *J Cereb Blood Flow Metab* **35,** 95–102.

Russell JC & Proctor SD (2006). Small animal models of cardiovascular disease: tools for the study of the roles of metabolic syndrome, dyslipidemia, and atherosclerosis. *Cardiovasc Pathol* **15,** 318–330.

Sabri O, Hellwig D, Schreckenberger M, Schneider R, Kaiser H-J, Wagenknecht G, Mull M & Buell U (2000). Influence of diabetes mellitus on regional cerebral glucose metabolism and regional cerebral blood flow. *Nucl Med Commun* **21,** 19–29.

Saisho Y (2014). Importance of beta cell function for the treatment of type 2 diabetes. *J Clin Med* **3,** 923–943.

Salas-Salvadó J, Bulló M, Babio N, Martínez-González MÁ, Ibarrola-Jurado N, Basora J, Estruch R, Covas MI, Corella D, Arós F, Ruiz-Gutiérrez V, Ros E & PREDIMED Study Investigators (2011). Reduction in the incidence of type 2 diabetes with the Mediterranean diet: results of the PREDIMED-Reus nutrition intervention randomized trial. *Diabetes Care* **34,** 14–19.

Salter MW & Beggs S (2014). Sublime microglia: expanding roles for the guardians of the CNS. *Cell* **158,** 15–24.

Sampey BP, Vanhoose AM, Winfield HM, Freemerman AJ, Muehlbauer MJ, Fueger PT, Newgard CB & Makowski L (2011). Cafeteria diet is a robust model of human metabolic syndrome with liver and adipose inflammation: comparison to high-fat

diet. *Obesity* **19,** 1109–1117.

Samuel VT & Shulman GI (2012). Mechanisms for insulin resistance: common threads and missing links. *Cell* **148,** 852–871.

Samuels LT, Reinecke RM & Ball HA (1942). Effect of diet on glucose tolerance and liver and muscle glycogen of hypophysectomized and normal rats. *Endocrinology* **31,** 42–45.

Sanchez-Lozada LG, Tapia E, Jimenez A, Bautista P, Cristobal M, Nepomuceno T, Soto V, Avila-Casado C, Nakagawa T, Johnson RJ, Herrera-Acosta J & Franco M (2007). Fructose-induced metabolic syndrome is associated with glomerular hypertension and renal microvascular damage in rats. *Am J Physiol Ren Physiol* **292,** F423–F429.

Santure M, Pitre M, Marette A, Deshaies Y, Lemieux C, Lariviere R, Nadeau A & Bachelard H (2002). Induction of insulin resistance by high-sucrose feeding does not raise mean arterial blood pressure but impairs haemodynamic responses to insulin in rats. *Br J Pharmacol* **137,** 185–196.

Sclafani A (1987). Carbohydrate taste, appetite, and obesity: an overview. *Neurosci Biobehav Rev* **11,** 131–153.

Sclafani A & Springer D (1976). Dietary obesity in adult rats: similarities to hypothalamic and human obesity syndromes. *Physiol Behav* **17,** 461–471.

Seghers V, Nakazaki M, DeMayo F, Aguilar-Bryan L & Bryan J (2000). Sur1 knockout mice. A model for K(ATP) channel-independent regulation of insulin secretion. *J Biol Chem* **275,** 9270–9277.

Shafat A, Murray B & Rumsey D (2009). Energy density in cafeteria diet induced hyperphagia in the rat. *Appetite* **52,** 34–38.

Sharma N, Okere IC, Barrows BR, Lei B, Duda MK, Yuan CL, Previs SF, Sharov VG,

Azimzadeh AM, Ernsberger P, Hoit BD, Sabbah H & Stanley WC (2008). High-sugar diets increase cardiac dysfunction and mortality in hypertension compared to low-carbohydrate or high-starch diets. *J Hypertens* **26,** 1402–1410.

Sharma S & Fulton S (2012). Diet-induced obesity promotes depressive-like behaviour that is associated with neural adaptations in brain reward circuitry. *Int J Obes* **37,** 382–389.

Sharma S, Zhuang Y & Gomez-Pinilla F (2012). High-fat diet transition reduces brain DHA levels associated with altered brain plasticity and behaviour. *Sci Rep* **2,** 1–8.

Shih AY, Blinder P, Tsai PS, Friedman B, Stanley G, Lyden PD & Kleinfeld D (2013). The smallest stroke: occlusion of one penetrating vessel leads to infarction and a cognitive deficit. *Nat Neurosci* **16,** 55–63.

Shimabukuro M, Higa N, Masuzaki H, Sata M & Ueda S (2016). Impact of individual metabolic risk components or its clustering on endothelial and smooth muscle cell function in men. *Cardiovasc Diabetol* **15,** 1–11.

Sinitskaya N, Gourmelen S, Schuster-Klein C, Guardiola-Lemaitre B, Pévet P & Challet E (2007). Increasing the fat-to-carbohydrate ratio in a high-fat diet prevents the development of obesity but not a prediabetic state in rats. *Clin Sci* **113,** 417–425.

Sleiman D, Al-Badri MR & Azar ST (2015). Effect of mediterranean diet in diabetes control and cardiovascular risk modification: a systematic review. *Front public Heal* **3,** 69.

Sokolova IA, Manukhina EB, Blinkov SM, Koshelev VB, Pinelis VG & Rodionov IM (1985). Rarefication of the arterioles and capillary network in the brain of rats with different forms of hypertension. *Microvasc Res* **30,** 1–9.

Sørensen LB, Møller P, Flint A, Martens M & Raben A (2003). Effect of sensory

perception of foods on appetite and food intake: a review of studies on humans. *Int J Obes* **27,** 1152–1166.

Sorond FA, Hollenberg NK, Panych LP & Fisher NDL (2010). Brain blood flow and velocity: correlations between magnetic resonance imaging and transcranial Doppler sonography. *J Ultrasound Med* **29,** 1017–1022.

South T, Holmes NM, Martire SI, Westbrook RF & Morris MJ (2014). Rats eat a cafeteria-style diet to excess but eat smaller amounts and less frequently when tested with chow. *PLoS One* **9,** e93506.

Speakman JR (2008). Thrifty genes for obesity, an attractive but flawed idea, and an alternative perspective: the "drifty gene" hypothesis. *Int J Obes* **32,** 1611–1617.

Stamler J, Stamler R, Neaton JD, Wentworth D, Daviglus ML, Garside D, Dyer AR, Liu K & Greenland P (1999). Low risk-factor profile and long-term cardiovascular and noncardiovascular mortality and life expectancy: findings for 5 large cohorts of young adult and middle-aged men and women. *JAMA* **282,** 2012–2018.

Stančáková A & Laakso M (2014). Genetics of metabolic syndrome. *Rev Endocr Metab Disord* **15,** 243–252.

Statistics Canada (2014). Metabolic syndrome in adults, 2012 to 2013. *Fact Sheet Cat #82-625-X201400114123*. Available at: http://www.statcan.gc.ca/pub/82-625-x/2014001/article/14123-eng.htm.

Steele EM, Baraldi LG, Laura M, Moubarac J, Mozaffarian D & Monteiro CA (2016). Ultra-processed foods and added sugars in the US diet: evidence from a nationally representative cross-sectional study. *BMJ Open* **6,** 1–9.

Sweazea KL, Lekic M & Walker BR (2010). Comparison of mechanisms involved in impaired vascular reactivity between high sucrose and high fat diets in rats. *Nutr*

Metab (Lond) **7,** 1–10.

Takechi R, Pallebage-Gamarallage MM, Lam V, Giles C & Mamo JC (2013). Nutraceutical agents with anti-inflammatory properties prevent dietary saturated-fat induced disturbances in blood-brain barrier function in wild-type mice. *J Neuroinflammation* **10,** 1–12.

Talmor-Barkan Y & Kornowski R (2017). The gut microbiome and cardiovascular risk: current perspective and gaps of knowledge. *Future Cardiol* **13,** 191–194.

Tchernof A & Després J-P (2013). Pathophysiology of human visceral obesity: an update. *Physiol Rev* **93,** 359–404.

Tennant KA & Brown CE (2013). Diabetes augments in vivo microvascular blood flow dynamics after stroke. *J Neurosci* **33,** 19194–19204.

Thaler JP, Yi CX, Schur EA, Guyenet SJ, Hwang BH, Dietrich MO, Zhao X, Sarruf DA, Izgur V, Maravilla KR, Nguyen HT, Fischer JD, Matsen ME, Wisse BE, Morton GJ, Horvath TL, Baskin DG, Tschop MH & Schwartz MW (2012). Obesity is associated with hypothalamic injury in rodents and humans. *J Clin Invest* **122,** 153–162.

The Look AHEAD Research Group (2013). Cardiovascular effects of intensive lifestyle intervention in type 2 diabetes. *N Engl J Med* **369,** 155–164.

The Look AHEAD Research Group (2014). Eight-year weight losses with an intensive lifestyle intervention: the Look AHEAD study. *Obesity* **22,** 5–13.

Thompson CS & Hakim AM (2009). Living beyond our physiological means. Small vessel disease of the brain is an expression of a systemic failure in arteriolar function: a unifying hypothesis. *Stroke* **40,** 1–9.

Tiehuis AM, Vincken KL, van den Berg E, Hendrikse J, Manschot SM, Mali WPTM, Kappelle LJ & Biessels GJ (2008). Cerebral perfusion in relation to cognitive

function and type 2 diabetes. *Diabetologia* **51,** 1321–1326.

Tran LT, Yuen VG & McNeill JH (2009). The fructose-fed rat: a review on the mechanisms of fructose-induced insulin resistance and hypertension. *Mol Cell Biochem* **332,** 145–159.

Turnbaugh PJ, Hamady M, Yatsunenko T, Cantarel BL, Duncan A, Ley RE, Sogin ML, Jones WJ, Roe BA, Affourtit JP, Egholm M, Henrissat B, Heath AC, Knight R & Gordon JI (2009*a*). A core gut microbiome in obese and lean twins. *Nature* **457,** 480–484.

Turnbaugh PJ, Ley RE, Mahowald MA, Magrini V, Mardis ER & Gordon JI (2006). An obesity-associated gut microbiome with increased capacity for energy harvest. *Nature* **444,** 1027–1131.

Turnbaugh PJ, Ridaura VK, Faith JJ, Rey FE, Knight R & Gordon JI (2009*b*). The Effect of Diet on the Human Gut Microbiome: A Metagenomic Analysis in Humanized Gnotobiotic Mice. *Sci Transl Med* **1,** 1–10.

Tyndall A V, Argourd L, Sajobi TT, Davenport MH, Forbes SC, Gill SJ, Parboosingh JS, Anderson TJ, Wilson BJ, Smith EE, Hogan DB, Hill MD & Poulin MJ (2016). Cardiometabolic risk factors predict cerebrovascular health in older adults: results from the Brain in Motion study. *Physiol Rep* **4,** e12733.

Tziomalos K, Athyros VG, Karagiannis A & Mikhailidis DP (2010). Endothelial dysfunction in metabolic syndrome: prevalence, pathogenesis and management. *Nutr Metab Cardiovasc Dis* **20,** 140–146.

Vague J (1947). La différenciation sexuelle; facteur déterminant des formes de l'obésité. *La Press médicale* **55,** 339.

Vaisse C, Clément K, Guy-Grand B & Froguel P (1998). A frameshift mutation in human

MC4R is associated with a dominant form of obesity. *Nat Genet* **20,** 113–114.

Valdearcos M, Robblee MM, Benjamin DI, Nomura DK, Xu AW & Koliwad SK (2014). Microglia dictate the impact of saturated fat consumption on hypothalamic inflammation and neuronal function. *Cell Rep* **9,** 2124–2138.

Valladolid-Acebes I, Fole A, Martín M, Morales L, Victoria Cano M, Ruiz-Gayo M & Olmo N Del (2013). Spatial memory impairment and changes in hippocampal morphology are triggered by high-fat diets in adolescent mice. Is there a role of leptin? *Neurobiol Learn Mem* **106,** 18–25.

Varga O, Harangi M, Olsson IAS & Hansen AK (2010). Contribution of animal models to the understanding of the metabolic syndrome: a systematic overview. *Obes Rev* **11,** 792–807.

Vasanji Z, Cantor EJF, Juric D, Moyen M & Netticadan T (2006). Alterations in cardiac contractile performance and sarcoplasmic reticulum function in sucrose-fed rats is associated with insulin resistance. *Am J Physiol - Cell Physiol* **291,** C772–C780.

Vinjé S, Stroes E, Nieuwdorp M & Hazen SL (2014). The gut microbiome as novel cardio-metabolic target: the time has come! *Eur Heart J* **35,** 883–887.

Vorhees C V. & Williams MT (2014). Assessing spatial learning and memory in rodents. *ILAR J* **55,** 310–332.

Wälchli T, Mateos JM, Weinman O, Babic D, Regli L, Hoerstrup SP, Gerhardt H, Schwab ME & Vogel J (2015). Quantitative assessment of angiogenesis, perfused blood vessels and endothelial tip cells in the postnatal mouse brain. *Nat Protoc* **10,** 53–74.

Walther G, Obert P, Dutheil F, Chapier R, Lesourd B, Naughton G, Courteix D & Vinet A (2015). Metabolic syndrome individuals with and without type 2 diabetes mellitus

present generalized vascular dysfunction, cross-sectional study. *Arterioscler Thromb Vasc Biol* **35,** 1022–1029.

Wardlaw JM, Sandercock PAG, Dennis MS & Starr J (2003). Is breakdown of the blood-brain barrier responsible for lacunar stroke, leukoaraiosis, and dementia? *Stroke* **34,** 806–812.

Willeumier KC, Taylor D V. & Amen DG (2011). Elevated BMI is associated with decreased blood flow in the prefrontal cortex using SPECT imaging in healthy adults. *Obesity* **19,** 1095–1097.

Williams RS, Heilbronn LK, Chen DL, Coster ACF, Greenfield JR & Samocha-Bonet D (2016*a*). Dietary acid load, metabolic acidosis and insulin resistance – Lessons from cross-sectional and overfeeding studies in humans. *Clin Nutr* **35,** 1084–1090.

Williams RS, Kozan P & Samocha-Bonet D (2016*b*). The role of dietary acid load and mild metabolic acidosis in insulin resistance in humans. *Biochimie* **124,** 171–177.

Winocur G & Greenwood CE (1993). High-fat diets impair conditional discrimination learning in rats. *Psychobiology* **21,** 286–292.

Winocur G & Greenwood CE (1999). The effects of high fat diets and environmental influences on cognitive performance in rats. *Behav Brain Res* **101,** 153–161.

Wong SK, Chin K-Y, Suhaimi FH, Fairus A & Ima-Nirwana S (2016). Animal models of metabolic syndrome: a review. *Nutr Metab (Lond)* **13,** 1–12.

World Health Organization (2016). Cardiovascular diseases (CVDs). *Fact Sheet*. Available at: http://www.who.int/mediacentre/factsheets/fs317/en/.

Yaffe K, Kanaya A, Lindquist K, Simonsick EM, Harris T, Shorr RI, Tylavsky FA & Newman AB (2004). The metabolic syndrome, inflammation, and risk of cognitive decline. *JAMA* **292,** 2237–2242.

Yang Q, Zhang Z, Gregg EW, Flanders WD, Merritt R & Hu FB (2014). Added sugar intake and cardiovascular diseases mortality among US adults. *JAMA Intern Med* **174,** 516–524.

Yates KF, Sweat V, Yau PL, Turchiano MM & Convit A (2012). Impact of metabolic syndrome on cognition and brain: a selected review of the literature. *Arterioscler Thromb Vasc Biol* **32,** 2060–2067.

Ye X, Gao X, Scott T & Tucker KL (2011). Habitual sugar intake and cognitive function among middle-aged and older Puerto Ricans without diabetes. *Br J Nutr* **106,** 1423–1432.

Yi C-X, Tschop MH, Woods SC & Hofmann SM (2012). High-fat-diet exposure induces IgG accumulation in hypothalamic microglia. *Dis Model Mech* **5,** 686–690.

Zheng H, Zheng Y, Wang D, Cai A, Lin Q, Zhao L, Chen M, Deng M, Ye X & Gao H (2017). Analysis of neuron–astrocyte metabolic cooperation in the brain of db/db mice with cognitive decline using 13 C NMR spectroscopy. *J Cereb Blood Flow Metab* **37,** 332–343.

Zhu H, Yoshimoto T, Imajo-Ohmi S, Dazortsava M, Mathivanan A & Yamashima T (2012). Why are hippocampal CA1 neurons vulnerable but motor cortex neurons resistant to transient ischemia? *J Neurochem* **120,** 574–585.

Appendix 1 – Additional Results

Telemetry recording of cardiovascular parameters over the period of once month

The Cafeteria diet significantly reduced diastolic and mean arterial pressures though did not impact systolic pressure. Moreover, the Cafeteria diet increased heart rate and pulse pressure. Statistical analysis was performed using linear mixed effects modeling with the restricted maximum likelihood (REML) method in IBM SPSS Statistics (v.23, IBM Corp., Armonk, NY). Values are estimated marginal means ± SEM, *** $p<0.001$.

	SD (N=2)	**CAF (N=3)**
Systolic blood pressure (mmHg)	134.1 ±0.7	132.5 ±0.6
Diastolic blood pressure (mmHg)	97.8 ±0.5	91.3 ±0.4 ***
Mean arterial pressure (mmHg)	112.5 ±0.5	108.6 ±0.4 ***
Pulse pressure (mmHg)	36.3 ±0.4	41.2 ±0.4 ***
Heart rate (bpm)	353 ±2	420 ±1.6 ***

Appendix 2 – Permission to Reprint Published Manuscripts

Figures and tables included in Chapter 1

Figure 1 was adapted from 'Pathophysiology of Human Visceral Obesity: an Update' (Tchernof & Després, 2013). Permission was not required from The American Physiological Society to reproduce this figure.

Figure 2 was adapted from 'The Pathobiology of Vascular Dementia' (Iadecola, 2013) with permission from Elsevier, license number 4093741066470.

Table 1 was adapted from 'Rodent Models for Metabolic Syndrome Research' (Panchal & Brown, 2011) which is an open access article distributed under the Creative Commons Attribution License.

Figure 3 was adapted from 'Animal Models of Metabolic Syndrome: a Review' (Wong et al., 2016) which is an open access article distributed under the Creative Commons Attribution License.

Publications reproduced with permission from the publishers

The article which comprised Chapter 2, 'A Physiological Characterization of the Cafeteria Diet Model of Metabolic Syndrome in the Rat' (Gomez-Smith *et al.*, 2016), was reproduced with permission from Elsevier, license number 3982720610118.

The appended article 'Enriched Rehabilitation Promotes Motor Recovery in Rats Exposed to Neonatal Hypoxia-Ischemia' was reproduced with permission from Elsevier, license number 4079321162224.

The appended article ‘Time Course of Neuronal Death Following Endothelin-1 Induced Focal Ischemia in Rats’ was reproduced with permission from Elsevier, license number 4079320109140.

The appended book chapter ‘Lost in Translation: Rethinking Approaches to Stroke Recovery’ was reproduced with permission from Elsevier, license number 4086500067915.

The appended article ‘How Can You Mend a Broken Brain? - Neurorestorative approaches to stroke recovery’ was reproduced with permission from Karger Publishers, license number 4079330317354.

Appendix 3 – Additional Publications

1) Schuch CP, Jeffers MS, Antonescu S, Nguemeni C, **Gomez-Smith M**, Pereira LO, Morshead CM & Corbett D (2016). Enriched Rehabilitation Promotes Motor Recovery in Rats Exposed to Neonatal Hypoxia-Ischemia. *Behav Brain Res*. **1**, 42-50.

   Statement of Author Contributions: M.G.S. performed 1/3 of common carotid artery surgeries and extensively edited early versions of the manuscript.

2) Nguemeni C, **Gomez-Smith M**, Jeffers MS, Schuch CP & Corbett D (2015). Time Course of Neuronal Death Following Endothelin-1 induced focal ischemia in rats. *J. Neurosci. Method* **15**, 72-6.

   Statement of Author Contributions: M.G.S. contributed significantly to the design of experiments, performed 1/3 of ET-1 stroke surgeries and cryosectioned 1/3 of brain tissue. M.G.S. also quantified all Fluoro-Jade C stained tissue and extensively edited all versions of the manuscript.

3) Corbett D, Jeffers M, Nguemeni C, **Gomez-Smith M** & Livingston-Thomas (2015). Lost in Translation: Rethinking Approaches to Stroke Recovery. *J Prog Brain Res*. **218**, 413-434.

   Statement of Author Contributions: M.G.S. wrote section 4: The Potential of Neuroplasticity to Enhance Stroke Recovery.

4) Corbett D, Nguemeni C & **Gomez-Smith M** (2014). How Can You Mend a Broken Brain? - Neurorestorative approaches to stroke recovery. *Cerebrovasc Dis*. **38**, 233-239.

Statement of Author Contributions: M.G.S. contributed to manuscript revisions.

Behavioural Brain Research 304 (2016) 42–50

Contents lists available at ScienceDirect

Behavioural Brain Research

journal homepage: www.elsevier.com/locate/bbr

Research report

Enriched rehabilitation promotes motor recovery in rats exposed to neonatal hypoxia-ischemia

Clarissa Pedrini Schuch[a,b], Matthew Strider Jeffers[a,h], Sabina Antonescu[a,h], Carine Nguemeni[a,h], Mariana Gomez-Smith[a,h], Lenir Orlandi Pereira[b], Cindi M. Morshead[c,d,e], Dale Corbett[a,f,g,h,*]

[a] Faculty of Medicine, University of Ottawa, Ottawa, ON, Canada
[b] Universidade Federal do Rio Grande do Sul, Porto Alegre, Brazil
[c] Institute of Medical Science, University of Toronto, Toronto, ON, Canada
[d] Department of Surgery, University of Toronto, Toronto, ON, Canada
[e] Institute of Biomaterials and Biomedical Engineering, University of Toronto, Toronto, ON, Canada
[f] Faculty of Medicine, University of Toronto, Toronto, ON, Canada
[g] Faculty of Medicine, Memorial University, St. John's, NL, Canada
[h] Canadian Partnership for Stroke Recovery, Ottawa, ON, Canada

HIGHLIGHTS

- A combination therapy of cyclosporine A and enriched rehabilitation is evaluated.
- Enriched rehabilitation promotes motor recovery.
- Sensitive behavioural tests can detect early impairments in hypoxic-ischemic rats.
- CsA given 2 weeks after HI is not therapeutically efficacious.

ARTICLE INFO

Article history:
Received 3 November 2015
Received in revised form 5 February 2016
Accepted 7 February 2016
Available online 10 February 2016

Keywords:
Perinatal asphyxia
Neonates
Recovery
Hypoxia-ischemia
Cyclosporine animal models

ABSTRACT

Despite continuous improvement in neonatology there is no clinically effective treatment for perinatal hypoxia ischemia (HI). Therefore, development of a new therapeutic intervention to minimize the resulting neurological consequences is urgently needed. The immature brain is highly responsive to environmental stimuli, such as environmental enrichment but a more effective paradigm is enriched rehabilitation (ER), which combines environmental enrichment with daily reach training. Another neurorestorative strategy to promote tissue repair and functional recovery is cyclosporine A (CsA). However, potential benefits of CsA after neonatal HI have yet to be investigated. The aim of this study was to investigate the effects of a combinational therapy of CsA and ER in attempts to promote cognitive and motor recovery in a rat model of perinatal hypoxic-ischemic injury. Seven-day old rats were submitted to the HI procedure and divided into 4 groups: CsA + Rehabilitation; CsA + NoRehabilitation; Vehicle + Rehabilitation; Vehicle + NoRehabilitation. Behavioural parameters were evaluated pre (experiment 1) and post 4 weeks of combinational therapy (experiment 2). Results of experiment 1 demonstrated reduced open field activity of HI animals and increased foot faults relative to shams in the ladder rung walking test. In experiment 2, we showed that ER facilitated acquisition of a staircase skilled-reaching task, increased number of zone crosses in open-field exploration and enhanced coordinated limb use during locomotion on the ladder rung task. There were no evident deficits in novel object recognition testing. Delayed administration of CsA, had no effect on functional recovery after neonatal HI. There was a significant reduction of cortical and hemispherical volume and hippocampal area, ipsilateral to arterial occlusion in HI animals; combinational therapy had no effect on these morphological measurements. In conclusion, the present study demonstrated that ER, but not CsA was the main contributor to enhanced recovery of motor ability after neonatal HI.

Abbreviations: HI, hypoxia-ischemia; ER, enriched rehabilitation; CsA, cyclosporine A; PND, postnatal day.

* Corresponding author at: Cellular & Molecular Medicine, Faculty of Medicine, University of Ottawa, Ottawa, ON K1H 8M5, Canada.
E-mail address: dcorbett@uottawa.ca (D. Corbett).

http://dx.doi.org/10.1016/j.bbr.2016.02.010
0166-4328/

1. Introduction

Perinatal hypoxia ischemia (HI) is one of the most common causes of mortality and morbidity in children [1,2]. Despite improvement in neonatal care there is no clinically effective treatment for this disorder. Therefore, development of a new therapeutic intervention to minimize the resulting neurological consequences of cerebral palsy, mental retardation and learning disabilities [3–5] is urgently needed.

The Rice-Vannucci model is widely used to study neonatal encephalic HI in rodents [6]. The main brain structures affected in this model are cerebral cortex, hippocampus, striatum and thalamus, mostly confined to the hemisphere ipsilateral to arterial occlusion [7,8]. As in humans, rats that experience cerebral HI have motor and cognitive deficits [9–14]. However, there is some inconsistency regarding motor impairments after HI lesion; some authors have found no impairment in forelimb use or motor coordination in adult rats exposed to neonatal HI [12,15,16].

Environmental enrichment has been used as a strategy to enhance neuroplasticity and to promote recovery of function following different types of brain injury such as stroke and HI [7,17–21]. Enriched housing provides sensory, cognitive and motor stimulation as well as social interaction by exposing groups of animals to a variety of objects such as ramps, toys, and other novel objects. Several studies have demonstrated that environmental enrichment can attenuate learning and memory deficits in HI rats [7,14,15,22]. However, motor impairments are not always rescued by exposure to an enriched environment. For example, some authors found no improvement on rotarod [15,19] and foot fault tests [23] thereby emphasizing the importance of conducting comprehensive test batteries. A more effective paradigm, especially for restoring upper limb function, is enriched rehabilitation (ER), which combines environmental enrichment with daily reach training [24]. Enriched rehabilitation improves forelimb and hindlimb motor function following both focal ischemic injury [24–26] as well as hemorrhagic stroke [27,28] in adult animals.

Another approach to enhance recovery is using drugs with pleiotropic actions such as Cyclosporine A (CsA) that has documented neurorestorative effects in adult animals with ischemic brain injury. This immunosuppressive drug enhances the activation of endogenous precursors to promote tissue repair that is correlated with functional recovery [29,30]. Additionally, CsA alters mitochondrial membrane permeability and transition pores so as to reduce oxidative damage [31,32] and recent data suggest that it reduces lipid peroxidation, apoptosis and neuroinflammation in a young rat model of closed head injury [33]. However, potential benefits of CsA after neonatal HI have yet to be investigated [34].

An emerging consensus is that interventions targeting single mechanisms are not successful in treating stroke and related neurological disorders. Instead, combination interventions targeting multiple mechanisms and thereby mimicking endogenous programs of neuroprotection and neural repair offer greater potential benefit [35]. Recently, we used this approach to show that ER combined with Erythropoietin (EPO) and epidermal growth factor (EGF) was more effective than the growth factors or ER alone in promoting behavioural recovery following forelimb motor cortex stroke in rats [36]. In the same vein, the present study was undertaken to examine effects of a combinational therapy consisting of CsA and ER in attempts to promote cognitive and motor recovery in a rat model of perinatal hypoxic-ischemia injury.

2. Materials and methods

2.1. Animals

Seven pregnant Sprague-Dawley rats were acquired from Charles River Laboratories (Montreal, Quebec, Canada) and housed on a reverse 12 h light/dark cycle until parturition with food and water freely available. At post-natal day 7 (PND) pups from the 7 dams were randomly divided into two experimental groups: HI (n = 17 females; n = 14 males) and sham (n = 9 females; n = 9 males). Subsequent behavioural testing was done during the dark phase. All procedures were in accordance with guidelines set by the Canadian Council on Animal Care and the University of Ottawa Animal Care Committee.

2.2. Surgical procedures

At PND 7, rat pups were anesthetized with isoflurane, had their left common carotid artery exposed, isolated from the nerve and vein and ligated using 4-0 surgical silk. After a 2.5 h delay, pups were placed in a hypoxic chamber for 90 min with O_2 levels and temperature maintained at 8% and 37 °C respectively [5,6]. Upon conclusion of this hypoxic episode, pups were returned to their home cage. Sham-operated animals were submitted to manipulation, anesthesia and neck incision, but did not receive arterial occlusion or exposure to the hypoxic environment.

2.3. Cyclosporine A (CsA) administration

Our initial plan was to begin CsA administration (15.0 mg/kg, i.p.) in the first 5–14 days after HI as we have done previously with ER and drug therapies in adult animals [25,36]. Unfortunately, we encountered an extremely high mortality rate (~50%) in neonatal rats which was due to toxicity of the CsA vehicle Cremophor EL [37] since equal numbers of vehicle and CsA treated pups died. Consequently, we delayed CsA until weaning (PND 21), when all HI pups were implanted subcutaneously on the flank with osmotic minipumps (Alzet, Cupertino, USA) delivering CsA (420 mg/mL; BioShop, Burlington, Canada) or vehicle (Cremophor EL; ethanol:cremophor—65:35). Rats were anesthetized during osmotic minipump implantation with 1.5%-2% isoflurane. Pumps had a total fill volume of 100 μl and pumped at a rate of 0.14 μl/h [2]. The vehicle and/or CsA solutions at this later developmental time point resulted in no deaths or detectable morbidity. Minipumps were kept in place until the end of experiments.

2.4. Enriched rehabilitation

At PND 21, after osmotic pump implantation, pups were weaned from their mothers and separated by sex (Fig. 1A). Animals in groups receiving ER were housed in large enrichment cages (groups of four to five, Fig. 1B) while those in non-rehabilitation groups were pair housed in standard cages. Experimental groups were defined with respect to ER condition and drug delivery. Rats were randomly divided into four experimental groups: (CsA or vehicle): CsA + Rehabilitation (n = 4 females; n = 4 males); CsA + NoRehabilitation (n = 5 females; n = 2 males); Vehicle + Rehabilitation (n = 4 females; n = 5 males); Vehicle + NoRehabilitation (n = 4 females; n = 3 males).

Enrichment cages contained objects of varied shapes and texture for exploration (i.e., shelves, plastic tubing, ladders, ramp) that were changed on a weekly basis. In addition to being housed in enriched environments, enriched groups were exposed to rehabilitative reach training 4 h/day, 6 days/week for 4 weeks (PND 21 until PND 48). Rehabilitation consisted of reaching for a food reward in a Plexiglas© chamber using only the impaired limb (right). The reaching apparatus was filled with 8 g of sugar pellets (45 mg; Research Diets, New Brunswick, NJ) and was used to encourage (rather than force) coordinated use of affected forelimb. Procedures for rehabilitative reach training were modified from those described previously [25]. Animals were trained to reach through a 1.1-cm-wide vertical slot to obtain food pellets situated in a well

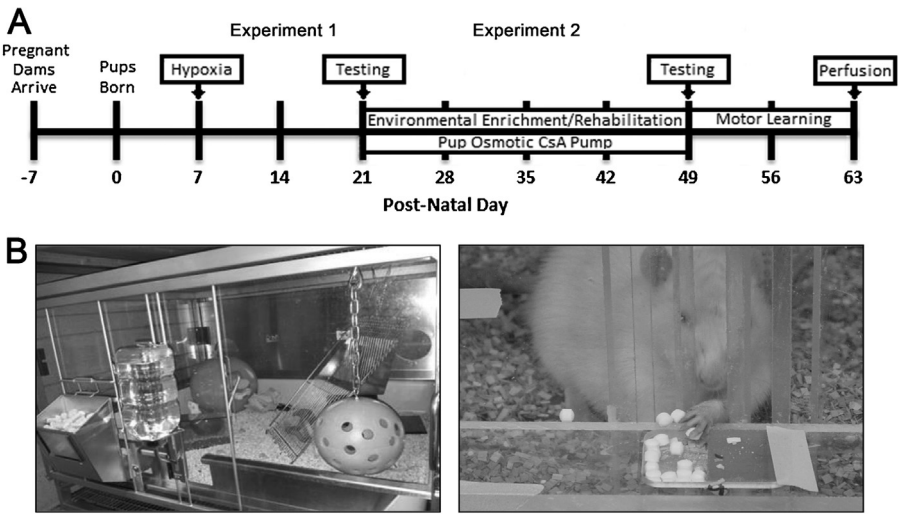

Fig. 1. (A) Time course of interventions. Experiment 1: motor function and cognitive tests at PND 17. Experiment 2: combinational therapy of cyclosporine A and enriched rehabilitation from PND 21 to 49 followed by motor learning performance (staircase test). (B) Enrichment cage shown on left, daily reach training shown on right.

2 cm from the front of a Plexiglas box on a shelf 3.5 cm high. The slot was positioned 1.4 cm from the right wall of the reaching box to discourage use of the left (unaffected) paw (Fig. 1B). At the end of each session remaining sugar pellets were weighed. The non-rehabilitation group did not receive rehabilitative therapy but to control for any possible effects of sugar on recovery, standard-treated animals were fed the average daily amount of sugar pellets eaten by an enriched animal (i.e., ~8 g/d). Animals were kept in enrichment cages until the end of experiments.

2.5. Behavioural testing

2.5.1. Cylinder test

To examine HI effects on spontaneous forelimb use during upright postural support movements [38,39], animals were placed into a clear Plexiglas© cylinder (20 cm in diameter) situated on a glass tabletop and videotaped from below. Each session consisted of 5 min in the cylinder or a minimum of 20 upright wall contacts. Forelimb wall contacts number (single-limb contacts and bilateral contacts) used for postural support was counted. Contralateral forelimb usage was calculated using the following equation [40]:

$$\text{Forelimb asymmetry}\,(\%) = \left[\frac{\left(\#\text{ofcontralateralcontact} + 1/2\#\text{ofbilateral}\right)}{(\#\text{ofipsilateral} + \text{contralateral} + \text{bilateralcontacts})}\right] * 100$$

2.5.2. Ladder rung test

Rats were trained (4 trials, twice in each direction) to cross a horizontal ladder situated 30 cm above a Table with variably spaced rungs [41]. Animals were videotaped crossing the apparatus in 4 trials using an irregular spaced rung pattern that was varied between each test session. Forelimb and hindlimb errors resulting in a limb falling through the plane of the bars (misses, deep slips, or slight slips) were counted. Steps precluding and following a stop were not counted. No significant differences in fore- and hindlimb errors were observed; therefore these errors were combined and expressed as total number of errors for each side (unaffected vs affected).

2.5.3. Open field

The rectangular open-field arena (98 cm × 98 cm × 30 cm) was divided in 16 zones (each zone was 24.5 × 24.5 cm). Animals were placed individually in the center, always facing the same direction, and were video-recorded for 5 min [10]. The distance traveled, number of crossings, instances of rearing and grooming, and latency to leave center of open field were measured automatically using EthoVision tracking software (Noldus Information Technology, Inc.).

2.5.4. Novel object recognition

This test is based on the natural behaviour of animals to spend more time exploring a new, rather than a formerly encountered object [42]. The novel object recognition test took place one day after open field testing. On the test day, a session consisting of two trials was given. The inter-trial interval was 5 min. In the first trial, two different objects were placed equidistant from the sidewalls. Rats were placed into the center of the arena and allowed to explore the two objects (A and B) for 5 min. Time spent exploring each object was recorded. During the second trial, one of the objects presented in the first trial was replaced by a novel object (B was changed to C) and rats were left in the box for 5 min. The time spent exploring both the familiar and novel object was recorded using EthoVision tracking software (Noldus Information Technology, Inc.). Exploration was defined by sniffing the object within a distance of 2 cm and/or touching it with the nose [42]. Object position was randomly assigned to avoid confounds of object and place preference. After each exposure, apparatus and objects were cleaned carefully with 70% alcohol to remove olfactory stimuli. Object preference index was calculated as follows: difference in exploration time in each object divided by the total time spent exploring the two objects.

2.5.5. Montoya staircase task

This test provides a sensitive measurement of independent forelimb skilled reaching and motor learning ability [43,44]. Staircase acquisition began after exposure to ER (6 weeks after HI). During the staircase training period all animals were mildly food restricted (~12 g of standard laboratory chow to maintain approximately 85–95% of their free-feeding body weight). Acquisition occurred over a 10-day period with animals receiving two 15-min trials/day beginning at PND 49.

2.6. Experiment 1: effects of neonatal hypoxia-ischemia on early motor and cognitive function

Ten days after hypoxic-ischemic surgery (PND 17), rat pups (sham (n = 18) and HI rats (n = 31)) were evaluated for deficits in motor and cognitive function using cylinder, ladder rung, open field and novel object recognition tests.

2.7. Experiment 2: combinational therapy of CsA and ER to promote motor recovery in rats exposed to neonatal HI

The same HI rats as in experiment 1 were divided into 4 experimental groups with respect to both an enriched rehabilitation (ER) condition and drug intervention: CsA + Rehabilitation (n = 8); CsA + No Rehabilitation (n = 7); Vehicle + Rehabilitation (n = 9); Vehicle + No Rehabilitation (n = 7). From PND 21 until PND 49 rats were exposed to the combinational therapy and then evaluated on the same motor and cognitive tasks (cylinder, ladder rung, open field, novel object recognition, and staircase task). Staircase acquisition occurred after exposure to the combinational therapy (i.e. PND 49-63).

2.8. Histological assessment

Following behavioural testing, animals were deeply anesthetized (5% isoflurane) and transcardially perfused with ice-cold 0.9% heparinized saline, followed by 4% paraformaldehyde (PFA) in phosphate-buffered saline (PBS). Brains were removed and post-fixed in 4% PFA overnight at 4 °C, then transferred into 20% sucrose-PBS until saturated. The brains were then frozen in isopentane on dry ice, sectioned on a cryostat at 20 μm and stained with cresyl violet to assess brain damage. Every 10th section of tissue was saved, which produced on average 50 sections per brain. Ten different coordinate planes for both the left and right hemispheres relative to Bregma (1.20, 0.70, 0.20, −0.30, −0.80, −1.30, −1.80, −2.30, −2.80, −3.30 mm) were measured using StereoInvestigator (MicroBrightfield Bioscience, Williston, Vermont, USA) software. The hippocampal area of both left and right hemispheres was also measured at −3.30 mm relative to Bregma. The surface area of each section was multiplied by both the section thickness (20 μm) and the interval between sections. This calculation results in an estimated volume of tissue in the space between each measured section. The sum of volumes for all measured sections was calculated to provide hemisphere and cortex volume for each animal.

2.9. Statistical analysis

Pretreatment data were analyzed using unpaired *T*-test and post-treatment data were analyzed by one-way or repeated-measures (staircase) analysis of variance (ANOVA). All analyses were followed by *post-hoc* tests for multiple comparisons, when appropriate. Brain damage (area and volume) was analyzed using Mann-Whitney U non-parametric tests. Experimenters performing volume and area analyses were blind to the experimental groups. Values are mean ± SEM. Statistical significance was set at $p < 0.05$. Statistics were performed using SPSS (SPSS, IBM, Armonk, New York).

3. Results

Since both male and female rats were included in this experiment, sex was initially included as an independent variable in all analyses. However, as no significant effects of sex were observed in any analyses this variable is not included in further discussion for simplicity of interpretation.

3.1. Infarct area and volume assessment

Hypoxia-ischemia resulted in injury primarily localized to the ipsilateral side (left). Animals were analyzed for hemisphere, cortex and hippocampal injury. Since there was no difference between HI groups, we collapsed animals by HI surgery and used the non-parametric Mann-Whitney *U* test to compare HI and sham animals. Mann-Whitney *U* tests showed that HI resulted in decreased volume of left hemisphere and cortex and also decreased area of left hippocampus while the right side was unaffected ($p < 0.001$); Fig. 2A–I.

3.2. Experiment 1: effects of neonatal HI on early motor and cognitive function

3.2.1. Cylinder test

In the cylinder test unpaired Student's *t*-test showed no difference in the proportion of touches between HI and sham rats at PND 17 ($p > 0.05$). Proportion of touches in HI rats using the unaffected (left) and affected paws 57% and 42% respectively in comparison to Sham rats that performed at 52% and 47% (data not shown).

3.2.2. Open field

Unpaired Student's *t*-test showed HI rats exhibited fewer zone crosses in the first minute of open-field exploration ($p < 0.05$) compared to Shams. There were no differences between groups when considering total number of crossings, distance and latency to leave arena center for the full 5-min trial (Table 1).

3.2.3. Ladder rung test

Horizontal ladder data analysis revealed a significantly greater number of foot slip errors per step for both right (affected; $p < 0.001$) and left (unaffected; $p < 0.05$) paws in HI animals (Fig. 3A). There were no significant differences in the number of steps required to cross the ladder (Sham: 59.33 ± 1.26; HI: 61.76 ± 1.84).

3.2.4. Novel object recognition

Novel object recognition, a test of declarative memory, wasn't affected by HI ($p > 0.05$). HI rats spent ~67% of time with the novel object while shams spent ~73% (Table 2).

3.3. Experiment 2: combinational therapy of CsA and ER to promote motor recovery in rats exposed to neonatal HI

3.3.1. Cylinder test

One-way ANOVA indicated no significant effects for *drug* ($F(1,30) = 1.2419$, $p > 0.05$) and *rehabilitation* ($F(1,30) = 0.0007$, $p > 0.05$) either for the affected (right) or unaffected (left) forelimb between groups ($p > 0.05$; data not shown).

3.3.2. Open field

We did not detect a significant *rehabilitation x drug* interaction ($F(3,27) = 0.003$, $p > 0.05$, therefore *rehabilitation* and *drug* main effects were assessed. One-way ANOVA indicated a significant *rehabilitation* effect ($F(1,30) = 6.5242$, $p < 0.01$) for crossing number during the first minute of open-field exploration. Once there was a significant main effect for *rehabilitation*, we collapsed groups across rehabilitated and non-rehabilitated animals. Unpaired Student's *t*-test showed ER rats had a greater number of zone crosses in the first minute of open-field exploration compared to non-rehabilitation animals ($p < 0.05$). Considering total number of crossings, distance

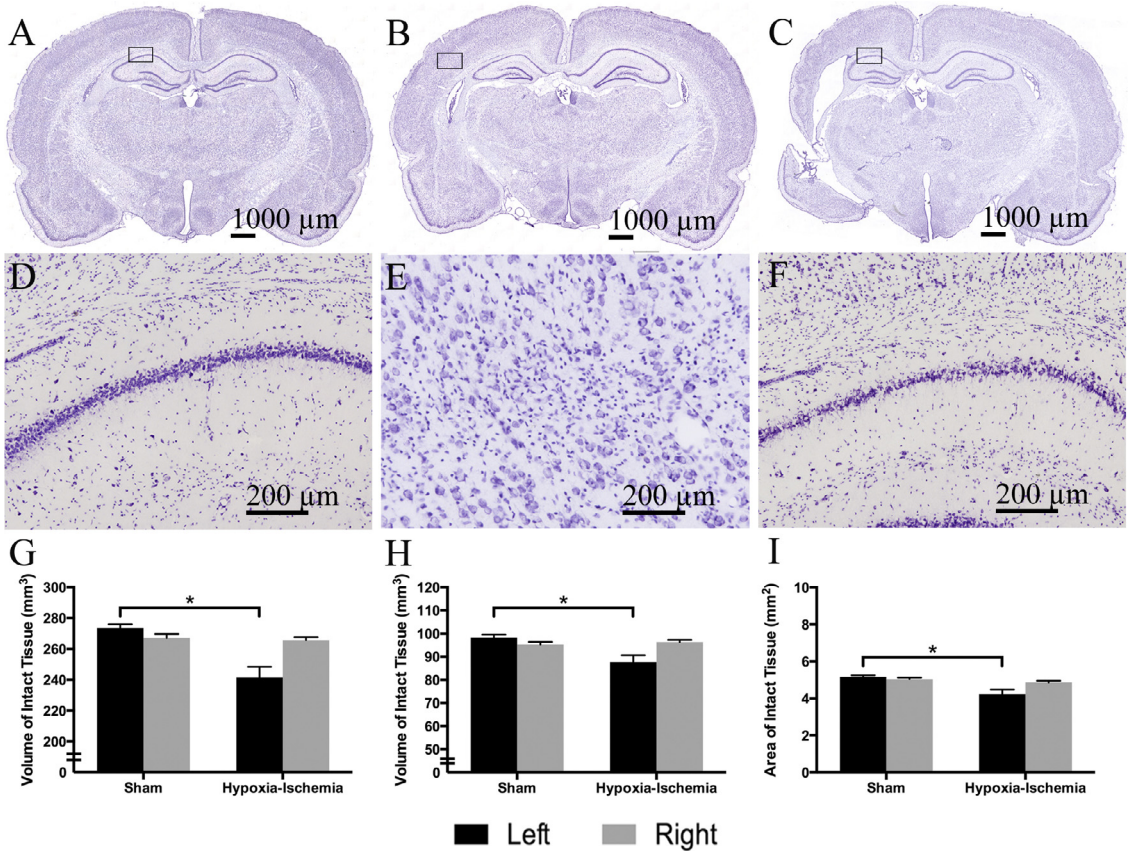

Fig. 2. Area and volume assessment of hemispheric, cortical and hippocampal tissue. Cresyl violet stained representative coronal sections of brain from (A) sham and (B, C) hypoxia-ischemia groups. Figures (D–F) show the inset regions from figures (A–C) respectively. (D) The CA1 region of the hippocampus in sham rats appeared to have a higher density of neurons than rats undergoing (F) hypoxia-ischemia. (E) Throughout the neocortex of HI rats, scattered microinfarcts were present. (G) Decreased total left (ligated) hemispheric volume of HI group compared to sham. (H) Decreased volume of left cortex in HI group compared to sham. (I) Decreased area of left hippocampus in HI group compared to sham. All data represent mean ± SEM using non-parametric Mann-Whitney *U* test (*$p < 0.001$). All structures in right side were unaffected relative to sham.

Table 1
Performance in the open-field task both prior to treatment (Experiment 1) and following rehabilitation and CsA treatment (Experiment 2A). In experiment 1, rats that received hypoxia-ischemia crossed between zones of the open field significantly less than those receiving a sham surgery. In Experiment 2, all animals received hypoxia-ischemia. No drug by group interaction was observed, but a significant main effect of rehabilitation showed that rats receiving rehab crossed between open field zones significantly more than those that did not receive rehab (2B). Unpaired student's *t*-test; *$p < 0.05$.

Experiment	Group	Crossings 1st minute	Total crossings	Distance (cm)	Latency (s)
1	Sham	*18.67 ± 8.1*	49.89 ± 8.2	1253.28 ± 133.5	24.19 ± 7.4
	Hypoxia-Ischemia	*11.23 ± 15.1**	39.26 ± 5.1	1253.39 ± 113.7	41.18 ± 10.2
2A	Vehicle + No Rehab	24.71 ± 1.8	130.57 ± 4.7	3354.65 ± 78.0	3.29 ± 0.7
	Vehicle + Rehab	32.78 ± 2.6	148.22 ± 13.1	3512.17 ± 185.6	4.39 ± 0.9
	CsA + No Rehab	28.14 ± 4.9	134.57 ± 17.1	3460.56 ± 334.4	2.93 ± 0.2
	CsA + Rehab	35.875 ± 2.4	149.38 ± 8.2	3554.65 ± 197.5	5.19 ± 2.5
2B	No Rehab	*26.43 ± 3.4*	132.57 ± 8.5	3407.60 ± 165.6	3.11 ± 0.3
	Rehab	*34.33 ± 1.5**	148.76 ± 7.9	3532.16 ± 134.6	4.77 ± 1.2

Unpaired Student's *t*-test.
* $p < 0.05$.

Table 2
Performance in the novel-object preference index prior to treatment (Experiment 1) and following rehabilitation and CsA treatment (Experiment 2). Rats receiving hypoxia-ischemia were not significantly impaired, relative to shams, on this task, and no effects of treatment on novel-object preference were observed.

Experiment	Groups	Proportion of Time with Novel (%)
1	Sham	73.13 ± 4.9
	Hypoxia-Ischemia	67.48 ± 3.8
2	Vehicle + No Rehab	57.33 ± 8.5
	Vehicle + Rehab	55.06 ± 7.6
	CsA + No Rehab	61.45 ± 6.1
	CsA + Rehab	67.31 ± 5.7

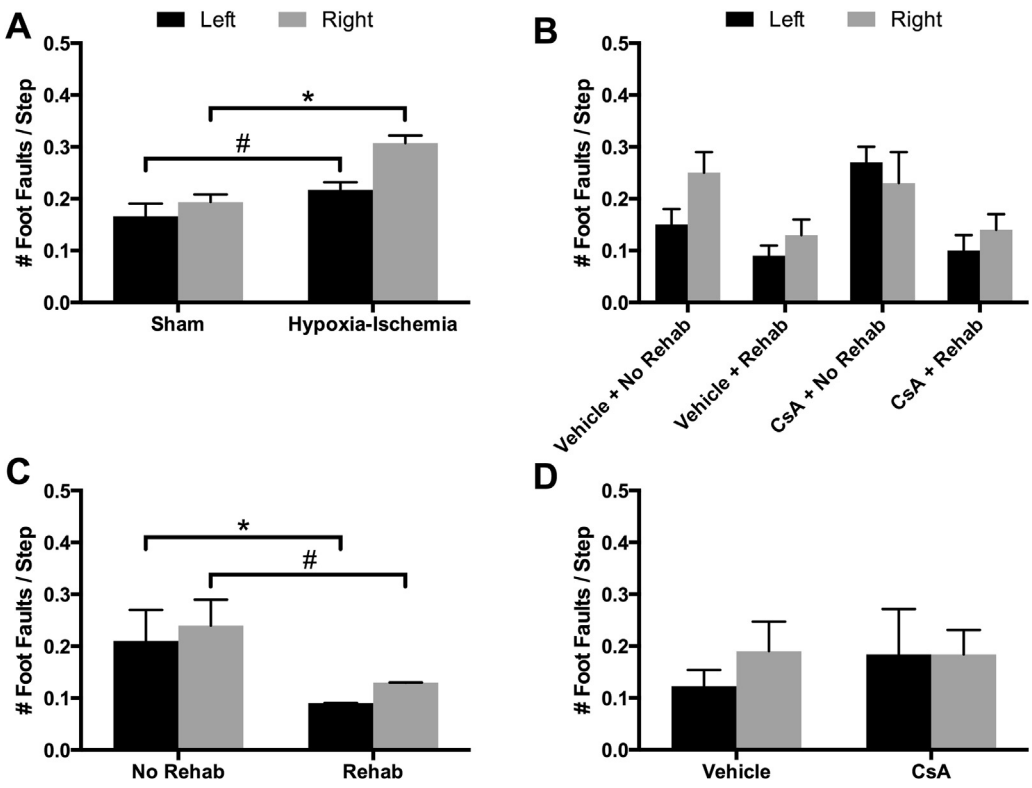

Fig. 3. Foot faults per step in ladder walking task, mean ± SEM. (A) In Experiment 1, animals in the HI group made significantly more errors with both the right and left paws in the ladder walking task. *p < 0.001; #p < 0.05. (B) Experiment 2, performance of all experimental conditions presented as number of errors per total of steps. All groups received HI injury. No significant time by group interaction was observed. (C) Post hoc analysis collapsing rehab and no rehab animals. Rehab condition demonstrated significant improvements over animals in the standard conditions both the affected and unaffected paws (*p < 0.001; #p < 0.05). (D) Post-hoc analysis collapsing CsA and vehicle animals for the left and right paw (p > 0.05). No significant differences between groups were observed.

and latency to leave arena center there is no difference between groups (Table 1).

3.3.3. Ladder rung test

One-way ANOVA indicated a *rehabilitation* effect ($F(1,30) = 16.0242$, $p < 0.001$) and a *drug* effect ($F(1,30) = 4.2336$, $p < 0.05$) for left (unaffected) paws in the horizontal ladder-rung test. There was also a significant main effect of *rehabilitation* ($F(1,30) = 6.756$, $p < 0.001$) for the right paws (affected, Fig. 3B). Collapsing rehab and no rehab animals, *post hoc* analysis showed that the rehab group makes significantly fewer errors than the no rehab group with right ($p < 0.01$) and left paws ($p < 0.001$, Fig. 3C). However, unpaired Student's *t*-test showed no significant difference between CsA and vehicle drug treatment for the left paws ($p > 0.05$; Fig. 3D). Additionally, there were no between-group differences in the number of steps required to cross the ladder (CsA + Rehab: 45.37 ± 1.26; CsA + NoRehab: 45.0 ± 1.58; Vehicle + Rehab: 47.87 ± 1.72; Vehicle + NoRehab: 46.85 ± 1.89).

3.3.4. Novel object recognition

Novel-object preference index wasn't affected by *rehabilitation* ($F(1,30) = 0.0310$, $p > 0.05$) or *drug* ($F(1,30) = 2.4356$, $p > 0.05$). Therefore, declarative memory was not influenced by combinational therapy (Table 2).

3.3.5. Montoya staircase task

Number of pellets retrieved for left paw (unaffected) increased within days; repeated measures ANOVA revealed significant *days* effect ($F(9,21) = 64.5623$, $p < 0.001$) representing a motor learning effect without differences between groups across time (Fig. 4A). Repeated measures ANOVA revealed a significant *rehabilitation* ($F(1,30) = 7.1776$, $p < 0.01$) and *days* effect ($F(9,21) = 26.5755$, $p < 0.001$) for affected forelimb (right, Fig. 4B). Collapsing rehab and no rehab animals, *post hoc* analysis showed that the no rehab group retrieved significantly fewer pellets than the rehab group across time ($p < 0.001$; Fig. 4C). The same difference is observed when comparing average group performances ($p < 0.001$; Fig. 4D).

4. Discussion

The Rice-Vannucci rat model of neonatal HI produces unilateral brain injury, causing damage mainly in the artery-occluded hemisphere [13]. In this model, most animals do not display any obvious locomotor or postural abnormalities so it is important to choose tests that are sufficiently sensitive to reveal sensorimotor and cognitive deficits.

In the first experiment, we investigated effects of neonatal HI event on early motor and cognitive function using a battery of tests. In a second experiment, we investigated the efficacy of a combined therapy of CsA and motor rehabilitation (i.e. enriched rehabilitation) on recovery of motor and cognitive function using the behavioural tests employed in experiment 1 and examined the acquisition of a novel skilled reaching task, the Montoya staircase.

In experiment 1 we found abnormalities in the open field and ladder tests but not in cylinder or novel object recognition tests. Open field evaluation conducted 17 days after injury showed that HI animals made fewer crossings than shams in the first minute of the test period, suggesting decreased exploratory activity or possibly increased anxiety [10,45]. Earlier studies have reported both hyper- and hypoactivity following neonatal hypoxia–ischemia [10,18,46] which may be due to differences in testing such as pre-exposing animals to the testing environment which results in habituation or averaging activity over long test sessions.

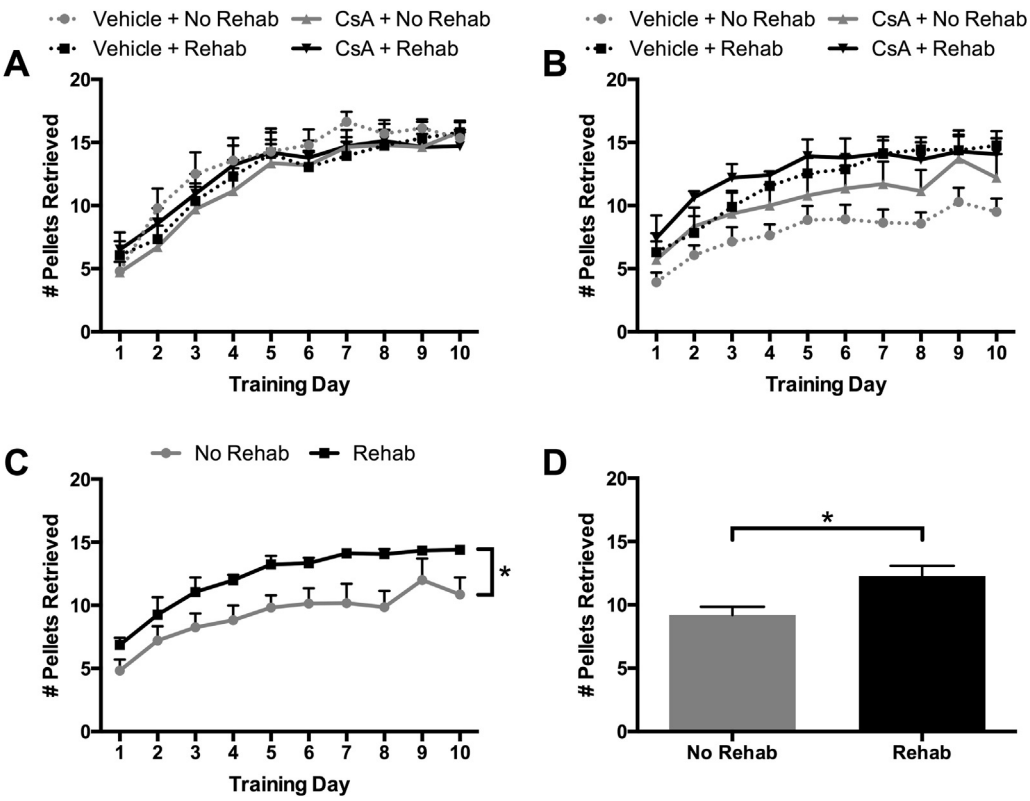

Fig. 4. Number of pellets retrieved in staircase reaching task averaged by training day, mean ± SEM. (D) All groups performed similarly with the left (unimpaired) paw in the staircase reaching task. (A) There was no significant time by group interaction for performance in the staircase reaching task with the right (impaired) paw. (B) Performance of rehab vs. non-rehab groups collapsed across time for the right paw. Animals in the rehab condition demonstrated superior performance over animals in the standard conditions at all time points (*$p < 0.001$). (C) Group performance for the right paw averaged across time. Overall, animals in rehab groups retrieved significantly more pellets than animals in groups that did not receive rehab (*$p < 0.001$).

Similarly, in the ladder rung test HI animals made significantly more foot faults than shams. Ladder rung walking has been reported to be sensitive in detecting long-term impairment in placement, stepping, and coordinated limb use during locomotion following different types of brain injury [25,41] in adult animals and the present findings show this also to be the case with HI injury (Fig. 3A).

The behavioural data in experiment 2 showed that ER produces significantly greater motor recovery than CsA therapy. Enriched rehabilitation increased number of zone crosses in open-field exploration and enhanced coordinated limb use on the ladder task and accelerated and improved new motor learning (i.e. acquisition of staircase skilled-reaching). Open field-testing conducted at PND 49 showed that ER animals exhibited a greater number of zone crossings in the first minute of open-field exploration when compared to non-rehabilitated animals. Ladder test outcomes suggest that the rehabilitation condition improved use of both affected and unaffected paws when compared to the non-rehabilitated group. In the staircase test, we found preserved motor learning capacity for all groups across time and greater functional improvement for ER groups independent of drug intervention. Contralateral (right) paw-reach performance was more impaired in non-rehabilitated rats indicating that this test is useful in detecting treatment effects. Enriched rehabilitation had no effect in the novel object recognition test.

In the present study CsA had no effect on behavioural outcomes relative to ER. A previous study reported that early CsA administration promoted endogenous neural precursor cell activation in mice [47]. However, other studies describing CsA effects on immature brain injury such as infarct volume [2,32,48,49] have produced inconsistent results. Based on the time window of other therapeutic interventions [50] it is possible that CsA administered 2 weeks after the HI procedure was too late to be efficacious since HI causes progressive damage and apoptosis in cerebral cortex, striatum and hippocampus [51,52] over the first several days after HI. Notably, there are reports that CsA administered immediately after or several hours after ischemic injury may attenuate cell death and protect the immature rat brain [2,32]. Unfortunately, Cremophor EL, the vehicle used to dissolve CsA proved so highly toxic in young rat pups that it precluded early CsA treatment. Our results suggest that very late CsA intervention has no effect on functional recovery after neonatal HI.

Assessment of HI injury shows clear hippocampal, cortical and hemispheric atrophy ipsilateral to arterial occlusion that was not affected by the combined therapy of CsA and ER. These results are in agreement with other findings [14,15,18,45,53] including a recent clinical trial in which CsA had no effect on infarct size [54].

In summary, the present study demonstrated that ER enhanced recovery of motor function after neonatal HI and improved learning of new motor skills. The present findings in an HI model are congruent with previous work reporting functional benefits of ER in models of focal ischemia [24–26] in adult animals. Interestingly, these studies found that there is an early “critical or sensitive” time window, lasting approximately 30 days after stroke in the adult rat, when ER is most effective. In the present study, the ER was initiated 14 days after HI injury and was very effective in enhancing motor learning (i.e. staircase acquisition), attenuating sensory-motor deficits (e.g. ladder test) and blunting the anxiety response in a novel environment (i.e. open-field). It remains to be determined if the “critical period” in the young brain remains open for a longer period of time than that of the adult brain.

Conflict of interest

The authors declare that there are no conflicts of interest.

Acknowledgments

This work was supported by grants from Heart and Stroke Foundation Canadian Partnership for Stroke Recovery and Emerging Leaders in the Americas Program (ELAP).

References

[1] D. Alonso-Alconada, A. Álvarez, O. Arteaga, A. Martínez-Ibargüen, E. Hilario, Neuroprotective effect of melatonin: a novel therapy against perinatal hypoxia-Ischemia, Int. J. Mol. Sci. 14 (2013) 9379–9395, http://dx.doi.org/10.3390/ijms14059379.
[2] J.H. Hwang, J.H. Lee, K.-H. Lee, E.J. Bae, D.K. Sung, Y.S. Chang, et al., Cyclosporine A attenuates hypoxic–ischemic brain injury in newborn rats, Brain Res. 1359 (2010) 208–215, http://dx.doi.org/10.1016/j.brainres.2010.08.047.
[3] B.J. Delsing, C.E. Catsman-Berrevoets, I.M. Appel, Early prognostic indicators of outcome in ischemic childhood stroke, Pediatr. Neurol. 24 (2001) 283–289, http://dx.doi.org/10.1016/S0887-8994(01) 00245-4.
[4] R.L. Holt, M.A. Mikati, Care for child development: basic science rationale and effects of interventions, Pediatr. Neurol. 44 (2011) 239–253, http://dx.doi.org/10.1016/j.pediatrneurol.2010.11.009.
[5] R.C. Vannucci, S.J. Vannucci, A model of perinatal hypoxic-ischemic brain damage, Ann. N. Y. Acad. Sci. 835 (1997) 234–249, http://dx.doi.org/10.1111/j.1749-6632.1997.tb48634.x.
[6] J.E. Rice, R.C. Vannucci, J.B. Brierley, The influence of immaturity on hypoxic-ischemic brain damage in the rat, Ann. Neurol. 9 (1981) 131–141, http://dx.doi.org/10.1002/ana.410090206.
[7] I.-C. Chou, T. Trakht, C. Signori, J. Smith, B.T. Felt, D.M. Vazquez, et al., Behavioral/environmental intervention improves learning after cerebral hypoxia-ischemia in rats, Stroke 32 (2001) 2192–2197, http://dx.doi.org/10.1161/hs0901.095656.
[8] W.J. Xia, M. Yang, T.F. Fok, K. Li, W.Y. Chan, P.-C. Ng, et al., Partial neuroprotective effect of pretreatment with tanshinone IIA on neonatal hypoxia-ischemia brain damage, Pediatr. Res. 58 (2005) 784–790, http://dx.doi.org/10.1203/01.PDR.0000180550.99162.BC.
[9] M.A. van der Kooij, F. Ohl, S.S. Arndt, A. Kavelaars, F. van Bel, C.J. Heijnen, Mild neonatal hypoxia-ischemia induces long-term motor- and cognitive impairments in mice, Brain. Behav. Immun. 24 (2010) 850–856, http://dx.doi.org/10.1016/j.bbi.2009.09.003.
[10] A. Lubics, D. Reglődi, A. Tamás, P. Kiss, M. Szalai, L. Szalontay, et al., Neurological reflexes and early motor behavior in rats subjected to neonatal hypoxic–ischemic injury, Behav. Brain Res. 157 (2005) 157–165, http://dx.doi.org/10.1016/j.bbr.2004.06.019.
[11] V.S. Ten, M. Bradley-Moore, J.A. Gingrich, R.I. Stark, D.J. Pinsky, Brain injury and neurofunctional deficit in neonatal mice with hypoxic-ischemic encephalopathy, Behav. Brain Res. 145 (2003) 209–219, http://dx.doi.org/10.1016/S0166-4328(03) 00146-3.
[12] T. Ikeda, K. Mishima, T. Yoshikawa, K. Iwasaki, M. Fujiwara, Y.X. Xia, et al., Selective and long-term learning impairment following neonatal hypoxic-ischemic brain insult in rats, Behav. Brain Res. 118 (2001) 17–25, http://dx.doi.org/10.1016/S0166-4328(00) 00287-4.
[13] E.M. Jansen, W.C. Low, Quantitative analysis of contralateral hemisphere hypertrophy and sensorimotor performance in adult rats following unilateral neonatal ischemic-hypoxic brain injury, Brain Res. 708 (1996) 93–99, http://dx.doi.org/10.1016/0006-8993(95) 01288-5.
[14] L.O. Pereira, N.S. Arteni, R.C. Petersen, A.P. da Rocha, M. Achaval, C.A. Netto, Effects of daily environmental enrichment on memory deficits and brain injury following neonatal hypoxia-ischemia in the rat, Neurobiol. Learn. Mem. 87 (2007) 101–108, http://dx.doi.org/10.1016/j.nlm.2006.07.003.
[15] J.J. Rojas, B.F. Deniz, P.M. Miguel, R. Diaz, D.E.S.É. Hermel, M. Achaval, et al., Effects of daily environmental enrichment on behavior and dendritic spine density in hippocampus following neonatal hypoxia-ischemia in the rat, Exp. Neurol. 241 (2013) 25–33, http://dx.doi.org/10.1016/j.expneurol.2012.11.026.
[16] E.F. Sanches, N.S. Arteni, F. Nicola, L. Boisserand, S. Willborn, C.A. Netto, Early hypoxia-ischemia causes hemisphere and sex-dependent cognitive impairment and histological damage, Neuroscience 237 (2013) 208–215, http://dx.doi.org/10.1016/j.neuroscience.2013.01.066.
[17] B.B. Johansson, P.V. Belichenko, Neuronal plasticity and dendritic spines: effect of environmental enrichment on intact and postischemic rat brain, J. Cereb. Blood Flow Metab. 22 (2002) 89–96, http://dx.doi.org/10.1097/00004647-200201000-00011.
[18] J.J. Rojas, B.F. Deniz, C.P. Schuch, J.V. Carletti, I. Deckmann, R. Diaz, et al., Environmental stimulation improves performance in the ox-maze task and recovers Na+, K+-ATPase activity in the hippocampus of hypoxic-ischemic rats, Neuroscience 291 (2015) 118–127, http://dx.doi.org/10.1016/j.neuroscience.2015.01.017.
[19] G. Horvath, D. Reglodi, G. Vadasz, J. Farkas, P. Kiss, Exposure to enriched environment decreases neurobehavioral deficits induced by neonatal glutamate toxicity, Int. J. Mol. Sci. 14 (2013) 19054–19066, http://dx.doi.org/10.3390/ijms140919054.
[20] A.L. Ohlsson, B.B. Johansson, Environment influences functional outcome of cerebral infarction in rats, Stroke 26 (1995) 644–649, http://dx.doi.org/10.1161/01.STR.26.4.644.
[21] D. Young, P.A. Lawlor, P. Leone, M. Dragunow, M.J. During, Environmental enrichment inhibits spontaneous apoptosis, prevents seizures and is neuroprotective, Nat. Med. 5 (1999) 448–453, http://dx.doi.org/10.1038/7449.
[22] H. van Praag, G. Kempermann, F.H. Gage, Neural consequences of environmental enrichment, Nat. Rev. Neurosci. 1 (2000) 191–198, http://dx.doi.org/10.1038/35044558.
[23] P. Kiss, G. Vadasz, B. Kiss-Illes, G. Horvath, A. Tamas, D. Reglodi, et al., Environmental enrichment decreases asphyxia-induced neurobehavioral developmental delay in neonatal rats, Int. J. Mol. Sci. 14 (2013) 22258–22273, http://dx.doi.org/10.3390/ijms141122258.
[24] J. Biernaskie, D. Corbett, Enriched rehabilitative training promotes improved forelimb motor function and enhanced dendritic growth after focal ischemic injury, J. Neurosci. 21 (2001) 5272–5280, doi:21/14/5272 [pii].
[25] J. Biernaskie, Efficacy of rehabilitative experience declines with time after focal ischemic brain injury, J. Neurosci. 24 (2004) 1245–1254, http://dx.doi.org/10.1523/JNEUROSCI.3834-03.2004.
[26] C.L. MacLellan, M.B. Keough, S. Granter-Button, G.A. Chernenko, S. Butt, D. Corbett, A critical threshold of rehabilitation involving brain-derived neurotrophic factor is required for poststroke recovery, Neurorehabil. Neural Repair 25 (2011) 740–748, http://dx.doi.org/10.1177/1545968311407517.
[27] C.L. MacLellan, N. Plummer, G. Silasi, A.M. Auriat, F. Colbourne, Rehabilitation promotes recovery after whole blood-induced intracerebral hemorrhage in rats, Neurorehabil. Neural Repair 25 (2011) 477–483, http://dx.doi.org/10.1177/1545968310395602.
[28] J. Caliaperumal, F. Colbourne, Rehabilitation improves behavioral recovery and lessens cell death without affecting iron, ferritin, transferrin, or inflammation after intracerebral hemorrhage in rats, neurorehabil, Neural Repair 28 (2014) 395–404, http://dx.doi.org/10.1177/1545968313517758.
[29] P. Dibajnia, C.M. Morshead, Role of neural precursor cells in promoting repair following stroke, Acta Pharmacol. Sin. 34 (2013) 78–90, http://dx.doi.org/10.1038/aps.2012.107.
[30] J. Hunt, A. Cheng, A. Hoyles, E. Jervis, C.M. Morshead, Cyclosporin A has direct effects on adult neural precursor cells, J. Neurosci. 30 (2010) 2888–2896, http://dx.doi.org/10.1523/JNEUROSCI.5991-09.2010.
[31] A.P. Halestrap, C.P. Connern, E.J. Griffiths, P.M. Kerr, Cyclosporin A binding to mitochondrial cyclophilin inhibits the permeability transition pore and protects hearts from ischaemia/reperfusion injury, Mol. Cell. Biochem. 174 (1997) 167–172 (accessed 05.10.15) http://www.ncbi.nlm.nih.gov/pubmed/9309682.
[32] P.-L. Leger, D. De Paulis, S. Branco, P. Bonnin, E. Couture-Lepetit, O. Baud, et al., Evaluation of cyclosporine A in a stroke model in the immature rat brain, Exp. Neurol. 230 (2011) 58–66, http://dx.doi.org/10.1016/j.expneurol.2010.06.009.
[33] N.A.A. Baky, L. Fadda, N.M. Al-Rasheed, N.M. Al-Rasheed, A. Mohamed, H. Yacoub, Neuroprotective effect of carnosine and cyclosporine-A against inflammation, apoptosis, and oxidative brain damage after closed head injury in immature rats, Toxicol. Mech. Methods. (2015) (accessed 05.10.15) http://www.tandfonline.com/doi/full/10.3109/15376516.2015.1070224.
[34] A. Tuladhar, C.M. Morshead, M.S. Shoichet, Circumventing the blood–brain barrier: local delivery of cyclosporin A stimulates stem cells in stroke-injured rat brain, J. Control. Release. 215 (2015) 1–11 (accessed 09.18.15) http://www.sciencedirect.com/science/article/pii/S0168365915300365.
[35] C. Iadecola, J. Anrather, Stroke research at a crossroad: asking the brain for directions, Nat. Neurosci. 14 (2011) 1363–1368, http://dx.doi.org/10.1038/nn.2953.
[36] M.S. Jeffers, a. Hoyles, C. Morshead, D. Corbett, Epidermal growth factor and erythropoietin infusion accelerate functional recovery in combination with rehabilitation, Stroke 45 (2014) 1856–1858, http://dx.doi.org/10.1161/STROKEAHA.114.005464.
[37] H. Gelderblom, J. Verweij, K. Nooter, A. Sparreboom, Cremophor EL: the drawbacks and advantages of vehicle selection for drug formulation, Eur. J. Cancer. 37 (2001) 1590–1598, http://dx.doi.org/10.1016/S0959-8049(01)00171-X.
[38] R.G. Mestriner, A.S. Pagnussat, L.S.B. Boisserand, L. Valentim, C.A. Netto, Skilled reaching training promotes astroglial changes and facilitated sensorimotor recovery after collagenase-induced intracerebral hemorrhage, Exp. Neurol. 227 (2011) 53–61, http://dx.doi.org/10.1016/j.expneurol.2010.09.009.
[39] T. Schallert, Behavioral tests for preclinical intervention assessment, NeuroRx 3 (2006) 497–504, http://dx.doi.org/10.1016/j.nurx.2006.08.001.
[40] M.T. Woodlee, A.M. Asseo-Garcia, X. Zhao, S.J. Liu, T.A. Jones, T. Schallert, Testing forelimb placing across the midline reveals distinct, lesion-dependent patterns of recovery in rats, Exp Neurol. 191 (2005) 310–317, http://dx.doi.org/10.1016/j.expneurol.2004.09.005.
[41] G.A. Metz, I.Q. Whishaw, Cortical and subcortical lesions impair skilled walking in the ladder rung walking test: a new task to evaluate fore- and hindlimb stepping, placing, and co-ordination, J. Neurosci. Methods 115 (2002) 169–179, http://dx.doi.org/10.1016/S0165-0270(02)00012-2.
[42] H. Plamondon, A. Morin, C. Charron, Chronic 17beta-estradiol pretreatment and ischemia-induced hippocampal degeneration and memory impairments:

a 6-month survival study, Horm. Behav. 50 (2006) 361–369, http://dx.doi.org/10.1016/j.yhbeh.2006.04.006.
[43] C.P. Montoya, L.J. Campbell-Hope, K.D. Pemberton, S.B. Dunnett, The staircase test: a measure of independent forelimb reaching and grasping abilities in rats, J. Neurosci. Methods 36 (1991) 219–228, http://dx.doi.org/10.1016/0165-0270(91) 90048-5.
[44] A.D.S. Pagnussat, S.M. Michaelsen, M. Achaval, C.A. Netto, Skilled forelimb reaching in Wistar rats: evaluation by means of Montoya staircase test, J. Neurosci. Methods 177 (2009) 115–121, http://dx.doi.org/10.1016/j.jneumeth.2008.10.001.
[45] J.V. Carletti, B.F. Deniz, P.M. Miguel, J.J. Rojas, J. Kolling, E.B. Scherer, et al., Folic acid prevents behavioral impairment and Na+,K+-ATPase inhibition caused by neonatal hypoxia–ischemia, Neurochem. Res. 37 (2012) 1624–1630, http://dx.doi.org/10.1007/s11064-012-0757-6.
[46] L. Iuvone, M.C. Geloso, E. Dell'Anna, Changes in open field behavior, spatial memory, and hippocampal parvalbumin immunoreactivity following enrichment in rats exposed to neonatal anoxia, Exp. Neurol. 139 (1996) 25–33, http://dx.doi.org/10.1006/exnr.1996.0077.
[47] A. Erlandsson, C.-H.A. Lin, F. Yu, C.M. Morshead, Immunosuppression promotes endogenous neural stem and progenitor cell migration and tissue regeneration after ischemic injury, Exp. Neurol. 230 (2011) 48–57, http://dx.doi.org/10.1016/j.expneurol.2010.05.018.
[48] A. Nakai, Y. Shibazaki, Y. Taniuchi, H. Miyake, A. Oya, T. Takeshita, Role of mitochondrial permeability transition in fetal brain damage in rats, Pediatr. Neurol. 30 (2004) 247–253, http://dx.doi.org/10.1016/j.pediatrneurol.2003.09.006.
[49] M. Puka-Sundvall, E. Gilland, H. Hagberg, Cerebral hypoxia-ischemia in immature rats: involvement of mitochondrial permeability transition? Dev. Neurosci. 23 (2001) 192–197 (46142).
[50] D. Corbett, M. Jeffers, C. Nguemeni, M. Gomez-Smith, J. Livingston-Thomas, Lost in translation: rethinking approaches to stroke recovery, Prog. Brain Res. 218 (2015) 413–434, http://dx.doi.org/10.1016/bs.pbr.2014.12.002.
[51] W. Nakajima, A. Ishida, M.S. Lange, K.L. Gabrielson, M.A. Wilson, L.J. Martin, et al., Apoptosis has a prolonged role in the neurodegeneration after hypoxic ischemia in the newborn rat, J. Neurosci. 20 (2000) 7994–8004, doi:20/21/7994 [pii].
[52] M.A. Hossain, Hypoxic-ischemic injury in neonatal brain: involvement of a novel neuronal molecule in neuronal cell death and potential target for neuroprotection, Int. J. Dev. Neurosci. 26 (2008) 93–101, http://dx.doi.org/10.1016/j.ijdevneu.2007.08.013.
[53] L.O. Pereira, A.C.P. Strapasson, P.M. Nabinger, M. Achaval, C.A. Netto, Early enriched housing results in partial recovery of memory deficits in female, but not in male, rats after neonatal hypoxia-ischemia, Brain Res. 1218 (2008) 257–266, http://dx.doi.org/10.1016/j.brainres.2008.04.010.
[54] N. Nighoghossian, Y. Berthezene, L. Mechtouff, L. Derex, T.H. Cho, T. Ritzenthaler, et al., Cyclosporine in acute ischemic stroke, Neurology 84 (2015) 2216–2223, http://dx.doi.org/10.1212/WNL.0000000000001639.

Journal of Neuroscience Methods 242 (2015) 72–76

Contents lists available at ScienceDirect

Journal of Neuroscience Methods

journal homepage: www.elsevier.com/locate/jneumeth

Basic Neuroscience

Time course of neuronal death following endothelin-1 induced focal ischemia in rats

Carine Nguemeni[a,e], Mariana Gomez-Smith[a,e], Matthew S. Jeffers[a,e], Clarissa Pedrini Schuch[d], Dale Corbett[a,b,c,e,*]

[a] Faculty of Medicine, University of Ottawa, Ottawa, ON, Canada
[b] Faculty of Medicine, Memorial University of Newfoundland, St. John's, NL, Canada
[c] Faculty of Medicine, University of Toronto, Toronto, ON, Canada
[d] Universidade Federal do Rio Grande do Sul, Brazil
[e] Canadian Partnership for Stroke Recovery, University of Ottawa, Ottawa, ON, Canada

HIGHLIGHTS

- We analyzed the time course of neuronal death in a rat model of ET-1 induced stroke targeting the forelimb motor cortex.
- Maximal infarct volume is achieved within 24 h of ischemia in this model.
- The process of neuronal degeneration is maximal within 24 h of ischemia.

ARTICLE INFO

Article history:
Received 18 September 2014
Received in revised form 8 December 2014
Accepted 3 January 2015
Available online 10 January 2015

Keywords:
Endothelin-1
Ischemic stroke
Neuronal death
Fluoro-Jade C

ABSTRACT

Background: Endothelin-1 (ET-1) induced focal ischemia is increasingly being used as a preclinical model of stroke. Here, we described for the first time, the time course of neuronal death and infarct evolution during the first 7 days following ischemia.
New method: We used hematoxylin and eosin (H&E) staining to evaluate infarct progression and Fluoro-Jade C (FJC) to quantify neuronal degeneration at 24, 48, 72 h and 7 days after ET-1 injection to the forelimb motor cortex in Sprague-Dawley rats.
Results: We found that infarct volume and neuronal degeneration are maximal at 24 h post-stroke. Neuronal degeneration is also significantly reduced within 7 days of stroke induction.
Comparison with existing method: This study is the first to provide a direct evaluation of both infarct volume evolution and neuronal death time course following ET-1 induced focal ischemia in the forelimb motor cortex.
Conclusion: This study describes the short-term time course of neuronal death and brain injury in the ET-1 stroke model, which provides a significant reference when determining the appropriate time to commence neuroprotective or recovery promoting strategies.

1. Introduction

Many animal models have been developed to mimic particular clinical features of stroke in an attempt to identify therapeutic targets and to develop effective post-stroke therapies (Canazza et al., 2014). However, almost every therapy developed in the preclinical setting has failed to translate successfully to clinic (O'Collins et al., 2006; Moskowitz, 2010). Models of focal ischemia have been associated with variable infarcts, mechanisms and size depending on the type of occlusion – permanent or transient, the duration of the occlusion and the agent responsible of the occlusion (microsphere, clot, filament, mechanical or chemical agent) (Carmichael, 2005). The extent of injury and the time course of cellular death (infarct core or more distal selective neuronal loss) within a model are crucial aspects for the stroke pathogenesis because they have a huge impact on the interpretation and the success of post-stroke interventions (Fisher et al., 2009). For instance, data suggest that some neuroprotective targets may have negative effects on recovery after stroke (Lo, 2008). Thus, by understanding how the injury evolves, it will be possible to administer a given intervention within

* Corresponding author at: Cellular & Molecular Medicine, Faculty of Medicine, University of Ottawa, Ottawa, ON K1H 8M5, Canada. Tel.: +1 613 562 5800x8177; fax: +1 613 562 54.
E-mail address: dcorbett@uottawa.ca (D. Corbett).

http://dx.doi.org/10.1016/j.jneumeth.2015.01.005
0165-0270/

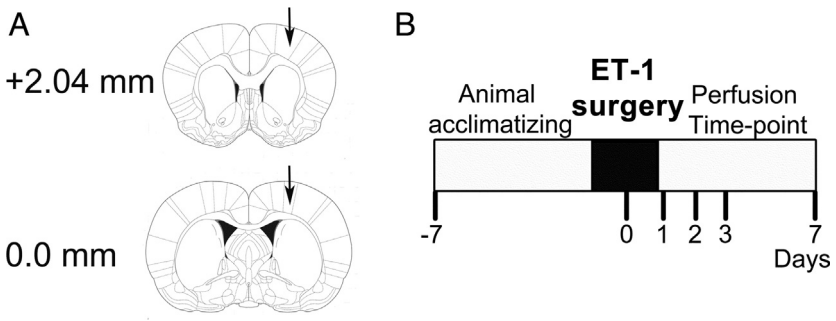

Fig. 1. Timeline of experimental procedures. (A) 2 μl of endothelin-1 (400 pmol/μl) was injected at each of two sites indicated by arrows in the rat forelimb motor cortex and (B) brains were extracted at 24, 48, 72 h and 7 days following ET-1 induced focal ischemia.

the appropriate time window, in order to improve efficacy and transferability.

Endothelin-1 (ET-1) is increasingly being used to induce focal ischemia in rodent models of stroke. ET-1 is a 21-amino acid peptide that acts as a vasoconstrictor (Yanagisawa et al., 1988), which can be microinjected to cause a transient and localized reduction in blood flow, resulting in ischemic damage (Macrae et al., 1993; Gilmour et al., 2004; Windle et al., 2006; Soleman et al., 2010). Unlike the original intraluminal suture model of middle cerebral artery occlusion that often results in very large infarcts, variable injury location (Dittmar et al., 2003; Strom et al., 2013) and debilitation, the ET-1 model results in rapid recovery from the surgical procedures and the injury size can easily be controlled. It also allows for specific targeting of any desired cortical or subcortical region by microinjection. The photothrombosis model is also reproducible and while primarily used to produce cortical injury (Matsuno et al., 1993) it can be used to create subcortical injury via stereotaxic implantation of a fibre optic probe (Barth and Mody, 2011). Moreover, this model allows for only limited vascular reperfusion (Carmichael, 2005). Occlusion of blood vessels resulting from ET-1 is followed by a slow and gradual reperfusion (Biernaskie et al., 2001) mimicking early reperfusion in human ischemic stroke (Barber et al., 1998).

The specific time course of cell death following ET-1 injection has not been systematically investigated. This is particularly important for recovery studies because if therapeutic interventions are given while injury is still evolving it becomes impossible to distinguish between neuroprotective versus restorative effects. Hence, the purpose of this study was to examine neuronal cell death during the first days following ET-1 injection in the forelimb motor cortex of rats. Herein, the area of infarction was estimated using hematoxylin and eosin staining (H&E), after which Fluoro-Jade C (FJC) labelling was used to confirm the specific temporal profile of degenerating neurons in more distal peri-infarct regions.

2. Materials and methods

2.1. Subjects

A total of 41 male Sprague-Dawley rats (Charles River Laboratories, Montreal, Canada) weighing 350–400 g at the time of surgery were used in this study. Rats were pair-housed in standard Plexiglas cages on a 12/12 h reverse light/dark cycle (lights off at 08:00) with ad libitum access to food and water. Animals were allowed to acclimate to the housing facility for 1 week prior to surgery. The University of Ottawa Animal Care Committee approved all experimental procedures. Two animals were removed from the study due to infarct sizes greater than two standard deviations from the mean, whereas two others were lost due to perfusion errors.

2.2. Endothelin-1 focal ischemia model

Rats were anesthetized with isoflurane (4% induction, 2% maintenance with oxygen 1–1.2 l/min) and secured in a stereotaxic frame. Endothelin-1 (Calbiochem, San Diego, California, 400 pmol/μl in sterile water) was injected at two sites of the right forelimb motor cortex. Each injection delivered 2 μl of ET-1 at a rate of 0.25 μl/min at the following coordinates relative to Bregma (Fig. 1A): anterior–posterior (AP): 0.0 and +2.0 mm; medial–lateral (ML): +2.5 mm. The dorso-ventral (DV) coordinates taken from cortex were: −2.4 mm for both the (AP) 0.0 mm and +2.0 mm sites. At each site, the injection was done in two sequences of 1 μL with a 1 min pause between each injection. At the end of the injection, the needle was left in place for 3 additional minutes before withdrawal. Five SHAM rats were treated identically except they received injections of sterile water instead of ET-1. Body temperature was maintained between 36.5 °C and 37.5 °C using a homoeothermic heating blanket throughout the surgery. After the ET-1 injections, the incision was sutured; a topical anaesthetic was applied (2% transdermal bupivacaine, 0.2 ml, Chiron, Guelph, Canada). Animals were then placed in a recovery chamber to maintain the body temperature at ∼37 °C until they recovered from anaesthesia. At this point, rats were given a single *s.c.* injection of buprenorphine (0.05 mg/kg, Reckitt Benckiser Pharmaceuticals Inc., Richmond, USA) and returned to their home cage.

2.3. Tissue preparation

At four distinct time points (24, 48, 72 h and 7 days) following surgery, rats were deeply anesthetized by *i.p.* administration of Euthanyl (149.5 mg/kg, Bimeda-MTC Health Inc., Cambridge, Canada) and transcardially perfused with heparinized saline, followed by 4% paraformaldehyde (PFA) in phosphate-buffered saline ($n = 8$/group, Fig. 1B). Brains were removed and post-fixed in 4% PFA overnight at 4 °C, then transferred to a solution of 20% sucrose (w/v) in 0.1 M phosphate buffer until saturated. Twenty microns thick sections were sectioned throughout the entire injured area. Sections at intervals of 200 μm were retained and stained with H&E or FJC for each animal. An average of 10 sections stained with H&E, covering the entire injured area were used to determine infarct volume.

2.4. Infarct volume assessment

The area of contralateral and intact ipsilateral tissue remaining was measured using Image J (downloaded for Mac OS X from public domain, NIH, USA, http://imagej.nih.gov/ij/) for each of the 10 sections sampled throughout the infarct. Infarct volume in mm^3 was calculated as follows: $\sum$[(area of contralesional

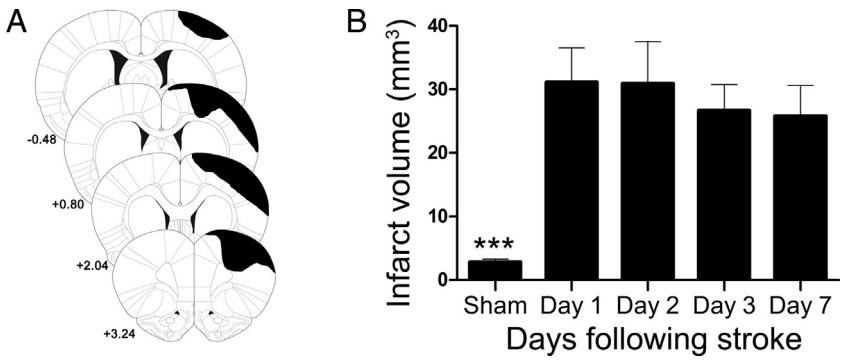

Fig. 2. Evaluation of ischemic damage with H&E staining. (A) Illustration of ischemic damage in a series of H&E stained sections representing the typical extent of injury in the rat cortex following ET-1 injection. (B) Cortical infarct volume following stroke in mm^3. Sham animals were injected with sterile water at the same coordinates as stroke animals and the brains were harvested 24 h after the injection to evaluate the damage. Five sham animals and eight animals for each of the stroke groups were analyzed. Values are expressed as mean ± SEM, *** indicates value of $p \leq 0.05$.

tissue – area of undamaged ipsilesional tissue) × distance between sections × thickness of sections] (Windle et al., 2006).

2.5. Fluoro-Jade C staining

FJC is a fluorescent dye derived from fluorescein which labels degenerating neurons. We used FJC (FJC, Histo-Chem Inc., AR, USA) to identify the temporal profile of neuronal death following ET-1 injection as per the protocol described by Schmued and colleagues (Schmued et al., 2005). Neurons labelled with FJC were quantified at 40X using the Optical Fractionator method in Stereo Investigator (Stereo Investigator® V10.0 MicroBrightField Bioscience, USA) on a Leica DMR microscope (Leica Microsystems, Germany). Four sections equally distributed throughout the infarct were analyzed from each animal ($n = 6$). The counting area was manually traced, defined as the cortical area in which Fluoro-Jade C-positive cells were present. The Optical Fractionator method created a 200 μm × 200 μm spaced grid that was superimposed onto the traced area containing FJC-positive cells. At each grid point, all cells within a randomly chosen 100 μm × 100 μm counting frame were counted.

2.6. Statistics

All analyses were conducted using the Statistical Package for the Social Sciences (SPSS v21.0.0 64 bit for Mac, IBM, USA). Data are expressed as mean ± standard error of the mean (SEM). Data were analyzed using a univariate analysis of variance (ANOVA). Tukey's honestly significant difference test (HSD) was used as a post hoc measure to determine differences between groups. These were considered statistically significant when $p < 0.05$. Experimenters performing all cell-counting and statistical analyses were blind to the experimental groups.

3. Results

3.1. Infarct volume quantification

Focal ischemia resulted in injury primarily localized to the forelimb motor cortex. All the animals were analyzed for cortical and striatal injury. Sham animals showed very minor cortical damage and no striatal injury (Fig. 2B). All the stroked rats showed cortical injury and we also detected some minor damage to the striatum in approximately half of the animals used for infarct volume quantification. There were no significant differences between the groups with respect to either cortical (Fig. 2A and Table 1, $n = 8$, $F_{(3,26)} = 0.243$, $p = 0.866$) or striatal infarct volume ($n = 2$–6, $F_{(3,26)} = 0.559$, $p = 0.647$) (Table 1). A schematic illustration of a typical infarction based on H&E staining is presented in Fig. 2A. Representative micrographs of H&E stained sections for a sham and a stroked rat are shown in Fig. 3C–E.

3.2. Time course of neuronal death

The number of FJC-positive cells was not statistically different between 24, 48 and 72 h following ET-1 injection. However, the number decreased significantly 7 days following stroke ($n = 6$, $F_{(3,20)} = 5.852$, $p = 0.005$, Fig. 2B). Furthermore, at 7 days, the area containing FJC-positive cells was significantly smaller compared to 24 h ($p = 0.009$) and 48 h ($p = 0.041$ Fig. 2C). The number of FJC positive cells and the areas of FJC positive cells are presented in Table 1. A representative micrograph of a FJC stained section is shown in Fig. 3 A–B.

4. Discussion

This study examined the temporal evolution of neuronal death and resulting infarct volume following stereotaxic injection of

Table 1
Infarct volume and neuronal death at different time points following ET-1 induced ischemia of the forelimb motor cortex.

Groups	Striatal infarct volume (mm^3)	Cortical infarct volume (mm^3)	FJC+ cell population number ($\times 10^3$)	Area containing FJC+ cells (mm^3)
Sham	0 ($n = 5$)	2.79 ± 0.47	–	–
24 h	5.25 ± 2.26 ($n = 4/8$)	31.0 ± 5.4	657.77 ± 123.81**	49.34 ± 8.81*
48 h	4.40 ± 1.57 ($n = 5/8$)	30.89 ± 6.60	560.95 ± 116.88*	44.68 ± 9.99*
72 h	1.84 ± 0.79 ($n = 4/8$)	26.36 ± 4.15	523.39 ± 120.36*	41.54 ± 8.03
7 days	3.30 ± 1.84 ($n = 3/8$)	25.77 ± 4.83	88.17 ± 9.32	13.58 ± 2.27

Five sham animals were analyzed for cortical and striatal infarct. They showed minor cortical damage and no striatal damage. Eight animals were analyzed for cortical and striatal infarct volume, FJC+ cells population and the area containing FJC+ cells. All the animals showed cortical injury but only a subset of rats had striatal damage. Data are presented as mean ± SEM. Significance by one-way ANOVA with Tukey HSD post hoc test.

* Value of $p \leq 0.05$.

** Value of $p \leq 0.005$ when compared to 7 days.

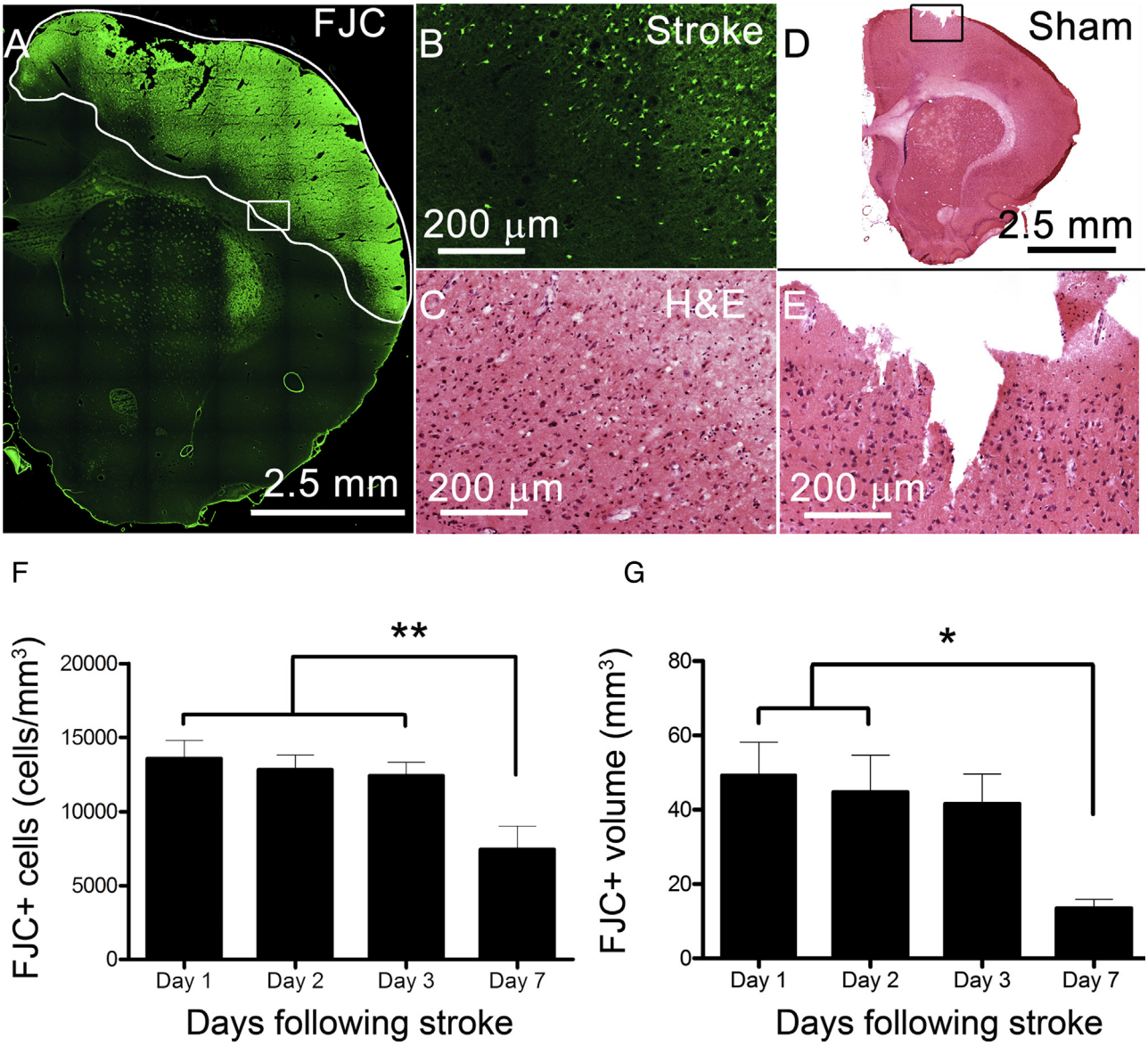

Fig. 3. Illustration of infarct volumes and cell death following ET-1. Representative images of Fluoro-Jade C staining (A and B), H&E staining (C–E) and time course of neuronal death (F and G) are shown. All images are taken at Bregma, approximately half-way between the two ET-1 injection sites. Images in (A and B) are taken from the same section. (A) Is a tile scan of the damaged hemisphere following stroke at 10× magnification, scale bar = 2.5 mm. The white line delineates the area containing FJC+ cortical cells. (B) Shows the region boxed in (A) at a 40× magnification illustrating the sharp border between dying and normal cortical cells, scale bar = 200 μm. (C) Shows H&E staining of the same region as in B at 40×. (D) Low power (10×) micrograph showing the needle track and minor cortical damage resulting from water injection in sham animals. (E) The region framed by the black square presented at 40×, scale bar = 200 μm. (F) The number of FJC-positive cells was quantified using stereological procedures at 40× magnification. (G) Volume estimate of the tissue containing dying neurons was defined by tracing the area where FJC-positive cells were found in the cortex including the ischemic core. Four sections from six animals per time point were analyzed. Values are expressed as mean ± SEM, *indicates value of $p \leq 0.05$, ** indicates value of $p \leq 0.005$.

ET-1 to the rat forelimb motor cortex. We found that at the 24 h time point infarct volume was maximal. In concordance with the infarct measurements, FJC staining showed that neuronal degeneration is also maximal at 24 h post-stroke; however, it decreased significantly 7 days after stroke while the infarct volume remained statistically unchanged. This timing of infarct development is similar to other models of permanent or transient ischemia in rodents (Chen et al., 2007; Liu et al., 2009). Together, these results suggest that treatments aiming to increase post-stroke recovery and plasticity would be unlikely to have confounding neuroprotective effects if initiated after 24 h. Although we did not perform an analysis of cell death in the first 2–4 h after ET-1 injection it is likely that injury is still progressing at these early time points.

The evolution of the infarct volume has been previously examined in other models of stroke (Garcia et al., 1993; Liu et al., 2009) but not following cortical injection of ET-1. Here, we examined the time course of infarct development up to 7 days after stroke. The lesion was mainly restricted to the cortex with minor loss of striatal tissue, as has been reported previously (Gilmour et al., 2004; Windle et al., 2006). In this study, we focused specifically on the fate of neurons. The rate and extent of neuronal death caused by stroke is variable, depending on the mechanism that triggers the cell death, the duration of the occlusion, and a number of other factors (Lipton, 1999). A factor that can also affect neuronal death and injury size is the rate of reperfusion. In fact, although blood flow restoration can prevent irreversible tissue injury, instant reperfusion can result in further tissue damage. The reperfusion injury has been described following the suture model of MCAo in rats, affecting infarct volume and neuronal death (Yang and Betz, 1994; Aronowski et al., 1997). Unlike those models, ET-1 allows for gradual and slow reperfusion lasting a number of hours (Biernaskie et al., 2001).

Since neuronal death following a relatively more gradual reperfusion could be delayed, as has been shown previously in models of global ischemia (Colbourne et al., 1999), it was important to rule out the possibility of protracted cell death following ET-1. To do this we employed FJC which was originally developed by Schmued and colleagues (Schmued et al., 2005) and has been successfully used to investigate neuronal death in several rodent models of neuronal degeneration (Bian et al., 2007; Wang et al., 2008; Chidlow et al., 2009). FJC+ labelling pinpointed the region where neurons were undergoing degeneration; which appeared maximal at 24 h following ET-1. Degenerating neurons were also identifiable at 48 and 72 h following stroke but only a limited number of dying neurons were FJC+ at 7 days after ET-1 injection. Initial mechanisms of neuronal degeneration are triggered within the first hours and days following ET-1 injection and the targeted cells then progress through the death cascade. This conclusion is supported by other studies showing that FJC+ cells also express apoptotic markers like caspase-3 and caspase-9 in a model of epilepsy (Wang et al., 2008). Apoptotic markers expression peak between 24 and 72 h post-ischemia in several models of stroke (Velier et al., 1999; Chaitanya and Babu, 2008) which correlates with the timeline of neuronal death as identified by FJC staining in the current study.

While the infarct volume per se did not change at 7-days post-stroke, the FJC-positive cell population significantly decreased compared to the pattern observed at 24 or 48 h. After stroke, in brain tissue stained with H & E, degenerating cells becomes eosinophilic and areas of high eosinophilic positive cells evolve into infarcts (Sun et al., 2006). The goal of this staining is to allow a macroscopic differentiation between damaged and undamaged tissue (Garcia et al., 1993). While dead neurons are stained by H&E and counted as part of the infarct estimations, scattered FJC+ cells were found also in peri-infarct regions distal to the core. This explains why the cortical volume containing degenerating neurons was greater than the infarct volume. Because the sections used at the different time points originated from different animals, it is impossible to follow the evolution of a neuronal population from the ischemic insult to death within the same animal using histological methods. However, both staining methods confirmed that there is a critical switch of the neuronal fate at 24 h post-ET-1 injection.

In conclusion, our results show that both neuronal death and overall tissue injury, peak at 24 h following ET-1 injection in the cortex of rats. These results set a maximum limit of 24 h post-stroke as the possible neuroprotection time window to consider when using this model in preclinical studies. Most importantly, any intervention aiming to target recovery mechanisms could be initiated 24 h after ET-1 without concerns of confounds arising from a neuroprotective action.

Acknowledgements

Research was funded by a joint grant from the European Stroke Network and the Canadian Stroke Network awarded to Dr. Corbett. C. Nguemeni was supported by funds provided by the Heart and Stroke Foundation Canadian Partnership for Stroke Recovery (CPSR). M. Gomez-Smith was supported by a doctoral fellowship from the Heart and Stroke Foundation. C. Pedrini Schuch received a visiting student award from Emerging Leaders in the Americas Program (ELATP) and the Heart and Stroke Foundation Canadian Partnership for Stroke Recovery. The authors thank Dr. Jessy Livingston-Thomas for her critical review of this manuscript and Anthony Carter for performing the surgery on Sham animals.

References

Aronowski J, Strong R, Grotta JC. Reperfusion injury: demonstration of brain damage produced by reperfusion after transient focal ischemia in rats. J Cereb Blood Flow Metab 1997;17(10):1048–56.

Barber PA, Davis SM, Infield B, Baird AE, Donnan GA, Jolley D, et al. Spontaneous reperfusion after ischemic stroke is associated with improved outcome. Stroke 1998;29(12):2522–8.

Barth AM, Mody I. Changes in hippocampal neuronal activity during and after unilateral selective hippocampal ischemia in vivo. J Neurosci 2011;31:851–60.

Bian GL, Wei LC, Shi M, Wang YQ, Cao R, Chen LW. Fluoro-Jade C can specifically stain the degenerative neurons in the substantia nigra of the 1-methyl-4-phenyl-1,2,3,6-tetrahydro pyridine-treated C57BL/6 mice. Brain Res 2007;1150:55–61.

Biernaskie J, Corbett D, Peeling J, Wells J, Lei H. A serial MR study of cerebral blood flow changes and lesion development following endothelin-1-induced ischemia in rats. Magn Reson Med 2001;46(4):827–30.

Canazza A, Minati L, Boffano C, Parati E, Binks S. Experimental models of brain ischemia: a review of techniques, magnetic resonance imaging, and investigational cell-based therapies. Front Neurol 2014;5:19.

Carmichael ST. Rodent models of focal stroke: size, mechanism, and purpose. NeuroRx 2005;2(3):396–409.

Chaitanya GV, Babu PP. Activation of calpain, cathepsin-b and caspase-3 during transient focal cerebral ischemia in rat model. Neurochem Res 2008;33(11):2178–86.

Chen F, Suzuki Y, Nagai N, Jin L, Yu J, Wang H, et al. Rodent stroke induced by photochemical occlusion of proximal middle cerebral artery: evolution monitored with MR imaging and histopathology. Eur J Radiol 2007;63(1):68–75.

Chidlow G, Wood JP, Sarvestani G, Manavis J, Casson RJ. Evaluation of Fluoro-Jade C as a marker of degenerating neurons in the rat retina and optic nerve. Exp Eye Res 2009;88(3):426–37.

Colbourne F, Li H, Buchan AM, Clemens JA. Continuing postischemic neuronal death in CA1: influence of ischemia duration and cytoprotective doses of NBQX and SNX-111 in rats. Stroke 1999;30(3):662–8.

Dittmar M, Spruss T, Schuierer G, Horn M. External carotid artery territory ischemia impairs outcome in the endovascular filament model of middle cerebral artery occlusion in rats. Stroke 2003;34(9):2252–7.

Fisher M, Feuerstein G, Howells DW, Hurn PD, Kent TA, Savitz SI, et al. Update of the stroke therapy academic industry roundtable preclinical recommendations. Stroke 2009;40(6):2244–50.

Garcia JH, Yoshida Y, Chen H, Li Y, Zhang ZG, Lian J, et al. Progression from ischemic injury to infarct following middle cerebral artery occlusion in the rat. Am J Pathol 1993;142(2):623–35.

Gilmour G, Iversen SD, O'Neill MF, Bannerman DM. The effects of intracortical endothelin-1 injections on skilled forelimb use: implications for modelling recovery of function after stroke. Behav Brain Res 2004;150(1–2):171–83.

Lipton P. Ischemic cell death in brain neurons. Physiol Rev 1999;79(4):1431–568.

Liu F, Schafer DP, McCullough LD. TTC, Fluoro-Jade B and NeuN staining confirm evolving phases of infarction induced by middle cerebral artery occlusion. J Neurosci Methods 2009;179(1):1–8.

Lo EH. A new penumbra: transitioning from injury into repair after stroke. Nat Med 2008;14(5):497–500.

Macrae IM, Robinson MJ, Graham DI, Reid JL, McCulloch J. Endothelin-1-induced reductions in cerebral blood flow: dose dependency, time course, and neuropathological consequences. J Cereb Blood Flow Metab 1993;13(2):276–84.

Matsuno H, Uematsu T, Umemura K, Takiguchi Y, Asai Y, Muranaka Y, et al. A simple and reproducible cerebral thrombosis model in rats induced by a photochemical reaction and the effect of a plasminogen–plasminogen activator chimera in this model. J Pharmacol Toxicol Methods 1993;29(3):165–73.

Moskowitz MA. Brain protection: maybe yes, maybe no. Stroke 2010;41(10 Suppl.):S85–6.

O'Collins VE, Macleod MR, Donnan GA, Horky LL, van der Worp BH, Howells DW. 1,026 experimental treatments in acute stroke. Ann Neurol 2006;59(3):467–77.

Schmued LC, Stowers CC, Scallet AC, Xu L. Fluoro-Jade C results in ultra high resolution and contrast labeling of degenerating neurons. Brain Res 2005;1035(1):24–31.

Soleman S, Yip P, Leasure JL, Moon L. Sustained sensorimotor impairments after endothelin-1 induced focal cerebral ischemia (stroke) in aged rats. Exp Neurol 2010;222(1):13–24.

Strom JO, Ingberg E, Theodorsson A, Theodorsson E. Method parameters' impact on mortality and variability in rat stroke experiments: a meta-analysis. BMC Neurosci 2013;14:41.

Sun L, Kuroiwa T, Ishibashi S, Katsumata N, Endo S, Mizusawa H. Transition of areas of eosinophilic neurons and reactive astrocytes to delayed cortical infarcts after transient unilateral forebrain ischemia in Mongolian gerbils. Acta Neuropathol 2006;111(1):21–8.

Velier JJ, Ellison JA, Kikly KK, Spera PA, Barone FC, Feuerstein GZ. Caspase-8 and caspase-3 are expressed by different populations of cortical neurons undergoing delayed cell death after focal stroke in the rat. J Neurosci 1999;19(14):5932–41.

Wang L, Liu YH, Huang YG, Chen LW. Time-course of neuronal death in the mouse pilocarpine model of chronic epilepsy using Fluoro-Jade C staining. Brain Res 2008;1241:157–67.

Windle V, Szymanska A, Granter-Button S, White C, Buist R, Peeling J, et al. An analysis of four different methods of producing focal cerebral ischemia with endothelin-1 in the rat. Exp Neurol 2006;201(2):324–34.

Yanagisawa M, Kurihara H, Kimura S, Goto K, Masaki T. A novel peptide vasoconstrictor, endothelin, is produced by vascular endothelium and modulates smooth muscle Ca2+ channels. J Hypertens Suppl 1988;6(4):S188–91.

Yang GY, Betz AL. Reperfusion-induced injury to the blood-brain barrier after middle cerebral artery occlusion in rats. Stroke 1994;25(8):1658–64, discussion 1664–5.

CHAPTER

Lost in translation: rethinking approaches to stroke recovery

19

Dale Corbett[†,1], **Matthew Jeffers**[*,§], **Carine Nguemeni**[*,§], **Mariana Gomez-Smith**[*,§], **Jessica Livingston-Thomas**[*,§]

*Faculty of Medicine, University of Ottawa, Ottawa, Ontario, Canada

[†]Heart & Stroke Foundation Canadian Partnership for Stroke Recovery and Department of Cellular & Molecular Medicine, University of Ottawa, Ottawa, Canada

[§]Canadian Partnership for Stroke Recovery, University of Ottawa, Ottawa, Ontario, Canada

[1]Corresponding author: Tel.: +1-613-562-5800ext.8177; Fax: +1-613-562-5435, e-mail address: dcorbett@uottawa.ca

Abstract

Stroke is the second leading cause of death and the preeminent cause of neurological disability. Attempts to limit brain injury after ischemic stroke with clot-dissolving drugs have met with great success but their use remains limited due to a narrow therapeutic time window and concern over serious side effects. Unfortunately, the neuroprotective strategy failed in clinical trials. A more promising approach is to promote recovery of function in people affected by stroke. Following stroke, there is a heightened critical period of plasticity that appears to be receptive to exogenous interventions (e.g., delivery of growth factors) designed to enhance neuroplasticity processes important for recovery. An emerging concept is that combinational therapies appear much more effective than single interventions in improving stroke recovery. One of the most promising interventions, with clinical feasibility, is enriched rehabilitation, a combination of environmental enrichment and task-specific therapy.

Keywords

recovery, neuroplasticity, enriched rehabilitation, stroke, animal models

1 THE PROBLEM OF STROKE

Stroke is the second leading cause of death worldwide and the leading cause of acquired neurological disabilities in the developed world (Feigin et al., 2014). The incidence of stroke varies by geographical region, so for example in Canada (population 35 million people) there are more than 50,000 new strokes each year.

Progress in Brain Research, Volume 218, ISSN 0079-6123, http://dx.doi.org/10.1016/bs.pbr.2014.12.002

The financial burden to the Canadian health care system is approximately $2.8 billion per year with an average cost of $50,000 for each new stroke patient in the 6-month period following stroke (Mittmann et al., 2012). In a disturbing trend, the risk of stroke in people under the age of 50 has increased by 24% in the last decade (Feigin et al., 2014; HSFC, 2014). Furthermore, these statistics underestimate the true magnitude of stroke since they account only for overt stroke. Silent or covert stroke resulting from small vessel disease is at least five times more common than overt stroke (Vermeer et al., 2007). Covert strokes are typically caused by small infarcts affecting subcortical brain structures and white matter (Roman et al., 2002). The subtle and insidious progression of covert stroke manifests as cognitive decline, abnormal gait, an increased risk of falls, depression, and often progresses to dementia (Arvanitakis et al., 2011; Srikanth et al., 2009; Wu et al., 2014).

2 STROKE PREVENTION AND ACUTE STROKE TREATMENT

Despite the progress made in treating heart disease and stroke, the incidence of stroke is predicted to double by mid-century (Ovbiagele et al., 2013). Aging is the most important risk factor for stroke with risk doubling every 10 years after the age of 55 (Wolf et al., 1991). In contrast to aging, which is a nonmodifiable risk factor, there are number of other risk factors that are comorbid with stroke (Goldstein et al., 2011). The increased occurrence of obesity induced by the typical Western diet, together with a sedentary lifestyle, often leads to the development of metabolic syndrome which consists of at least three of the following five modifiable risk factors: high blood pressure, abdominal obesity, elevated triglycerides, hyperglycemia, and low-HDL cholesterol (Eckel et al., 2010). Those factors can contribute both independently or in combination to impair the peripheral and cerebrovasculature. Preclinical data have shown that exposing animals to a Western diet (high in fat, sugar, and sodium) for a long period prior to injury creates a comorbid condition that impairs vascular function and increases ischemic damage (Deutsch et al., 2009; Langdon et al., 2011). Interventions like diet change and physical exercise have the potential to reduce stroke incidence and improve poststroke recovery (He et al., 2006; Middleton et al., 2013), but the implementation of these lifestyle changes has yet to become widely incorporated into poststroke best practices.

Thrombolysis with recombinant tissue plasminogen activator (t-PA) is the only drug approved for the treatment of acute stroke (NINDS, 1995). The relatively narrow time window for t-PA (3–4.5 h from stroke onset) and serious side effects, including intracerebral hemorrhage, limits its use to 5–10% of the overall stroke population (Iadecola and Anrather, 2011a,b; Jauch et al., 2013). Unfortunately, many patients benefiting from t-PA are left with significant functional impairments.

Another approach has been to use drugs to reduce ischemic injury once stroke has occurred. Unfortunately, all drugs that appeared to be neuroprotective in animal models subsequently failed in clinical trials (O'Collins et al., 2006). While many of the clinical trials were flawed, a major problem was that the animal models failed

to reflect the clinical heterogeneity and comorbidities of human stroke (Carmichael, 2005). For example, neuroprotectant efficacy was often solely evaluated by histological endpoints (i.e., cell counts and infarct volumes) at short survival times (usually within 7 days), where in clinical settings, the primary outcomes are long-term neurological function and daily life independence (Goldie et al., 2014). Small sample size, gender differences, and age are other factors that are often not considered and ultimately limit the translation of preclinical studies to clinic (Dirnagl, 2006; Fisher et al., 2009; Kimmelman et al., 2014).

It is becoming increasingly apparent that regenerative and rehabilitative interventions offer the best opportunity for stroke patients to regain mobility and independence. Unlike acute neuroprotection or thrombolysis, rehabilitation provides a longer time window for intervention (i.e., months, years) and is not limited to ischemic stroke, as is the case with t-PA. Surprisingly, interest in using rehabilitative and recovery strategies has been relatively neglected until recently. The observation that spontaneous recovery can occur for many years following stroke (Cramer, 2008) has created growing interest in poststroke neuroplasticity, which, as discussed below, has great potential for enhancing functional recovery. Nonetheless, it is critical that neurorestorative approaches to stroke recovery avoid the mistakes that plagued the stroke neuroprotection field.

3 THE USE OF ANIMAL MODELS TO ASSESS STROKE RECOVERY

Many patients make rapid gains in motor function in the first weeks after their stroke followed by a later phase (3–4 months poststroke) where recovery appears to plateau (Jorgensen et al., 1995; Kwakkel et al., 2003; Lai et al., 2002; Page et al., 2004). Gradual improvement may then take place at a greatly reduced rate over many years but rarely results in full recovery. Presently, many preclinical studies employ animal models in which recovery occurs both rapidly (e.g., 1–2 weeks) and completely after stroke. This mismatch is problematic, since interventions may appear artificially effective in animal models, in which there is already substantial spontaneous recovery. One of the most important lessons learned from failed neuroprotection trials is that animal stroke models must incorporate key features of human stroke, including *chronicity* of functional impairment, in order to avoid translational failure (Carmichael, 2005; Murphy and Corbett, 2009). While there are numerous animal models being used to evaluate recovery from stroke, one that is gaining more widespread use is the endothelin-1 (ET-1) model that creates injury as a result of temporary vasoconstrictive action following stereotaxic injection. In contrast to the intraluminal suture model, ET-1 can be used to target any cortical (e.g., forelimb motor cortex) or subcortical site to create injury and results in a gradual reperfusion, similar to most cases of human stroke (Windle et al., 2006). Using this model, we have been able to achieve long-lasting sensory-motor deficits that improve, but do not fully resolve, following different therapeutic interventions such as enriched

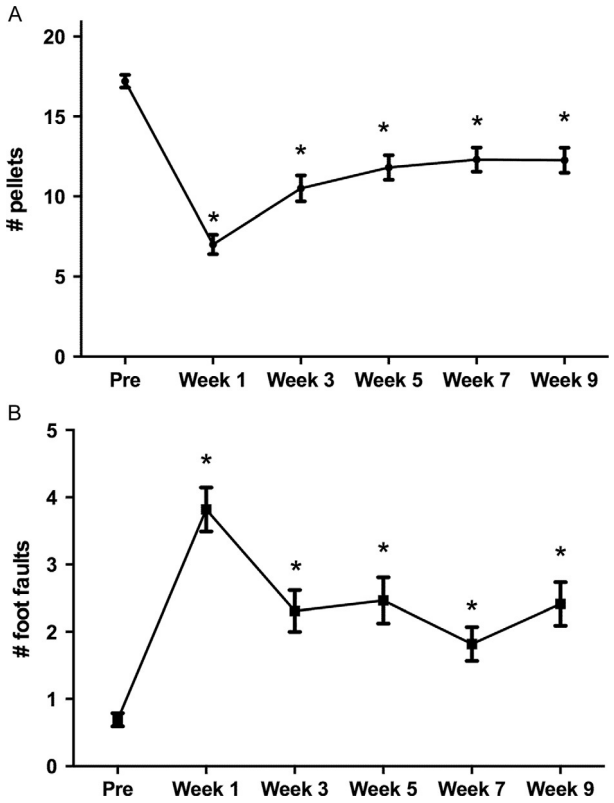

FIGURE 1

Persistent behavioral impairments following endothelin-1-induced stroke in the forelimb motor cortex of rats. ET-1 stroke in rats produces long-lasting impairments in skilled reaching assessed using the Montoya staircase apparatus (A). Note the limited spontaneous recovery occurring in the first few weeks after stroke and a subsequent plateau in recovery from week 5 onward. Similar chronic impairments in hindlimb function are apparent in the tapered beam task (B). In order to avoid translational failure, preclinical stroke recovery models need to ensure that behavioral deficits are chronic as in human stroke. $^{*}p<0.001$ versus prestroke reaching baseline, $N=24$.

rehabilitation (ER; Biernaskie and Corbett, 2001; Jeffers et al., 2014; MacLellan et al., 2011; Fig. 1). In addition, it is important to use a battery of behavioral tests to assess recovery since improved performance on one task may not be evident on other tests. In our experience, the most sensitive behavioral test involves a skilled reaching task, such as the single pellet reaching task or Montoya staircase test (Biernaskie and Corbett, 2001; Grabowski et al., 1993; Whishaw et al., 2008; Whishaw and Pellis, 1990). While both tests require extensive prestroke training they have high clinical relevance, since upper limb deficits are a common and persistent

problem in human stroke (Kwakkel et al., 2003; Wade et al., 1985) and, therefore, should be part of any rodent behavioral test battery to assess stroke recovery.

4 THE POTENTIAL OF NEUROPLASTICITY TO ENHANCE STROKE RECOVERY

Our understanding of how the brain adapts to its environment, particularly after injury, has expanded dramatically in the last 30 years. We now know that the adult brain can be reshaped by experience, by use-dependent neuronal activity as well as in response to injury throughout the lifespan. In the adult-injured brain and in the developing immature brain, a critical window of opportunity exists during which external experience-driven stimuli as well as intrinsic internal processes drive rapid and profound remodeling of neural circuits.

In the human brain, the first year of life is characterized by a large increase in cortical synaptic density that is abruptly followed by a slow process of synaptic pruning lasting several years. From puberty onward, the number of synapses in the human brain remains stable (Huttenlocher, 1979). Despite the large number of synapses in the brain during infancy, morphologically they are immature and it is through experience-dependent and experience-expectant events that synapse morphology adapts to strengthen synaptic connections (Greenough et al., 1987; Grossman et al., 2002). Indeed, Greenough observed that both rearing healthy juvenile rats in a complex environment (Greenough and Volkmar, 1973) and training adult rats to perform a reaching task (Greenough et al., 1985) lead to more extensive dendritic branching in the visual and motor cortices, respectively. Moreover, these events need to occur along a specific timeline otherwise normal circuitry and ensuing function will be irreversibly impaired. Hubel and Wiesel's classic experiments involving monocular deprivation in kittens showed that the first 10–12 weeks of a kitten's life are critical in the appropriate formation of visual cortex ocular dominance columns (Hubel and Wiesel, 1970). Current research in neuroplasticity is focused on identifying the mechanisms that are involved in the closing of the critical window, as they could potentially be targets for poststroke therapies. One process that may limit neuroplastic potential during development is the onset and expansion of myelination, along with myelin-associated growth inhibitors, within the central nervous system and the consequent regression of growth-promoting factors such as GAP-43 (Kapfhammer and Schwab, 1994).

A host of spontaneous changes occur in the brain immediately following stroke, only some of which participate directly in postinjury repair. Ionic imbalance and cell death due to nutrient deprivation, neurotransmitter excitotoxicity, and excess free radical generation must first subside before spontaneous or rehabilitation-based recovery can occur (Hossmann, 2006). Similar to the developing brain, dendritic structure and synaptic density undergo extensive remodeling within the first few days after stroke. For example, Brown and colleagues, using two-photon fluorescence microscopy, found a five- to eight-fold increase in spine formation in

peri-infarct cortex following photothrombotic stroke in mice. Growth was maximal within 1–2 weeks postinjury but remained constant for at least 6 weeks. Moreover, this change in synaptic morphology proximal to the infarcted tissue was not seen more distally (1.5 mm) indicating a geographic specificity for this phenomenon (Brown et al., 2007). Contralesional motor reorganization also takes place after stroke; however, the precise role that plays in functional outcome is not fully understood. Small unilateral infarcts greatly increase the receptive field size of the somatosensory cortex in both the ipsi- and contralesional cortices (Reinecke et al., 2003). Human studies have also demonstrated increases in contralesional activity that subsides as recovery occurs (Liepert et al., 2000) and inhibition of this cortical tissue has led to increased recovery of motor function in some studies (Nowak et al., 2008). However, animal studies have shown that the effects of contralesional inhibition vary depending on the severity of the stroke, and in some cases, functional gains can be lost through inhibition of the homologous cortical tissue (Biernaskie et al., 2005). These contrasting studies show that structural reorganization of both peri- and contralesional tissues are important for stroke recovery, but further study is required to discern the specific roles that each region plays in the recovery process.

Poststroke interventions can be used to identify some of the mechanisms contributing to poststroke recovery. Compelling evidence points to the reorganization of motor maps in the ipsilesional cortex as an important determinant of stroke recovery as a result of rehabilitative training (Nudo et al., 1996). Enhanced dendritic arborization in this region has also been demonstrated to occur in conjunction with rehabilitation (Biernaskie and Corbett, 2001; Jones et al., 1999). These phenomena of rehabilitation-induced increases in dendritic arborization and motor map reorganization appear to occur in tandem (Hickmott and Steen, 2005). Thus, structural modification of the perilesional cortex appears to be a major driving force of poststroke functional recovery and is likely mediated by a cascade of stroke-induced changes in gene and protein expression.

Our lab was the first to demonstrate the existence of a critical period, similar to the one observed in development, during which potential for recovery is optimal, and after which interventions are less effective. Indeed, Biernaskie and colleagues showed that when rats were exposed to a form of rehabilitation, termed ER which combines daily reach training with chronic exposure to an enriched environment early after stroke (5 or 14 days poststroke), the animals showed significant recovery compared to control animals. When ER was postponed to 30 days, it lost its effectiveness (Biernaskie et al., 2004) and did not induce structural remodeling in the cortex. We have also recently shown that ER effectively increases synaptic activity in the peri-infarct cortex during this critical time window. Four groups of rats underwent different types of rehabilitation following ET-1 focal ischemia of the forelimb motor cortex. Untreated animals were compared to those receiving only reach training, environmental enrichment, or ER. The animals that received the combination therapy (ER) showed the strongest increase in synaptic activity in the peri-infarct region as determined by increased expression of the immediate early gene FosB/ΔFosB (Clarke et al., 2014).

Additional efforts to modulate beneficial neuroplastic processes underlying structural reorganization have taken several forms. As stated above, excitation of ipsilesional and inhibition of contralesional cortical networks with transcranial magnetic stimulation (TMS) has been successfully used to restore some functions lost in stroke (Raux et al., 2010; Takeuchi et al., 2005). Intensive, task-specific practice using constraint-induced movement therapy, which encourages motor map reorganization, has also provided clinical benefits (Liepert et al., 2000; Wolf et al., 2006). Other groups have attempted to alter the cortical excitatory–inhibitory balance to enhance plasticity and recovery of function in animals using pharmacological approaches (Clarkson et al., 2010). More recently, research has begun to combine these approaches in conjunction with rehabilitative therapies to accelerate recovery beyond what is possible with either treatment alone (Jeffers et al., 2014).

A host of proteins exhibit differential expression patterns poststroke, such as those controlling axonal guidance and cytoskeletal modification, extracellular matrix function, growth factors, transcription factors as well as DNA-modifying genes (Overman and Carmichael, 2014). Although the molecular events occurring in the brain after stroke are complex, there is a general consensus that proteins inhibiting plasticity are downregulated shortly after stroke while those promoting plasticity are upregulated (Carmichael et al., 2005; Murphy and Corbett, 2009; Fig. 2). An initial or "trigger" phase during the first 3 days following stroke involves axonal sprouting proximal to the lesion resulting from synchronized neuronal activity in the perilesional cortex (Carmichael and Chesselet, 2002). Immediately after this initial phase, several growth-promoting proteins, such as GAP-43, CAP23, c-jun, and SPRR1, are increased maximally for several weeks at which point they slowly taper off (Carmichael et al., 2005). It is at this time point, 1 month after stroke, when new patterns of axonal projections are detectable (Carmichael et al., 2001). Growth inhibitory gene expression occurs within the immediate vicinity of the infarct but also throughout the entire brain. Shortly after stroke, a glial scar is formed around the core of the infarct through the recruitment of reactive astrocytes that synthesize large amounts of chondroitin sulfate proteoglycans (Carmichael et al., 2005). Cell death, oxidative DNA, and protein damage occur in this area. In the rest of the brain parenchyma, perineuronal nets break down shortly after stroke. Thus, both growth-promoting and growth-inhibitory molecules represent promising target for enhancing stroke recovery. One molecule that appears particularly important for recovery is brain-derived neurotrophic factor (BDNF). BDNF is the most widely expressed neurotrophin in the central nervous system (Park and Poo, 2013) and plays a pivotal role in cell survival, neurite outgrowth, dendritic spine formation, and the initiation of neural stem cell differentiation. In a rat model of stroke, BDNF has been shown to be required for poststroke recovery since ventricular infusion of a BDNF antisense mRNA negates the beneficial effects of an ER intervention (Ploughman et al., 2009). Similarly, interfering with BDNF reduces the amount of spontaneous recovery in a mouse model of photothrombotic stroke (Clarkson et al., 2011). The identification of a human genetic variant of the BDNF gene, Val66Met, has also been very revealing. Val66Met carriers have worse outcomes after hemorrhagic stroke

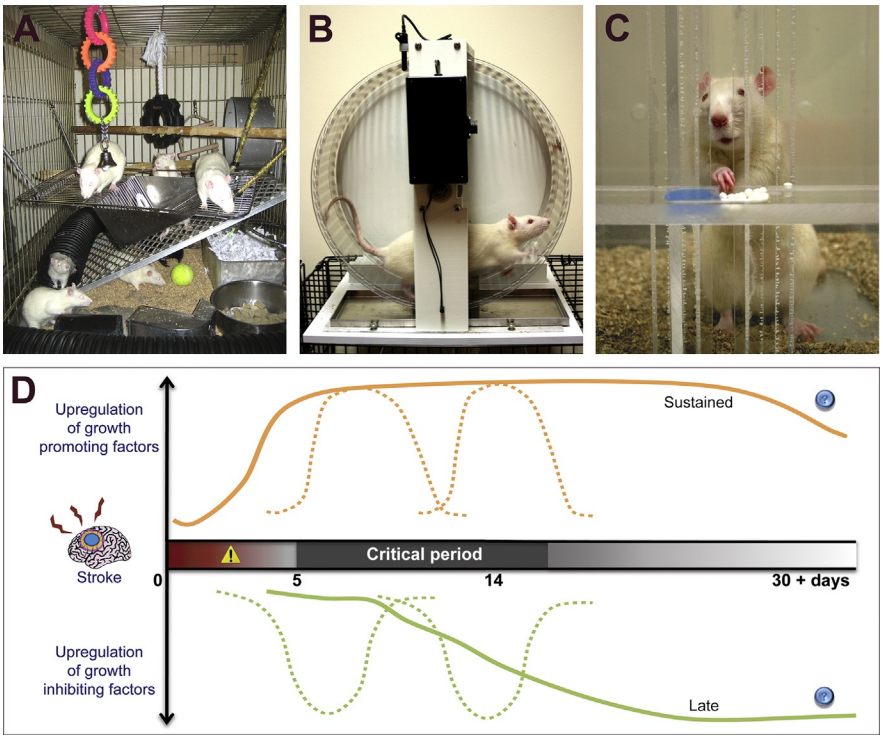

FIGURE 2

Enriched rehabilitation (ER) and the critical period for poststroke recovery. In rats, ER promotes recovery of skilled reaching in the Montoya staircase apparatus following ET-1-induced focal ischemia (Biernaskie and Corbett, 2001; Biernaskie et al., 2004; MacLellan et al., 2011). The protocol consists of enriched housing (A) and/or running exercise (B) in combination with daily reach training (C) of the impaired limb. Rats are housed in enriched environments starting 5–14 days after stroke (D). The timing of rehabilitation is designed to engage multiple neuroplasticity processes during the early poststroke recovery period when there is a sustained upregulation of growth-promoting genes (solid red (dark gray in the print version) line in D). Most growth-inhibitory genes (solid green (light gray in the print version) line) tend to be upregulated more gradually, several weeks after stroke, toward the end of the critical period for stroke recovery. Several growth-promoting and growth-inhibiting genes are transiently upregulated (dashed lines) in the early and mid poststroke recovery phase. This critical period observed in animal studies may be different in humans where spontaneous recovery can extend for several months after stroke.

Data in (D) adapted from Carmichael et al. (2005). Figure modified from Murphy and Corbett (2009).

(Siironen et al., 2007) and show evidence of reduced cortical plasticity (Di Lazzaro et al., 2014; Kleim et al., 2006) including reducing the beneficial effects of rTMS on motor recovery after stroke (Chang et al., 2014).

Research into inactivation of Nogo, a powerful neurite outgrowth inhibitor (Huber and Schwab, 2000), is showing considerable potential for translation to

the clinic. In cell culture (Montani et al., 2009), *ex vivo* experiments (Zagrebelsky et al., 2010), neurite expansion, and size of growth cones were enhanced in Nogo-A knockout animals and animals treated with an anti-Nogo-A antibody. Many studies have focused on the regenerative properties of blocking Nogo-A in spinal cord repair and in animal models of stroke (Freund et al., 2009; Markus et al., 2005; Papadopoulos et al., 2002; Tsai et al., 2011; Zorner and Schwab, 2010). A recent study by Wahl and colleagues provides strong evidence that blockade of Nogo-A combined with rehabilitation in a time-dependent manner is an extremely effective approach to enhance stroke recovery (Wahl et al., 2014).

5 EXOGENOUS AND ENDOGENOUS STEM CELL APPROACHES TO ENHANCE STROKE RECOVERY

Approaches to facilitate poststroke recovery have explored the promise of both exogenous and endogenous stem cells to replace lost neuronal networks. Exogenous cell delivery has encountered two major challenges that limit functional benefits: (1) even with immunosuppression, a large proportion of the transplanted cells die shortly after transplantation (Kelly et al., 2004) and (2) transplants tend to be directed to the peri-infarct tissue, which has the most potential for enabling poststroke recovery, but risks damaging this tissue even further (Moshayedi and Carmichael, 2013). Despite these limitations, exogenous cell delivery methods have shown functional improvements in both skilled and general sensorimotor outcome measures (Andrews et al., 2008). Methodologies to overcome these challenges, such as cell scaffolding and delivery into the ischemic core or cortex with hyaluronan gels (Wang et al., 2012; Zhong et al., 2010) and intravenous cell delivery (Komatsu et al., 2010) represent significant advancements in this field.

Since the discovery of endogenous adult neural precursor cells (Reynolds and Weiss, 1992), an intensive research effort has been directed to identifying the properties of these cells as a possible alternative to exogenous cell delivery. It has been repeatedly demonstrated that ischemic injury results in activation of neural precursor cells and their subsequent migration toward the site of damage (Parent et al., 2002). These cells also have the ability to adopt a mature cellular phenotype and functionally integrate into the surrounding tissue (Hou et al., 2008; Yamashita et al., 2006). However, given the debilitating effects of stroke, it seems unlikely the brain's endogenous neural precursor cell response alone is sufficient to support functional recovery. Attempts to augment the neural precursor cell proliferation and migration response have been successful through application of a wide variety of exogenous growth factors, and more recently through the use of immunosuppressive drugs (Erlandsson et al., 2011). These studies have revealed functional benefits in stroke recovery that correlate with the expansion of the neural precursor cell population (Kolb et al., 2007). However, the role that these cells are playing in recovery of function is still unclear. Indeed, in some cases, it has been demonstrated that beneficial behavioral effects can still be observed from treatments that are classically associated with increased neural precursor cell proliferation, even when neurogenesis

has been eliminated (Meshi et al., 2006). This raises questions of whether or not endogenous neurogenesis plays a direct role in stroke recovery. In the case of both exogenous and endogenous cell recruitment for promoting stroke recovery, it has been suggested that the beneficial effects are the result of cortical reorganization through alternative mechanisms, such as growth factor release or stabilization of surviving tissue (Savitz, 2013).

Stroke recovery research has largely revolved around restoring lost *motor* function. Section 4 illustrates the concentrated efforts on understanding the molecular mechanisms underlying recovery and development of new treatment targets. Poststroke cognitive impairments are also common and have a debilitating effect on quality of life; however, this research area has received much less attention. Section 6 addresses the state of this field and the specific challenges associated with modeling cognitive impairments.

6 STROKE RECOVERY: WHAT ABOUT COGNITION?

Cognitive dysfunction occurs in 22–40% of stroke survivors (Douiri et al., 2013; Pohjasvaara et al., 2002), resulting in learning and memory impairments and deficits in executive functions, such as planning, behavioral flexibility, and attention set-shifting ability (Kelly-Hayes et al., 1998; Pendlebury and Rothwell, 2009; Pohjasvaara et al., 2002). Furthermore, poststroke depression (PSD) may be prevalent in as many as a third of survivors (Burvill et al., 1997; Whyte and Mulsant, 2002). The relationship between stroke and depression remains unclear since damage to brain circuitry directly involved in regulating mood, as well as reactive depression, can result from stroke (Gainotti and Marra, 2002). The degree to which PSD and cognitive impairments affect one another has not been well elucidated (Terroni et al., 2012). Impairments in cognition and emotion can persist for years (Douiri et al., 2013) and are associated with higher rates of long-term poststroke disability (Burvill et al., 1997; Patel et al., 2002) and increased burden on caregivers (Forsberg-Warleby et al., 2004; Rigby et al., 2009).

Not surprisingly, preclinical research has focused almost exclusively on studying poststroke motor impairments since these deficits, unlike cognition and depression, are more obvious and far easier to study in animal models. Another reason for the paucity of animal studies investigating cognitive dysfunction is that the most widely used model of focal ischemia in rodents, the intraluminal suture middle cerebral artery occlusion model (Longa et al., 1989), predominantly affects sensory-motor circuitry. While cognitive impairment (e.g., spatial mapping) has been reported with this model, the apparent deficits are difficult to dissociate from sensory-motor dysfunction. Meanwhile, PSD is rarely examined in animal stroke models (Loubinoux et al., 2012). However, with the development of alternative stroke models (e.g., ET-1 and photothrombosis models), it is possible to target regions of the brain associated with specific cognitive functions, while leaving motor function intact (Cordova et al., 2014). Using these models, it is possible to conduct systematic evaluations into the

nature of poststroke cognitive deficits and ensuing recovery, and to determine how nonmotor brain areas respond to poststroke treatments.

Numerous well-established behavioral tests can be applied in the study of poststroke cognition. For instance, spatial learning and memory can be evaluated using the Morris water maze, the Barnes maze, or the radial arm maze (Carter and Shieh, 2010). For assessing higher cognitive functions, tasks become more elaborate. Clinically, executive dysfunction is evaluated using the Stroop Task, the Wisconsin Card Sorting Task, and the Trail Making Test, among others (Pohjasvaara et al., 2002). In animals, executive function can be assessed with different paradigms; a particularly promising approach employs attention set-shifting tests whereby an animal is taught to associate a reward with a particular stimulus dimension (e.g., an odor) that predicts food reward which is then changed within and/or across dimensions (e.g., type of digging material in a pot hiding the food reward). An alternative test includes the T-maze Win/Shift-Win/Stay tests that evaluate an animal's ability to shift response strategies once the rule signaling reward has changed (i.e., Win-Shift to Win-Stay strategy; Colbourne and Corbett, 1995). These cognitive tests are much more time consuming than simple Morris water maze tests (or motor tests) but better reflect the types of cognitive impairments encountered in human stroke.

Using the appropriate cognitive tests, it becomes possible to investigate recovery-enhancing treatments including rehabilitation. The goal of rehabilitation is to engage activity-dependent cues that optimize neuroplastic changes in the poststroke brain microenvironment (Carmichael, 2008; Cramer et al., 2011; Hicks et al., 2007; Ratan and Noble, 2009). In clinical practice, cognitive rehabilitation includes concurrently administered training components specifically targeted to each type of deficit present (e.g., attention, memory, problem solving), as well as compensatory strategy training (e.g., keeping a notebook, using mnemonic strategies) (Cicerone et al., 2000; Eslinger et al., 2013). Patients receiving rehabilitation can exhibit some recovery on cognitive measurements, and show improved performance on activities of daily living (Cicerone et al., 2000; Desmond et al., 1996). However, the degree to which true recovery processes have occurred, rather than implementation of compensatory techniques, is unclear.

In an attempt to augment recovery beyond that achieved by traditional rehabilitation, additional treatments have been explored in the clinical setting. These include interventions that alter cortical excitability, such as TMS (Cao et al., 2014) and transcranial direct current stimulation (Miniussi et al., 2008); music therapy which stimulates diverse cognitive and emotional neural pathways (Sarkamo et al., 2008), and various pharmacological approaches including the use of antidepressant drugs and dopamine agonists (Eslinger et al., 2013; Parton et al., 2005). The effective time window for rehabilitation of cognitive dysfunction is unknown, and may or may not involve similar mechanisms as motor rehabilitation, which is most effective in the subacute and acute poststroke stages (although some therapies are effective in the chronic phase; Liepert et al., 2000; Wolf et al., 2006). Similarly, the use of repetition and increasing intensity over time are hallmarks of motor and

aphasia rehabilitation and would be expected to influence cognitive recovery, but there is presently a knowledge gap in this area.

Animal studies of cognitive rehabilitation are exceedingly rare. As previously discussed, environmental enrichment comprises physical activity, social stimulation, and cognitive activity, thereby representing a combination therapy. Environmental enrichment improves cognition in several neurodegenerative disorders, including Alzheimer's, Huntington's, and Parkinson's diseases (for review, see Hannan, 2014) and reverse depression-like behavior in mice (Jha et al., 2011). These reports along with evidence that environmental enrichment improves poststroke motor deficits (Biernaskie and Corbett, 2001; Clarke et al., 2009; Farrell et al., 2001) hold great promise for the investigation of its use in a poststroke cognitive dysfunction model.

Recently, our laboratory developed a novel cognitive rehabilitation paradigm using a Hebb–Williams maze to encourage cognitive stimulation through exploration of changing maze environments. Hebb–Williams maze exposure was combined with physical activity and the combination, but not the single interventions alone, improved working memory in healthy animals (Langdon and Corbett, 2012), and contributed to improve cognitive performance in an animal model of vascular dementia (Langdon et al., 2013).

With an increasing interest in modeling cognitive deficits using focal ischemic models, much remains to be determined about the nature of poststroke plasticity of nonmotor brain areas. Questions regarding the existence of a similar permissive neuroplastic time window, the degree to which cognition-dependent rehabilitation may be effective, and issues such as rehabilitation repetition and intensity thresholds remain to be investigated.

7 FUTURE DIRECTIONS: A HOLISTIC APPROACH TO STROKE RECOVERY

In retrospect, the "silver bullet" approach (e.g., blocking free radicals) that typified the stroke neuroprotection field was naive given the complexity of the ischemic cell death cascade (Iadecola and Anrather, 2011b; Ratan and Noble, 2009). In contrast, interventions with pleiotropic, complementary effects that mimic the brain's intrinsic attempt to limit ischemic damage are more likely to provide effective neuroprotection than a single target approach. This is best illustrated by long-duration postischemic hypothermia that is now widely used to treat cardiac arrest and perinatal asphyxia (Bernard et al., 2002; Nguyen et al., 2013). Postischemic hypothermia, unlike neuroprotective drugs, provided permanent histological and functional protection (Colbourne and Corbett, 1994; Colbourne and Corbett, 1995) in multiple animal stroke models due to its simultaneous interference with multiple molecular and cellular events in the ischemic cascade (Bao and Xu, 2013). Other examples of effective interventions targeting multiple mechanisms include exercise and ischemic preconditioning (Iadecola and Anrather, 2011b).

As with neuroprotection, combinational therapies have considerable potential to provide optimal gains in functional recovery following stroke by tapping into multiple, complementary mechanisms underlying neuroplasticity and repair. Environmental enrichment has long been known to be an effective "cocktail" intervention for restoring behavioral recovery after brain injury (Johansson and Ohlsson, 1996; Kolb et al., 1998; Murphy and Corbett, 2009; Will et al., 2004). To this end, we have combined environmental enrichment with daily bouts of reach training (i.e., ER) to achieve an even more effective intervention for enhancing poststroke recovery (Biernaskie and Corbett, 2001; Biernaskie et al., 2004). As described above, the individual components of ER (i.e., reach training, environmental enrichment) are less effective than ER in activating cortical peri-infarct neurons (Clarke et al., 2014) implicated in recovery of sensory-motor function (Carmichael, 2006; Murphy and Corbett, 2009; Nudo et al., 1996). Collectively, the individual elements of ER complement one another to enhance different neuroplasticity processes (e.g., upregulation of growth factors, angiogenesis, sprouting; Sale et al., 2009; Will et al., 2004) and to date ER represents the most effective preclinical intervention for facilitating poststroke recovery (Clarke et al., 2014; Murphy and Corbett, 2009). In an extension of this work, Jeffers and colleagues reported that a growth factor cocktail combined with ER resulted in more rapid recovery in rats with stroke targeting the forelimb motor cortex. Again the combination treatment was more effective than ER or the growth factors alone (Jeffers et al., 2014). It is important to note that this study was the first to demonstrate that an intervention (ER + growth factors) was superior to what might be considered existing preclinical best practice (i.e., ER). By including a "best practice" control (instead of nontreated controls) in preclinical studies, as is done routinely in clinical studies, the likelihood of translational failure to the clinic will be reduced (Dirnagl, 2006; Fisher et al., 2009; Jeffers et al., 2014).

Single intervention studies are appealing because of their simplicity and cost effectiveness, however, the track record of monotherapeutic approaches in stroke is very poor and must at some point be abandoned (Iadecola and Anrather, 2011b; Ratan and Noble, 2009). One promising multimodal preclinical treatment is ER which activates the brain's own self-repair and reorganizational programs. Furthermore, ER can be adapted to the clinical setting and preliminary findings in stroke patients are encouraging (Janssen et al., 2014). Combining ER with adjunctive therapies (e.g., drugs, electrical stimulation) to further enhance stroke recovery is a promising avenue for future research, however, the sequence and timing of the individual components of the combination therapy may be critical in determining the optimal efficacy (Wahl et al., 2014).

ACKNOWLEDGMENTS

Operating grants to D. C. from the Canadian Institutes for Health Research (CIHR), the Heart and Stroke Foundation of Canada, the Canadian Partnership for Stroke Recovery, and the Canadian Stroke Network are gratefully acknowledged. D. C. was the recipient of a Tier 1 Canada Research Chair in Stroke and Neuroplasticity.

REFERENCES

Andrews, E.M., Tsai, S.Y., Johnson, S.C., Farrer, J.R., Wagner, J.P., Kopen, G.C., Kartje, G.L., 2008. Human adult bone marrow-derived somatic cell therapy results in functional recovery and axonal plasticity following stroke in the rat. Exp. Neurol. 211 (2), 588–592.

Arvanitakis, Z., Leurgans, S.E., Barnes, L.L., Bennett, D.A., Schneider, J.A., 2011. Microinfarct pathology, dementia, and cognitive systems. Stroke 42 (3), 722–727.

Bao, L., Xu, F., 2013. Fundamental research progress of mild hypothermia in cerebral protection. Springerplus 2 (1), 306.

Bernard, S.A., Gray, T.W., Buist, M.D., Jones, B.M., Silvester, W., Gutteridge, G., Smith, K., 2002. Treatment of comatose survivors of out-of-hospital cardiac arrest with induced hypothermia. N. Engl. J. Med. 346 (8), 557–563.

Biernaskie, J., Corbett, D., 2001. Enriched rehabilitative training promotes improved forelimb motor function and enhanced dendritic growth after focal ischemic injury. J. Neurosci. 21 (14), 5272–5280.

Biernaskie, J., Chernenko, G., Corbett, D., 2004. Efficacy of rehabilitative experience declines with time after focal ischemic brain injury. J. Neurosci. 24 (5), 1245–1254.

Biernaskie, J., Szymanska, A., Windle, V., Corbett, D., 2005. Bi-hemispheric contribution to functional motor recovery of the affected forelimb following focal ischemic brain injury in rats. Eur. J. Neurosci. 21 (4), 989–999.

Brown, C.E., Li, P., Boyd, J.D., Delaney, K.R., Murphy, T.H., 2007. Extensive turnover of dendritic spines and vascular remodeling in cortical tissues recovering from stroke. J. Neurosci. 27 (15), 4101–4109.

Burvill, P., Johnson, G., Jamrozik, K., Anderson, C., Stewart-Wynne, E., 1997. Risk factors for post-stroke depression. Int. J. Geriatr. Psychiatry 12 (2), 219–226.

Cao, L., Zhao, R., Huo, S., Du, J.B., Liu, L., Zhang, Y.M., Song, W.Q., 2014. Effects of repetitive transcranial magnetic stimulation on cognitive impairment in stroke patients: a meta-analysis. Mol. Neurobiol.

Carmichael, S.T., 2005. Rodent models of focal stroke: size, mechanism, and purpose. NeuroRx 2 (3), 396–409.

Carmichael, S.T., 2006. Cellular and molecular mechanisms of neural repair after stroke: making waves. Ann. Neurol. 59 (5), 735–742.

Carmichael, S.T., 2008. Themes and strategies for studying the biology of stroke recovery in the poststroke epoch. Stroke 39 (4), 1380–1388.

Carmichael, S.T., Chesselet, M.F., 2002. Synchronous neuronal activity is a signal for axonal sprouting after cortical lesions in the adult. J. Neurosci. 22 (14), 6062–6070.

Carmichael, S.T., Wei, L., Rovainen, C.M., Woolsey, T.A., 2001. New patterns of intracortical projections after focal cortical stroke. Neurobiol. Dis. 8 (5), 910–922.

Carmichael, S.T., Archibeque, I., Luke, L., Nolan, T., Momiy, J., Li, S., 2005. Growth-associated gene expression after stroke: evidence for a growth-promoting region in peri-infarct cortex. Exp. Neurol. 193 (2), 291–311.

Carter, M., Shieh, J., 2010. Guide to Research Techniques in Neuroscience. Academic Press, New York.

Chang, W.H., Bang, O.Y., Shin, Y.I., Lee, A., Pascual-Leone, A., Kim, Y.H., 2014. BDNF polymorphism and differential rTMS effects on motor recovery of stroke patients. Brain Stimul. 7 (4), 553–558.

Cicerone, K.D., Dahlberg, C., Kalmar, K., Langenbahn, D.M., Malec, J.F., Bergquist, T.F., Felicetti, T., Giacino, J.T., Harley, J.P., Harrington, D.E., Herzog, J., Kneipp, S.,

Laatsch, L., Morse, P.A., 2000. Evidence-based cognitive rehabilitation: recommendations for clinical practice. Arch. Phys. Med. Rehabil. 81 (12), 1596–1615.
Clarke, J., Mala, H., Windle, V., Chernenko, G., Corbett, D., 2009. The effects of repeated rehabilitation "tune-ups" on functional recovery after focal ischemia in rats. Neurorehabil. Neural Repair 23 (9), 886–894.
Clarke, J., Langdon, K.D., Corbett, D., 2014. Early poststroke experience differentially alters periinfarct layer II and III cortex. J. Cereb. Blood Flow Metab. 34 (4), 630–637.
Clarkson, A.N., Huang, B.S., Macisaac, S.E., Mody, I., Carmichael, S.T., 2010. Reducing excessive GABA-mediated tonic inhibition promotes functional recovery after stroke. Nature 468 (7321), 305–309.
Clarkson, A.N., Overman, J.J., Zhong, S., Mueller, R., Lynch, G., Carmichael, S.T., 2011. AMPA receptor-induced local brain-derived neurotrophic factor signaling mediates motor recovery after stroke. J. Neurosci. 31 (10), 3766–3775.
Colbourne, F., Corbett, D., 1994. Delayed and prolonged post-ischemic hypothermia is neuroprotective in the gerbil. Brain Res. 654, 265–272.
Colbourne, F., Corbett, D., 1995. Delayed postischemic hypothermia: a six month survival study using behavioral and histological assessments of neuroprotection. J. Neurosci. 15, 7250–7260.
Cordova, C.A., Jackson, D., Langdon, K.D., Hewlett, K.A., Corbett, D., 2014. Impaired executive function following ischemic stroke in the rat medial prefrontal cortex. Behav. Brain Res. 258, 106–111.
Cramer, S.C., 2008. Repairing the human brain after stroke. II. Restorative therapies. Ann. Neurol. 63 (5), 549–560.
Cramer, S.C., Sur, M., Dobkin, B.H., O'Brien, C., Sanger, T.D., Trojanowski, J.Q., Rumsey, J.M., Hicks, R., Cameron, J., Chen, D., Chen, W.G., Cohen, L.G., deCharms, C., Duffy, C.J., Eden, G.F., Fetz, E.E., Filart, R., Freund, M., Grant, S.J., Haber, S., Kalivas, P.W., Kolb, B., Kramer, A.F., Lynch, M., Mayberg, H.S., McQuillen, P.S., Nitkin, R., Pascual-Leone, A., Reuter-Lorenz, P., Schiff, N., Sharma, A., Shekim, L., Stryker, M., Sullivan, E.V., Vinogradov, S., 2011. Harnessing neuroplasticity for clinical applications. Brain 134 (Pt. 6), 1591–1609.
Desmond, D.W., Moroney, J.T., Sano, M., Stern, Y., 1996. Recovery of cognitive function after stroke. Stroke 27 (10), 1798–1803.
Deutsch, C., Portik-Dobos, V., Smith, A.D., Ergul, A., Dorrance, A.M., 2009. Diet-induced obesity causes cerebral vessel remodeling and increases the damage caused by ischemic stroke. Microvasc. Res. 78 (1), 100–106.
Di Lazzaro, V., Pellegrino, G., Di Pino, G., Corbetto, M., Ranieri, F., Brunelli, N., Paolucci, M., Bucossi, S., Ventriglia, M.C., Brown, P., Capone, F., 2014. Val66Met BDNF gene polymorphism influences human motor cortex plasticity in acute stroke. Brain Stimul. 7 (6), 841–848. http://dx.doi.org/10.1016/j.brs.2014.10.001.
Dirnagl, U., 2006. Bench to bedside: the quest for quality in experimental stroke research. J. Cereb. Blood Flow Metab. 26 (12), 1465–1478.
Douiri, A., Rudd, A.G., Wolfe, C.D., 2013. Prevalence of poststroke cognitive impairment: South London Stroke Register 1995–2010. Stroke 44 (1), 138–145.
Eckel, R.H., Alberti, K.G., Grundy, S.M., Zimmet, P.Z., 2010. The metabolic syndrome. Lancet 375 (9710), 181–183.
Erlandsson, A., Lin, C.H., Yu, F., Morshead, C.M., 2011. Immunosuppression promotes endogenous neural stem and progenitor cell migration and tissue regeneration after ischemic injury. Exp. Neurol. 230 (1), 48–57.

Eslinger, P.J., Flaherty-Craig, C.V., Chakara, F.M., 2013. Rehabilitation and management of executive function disorders. Handb. Clin. Neurol. 110, 365–376.
Farrell, R., Evans, S., Corbett, D., 2001. Environmental enrichment enhances recovery of function but exacerbates ischemic cell loss. Neuroscience 107, 585–592.
Feigin, V.L., Forouzanfar, M.H., Krishnamurthi, R., Mensah, G.A., Connor, M., Bennett, D.A., Moran, A.E., Sacco, R.L., Anderson, L., Truelsen, T., O'Donnell, M., Venketasubramanian, N., Barker-Collo, S., Lawes, C.M., Wang, W., Shinohara, Y., Witt, E., Ezzati, M., Naghavi, M., Murray, C., 2014. Global and regional burden of stroke during 1990–2010: findings from the Global Burden of Disease Study 2010. Lancet 383 (9913), 245–254.
Fisher, M., Feuerstein, G., Howells, D.W., Hurn, P.D., Kent, T.A., Savitz, S.I., Lo, E.H., 2009. Update of the stroke therapy academic industry roundtable preclinical recommendations. Stroke 40 (6), 2244–2250.
Forsberg-Warleby, G., Moller, A., Blomstrand, C., 2004. Psychological well-being of spouses of stroke patients during the first year after stroke. Clin. Rehabil. 18, 430–437.
Freund, P., Schmidlin, E., Wannier, T., Bloch, J., Mir, A., Schwab, M.E., Rouiller, E.M., 2009. Anti-Nogo-A antibody treatment promotes recovery of manual dexterity after unilateral cervical lesion in adult primates—re-examination and extension of behavioral data. Eur. J. Neurosci. 29 (5), 983–996.
Gainotti, G., Marra, C., 2002. Determinants and consequences of post-stroke depression. Curr. Opin. Neurol. 15 (1), 85–89.
Goldie, F.C., Fulton, R.L., Frank, B., Lees, K.R., 2014. Interdependence of stroke outcome scales: reliable estimates from the Virtual International Stroke Trials Archive (VISTA). Int. J. Stroke 9 (3), 328–332.
Goldstein, L.B., Bushnell, C.D., Adams, R.J., Appel, L.J., Braun, L.T., Chaturvedi, S., Creager, M.A., Culebras, A., Eckel, R.H., Hart, R.G., Hinchey, J.A., Howard, V.J., Jauch, E.C., Levine, S.R., Meschia, J.F., Moore, W.S., Nixon, J.V., Pearson, T.A., 2011. Guidelines for the primary prevention of stroke: a guideline for healthcare professionals from the American Heart Association/American Stroke Association. Stroke 42 (2), 517–584.
Grabowski, M., Brundkin, P., Johansson, B.B., 1993. Paw-reaching, sensorimotor, and rotational behavior after brain infarction in rats. Stroke 24, 889–895.
Greenough, W.T., Volkmar, F.R., 1973. Pattern of dendritic branching in occipital cortex of rats reared in complex environments. Exp. Neurol. 40 (2), 491–504.
Greenough, W.T., Larson, J.R., Withers, G.S., 1985. Effects of unilateral and bilateral training in a reaching task on dendritic branching of neurons in the rat motor-sensory forelimb cortex. Behav. Neural Biol. 44, 301–314.
Greenough, W.T., Black, J.E., Wallace, C.S., 1987. Experience and brain development. Child Dev. 58 (3), 539–559.
Grossman, A.W., Churchill, J.D., Bates, K.E., Kleim, J.A., Greenough, W.T., 2002. A brain adaptation view of plasticity: is synaptic plasticity an overly limited concept? Prog. Brain Res. 138, 91–108.
Hannan, A.J., 2014. Environmental enrichment and brain repair: harnessing the therapeutic effects of cognitive stimulation and physical activity to enhance experience-dependent plasticity. Neuropathol. Appl. Neurobiol. 40 (1), 13–25.
He, F.J., Nowson, C.A., MacGregor, G.A., 2006. Fruit and vegetable consumption and stroke: meta-analysis of cohort studies. Lancet 367 (9507), 320–326.

Hickmott, P.W., Steen, P.A., 2005. Large-scale changes in dendritic structure during reorganization of adult somatosensory cortex. Nat. Neurosci. 8 (2), 140–142.
Hicks, A.U., Hewlett, K., Windle, V., Chernenko, G., Ploughman, M., Jolkkonen, J., Weiss, S., Corbett, D., 2007. Enriched environment enhances transplanted subventricular zone stem cell migration and functional recovery after stroke. Neuroscience 146 (1), 31–40.
Hossmann, K.A., 2006. Pathophysiology and therapy of experimental stroke. Cell. Mol. Neurobiol. 26 (7–8), 1057–1083.
Hou, S.W., Wang, Y.Q., Xu, M., Shen, D.H., Wang, J.J., Huang, F., Yu, Z., Sun, F.Y., 2008. Functional integration of newly generated neurons into striatum after cerebral ischemia in the adult rat brain. Stroke 39 (10), 2837–2844.
HSFC, 2014. Heart and stroke foundation of Canada annual report 2014.
Hubel, D.H., Wiesel, T.N., 1970. The period of susceptibility to the physiological effects of unilateral eye closure in kittens. J. Physiol. 206 (2), 419–436.
Huber, A.B., Schwab, M.E., 2000. Nogo-A, a potent inhibitor of neurite outgrowth and regeneration. Biol. Chem. 381 (5–6), 407–419.
Huttenlocher, P.R., 1979. Synaptic density in human frontal cortex—developmental changes and effects of aging. Brain Res. 163 (2), 195–205.
Iadecola, C., Anrather, J., 2011a. The immunology of stroke: from mechanisms to translation. Nat. Med. 17 (7), 796–808.
Iadecola, C., Anrather, J., 2011b. Stroke research at a crossroad: asking the brain for directions. Nat. Neurosci. 14 (11), 1363–1368.
Janssen, H., Ada, L., Bernhardt, J., McElduff, P., Pollack, M., Nilsson, M., Spratt, N.J., 2014. An enriched environment increases activity in stroke patients undergoing rehabilitation in a mixed rehabilitation unit: a pilot non-randomized controlled trial. Disabil. Rehabil. 36 (3), 255–262.
Jauch, E.C., Saver, J.L., Adams Jr., H.P., Bruno, A., Connors, J.J., Demaerschalk, B.M., Khatri, P., McMullan Jr., P.W., Qureshi, A.I., Rosenfield, K., Scott, P.A., Summers, D.R., Wang, D.Z., Wintermark, M., Yonas, H., 2013. Guidelines for the early management of patients with acute ischemic stroke: a guideline for healthcare professionals from the American Heart Association/American Stroke Association. Stroke 44 (3), 870–947.
Jeffers, M.S., Hoyles, A., Morshead, C., Corbett, D., 2014. Epidermal growth factor and erythropoietin infusion accelerate functional recovery in combination with rehabilitation. Stroke 45, 1856–1858.
Jha, S., Dong, B., Sakata, K., 2011. Enriched environment treatment reverses depression-like behavior and restores reduced hippocampal neurogenesis and protein levels of brain-derived neurotrophic factor in mice lacking its expression through promoter IV. Transl. Psychiatry 1, e40.
Johansson, B.B., Ohlsson, A.L., 1996. Environment, social interaction, and physical activity as determinants of functional outcome after cerebral infarction in the rat. Exp. Neurol. 139 (2), 322–327.
Jones, T.A., Chu, C.J., Grande, L.A., Gregory, A.D., 1999. Motor skills training enhances lesion-induced structural plasticity in the motor cortex of adult rats. J. Neurosci. 19, 10153–10163.
Jorgensen, H.S., Nakayama, H., Raaschou, H.O., Olsen, T.S., 1995. Recovery of walking function in stroke patients: the Copenhagen Stroke Study. Arch. Phys. Med. Rehabil. 76 (1), 27–32.

Kapfhammer, J.P., Schwab, M.E., 1994. Inverse patterns of myelination and GAP-43 expression in the adult CNS: neurite growth inhibitors as regulators of neuronal plasticity? J. Comp. Neurol. 340 (2), 194–206.

Kelly, S., Bliss, T.M., Shah, A.K., Sun, G.H., Ma, M., Foo, W.C., Masel, J., Yenari, M.A., Weissman, I.L., Uchida, N., Palmer, T., Steinberg, G.K., 2004. Transplanted human fetal neural stem cells survive, migrate, and differentiate in ischemic rat cerebral cortex. Proc. Natl. Acad. Sci. U.S.A. 101 (32), 11839–11844.

Kelly-Hayes, M., Robertson, J.T., Broderick, J.P., Duncan, P.W., Hershey, L.A., Roth, E.J., Thies, W.H., Trombly, C.A., 1998. The American Heart Association stroke outcome classification: executive summary. Circulation 97 (24), 2474–2478.

Kimmelman, J., Mogil, J.S., Dirnagl, U., 2014. Distinguishing between exploratory and confirmatory preclinical research will improve translation. PLoS Biol. 12 (5), e1001863.

Kleim, J.A., Chan, S., Pringle, E., Schallert, K., Procaccio, V., Jimenez, R., Cramer, S.C., 2006. BDNF val66met polymorphism is associated with modified experience-dependent plasticity in human motor cortex. Nat. Neurosci. 9 (6), 735–737.

Kolb, B., Forgie, M., Gibb, R., Gorny, G., Rowntree, S., 1998. Age, experience and the changing brain. Neurosci. Biobehav. Rev. 22, 143–159.

Kolb, B., Morshead, C., Gonzalez, C., Kim, M., Gregg, C., Shingo, T., Weiss, S., 2007. Growth factor-stimulated generation of new cortical tissue and functional recovery after stroke damage to the motor cortex of rats. J. Cereb. Blood Flow Metab. 27 (5), 983–997.

Komatsu, K., Honmou, O., Suzuki, J., Houkin, K., Hamada, H., Kocsis, J.D., 2010. Therapeutic time window of mesenchymal stem cells derived from bone marrow after cerebral ischemia. Brain Res. 1334, 84–92.

Kwakkel, G., Kollen, B.J., van der Grond, J., Prevo, A.J., 2003. Probability of regaining dexterity in the flaccid upper limb: impact of severity of paresis and time since onset in acute stroke. Stroke 34 (9), 2181–2186.

Lai, S.M., Studenski, S., Duncan, P.W., Perera, S., 2002. Persisting consequences of stroke measured by the stroke impact scale. Stroke 33 (7), 1840–1844.

Langdon, K.D., Corbett, D., 2012. Improved working memory following novel combinations of physical and cognitive activity. Neurorehabil. Neural Repair 26 (5), 523–532.

Langdon, K.D., Clarke, J., Corbett, D., 2011. Long-term exposure to high fat diet is bad for your brain: exacerbation of focal ischemic brain injury. Neuroscience 182, 82–87.

Langdon, K.D., Granter-Button, S., Harley, C.W., Moody-Corbett, F., Peeling, J., Corbett, D., 2013. Cognitive rehabilitation reduces cognitive impairment and normalizes hippocampal CA1 architecture in a rat model of vascular dementia. J. Cereb. Blood Flow Metab. 33 (6), 872–879.

Liepert, J., Bauder, H., Wolfgang, H.R., Miltner, W.H., Taub, E., Weiller, C., 2000. Treatment-induced cortical reorganization after stroke in humans. Stroke 31 (6), 1210–1216.

Longa, E.L., Weinstein, P.R., Carlson, S., Cummins, R., 1989. Reversible middle cerebral artery occlusion without craniectomy in rats. Stroke 20, 84–91.

Loubinoux, I., Kronenberg, G., Endres, M., Schumann-Bard, P., Freret, T., Filipkowski, R.K., Kaczmarek, L., Popa-Wagner, A., 2012. Post-stroke depression: mechanisms, translation and therapy. J. Cell. Mol. Med. 16 (9), 1961–1969.

MacLellan, C.L., Keough, M.B., Granter-Button, S., Chernenko, G.A., Butt, S., Corbett, D., 2011. A critical threshold of rehabilitation involving brain-derived neurotrophic factor is required for poststroke recovery. Neurorehabil. Neural Repair 25 (8), 740–748.

Markus, T.M., Tsai, S.Y., Bollnow, M.R., Farrer, R.G., O'Brien, T.E., Kindler-Baumann, D.R., Rausch, M., Rudin, M., Wiessner, C., Mir, A.K., Schwab, M.E., Kartje, G.L., 2005. Recovery and brain reorganization after stroke in adult and aged rats. Ann. Neurol. 58 (6), 950–953.

Meshi, D., Drew, M.R., Saxe, M., Ansorge, M.S., David, D., Santarelli, L., Malapani, C., Moore, H., Hen, R., 2006. Hippocampal neurogenesis is not required for behavioral effects of environmental enrichment. Nat. Neurosci. 9 (6), 729–731.

Middleton, L.E., Corbett, D., Brooks, D., Sage, M.D., Macintosh, B.J., McIlroy, W.E., Black, S.E., 2013. Physical activity in the prevention of ischemic stroke and improvement of outcomes: a narrative review. Neurosci. Biobehav. Rev. 37 (2), 133–137.

Miniussi, C., Cappa, S.F., Cohen, L.G., Floel, A., Fregni, F., Nitsche, M.A., Oliveri, M., Pascual-Leone, A., Paulus, W., Priori, A., Walsh, V., 2008. Efficacy of repetitive transcranial magnetic stimulation/transcranial direct current stimulation in cognitive neurorehabilitation. Brain Stimul. 1 (4), 326–336.

Mittmann, N., Seung, S.J., Hill, M.D., Phillips, S.J., Hachinski, V., Cote, R., Buck, B.H., Mackey, A., Gladstone, D.J., Howse, D.C., Shuaib, A., Sharma, M., 2012. Impact of disability status on ischemic stroke costs in Canada in the first year. Can. J. Neurol. Sci. 39 (6), 793–800.

Montani, L., Gerrits, B., Gehrig, P., Kempf, A., Dimou, L., Wollscheid, B., Schwab, M.E., 2009. Neuronal Nogo-A modulates growth cone motility via Rho-GTP/LIMK1/cofilin in the unlesioned adult nervous system. J. Biol. Chem. 284 (16), 10793–10807.

Moshayedi, P., Carmichael, S.T., 2013. Hyaluronan, neural stem cells and tissue reconstruction after acute ischemic stroke. Biomatter 3 (1), e23863.

Murphy, T.H., Corbett, D., 2009. Plasticity during stroke recovery: from synapse to behaviour. Nat. Rev. Neurosci. 10 (12), 861–872.

Nguyen, A., Armstrong, E.A., Yager, J.Y., 2013. Evidence for therapeutic intervention in the prevention of cerebral palsy: hope from animal model research. Semin. Pediatr. Neurol. 20 (2), 75–83.

NINDS, 1995. Tissue plasminogen activator for acute ischemic stroke. The National Institute of Neurological Disorders and Stroke rt-PA Stroke Study Group. N. Engl. J. Med. 333, 1581–1587.

Nowak, D.A., Grefkes, C., Dafotakis, M., Eickhoff, S., Kust, J., Karbe, H., Fink, G.R., 2008. Effects of low-frequency repetitive transcranial magnetic stimulation of the contralesional primary motor cortex on movement kinematics and neural activity in subcortical stroke. Arch. Neurol. 65 (6), 741–747.

Nudo, R.J., Milliken, G.W., Jenkins, W.M., Merzenich, M.M., 1996. Use-dependent alterations of movement representations in primary motor cortex of adult squirrel monkeys. J. Neurosci. 16 (2), 785–807.

O'Collins, V.E., Macleod, M.R., Donnan, G.A., Horky, L.L., van der Worp, B.H., Howells, D.W., 2006. 1,026 experimental treatments in acute stroke. Ann. Neurol. 59 (3), 467–477.

Ovbiagele, B., Goldstein, L.B., Higashida, R.T., Howard, V.J., Johnston, S.C., Khavjou, O.A., Lackland, D.T., Lichtman, J.H., Mohl, S., Sacco, R.L., Saver, J.L., Trogdon, J.G., 2013. Forecasting the future of stroke in the United States: a policy statement from the American Heart Association and American Stroke Association. Stroke 44 (8), 2361–2375.

Overman, J.J., Carmichael, S.T., 2014. Plasticity in the injured brain: more than molecules matter. Neuroscientist 20 (1), 15–28.

Page, S.J., Gater, D.R., Bach, Y.R.P., 2004. Reconsidering the motor recovery plateau in stroke rehabilitation. Arch. Phys. Med. Rehabil. 85 (8), 1377–1381.
Papadopoulos, C.M., Tsai, S.Y., Alsbiei, T., O'Brien, T.E., Schwab, M.E., Kartje, G.L., 2002. Functional recovery and neuroanatomical plasticity following middle cerebral artery occlusion and IN-1 antibody treatment in the adult rat. Ann. Neurol. 51 (4), 433–441.
Parent, J.M., Vexler, Z.S., Gong, C., Derugin, N., Ferriero, D.M., 2002. Rat forebrain neurogenesis and striatal neuron replacement after focal stroke. Ann. Neurol. 52 (6), 802–813.
Park, H., Poo, M.M., 2013. Neurotrophin regulation of neural circuit development and function. Nat. Rev. Neurosci. 14 (1), 7–23.
Parton, A., Coulthard, E., Husain, M., 2005. Neuropharmacological modulation of cognitive deficits after brain damage. Curr. Opin. Neurol. 18 (6), 675–680.
Patel, M.D., Coshall, C., Rudd, A.G., Wolfe, C.D., 2002. Cognitive impairment after stroke: clinical determinants and its associations with long-term stroke outcomes. J. Am. Geriatr. Soc. 50 (4), 700–706.
Pendlebury, S.T., Rothwell, P.M., 2009. Prevalence, incidence, and factors associated with pre-stroke and post-stroke dementia: a systematic review and meta-analysis. Lancet Neurol. 8 (11), 1006–1018.
Ploughman, M., Windle, V., MacLellan, C.L., White, C., Dore, J.J., Corbett, D., 2009. Brain-derived neurotrophic factor contributes to recovery of skilled reaching after focal ischemia in rats. Stroke 40, 1490–1495.
Pohjasvaara, T., Leskela, M., Vataja, R., Kalska, H., Ylikoski, R., Hietanen, M., Leppavuori, A., Kaste, M., Erkinjuntti, T., 2002. Post-stroke depression, executive dysfunction and functional outcome. Eur. J. Neurol. 9 (3), 269–275.
Ratan, R.R., Noble, M., 2009. Novel multi-modal strategies to promote brain and spinal cord injury recovery. Stroke 40 (3 Suppl.), S130–S132.
Raux, M., Xie, H., Similowski, T., Koski, L., 2010. Facilitatory conditioning of the supplementary motor area in humans enhances the corticophrenic responsiveness to transcranial magnetic stimulation. J. Appl. Physiol. (1985) 108 (1), 39–46.
Reinecke, S., Dinse, H.R., Reinke, H., Witte, O.W., 2003. Induction of bilateral plasticity in sensory cortical maps by small unilateral cortical infarcts in rats. Eur. J. Neurosci. 17 (3), 623–627.
Reynolds, B.A., Weiss, S., 1992. Generation of neurons and astrocytes from isolated cells of the adult mammalian central nervous system. Science 255 (5052), 1707–1710.
Rigby, H., Gubitz, G., Eskes, G., Reidy, Y., Christian, C., Grover, V., Phillips, S., 2009. Caring for stroke survivors: baseline and 1-year determinants of caregiver burden. Int. J. Stroke 4 (3), 152–158.
Roman, G.C., Erkinjuntti, T., Wallin, A., Pantoni, L., Chui, H.C., 2002. Subcortical ischaemic vascular dementia. Lancet Neurol. 1 (7), 426–436.
Sale, A., Berardi, N., Maffei, L., 2009. Enrich the environment to empower the brain. Trends Neurosci. 32 (4), 233–239.
Sarkamo, T., Tervaniemi, M., Laitinen, S., Forsblom, A., Soinila, S., Mikkonen, M., Autti, T., Silvennoinen, H.M., Erkkila, J., Laine, M., Peretz, I., Hietanen, M., 2008. Music listening enhances cognitive recovery and mood after middle cerebral artery stroke. Brain 131 (Pt. 3), 866–876.
Savitz, S.I., 2013. Cell therapies: careful translation from animals to patients. Stroke 44 (6 Suppl. 1), S107–S109.

Siironen, J., Juvela, S., Kanarek, K., Vilkki, J., Hernesniemi, J., Lappalainen, J., 2007. The Met allele of the BDNF Val66Met polymorphism predicts poor outcome among survivors of aneurysmal subarachnoid hemorrhage. Stroke 38 (10), 2858–2860.

Srikanth, V., Beare, R., Blizzard, L., Phan, T., Stapleton, J., Chen, J., Callisaya, M., Martin, K., Reutens, D., 2009. Cerebral white matter lesions, gait, and the risk of incident falls: a prospective population-based study. Stroke 40 (1), 175–180.

Takeuchi, N., Chuma, T., Matsuo, Y., Watanabe, I., Ikoma, K., 2005. Repetitive transcranial magnetic stimulation of contralesional primary motor cortex improves hand function after stroke. Stroke 36 (12), 2681–2686.

Terroni, L., Sobrieto, M.F.M., Conforto, A.B., Adda, C.C., Guajardo, V.D., de Lucia, M.-C.S., Fraguas, R., 2012. Association among depression, cognitive impairment and executive dysfunction after stroke. Dement. Neuropsychol. 6, 152–157.

Tsai, S.Y., Papadopoulos, C.M., Schwab, M.E., Kartje, G.L., 2011. Delayed anti-nogo-a therapy improves function after chronic stroke in adult rats. Stroke 42 (1), 186–190.

Vermeer, S.E., Longstreth Jr., W.T., Koudstaal, P.J., 2007. Silent brain infarcts: a systematic review. Lancet Neurol. 6 (7), 611–619.

Wade, D.T., Wood, V.A., Hewer, R.L., 1985. Recovery after stroke—the first 3 months. J. Neurol. Neurosurg. Psychiatry 48 (1), 7–13.

Wahl, A.S., Omlor, W., Rubio, J.C., Chen, J.L., Zheng, H., Schroter, A., Gullo, M., Weinmann, O., Kobayashi, K., Helmchen, F., Ommer, B., Schwab, M.E., 2014. Neuronal repair. Asynchronous therapy restores motor control by rewiring of the rat corticospinal tract after stroke. Science 344 (6189), 1250–1255.

Wang, Y., Cooke, M.J., Morshead, C.M., Shoichet, M.S., 2012. Hydrogel delivery of erythropoietin to the brain for endogenous stem cell stimulation after stroke injury. Biomaterials 33 (9), 2681–2692.

Whishaw, I.Q., Pellis, S.M., 1990. The structure of skilled forelimb reaching in the rat: a proximally driven movement with a single distal rotatory component. Behav. Brain Res. 41 (1), 49–59.

Whishaw, I.Q., Alaverdashvili, M., Kolb, B., 2008. The problem of relating plasticity and skilled reaching after motor cortex stroke in the rat. Behav. Brain Res. 192 (1), 124–136.

Whyte, E.M., Mulsant, B.H., 2002. Post stroke depression: epidemiology, pathophysiology, and biological treatment. Biol. Psychiatry 52 (3), 253–264.

Will, B., Galani, R., Kelche, C., Rosenzweig, M.R., 2004. Recovery from brain injury in animals: relative efficacy of environmental enrichment, physical exercise or formal training (1990–2002). Prog. Neurobiol. 72 (3), 167–182.

Windle, V., Szymanska, A., Granter-Button, S., White, C., Buist, R., Peeling, J., Corbett, D., 2006. An analysis of four different methods of producing focal cerebral ischemia with endothelin-1 in the rat. Exp. Neurol. 201 (2), 324–334.

Wolf, P.A., D'Agostino, R.B., Belanger, A.J., Kannel, W.B., 1991. Probability of stroke: a risk profile from the Framingham Study. Stroke 22 (3), 312–318.

Wolf, S.L., Winstein, C.J., Miller, J.P., Taub, E., Uswatte, G., Morris, D., Giuliani, C., Light, K.E., Nichols-Larsen, D., 2006. Effect of constraint-induced movement therapy on upper extremity function 3 to 9 months after stroke: the EXCITE randomized clinical trial. JAMA 296 (17), 2095–2104.

Wu, R.H., Li, Q., Tan, Y., Liu, X.Y., Huang, J., 2014. Depression in silent lacunar infarction: a cross-sectional study of its association with location of silent lacunar infarction and vascular risk factors. Neurol. Sci. 35 (10), 1553–1559.

Yamashita, T., Ninomiya, M., Hernandez Acosta, P., Garcia-Verdugo, J.M., Sunabori, T., Sakaguchi, M., Adachi, K., Kojima, T., Hirota, Y., Kawase, T., Araki, N., Abe, K., Okano, H., Sawamoto, K., 2006. Subventricular zone-derived neuroblasts migrate and differentiate into mature neurons in the post-stroke adult striatum. J. Neurosci. 26 (24), 6627–6636.

Zagrebelsky, M., Schweigreiter, R., Bandtlow, C.E., Schwab, M.E., Korte, M., 2010. Nogo-A stabilizes the architecture of hippocampal neurons. J. Neurosci. 30 (40), 13220–13234.

Zhong, J., Chan, A., Morad, L., Kornblum, H.I., Fan, G., Carmichael, S.T., 2010. Hydrogel matrix to support stem cell survival after brain transplantation in stroke. Neurorehabil. Neural Repair 24 (7), 636–644.

Zorner, B., Schwab, M.E., 2010. Anti-Nogo on the go: from animal models to a clinical trial. Ann. N. Y. Acad. Sci. 1198 (Suppl. 1), E22–E34.

Review

Cerebrovascular Diseases

Cerebrovasc Dis 2014;38:233–239
DOI: 10.1159/000368887

Received: September 25, 2014
Accepted: October 6, 2014
Published online: November 13, 2014

How Can You Mend a Broken Brain? – Neurorestorative Approaches to Stroke Recovery

Dale Corbett[a–d] Carine Nguemeni[a, b] Mariana Gomez-Smith[a, b]

[a]Department of Cellular & Molecular Medicine, Faculty of Medicine, [b]Canadian Partnership for Stroke Recovery, University of Ottawa, Ottawa, Ont., [c]Faculty of Medicine, Memorial University of Newfoundland, St. John's, Nfld., and [d]Faculty of Medicine, University of Toronto, Toronto, Ont., Canada

Key Words
Stroke recovery · Neuroplasticity · Enriched rehabilitation · Functional outcome

Abstract
Background: Stroke is a devastating disorder that strikes approximately 15 million people worldwide. While most patients survive stroke, many are left with lifelong impairments, thereby making stroke the leading cause of permanent neurological disability. Despite this, there are a few options for treatment of acute stroke. Restoration of blood flow using clot-dissolving drugs has produced impressive benefits in some patients. However, for these drugs to be effective, they must be given soon after stroke onset and relatively only a few stroke patients reach hospital within this time. Side effects of these compounds further limit their use. ***Summary:*** Enhancing the brain's endogenous capacity for reorganization and self-repair offers the most promise for victims of stroke. Indeed, many stroke patients show considerable spontaneous functional improvement. Findings in the last 15 years suggest that stroke and related injury create a cerebral milieu similar to that of early brain development, a period characterized by rapid neuronal growth and neuroplasticity. A variety of interventions (e.g., stem cells, delivery of growth factors) are currently being explored in order to enhance neuroplasticity and reorganizational processes that are important for recovery of function. An emerging concept is that combinational or 'cocktail' therapies are more effective than single interventions in improving stroke recovery. Among these, one of the most promising therapies is enriched rehabilitation, a combination of environmental enrichment and task-specific therapy (e.g., reach training). ***Key Messages:*** Neurorestorative approaches to brain reorganization and repair are providing new insights into how neural circuits respond to injury and how this knowledge can be used for optimizing stroke rehabilitation practice.

Introduction

Stroke is the leading cause of adult neurological disability and the second leading cause of death worldwide. Attempts to reduce the incidence of stroke are being countered by an aging population and rising rates of obesity and metabolic disturbances as a result of a sedentary lifestyle and poor diet [1]. Despite significant advances in our understanding of the pathophysiology of stroke, all neuroprotective drug trials failed leaving t-PA as the only effective treatment for acute stroke [2]. Unfortunately, the limited time window and side effects limit its use to a

KARGER

E-Mail karger@karger.com
www.karger.com/ced

1015–9770/14/0384–0233$39.50/0

Dale Corbett, PhD
Department of Cellular & Molecular Medicine, Faculty of Medicine
Roger Guindon Hall, 3510G, University of Ottawa
451 Smyth Rd., Ottawa, ON, K1H 8M5 (Canada)
E-Mail dcorbett@uottawa.ca

relatively small percentage of stroke patients [3]. Furthermore, many patients benefitting from t-PA are still left with significant disabilities. In recent years, research in the stroke field has begun to shift from acute stroke to the stroke recovery phase. This change in emphasis has been triggered by a dramatic increase in our understanding of neuroplasticity and its potential to reorganize and restore function to the stroke-damaged brain [4–8, 26]. Clearly, neurorestorative interventions, including rehabilitation, offer the most hope for stroke survivors because the therapeutic time window is not limited to minutes to hours, as for t-PA, but instead applicable to weeks, months, and years and can be applied to any type of stroke, including hemorrhagic stroke.

Modeling Stroke Recovery

An important lesson from the failed stroke neuroprotection trials is that preclinical models, while never perfectly mimicking human stroke, must nonetheless capture essential features of the disease in order to avoid generating false positive results with subsequent translational failure [9–11]. For example, most stroke patients have residual deficits even years after their injury [12]. Thus, it is essential to develop animal models that also produce similar chronic functional deficits. An increasingly popular model uses endothelin-1 (ET-1), which when stereotaxically injected induces vasoconstriction followed by a gradual reperfusion, similar to human ischemic stroke [13]. The ensuing long-lasting, sensory-motor deficits make it ideal for stroke recovery studies. In addition to choosing an appropriate stroke model, it is essential to employ a sensitive battery of sensory-motor tests since recovery on one test does not guarantee recovery on other tests. Impairment of the upper limb after stroke is very common and the deficits are often persistent [14]. Therefore, a reaching task should be part of any rodent behavioral test battery to assess stroke recovery. Particularly useful, due to their great sensitivity and clinical relevance, are tests of skilled reaching such as the Montoya staircase or single pellet reaching test [4, 14–17].

Stroke Rehabilitation – Missed Opportunities?

An emerging view of the last 15 years is that stroke recreates a cerebral milieu similar to that of early brain development, a period characterized by rapid brain growth and remodeling of synaptic connections. The adult brain responds to stroke by increasing dendritic growth, forming new synapses, reorganizing functional maps, and by upregulating growth factors [6, 18–20] – all processes thought to contribute to behavioral recovery. Complex changes in growth-promoting and growth-inhibitory genes have been revealed following cortical stroke in rats [20, 21]. The general pattern is that growth inhibitory proteins (e.g., Nogo) are inhibited for several weeks after stroke but thereafter begin to show increased expression. Conversely, growth-promoting genes, including Gap-43, are highly expressed in the first days after stroke. This pattern of post-stroke gene expression is suggestive of a 'permissive neural niche' for stroke recovery in the first few weeks after injury [20]. While the experience of stroke patients varies considerably depending on injury severity, disease comorbidity, staffing, and resource issues, it is the case that in the first few weeks after stroke, many patients are alone as much as 60% of their time and inactive during 75% of their waking hours [22]. Except for the period allocated for therapy sessions, the lack of stimulation, exercise, and socialization is striking. Further, current rehabilitation practice is often not early, nor intense, and most clinical trials are conducted in the chronic phase (i.e., >6 months) of stroke recovery [23].

Enriched Rehabilitation and Stroke Recovery

Many of the reparative gene programs initiated by stroke are profoundly affected by behavioral and environmental experience, such as housing animals in enriched environments (large cages with novel objects to provide exercise, sensory-motor, social and cognitive stimulation) or providing running exercise [24, 27, 28]. For example, environmental enrichment, like exercise, increases levels of growth factors, neurogenesis, and angiogenesis [28–31]. While many studies have shown that environmental enrichment improves motor recovery after stroke [27], the benefits are primarily seen on gross tests of sensory-motor function such as rotarod or neurologic test batteries and not tests of reaching that require fine motor skills [4, 32]. Accordingly, we developed a rehabilitation paradigm, termed enriched rehabilitation (ER) that combines the social, sensory-motor, and cognitive stimulation inherent to environmental enrichment with daily reach training in order to provide task-specific therapy of the affected limb, following forelimb cortical stroke in rats (fig. 1a–c). This paradigm has been successfully used to improve recovery of skilled reaching in rats following different forms of ischemic and hemorrhagic stroke [33–35].

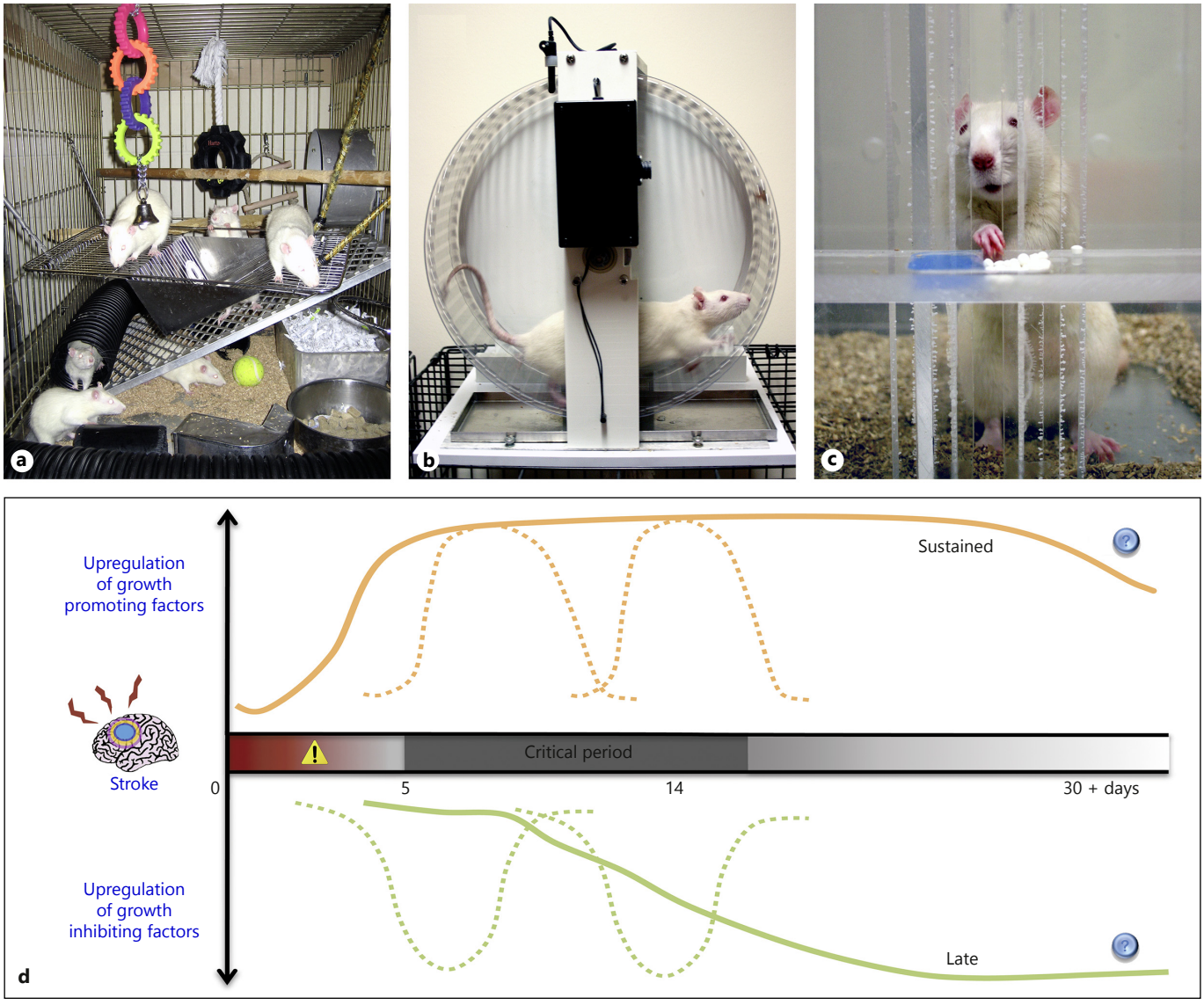

Fig. 1. Enriched rehabilitation paradigm and the critical period of post-stroke rehabilitation. After stroke, skilled use of the affected hand (or paw) is highly resistant to recovery in both humans and animals. In rats, enriched rehabilitation produces substantial improvements in the recovery of skilled reaching [25, 34–36, 67]. The protocol consists of enriched housing (**a**) and/or running exercise (**b**) in combination with several hours of daily reach training (**c**) of the impaired limb. Rats are housed in enriched environments starting 5–14 days after stroke (**d**). The timing of rehabilitation is designed to optimally engage neuroplasticity processes during the critical period of the early post-stroke recovery phase, during which a sustained upregulation of growth-promoting genes predominates (solid red line in part **d**). Most growth-inhibitory genes (solid green line) tend to be upregulated gradually, several weeks after stroke, toward the end of the critical period of stroke recovery. A few growth-promoting and growth-inhibiting genes are transiently upregulated (dashed lines) in the early and mid post-stroke recovery period. This critical period is observed in animal studies and might be different in the case of human stroke, where spontaneous recovery can extend for the first 90 days after injury. Data in part **d** is adapted from [20, 21]. Figure modified from [4].

Rehabilitation: Timing and the Concept of Critical Periods

In addition to improving behavioral recovery, a key effect of ER is that it increases dendritic length and complexity of layer V motor neurons in the stroke-damaged brain [25], suggesting that this structural modification may be contributing to the improved outcome. In support of this notion are animal studies showing that delayed initiation of ER until 30 days after stroke does not result in improved functional recovery nor does it alter layer V dendrites. These findings suggest there is 'critical or sensitive period' lasting several weeks after stroke when brain plasticity processes (fig. 1d) are optimally responsive to rehabilitation [4, 36]. Interestingly, this critical period coincides with the rising waves of growth-promoting genes that appear to peak 30 days after stroke [20]. While there is general consensus that post-stroke rehabilitation should be started sooner rather than later, there is no agreement as to exactly when it should start or when it is too late to achieve substantial benefit [23, 37, 38]. Animal studies, including some of our own research [4, 23, 36], have helped guide clinical studies including the recent EXPLICIT stroke trial evaluating early constraint-induced movement therapy [39], although an earlier constraint therapy study reported negative [40] outcomes. However, results may be influenced not only by timing, but also by the type and intensity of the intervention since early aphasia therapy [41] and early physical activity [42, 43] are associated with better outcomes.

Brain Derived Neurotrophic Factor and Stroke Recovery

Brain Derived Neurotrophic Factor (BDNF) is the most highly expressed growth factor in the human brain and plays an essential role in neuroplasticity in both the intact and the damaged brain by increasing neuronal survival, synaptogenesis, angiogenesis, and neurogenesis [44]. Administration of BDNF in shortly after stroke reduces injury [45], whereas delayed administration is associated with improved sensory-motor recovery [46, 47]. Our laboratory has investigated the possible role of BDNF in mediating the behavioral recovery induced by rehabilitation. Notably, blocking BDNF in the rat negates the benefits of rehabilitation-induced recovery after sensory-motor cortex stroke [48], while selective blockade of BDNF signaling in the peri-infarct cortex attenuates glutamate, AMPAR-mediated spontaneous motor recovery in mice subjected to photothrombotic stroke [49]. In related work [34], it was found that a critical amount or 'threshold' of post-stroke reaching rehabilitation must be met to obtain functional recovery. Animals exceeding this threshold exhibited forelimb recovery and showed significant increases in motor cortex BDNF levels, while rats receiving less rehabilitation did not recover and BDNF levels remained at control levels. These findings clearly indicate that BDNF plays a key role in post-stroke rehabilitation and consequently BDNF may be an important target to enhance recovery in stroke patients.

Stem Cells and Stroke Recovery

The identification of at least two neurogenic zones in the rodent and human brain created optimism for brain repair and stroke recovery because neural stem cells and their progenitors, collectively termed neural precursor cells (NPCs), were observed to migrate toward an injury site [50–52]. Direct delivery of NPCs [53–56] or mobilization of endogenous NPCs with growth factors or drugs [57, 58] improves recovery after stroke but in most of these studies, the behavioral effects are rather small. Mesenchymal stem cells appear to be especially effective in restoring function after focal stroke. Indeed, in one recent review, it was noted that approximately 95% of studies reported improved functional outcomes [59]. However, similar impressive outcomes were noted in early neuroprotection reviews, so a more cautious and critical assessment of stem cell studies is clearly warranted. For example, many of the mesenchymal stem cell studies used rather crude neurological test scores and simple balance tests that tend to resolve rather quickly without intervention [4]. Thus, it will be important to demonstrate that stem cell therapies are effective with more demanding behavioral tests where spontaneous recovery is limited.

New Approaches to Brain Repair – Combination Therapies

Increasing evidence indicates that the causes of ischemic cell death are *multi-factorial* [3]. Furthermore, the brain responds to vascular insults by marshalling a wide array of self-protective mechanisms [3, 60] that stand in marked contrast to the *single-target* approach commonly employed in neuroprotection [61]. When interventions (e.g., hypothermia) target multiple, instead of single mechanisms, the results are impressive [3, 62]. Similarly,

a more effective approach might be to use a 'cocktail' intervention to exploit multiple complementary neuroplastic mechanisms to restore post-stroke recovery. For example, each of the individual elements of enriched rehabilitation (exercise, socialization, cognitive stimulation, reach training) has some therapeutic potential but collectively provide a powerful intervention by acting upon multiple complementary processes of neuroplasticity (e.g., upregulation of growth factors, angiogenesis, dendritic sprouting) [27, 63]. This was illustrated in a recent experiment showing that ER, but not enriched environments or reach training alone, strongly activated neurons in layer II and III peri-infarct cortex [64], a region thought to be critical for recovery of sensory-motor function [4, 65, 66]. These findings indicate that a *combination* of environmental enrichment and task-specific rehabilitation targeting the main functional deficit (i.e., skilled reaching) most effectively increases neuronal activity around the lesion. Similarly, in more recent work, we found that serial administration of epidermal growth factor and erythropoietin induced mobilization of the endogenous NPC pool and resulted in significantly faster and more complete recovery after cortical stroke in rats when it was combined with ER [67]. This is the first demonstration that stem cell therapy produces an additive benefit in stroke recovery beyond what can be achieved with an optimized rehabilitation paradigm. This is important because stem cell therapies (or other interventions) will likely not be employed unless they provide benefit in beyond what is already achieved through current best practice (i.e., rehabilitation).

Designing preclinical and clinical studies using combination therapies is more complicated and costly than traditional single intervention studies. Nonetheless, the efficacy of single interventions in stroke is abysmal and sooner or later, this 'silver bullet' approach must be abandoned [3]. Adapting preclinical enrichment paradigms to the clinic is possible and early results with enriched rehabilitation in stroke patients are encouraging [68]. Clearly the post-stroke environment has the potential to significantly impact the brain's intrinsic restorative programs and in so doing profoundly affect stroke recovery. Indeed, enriched rehabilitation, unlike many other preclinical post-stroke interventions, has shown consistent benefits across laboratories and stroke models [25, 35, 69].

Funding

Operating grants from the Canadian Institutes for Health Research (CIHR), the Heart and Stroke Foundation of Canada and the Canadian Stroke Network to DC are gratefully acknowledged. D. Corbett was the recipient of a Tier 1 Canada Research Chair in Stroke and Neuroplasticity.

Disclosure Statement

No conflicts of interest.

Ethics

All research conducted by the authors described in this article conformed to the guidelines established by the Canadian Council on Animal Care and were approved by the institutional animal care committees of Memorial University of Newfoundland and the University of Ottawa.

References

1 Feigin VL, Forouzanfar MH, Krishnamurthi R, Mensah GA, Connor M, Bennett DA, Moran AE, Sacco RL, Anderson L, Truelsen T, O'Donnell M, Venketasubramanian N, Barker-Collo S, Lawes CM, Wang W, Shinohara Y, Witt E, Ezzati M, Naghavi M, Murray C: Global and regional burden of stroke during 1990–2010: findings from the global burden of disease study 2010. Lancet 2014;383:245–254.

2 O'Collins VE, Macleod MR, Donnan GA, Horky LL, van der Worp BH, Howells DW: 1,026 experimental treatments in acute stroke. Ann Neurol 2006;59:467–477.

3 Iadecola C, Anrather J: Stroke research at a crossroad: asking the brain for directions. Nat Neurosci 2011;14:1363–1368.

4 Murphy TH, Corbett D: Plasticity during stroke recovery: from synapse to behaviour. Nat Rev Neurosci 2009;10:861–872.

5 Nudo RJ, Wise BM, SiFuentes F, Milliken GW: Neural substrates for the effects of rehabilitative training on motor recovery after ischemic infarct. Science 1996;272:1791–1794.

6 Nudo RJ: Postinfarct cortical plasticity and behavioral recovery. Stroke 2007;38:840–845.

7 Dancause N, Nudo RJ: Shaping plasticity to enhance recovery after injury. Prog Brain Res 2011;192:273–295.

8 Carmichael ST, Krakauer JW: The promise of neuro-recovery after stroke: introduction. Stroke 2013;44(6 suppl 1):S103.

9 Fisher M, Feuerstein G, Howells DW, Hurn PD, Kent TA, Savitz SI, Lo EH; STAIR Group: Update of the stroke therapy academic industry roundtable preclinical recommendations. Stroke 2009;40:2244–2250.

10 Dirnagl U, Lauritzen M: Improving the quality of biomedical research: guidelines for reporting experiments involving animals. J Cereb Blood Flow Metab 2011;31:989–990.

11 Dirnagl U: Bench to bedside: the quest for quality in experimental stroke research. J Cereb Blood Flow Metab 2006;26:1465–1478.

12 Dobkin BH: Clinical practice. Rehabilitation after stroke. N Engl J Med 2005;352:1677–1684.

13 Windle V, Szymanska A, Granter-Button S, White C, Buist R, Peeling J, Corbett D: An analysis of four different methods of producing focal cerebral ischemia with endothelin-1 in the rat. Exp Neurol 2006;201:324–334.

14 Wade DT, Wood VA, Hewer RL: Recovery after stroke – the first 3 months. J Neurol Neurosurg Psychiatry 1985;48:7–13.
15 Iwaniuk AN, Whishaw IQ: On the origin of skilled forelimb movements. Trends Neurosci 2000;23:372–376.
16 Bury SD, Jones TA: Unilateral sensorimotor cortex lesions in adult rats facilitate motor skill learning with the 'Unaffected' forelimb and training-induced dendritic structural plasticity in the motor cortex. J Neurosci 2002;22:8597–8606.
17 Maldonado MA, Allred RP, Felthauser EL, Jones TA: Motor skill training, but not voluntary exercise, improves skilled reaching after unilateral ischemic lesions of the sensorimotor cortex in rats. Neurorehabil Neural Repair 2008;22:250–261.
18 Cramer SC, Chopp M: Recovery recapitulates ontogeny. Trends Neurosci 2000;23:265–271.
19 Jones TA, Chu CJ, Grande LA, Gregory AD: Motor skills training enhances lesion-induced structural plasticity in the motor cortex of adult rats. J Neurosci 1999;19:10153–10163.
20 Carmichael ST, Archibeque I, Luke L, Nolan T, Momiy J, Li S: Growth-associated gene expression after stroke: evidence for a growth-promoting region in peri-infarct cortex. Exp Neurol 2005;193:291–311.
21 Li S, Carmichael ST: Growth-associated gene and protein expression in the region of axonal sprouting in the aged brain after stroke. Neurobiol Dis 2006;23:362–373.
22 Bernhardt J, Dewey H, Thrift A, Donnan G: Inactive and alone: physical activity within the first 14 days of acute stroke unit care. Stroke 2004;35:1005–1009.
23 Krakauer JW, Carmichael ST, Corbett D, Wittenberg GF: Getting neurorehabilitation right: what can be learned from animal models? Neurorehabil Neural Repair 2012;26:923–931.
24 Kolb B, Forgie M, Gibb R, Gorny G, Rowntree S: Age, experience and the changing brain. Neurosci Biobehav Rev 1998;22:143–159.
25 Biernaskie J, Corbett D: Enriched rehabilitative training promotes improved forelimb motor function and enhanced dendritic growth after focal ischemic injury. J Neurosci 2001;21:5272–5280.
26 Dancause N, Barbay S, Frost SB, Plautz EJ, Chen D, Zoubina EV, Stowe AM, Nudo RJ: Extensive cortical rewiring after brain injury. J Neurosci 2005;25:10167–10179.
27 Will B, Galani R, Kelche C, Rosenzweig MR: Recovery from brain injury in animals: relative efficacy of environmental enrichment, physical exercise or formal training (1990–2002). Prog Neurobiol 2004;72:167–182.
28 Swain RA, Harris AB, Wiener EC, Dutka MV, Morris HD, Theien BE, Konda S, Engberg K, Lauterbur PC, Greenough WT: Prolonged exercise induces angiogenesis and increases cerebral blood volume in primary motor cortex of the rat. Neuroscience 2003;117:1037–1046.
29 Cotman CW, Berchtold NC, Christie LA: Exercise builds brain health: key roles of growth factor cascades and inflammation. Trends Neurosci 2007;30:464–472.
30 Kleim JA, Cooper NR, Vandenberg PM: Exercise induces angiogenesis but does not alter movement representations within rat motor cortex. Brain Res 2002;934:1–6.
31 van Praag H, Christie BR, Sejnowski TJ, Gage FH: Running enhances neurogenesis, learning and long term potentiation. Proc Natl Acad Sci U S A 1999;96:13427–13431.
32 Grabowski M, Brundkin P, Johansson BB: Paw-reaching, sensorimotor, and rotational behavior after brain infarction in rats. Stroke 1993;24:889–895.
33 Biernaskie J, Corbett D, Peeling J, Wells J, Lei H: A serial MR study of cerebral blood flow changes and lesion development following endothelin-1-induced ischemia in rats. Magn Reson Med 2001;46:827–830.
34 MacLellan CL, Keough MB, Granter-Button S, Chernenko GA, Butt S, Corbett D: A critical threshold of rehabilitation involving brain-derived neurotrophic factor is required for poststroke recovery. Neurorehabil Neural Repair 2011;25:740–748.
35 Caliaperumal J, Colbourne F: Rehabilitation improves behavioral recovery and lessens cell death without affecting iron, ferritin, transferrin, or inflammation after intracerebral hemorrhage in rats. Neurorehabil Neural Repair 2014;28:395–404.
36 Biernaskie J, Chernenko G, Corbett D: Efficacy of rehabilitative experience declines with time after focal ischemic brain injury. J Neurosci 2004;24:1245–1254.
37 Korner-Bitensky N: When does stroke rehabilitation end? Int J Stroke 2013;8:8–10.
38 Bernhardt J, Indredavik B, Langhorne P: When should rehabilitation begin after stroke? Int J Stroke 2013;8:5–7.
39 Nijland RH, van Wegen EE, Harmeling-van der Wel BC, Kwakkel G: Accuracy of physical therapists' early predictions of upper-limb function in hospital stroke units: the EPOS Study. Phys Ther 2013;93:460–469.
40 Dromerick AW, Lang CE, Birkenmeier RL, Wagner JM, Miller JP, Videen TO, Powers WJ, Wolf SL, Edwards DF: Very Early Constraint-Induced Movement during Stroke Rehabilitation (VECTORS): A single-center RCT. Neurology 2009;73:195–201.
41 Godecke E, Ciccone NA, Granger AS, Rai T, West D, Cream A, Cartwright J, Hankey GJ: A comparison of aphasia therapy outcomes before and after a very early rehabilitation programme following stroke. Int J Lang Commun Disord 2014;49:149–161.
42 West T, Churilov L, Bernhardt J: Early physical activity and discharge destination after stroke: a comparison of acute and comprehensive stroke unit care. Rehabil Res Pract 2013;2013:498014.
43 Askim T, Bernhardt J, Salvesen O, Indredavik B: Physical activity early after stroke and its association to functional outcome 3 months later. J Stroke Cerebrovasc Dis 2014;23:e305–e312. DOI: 10.1016/j.jstrokecerebrovasdis.2013.12.011. Epub 2014.
44 Park H, Poo MM: Neurotrophin regulation of neural circuit development and function. Nat Rev Neurosci 2013;14:7–23.
45 Schabitz WR, Sommer C, Zoder W, Kiessling M, Schwaninger M, Schwab S: Intravenous brain-derived neurotrophic factor reduces infarct size and counterregulates Bax and Bcl-2 expression after temporary focal cerebral ischemia. Stroke 2000;31:2212–2217.
46 Schabitz WR, Berger C, Kollmar R, Seitz M, Tanay E, Kiessling M, Schwab S, Sommer C: Effect of brain-derived neurotrophic factor treatment and forced arm use on functional motor recovery after small cortical ischemia. Stroke 2004;35:992–997.
47 Schabitz WR, Steigleder T, Cooper-Kuhn CM, Schwab S, Sommer C, Schneider A, Kuhn HG: Intravenous brain-derived neurotrophic factor enhances poststroke sensorimotor recovery and stimulates neurogenesis. Stroke 2007;38:2165–2172.
48 Ploughman M, Windle V, MacLellan CL, White C, Dore JJ, Corbett D: Brain-derived neurotrophic factor contributes to recovery of skilled reaching after focal ischemia in rats. Stroke 2009;40:1490–1495.
49 Clarkson AN, Overman JJ, Zhong S, Mueller R, Lynch G, Carmichael ST: AMPA receptor-induced local brain-derived neurotrophic factor signaling mediates motor recovery after stroke. J Neurosci 2011;31:3766–3775.
50 Chen J, Li Y, Wang L, Zhang Z, Lu D, Lu M, Chopp M: Therapeutic benefit of intravenous administration of bone marrow stromal cells after cerebral ischemia in rats. Stroke 2001;32:1005–1011.
51 Veizovic T, Beech JS, Stroemer RP, Watson WP, Hodges H: Resolution of stroke deficits following contralateral grafts of conditionally immortal neuroepithelial stem cells. Stroke 2001;32:1012–1019.
52 Parent JM, Vexler ZS, Gong C, Derugin N, Ferriero DM: Rat forebrain neurogenesis and striatal neuron replacement after focal stroke. Ann Neurol 2002;52:802–813.
53 Zhao LR, Duan WM, Reyes M, Keene CD, Verfaillie CM, Low WC: Human bone marrow stem cells exhibit neural phenotypes and ameliorate neurological deficits after grafting into the ischemic brain of rats. Exp Neurol 2002;174:11–20.
54 Bliss TM, Kelly S, Shah AK, Foo WC, Kohli P, Stokes C, Sun GH, Ma M, Masel J, Kleppner SR, Schallert T, Palmer T, Steinberg GK: Transplantation of hNT neurons into the ischemic cortex: cell survival and effect on sensorimotor behavior. J Neurosci Res 2006;83:1004–1014.
55 Hicks AU, Hewlett K, Windle V, Chernenko G, Ploughman M, Jolkkonen J, Weiss S, Corbett D: Enriched environment enhances transplanted subventricular zone stem cell migration and functional recovery after stroke. Neuroscience 2007;146:31–40.

56 Zhang L, Li Y, Zhang C, Chopp M, Gosiewska A, Hong K: Delayed administration of human umbilical tissue-derived cells improved neurological functional recovery in a rodent model of focal ischemia. Stroke 2011;42:1437–1444.

57 Kolb B, Morshead C, Gonzalez C, Kim M, Gregg C, Shingo T, Weiss S: Growth factor-stimulated generation of new cortical tissue and functional recovery after stroke damage to the motor cortex of rats. J Cereb Blood Flow Metab 2007;27:983–997.

58 Erlandsson A, Lin CH, Yu F, Morshead CM: Immunosuppression promotes endogenous neural stem and progenitor cell migration and tissue regeneration after ischemic injury. Exp Neurol 2011;230:48–57.

59 Eckert MA, Vu Q, Xie K, Yu J, Liao W, Cramer SC, Zhao W: Evidence for high translational potential of mesenchymal stromal cell therapy to improve recovery from ischemic stroke. J Cereb Blood Flow Metab 2013;33:1322–1334.

60 Moskowitz MA, Lo EH, Iadecola C: The science of stroke: mechanisms in search of treatments. Neuron 2010;67:181–198.

61 Lo EH: Degeneration and repair in central nervous system disease. Nat Med 2010;16:1205–1209.

62 Colbourne F, Corbett D: Delayed and prolonged post-ischemic hypothermia is neuroprotective in the gerbil. Brain Res 1994;654:265–272.

63 Sale A, Berardi N, Maffei L: Enrich the environment to empower the brain. Trends Neurosci 2009;32:233–239.

64 Clarke J, Langdon KD, Corbett D: Early post-stroke experience differentially alters periinfarct layer II and III cortex. J Cereb Blood Flow Metab 2014;34:630–637.

65 Nudo RJ, Milliken GW, Jenkins WM, Merzenich MM: Use-dependent alterations of movement representations in primary motor cortex of adult squirrel monkeys. J Neurosci 1996;16:785–807.

66 Carmichael ST: Cellular and molecular mechanisms of neural repair after stroke: making waves. Ann Neurol 2006;59:735–742.

67 Jeffers MS, Hoyles A, Morshead C, Corbett D: Epidermal growth factor and erythropoietin infusion accelerate functional recovery in combination with rehabilitation. Stroke 2014;45:1856–1858.

68 Janssen H, Ada L, Bernhardt J, McElduff P, Pollack M, Nilsson M, Spratt NJ: An enriched environment increases activity in stroke patients undergoing rehabilitation in a mixed rehabilitation unit: a pilot non-randomized controlled trial. Disabil Rehabil 2014;36:255–262.

69 Madinier A, Quattromani MJ, Sjolund C, Ruscher K,Wieloch T: Enriched housing enhances recovery of limb placement ability and reduces aggrecan-containing perineuronal nets in the rat somatosensory cortex after experimental stroke. PLoS One 2014;9:e93121.